Terms and Conditions of Use of Digitised Theses from Trinity College Library Dublin

Copyright statement

All material supplied by Trinity College Library is protected by copyright (under the Copyright and Related Rights Act, 2000 as amended) and other relevant Intellectual Property Rights. By accessing and using a Digitised Thesis from Trinity College Library you acknowledge that all Intellectual Property Rights in any Works supplied are the sole and exclusive property of the copyright and/or other IPR holder. Specific copyright holders may not be explicitly identified. Use of materials from other sources within a thesis should not be construed as a claim over them.

A non-exclusive, non-transferable licence is hereby granted to those using or reproducing, in whole or in part, the material for valid purposes, providing the copyright owners are acknowledged using the normal conventions. Where specific permission to use material is required, this is identified and such permission must be sought from the copyright holder or agency cited.

Liability statement

By using a Digitised Thesis, I accept that Trinity College Dublin bears no legal responsibility for the accuracy, legality or comprehensiveness of materials contained within the thesis, and that Trinity College Dublin accepts no liability for indirect, consequential, or incidental, damages or losses arising from use of the thesis for whatever reason. Information located in a thesis may be subject to specific use constraints, details of which may not be explicitly described. It is the responsibility of potential and actual users to be aware of such constraints and to abide by them. By making use of material from a digitised thesis, you accept these copyright and disclaimer provisions. Where it is brought to the attention of Trinity College Library that there may be a breach of copyright or other restraint, it is the policy to withdraw or take down access to a thesis while the issue is being resolved.

Access Agreement

By using a Digitised Thesis from Trinity College Library you are bound by the following Terms & Conditions. Please read them carefully.

I have read and I understand the following statement: All material supplied via a Digitised Thesis from Trinity College Library is protected by copyright and other intellectual property rights, and duplication or sale of all or part of any of a thesis is not permitted, except that material may be duplicated by you for your research use or for educational purposes in electronic or print form providing the copyright owners are acknowledged using the normal conventions. You must obtain permission for any other use. Electronic or print copies may not be offered, whether for sale or otherwise to anyone. This copy has been supplied on the understanding that it is copyright material and that no quotation from the thesis may be published without proper acknowledgement.

The interaction of clumping factor B and iron-regulated surface determinant protein A of *Staphylococcus aureus* with the squamous epithelial cell envelope protein loricrin

A thesis submitted for the degree of Doctor in Philosophy

by

Michelle Mulcahy

Moyne Institute of Preventive Medicine
Department of Microbiology
Trinity College

January 2013

Declaration

I hereby declare that this thesis has not previously been submitted for a degree at this or any other university and that it is my own work except where it is duly acknowledged in the text.

I agree that this thesis may be lent or copied at the discretion of the Librarian, Trinity College Dublin.

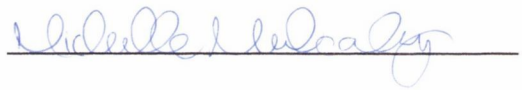

Michelle Mulcahy

Acknowledgements

Firstly I would like to thank my supervisor Prof. Tim Foster for giving me the opportunity to be part of his research group. I am very grateful for his dedication, advice and expertise over the course of my project. I would also like to thank Dr. Rachel McLoughlin for the training, guidance and encouragement she provided during my *in vivo* work. I would like to extend my gratitude toward the members of my thesis committee for their help and advice. I would also like to thank my funding body Science Foundation Ireland. Many thanks to Barry Moran for his help with the FACs analysis. I also owe many thanks to everyone in the faculty of Science who donated squames, particularly those who donated frequently.

I cannot convey enough gratitude towards my fellow members of the Foster lab both past and present, including Dee, Joan, Helen, Ian, Fiona, Emma, Marta, Tara, Niamh and Simon. For her endless advice and guidance I would especially like to thank Dr. Joan Geoghegan. Special thanks to Dee for making more blood plates for me than for the rest of the lab combined! I owe a world of thanks to Emma, Marta, Tara and Niamh for their support and advice, as well as the giggles, cake and many, many cups of tea we have shared for the last four years! I would also like to express my gratitude to Alison, Belinda, Mieskzo and Kate in the McLoughlin lab for all of their help with those crazy FVB mice! I would particularly like to thank Kate for performing the *in vivo* infection model. Many thanks to everyone in the Moyne for making it such a lovely place to work, especially Jayne, Noreen, Caroline and everyone in the prep room.

I would also like to thank all of my friends particularly Sinead, Sonia, Clare and Michelle for providing a wonderful distraction from the lab and for having the patience to put up with me on a bad science day! A very special thank you to my boyfriend Dave for always being there to listen to my worries, to walk me home after a late night in the lab and for always knowing when to turn up with a cup of tea and a bar of chocolate! Finally I would like to thank my family for their infinite encouragement, love and support. I will be eternally indebted to them.

Summary

Staphylococcus aureus permanently colonises the anterior nares of 20% of the human population while the remainder is colonised intermittently. Clumping factor B (ClfB) is a surface-expressed staphylococcal protein that plays a role in nasal colonisation. ClfB promotes bacterial adherence to human desquamated epithelial cells (squames) and ClfB-deficient strains of *S. aureus* displayed a significantly reduced ability to colonise the nares of rodents and healthy human volunteers. The iron-regulated surface determinant protein A (IsdA) is also involved in nasal colonisation. IsdA promotes bacterial adherence to squames and an interaction between IsdA and loricrin has been suggested. ClfB binds to the αC-region of fibrinogen and to the tail region of the surface-exposed squamous cell protein cytokeratin 10 (K10). The ClfB-binding site within K10 was localised to the glycine serine-rich omega loops in the K10 tail. Unpublished evidence from E. Walsh and T.J. Foster suggested that ClfB binds to loricrin, another structural protein present in the cornified envelope. Loricrin is almost entirely composed of omega loop structures similar to those in K10 and represents another potential ligand for ClfB on squames.

The interaction between ClfB and loricrin was investigated by constructing and purifying recombinant GST-tagged loricrin and the minimal ligand-binding N2N3 region of ClfB. Solid phase binding assays and SPR analysis revealed that ClfB bound to loricrin with a similar affinity to fibrinogen and K10. In order to determine whether a ClfB-binding site existed within loricrin, individual human loricrin loop regions were constructed and purified. rClfB bound to all loop regions but bound to loop region 2v with the highest affinity. ClfB promoted adherence of *S. aureus* to loricrin compared to a ClfB-deficient mutant. ClfB expressed on the surface of *Lactococcus lactis* also promoted bacterial adhesion to loricrin compared to a control strain.

ClfB binds fibrinogen and K10 using the "dock, lock and latch" mechanism. In order to determine whether ClfB binds loricrin using this mechanism, ClfB N2N3 mutants lacking the lock-latch region were constructed and purified. A Δlock-latch mutant of ClfB exhibited reduced binding to each ligand in solid phase assays indicating that ClfB binds each ligand using the

"dock, lock and latch" mechanism. Pre-incubation of *S. aureus* and recombinant ClfB with loricrin L2v inhibited binding to K10 and fibrinogen, confirming that loricrin binds the same region within ClfB as K10 and fibrinogen.

The ability of loricrin to act as a ligand for ClfB on the surface of squames was investigated. Human squames were probed with anti-loricrin IgG using flow cytometry and whole cell dot immunoblotting. The results indicated that loricrin is surface-exposed. Furthermore, loricrin region L2v inhibited ClfB-mediated adherence of *S. aureus* to human squames. To investigate whether the interaction between ClfB and loricrin was sufficient to facilitate *S. aureus* nasal colonisation, a murine model of nasal colonisation was established using loricrin-deficient ($Lor^{-/-}$) mice. In the absence of loricrin, *S. aureus* nasal colonisation was significantly impaired. Furthermore S. aureus Δ*clfB* colonised wild-type mice less efficiently than the parental strain. In contrast, a similar lower level of colonisation was observed with both the parental strain and the $ClfB^{-}$ mutant in $Lor^{-/-}$ mice, indicating that loricrin is the primary ligand for ClfB in the nose. The ability of ClfB to support nasal colonisation by binding loricrin *in vivo* was confirmed by the ability of *Lactococcus lactis* expressing ClfB to be retained in the nares of WT mice but not in $Lor^{-/-}$ mice.

The interaction between IsdA and loricrin was assessed. IsdA-deficient strains of *S. aureus* and *S. aureus* Δ*clfB* were constructed. *S. aureus* Δ*isdA* displayed no reduction in binding to recombinant loricrin or K10. Furthermore, *S. aureus* expressing IsdA but lacking ClfB and *L. lactis* expressing IsdA failed to adhere to loricrin or K10, indicating that IsdA does not facilitate bacterial adherence to loricrin. Recombinant IsdA exhibited weak binding to loricrin and K10 in binding assays but this interaction could not be confirmed using SPR. IsdA promoted bacterial adherence to squames. However pre-incubation of bacteria with loricrin region L2v did not inhibit IsdA-mediated squame adherence. Colonisation of mouse nares by *S. aureus* Δ*isdA* was significantly reduced compared to colonisation by the parental *S. aureus* strain whereas no difference in colonisation in $Lor^{-/-}$ mice was observed. However due to the *in vitro* results generated, IsdA may not promote nasal colonisation through an interaction with loricrin in the nares.

Publications

Mulcahy, M.E., Geoghegan, J.A., Monk, I.R., O'Keeffe, K.M., Walsh, E.J., Foster, T.J. and McLoughlin, R.M. (2012) Nasal Colonisation by *Staphylococcus aureus* Depends upon Clumping Factor B Binding to the Squamous Epithelial Cell Envelope Protein Loricrin. PLoS Pathogens, 8(12): e1003092. doi:10.1371/journal.ppat.1003092

Contents

Chapter 2 Materials and Methods

List of tables

List of figures

Key to abbreviations

Single letter amino acid code

A	Alanine
C	Cysteine
D	Aspartic acid
E	Glutamic acid
F	Phenylalanine
G	Glycine
H	Histidine
I	Isoleucine
K	Lysine
L	Leucine
M	Methionine
N	Asparagine
P	Proline
Q	Glutamine
R	Arginine
S	Serine
T	Threonine
V	Valine
W	Tryptophan
Y	Tyrosine

Nucleotides

A	Adenine
T	Thymine
C	Cytosine
G	Guanine

Key to abbreviations	
Amp	Ampicillin
AnTc	Anhydrotetracycline
aa	amino acid
bp	base pair(s)
BSA	bovine serum albumin
Cm	Chloramphenicol
DNA	deoxyribonucleic acid
dNTP	deoxy nucleoside triphosphate
EDTA	ethylenediaminetetraacetic acid
ELISA	enzyme linked immunosorbent assay
Erm	Erythromycin
Fg	fibrinogen
Fn	fibronectin
GST	glutathione S-transferase
h	hour(s)
HK10	human cytokeratin YY loop
HLor	human loricrin
Ig	immunoglobulin
V_H	variable immunoglobulin heavy chain
K10	cytokeratin 10
Kan	Kanamycin
kb	kilobase pair
kDa	kilodalton
MK10	murine cytokeratin 10 tail region
min	minute(s)
MLor	murine loricrin
nt	nucleotides
OD	optical density
PBS	phosphate buffered saline

Key to abbreviations	
PCR	polymerase chain reaction
rpm	revolutions per minute
SDS-PAGE	sodium dodecyl sulfate polyacrylamide gel electrophoresis
SPR	surface plasmon resonance
s	second
Sm	Streptomycin
Tris	trishydroxymethylaminomethane
TSA	trypticase soy agar
TSB	trypticase soy broth
BHI	brain-heart infusion medium
v/v	volume per volume
w/v	weight per volume
WT	wild-type

Chapter 1
Introduction

1.1 The characteristics of *Staphylococcus aureus*

Bacteria of the genus *Staphylococcus* are non-motile, Gram-positive spheres that have the appearance of grape-like clusters when viewed under a microscope. Bacteria of this genus are most closely related to *Enterococcus*, *Bacillus* and *Listeria*. Molecular typing and genetic analyses have placed the staphylococci in the *Bacillus-Lactobacillus-Streptococcus* cluster of the *Micrococcaceae* (Stackebrandt and Teuber 1988). The genus *Staphylococcus* now encompasses at least 45 species and 21 subspecies (Drancourt and Raoult 2002; Novakova *et al.* 2010; Supre *et al.* 2010). Other characteristics inherent to staphylococci include a low percentage of G and C (30 – 40 %) in genomic DNA, resistance to desiccation and a high tolerance to salt (up to 3.5 M NaCl).

Staphylococcus aureus is distinguishable from other staphylococci due to its gold pigmentation and its ability to ferment mannitol, as well as production of a thermostable DNase. It also secretes the zymogen coagulase which can bind to and activate prothrombin, converting fibrinogen to fibrin and promoting clot formation. The expression and production of extracellular coagulase differentiates *S. aureus* from coagulase-negative staphylococci (CoNS). *S. aureus* is considered more virulent than coagulase-negative staphylococci (CoNS) (Fahlberg and Marston 1960; Marston and Fahlberg 1960), although CoNS species such as *S. epidermidis*, *S. lugdunensis* and *S. haemolyticus* have been shown to cause serious human infections.

1.2 *S. aureus* colonisation

S. aureus permanently colonises approximately 20% of the population, while the remainder are intermittent carriers. Nasal carriage is a known risk factor for infection which can often be attributed to an autologous strain (von Eiff C 2001; Wertheim *et al.* 2005; Munoz *et al.* 2008). However carriers may be immunologically adapted their own strain, since *S. aureus* bacteraemia-related death was found to be significantly higher in non-carriers compared to carriers (Wertheim *et al.* 2004).

Historically, individuals were separated into one of three classes of *S. aureus* carriage: persistent (~20%), intermittent (~30%) and non-carriers (~50%) based on the prevalence of *S. aureus* in an individuals' nasal swab culture (Eriksen *et al.* 1995; Hu *et al.* 1995; Wertheim *et al.* 2005). However, more recent studies have re-classified *S. aureus* nasal carriage types based on antibody titre profiles and the ability to eliminate *S. aureus* strains from the nares (van Belkum *et al.* 2009). Human volunteers of known carrier status were artificially colonised with a mixture of *S. aureus* strains. *S. aureus* was eliminated from the nares of intermittent carriers and non-carriers at a similar rate whereas in persistent carriers the duration of colonisation was significantly higher. In addition, intermittent carriers and non-carriers shared similar anti-staphylococcal antibody profiles. This is in agreement with previous studies that have shown that persistent carriers have a higher risk for *S. aureus* infection compared to intermittent and non-carriers (Nouwen *et al.* 2005). Furthermore, the interaction between *S. aureus* and the host was shown to be highly specific as persistent carriers artificially colonised with a mixed culture could specifically re-acquire their autologous strain.

S. aureus primarily colonises the moist squamous epithelium of the anterior nares (Cole *et al.* 2001). The epithelium of the anterior nares is stratified and is composed of layers of squamous cells which mature as they progress from basal layers to the exposed surface. *S. aureus* attaches to nasal desquamated epithelial cells (squames) which are cornified, dead cells that are eventually sloughed off the surface of the nasal epithelium (Peacock *et al.* 2001). This process of cell cornification is described in detail in section 1.6. Other studies have suggested that *S. aureus* also adheres to ciliated nasal epithelial cells that are found deeper inside the nasal cavity, possibly through the interaction of the surface-expressed polyanionic polymer wall teichoic acid with an unknown ligand (Shuter *et al.* 1996; Clement *et al.* 2005; Weidenmaier and Peschel 2008). *S. aureus* can also be found at secondary sites throughout the body such as the skin, pharynx, axillae and perineum.

1.2.1 Determinants of nasal carriage

1.2.1.1 Host factors

Host factors involved in nasal colonisation by *S. aureus* are poorly understood. When *S. aureus* colonises the anterior nares it must overcome both innate and adaptive immune responses controlled by nasal-associated lymphoid tissue (NALT). Therefore, polymorphisms in genes associated with innate immune defence may be determinants of nasal carriage. Genetic studies have reported that single nucleotide polymorphisms in the glucocorticoid receptor, C-reactive proteins, interleukin-4 and complement cascade inhibitor proteins are associated with persistent *S. aureus* nasal carriage (van den Akker *et al.* 2006; Emonts *et al.* 2008; Ruimy *et al.* 2010) as well as polymorphic variations in the vitamin D receptor gene in patients with type I diabetes (Panierakis *et al.* 2009). In addition, studies have characterised innate immune mechanisms in the nasal cavity that can influence colonisation status. Reduction in the expression of anti-microbial peptides in nasal secretions such as human β-defensin-3 (Zanger *et al.* 2011) as well as alterations in the expression of pathogen recognition receptors such as toll-like receptor-2 on the nasal epithelium (Gonzalez-Zorn *et al.* 2005) have been shown to influence colonisation. In addition, the presence of haemoglobin in nasal secretions can contribute to nasal colonisation (Pynnonen *et al.* 2011) by promoting surface colonisation and preventing expression of the accessory gene regulator (Agr) quorum sensing system.

1.2.1.2 Bacterial factors

A fundamental characteristic that dictates the interaction between *S. aureus* and the host during nasal colonisation is adhesion of the bacterium to nasal epithelial surfaces. This is a multifactorial process which depends upon specific interactions between adhesins on the bacterial cell surface and their target ligands in the epithelium. *S. aureus* has developed a broad spectrum of factors that contribute to nasal colonisation. These proteins are functionally redundant in nature as many adhesins involved in nasal colonisation play other important roles in virulence or immune evasion. The surface proteins and other

factors involved in *S. aureus* nasal colonisation are described in section 1.3, 1.4 and 1.5.

Due to the conserved core genome of *S. aureus*, discriminating chromosomal factors between carrier and infecting strains may be difficult to identify. The majority of differences between *S. aureus* strains arise from the acquisition of mobile genetic elements which may encode factors that promote colonisation. Examples of such factors include the staphylococcal cassette chromosome (SCC) *mec*-encoded surface protein Pls (Huesca *et al.* 2002) and the bacteriophage-encoded adhesin SasX (Li *et al.* 2012) which are discussed in detail in sections 1.4.4 and 1.4.6, respectively. Furthermore, phages inserting into the chromosomal gene coding for β-haemolysin are detected in about 90% of carrier isolates (Goerke *et al.* 2009).

The essential WalKR two-component system has been implicated as the master regulatory system during *S. aureus* adaptation in the initial stages of nasal colonisation. An increase in expression of *walKR* mRNA was observed in the nares of humans and in the cotton rat (Burian *et al.* 2010; Burian *et al.* 2010). Target genes for WalKR include *sceD* and *tagO*, the gene products of which have been shown to play a role in nasal colonisation. Conversely, major regulatory systems that drive the expression of virulence factor genes such as the Agr quorum sensing system, the virulence gene regulatory system Sae or the alternative sigma factor B were all found to be inactive during nasal colonisation.

As well as factors that are inherent to the bacteria and the host, other niche-specific features that can influence colonisation. Commensal flora are known to inhibit pathogen colonisation and the phenomenon of bacterial interference has been shown to negatively affect nasal colonisation of *S. aureus*. Negative associations with *S. aureus* and corynebacterium species have been documented (Uehara *et al.* 2000; Lina *et al.* 2003), more than likely due to competition for the same niche. In addition, an inverse correlation between colonisation of *S. aureus* and *Streptococcus pneumoniae* in children has been reported, which suggests that the nares may be a competitive environment for both organisms (Regev-Yochay *et al.* 2004). A recent study has reported that

production of H_2O_2 by *S. pneumoniae* in the nasopharynx can trigger the induction of lysogenic phages in *S. aureus*, which is lethal for the bacteria (Selva *et al.* 2009). Furthermore, the widespread use of a polyvalent pneumococcal vaccine has led to an increase in *S. aureus* carriage rates in recipients of the vaccine (van Gils *et al.* 2011).

The production of the serine protease Esp by *S. epidermidis* has a negative effect on *S. aureus* nasal colonisation. Esp-producing strains of *S. epidermidis* introduced into the nares of healthy human carriers could eliminate *S. aureus* from the nose, whereas a mutant strain deficient in Esp, as well as wild-type Esp-negative strains had no effect (Iwase *et al.* 2010). This suggested that Esp dispersed *S. aureus* biofilms in the nose. However no evidence of biofilm formation by *S. aureus* in the nares has been reported (Burian *et al.* 2010; Ten Broeke-Smits *et al.* 2010). Alternatively, Esp may be able to degrade the keratinous squamous epithelium, preventing keratin-binding surface proteins such as ClfB from promoting attachment. In addition, Esp-producing strains of *S. epidermidis* instilled in the nares of mice prevented subsequent colonisation by a methicillin-resistant *S. aureus* (MRSA) strain (Park *et al.* 2011).

1.2.2 *S. aureus* disease

S. aureus is a significant cause of infection. The most common types of *S. aureus* infections are superficial skin lesions such as boils, impetigo and abscesses. It can also gain entry to the bloodstream by breach of the skin or mucosal barrier, causing bacteraemia or septicaemia. Bacteraemia can result in dissemination to and infection of internal tissues such as bone (osteomyelitis), joints (septic arthritis), lungs (pneumonia), and heart valves (endocarditis) (Lowy 1998). Treatment of invasive *S. aureus* infections relies heavily on the use of antimicrobial agents, to which the organism is increasingly developing resistance (discussed in section 1.9). Resistance to β-lactams including penicillins, cephalosporins and cephamycins is caused by the *mecA*-encoded penicillin-binding protein 2a found in MRSA. The glycopeptide vancomycin is the last conventional antibiotic to which MRSA was susceptible. However intermediate resistance to vancomycin by vancomycin-intermediate *S. aureus* (VISA) strains is frequently encountered and isolated cases of high-level

resistance have been reported (Flannagan *et al.* 2003; Weigel *et al.* 2003). New antibiotics including linezolid (Zyvox) have been developed specifically to deal with serious MRSA infection (Brickner *et al.* 2008). However, *S. aureus* resistance to linezolid has been reported (Locke *et al.* 2010; Mendes *et al.* 2010; Morales *et al.* 2010; LaMarre *et al.* 2011).

Atopic dermatitis (AD) is a chronic skin inflammatory disorder. *S. aureus* skin colonisation is a known risk factor in the severity of AD disease (Machura *et al.* 2008). The release of superantigenic toxins by *S. aureus* has been shown to trigger AD and to contribute to its severity (Leung *et al.* 1993; Campbell and Kemp 1998; Tomi *et al.* 2005). *S. aureus* nasal colonisation in the first year of life is associated with the subsequent occurrence of AD in later childhood years (Lebon *et al.* 2009). *S. aureus* transiently colonises 5% of adults with healthy human skin whereas it can be isolated from lesions in 90% of adults with AD (Leyden *et al.* 1974; Hauser *et al.* 1985). *S. aureus* surface proteins ClfB, protein A and Fibronectin-binding proteins might be associated with AD (discussed in sections 1.4.1.2, 1.4.5 and 1.4.2, respectively). The most important host factors are loss-of function mutations in the cornified cell envelope protein filaggrin (discussed in section 1.7.3).

1.3 Components of the cell wall

The *S. aureus* cell wall is predominantly made up of peptidoglycan, with wall teichoic acids, lipoteichoic acids and small amounts of protein encompassing the remainder. Peptidoglycan constitutes approximately 60% of the cell wall. It consists of glycan strands made of repeating disaccharide units of N-acetylglucosamine and N-acetylmuramic acid (GlcNAc-(β1-4)-MurNAc) (Ghuysen and Strominger 1963). MurNAc moieties in the glycan chains are cross-linked by short tetrapeptides (L-Ala-D-Glu-L-Lys-D-Ala) to generate a rigid three-dimensional cell wall network. This is polymerized by translocases and transpeptidases (penicillin-binding proteins) to generate peptidoglycan strands that are crosslinked with other strands. Pentaglycine interpeptide bridges link the tetrapeptide units of neighbouring glycan chains (Figure 1.1). *S. aureus* peptidoglycan is susceptible to cleavage by the endopeptidase lysostaphin due to 6 O-acetylation of muramic acid (Schleifer and Kandler 1972).

The cell wall acts as a protective barrier against osmotic lysis and membrane-damaging compounds. It also allows transport and assembly of surface components and proteins that interact with the extracellular environment. The cell wall in Gram-positive bacteria is considerably thicker than that of Gram-negative bacteria.

1.3.1 Teichoic acids

Teichoic acids (TA) are a major component of the *S. aureus* cell wall. Two types of TAs are produced from separate biochemical pathways that are either covalently linked to peptidoglycan (wall teichoic acids) or are linked to the cytoplasmic membrane (lipoteichoic acids). Wall teichoic acid (WTA) is made up of ribitol-phosphate polymers substituted with N-acetylglucosamine and D-alanine residues (Ward 1981; Endl *et al.* 1983; Collins *et al.* 2002). It is covalently linked to peptidoglycan via a disaccharide consisting of GluNAc and N-acetylmannosamine, which is followed by two units of glycerol phosphate (Yokoyama *et al.* 1989; Brown *et al.* 2008). Lipoteichoic acid (LTA) polymers of *S. aureus* consist of glycerol phosphate units substituted with D-alanine. They are attached to the cytoplasmic membrane via a glycolipid anchor (Xia *et al.* 2010).

TAs play a role in bacterial resistance to environmental stress. They have also been shown to modulate enzyme activity and cation concentrations in the cell envelope. Higher levels of D-alanine substitution in WTA and L-lysine modifications on phosphatidylglycerol promote resistance to defensins, kinocidins and cationic antibiotics like vancomycin (Peschel *et al.* 1999; Peschel *et al.* 2001; Collins *et al.* 2002; Weidenmaier *et al.* 2005). Furthermore, WTA also confers protection against human skin fatty acids (Kohler *et al.* 2009). Resistance to heat stress and low osmolarity is enhanced by both types of TA (Vergara-Irigaray *et al.* 2008; Oku *et al.* 2009).

WTA has been shown to play an important role in nasal colonisation by *S. aureus* (Weidenmaier *et al.* 2004). In a cotton rat model of nasal colonisation, a WTA-deficient mutant was almost completely eliminated from the cotton rat nose after 1 day compared to a wild-type strain whereas a mutant deficient in

sortase-linked surface proteins persisted for longer (Weidenmaier *et al.* 2008), indicating that WTA plays a crucial role in the initial stages of nasal colonisation while surface proteins may be more important for persistence and maintenance of colonisation. This is in agreement with transcriptional studies that showed an increased expression of WTA biosynthesis genes *tag*O and *tar*K in the nares in the initial stages of colonisation (Burian *et al.* 2010; Burian *et al.* 2010). Furthermore, a WTA-deficient mutant displayed significantly impaired adhesion to human nasal cells (Weidenmaier *et al.* 2004). A ligand for WTA in the nose has not yet been identified, although an interaction with lectin-like receptors and the scavenger receptor-specific ligand polyinosinic acid has been suggested. WTA also promotes bacterial adherence to endothelial cells and a WTA-deficient mutant displayed attenuated virulence in a rabbit model of endocarditis (Weidenmaier *et al.* 2005).

1.3.2 Capsular Polysaccharide

Capsular polysaccharide (CP) is produced by the majority of *S. aureus* clinical isolates (O'Riordan and Lee 2004; Roghmann *et al.* 2005). Although 11 serotypes of CP have been identified, the structurally similar CP serotype-5 and CP serotype-8 are the predominant CPs in *S. aureus* human isolates. Expression of serotype CP5 and CP8 is associated with increased virulence in animal infection models (Nilsson *et al.* 1997; Thakker *et al.* 1998; Luong and Lee 2002; Roghmann *et al.* 2005). Expression of CP also enhances virulence by conferring bacterial resistance to phagocytosis (O'Riordan and Lee 2004). Expression of CP can reduce *S. aureus* clumping factor A-mediated adherence to fibrinogen and platelets (Risley *et al.* 2007) by masking the protein binding site. CP antigens were the earliest purified experimental vaccines to protect against *S. aureus* infection.

Expression of CP is strongly influenced by growth conditions and different growth media have been shown to affect CP production (Sutra *et al.* 1990; Dassy *et al.* 1991; Stringfellow *et al.* 1991; Poutrel *et al.* 1995). CP production *in vivo* has been demonstrated in many studies. In particular, *in vivo* expression of CP5 was demonstrated in *S. aureus* strains colonising the nares of mice (Kiser *et al.* 1999). A capsule-deficient mutant displayed significantly

reduced rates of carriage. These results suggest a role for CP production in nasal colonisation by *S. aureus*. CP production may protect the bacteria from desiccation in the nasal cavity and may protect against IgA-mediated clearance from the nares (Kiser *et al.* 1999).

1.3.3 Sorting

Several staphylococcal surface proteins that are in involved in colonisation of the nares by adhesion to squames, invasion and immune evasion are translocated across the bacterial membrane using the secretory (Sec) translocation pathway and are then covalently attached to the peptidoglycan layer of the cell wall by a process known as 'sorting'. Protein precursors contain an N-terminal signal sequence which directs them into the Sec pathway. Membrane anchored signal peptidase enzymes cleave the signal sequence upon translocation across the cytoplasmic membrane (Cregg *et al.* 1996; Mazmanian *et al.* 2001). At the C-terminus a hydrophobic, membrane-spanning domain followed by a number of positively charged residues anchors the cleaved peptide and allows subsequent covalent attachment to the cell wall by a sortase enzyme (Fischetti *et al.* 1990; Navarre and Schneewind 1999; Mazmanian *et al.* 2001).

In *S. aureus,* sorting is mediated by two membrane-bound transpeptidases known as sortase (Srt) A and SrtB (Mazmanian *et al.* 2001; Pallen *et al.* 2001). SrtA recognises the C-terminal LPXTG sorting signal carried by the majority of *S. aureus* surface proteins. The gene for SrtB is located within the iron-regulated surface determinant (*isd*) gene cluster of *S. aureus* and SrtB is responsible for anchoring IsdC through recognition of a C-terminal NPQTN motif (Mazmanian *et al.* 2002). The threonine and glycine residues of the LPXTG motif undergo nucleophilic attack by the SrtA active site (Figure 1.1). A thioester linked intermediate is then formed by SrtA and the carbonyl group of the C-terminal threonine. This intermediate is resolved by covalently attaching the surface protein to the pentaglycine crossbridge of peptidoglycan, restoring the enzyme active site. The linked surface protein is then incorporated into the cell wall envelope via the transglycosylation and transpeptidation reactions of cell wall biosynthesis.

The crystal structure of the N-terminal catalytic domain of SrtA in complex with an LPXTG peptide has been solved (Liew *et al.* 2004; Zong *et al.* 2004) and showed that proline and threonine residues of the LPXTG motif are held in position within the substrate binding pocket of SrtA by hydrophobic interactions with residues near the sortase active site. Recognition of LPXTG is highly stringent and substitutions at positions 1, 2, 4 and 5 are not tolerated (Kruger *et al.* 2004). SrtA plays a crucial role in the correct anchoring of surface proteins involved in virulence and colonisation. *S. aureus srtA* mutants cannot correctly anchor LPXTG-motif surface proteins and are attenuated in animal infection models of septic arthritis and endocarditis (Jonsson *et al.* 2002; Weiss *et al.* 2004). SrtA mutants also displayed a significantly reduced ability to colonise rodent nares in murine and cotton rat models of nasal colonisation (Schaffer *et al.* 2006; Weidenmaier and Peschel 2008).

1.4 Staphylococcal Virulence Factors

1.4.1 Fibrinogen binding proteins

Fibrinogen is a soluble 340 kDa glycoprotein present in plasma (Figure 1.2). It is cleaved by thrombin and then converted to fibrin, a major component of fibrin clots. Fibrinogen plays a key role in blood clotting, inflammation and wound healing and can also act as a bridging molecule for platelet aggregation (Herrick *et al.* 1999).

The fibrinogen structure comprises two subunits both of which consist of three non-identical polypeptide chains designated Aα, Bβ and γ. The N-terminal regions of each chain are crosslinked by disulfide bond formation to form a central knot known as the E domain. The molecule also contains two outer D domains consisting of the C-termini of the Bβ- and γ-chains and the central region of the Aα-chain. The D domains are connected to the E domain by triple helical coiled-coils held together by disulfide bonds (Herrick *et al.* 1999). The C-terminal region of each Aα-chain consists of the αC-connector and the globular αC-domain (Rudchenko *et al.* 1996; Tsurupa *et al.* 2002; Burton *et al.* 2006). The N-terminal ends of the α- and β-chains represent fibrinopeptides A

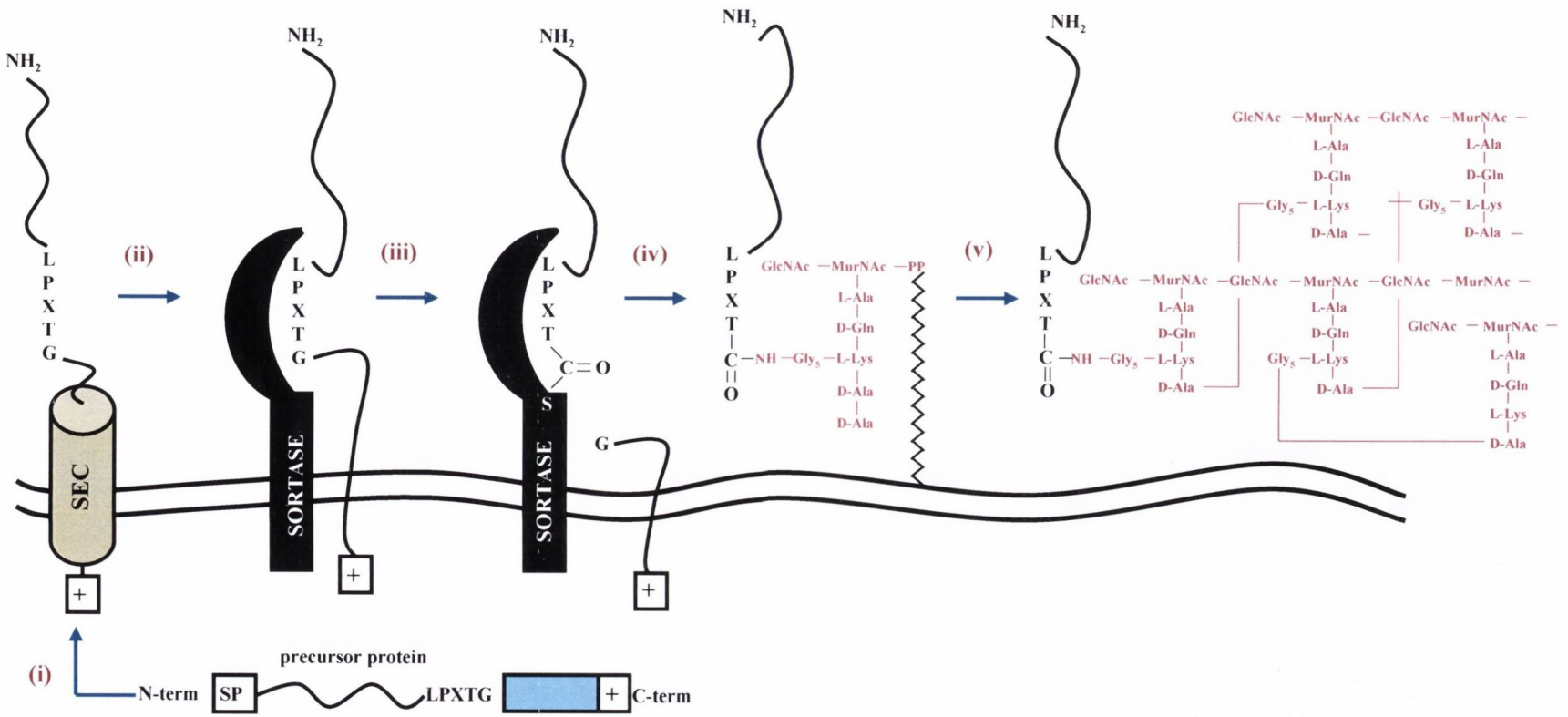

Figure 1.1. Surface protein anchoring in *Staphylococcus aureus*.

(**i**) Export. Precursor proteins are directed into the Sec pathway where the signal peptide (SP) is removed. (**ii**) Retention. The C-terminal sorting signal retains polypeptides within the secretory pathway. (**iii**) Cleavage. Sortase cleaves between residues T and G of the LPXTG motif forming a thioester enzyme intermediate. (**iv**) Linkage. The acyl-enzyme intermediate is resolved, and an amide bond is formed between the surface protein and the uncross-linked pentaglycine bridge on lipid II (**v**) Cell wall incorporation. Lipid-linked surface protein is incorporated into the cell wall peptidoglycan by transglycosylation and transpeptidation.

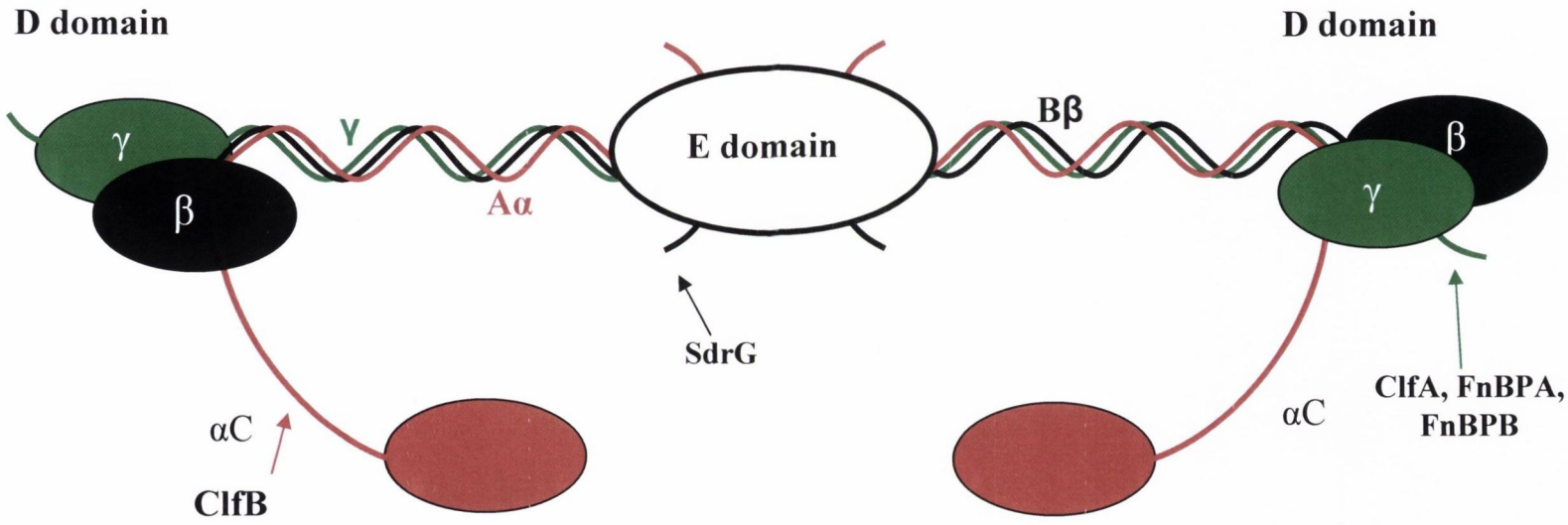

Figure 1.2. Structure of human fibrinogen.

Fibrinogen consists of two identical disulfide-linked subunits, each composed of three non-identical polypeptide chains, Aα, Bβ and γ. Fibrinogen can be divided into 4 major regions, the central E region, 2 identical terminal D regions and the αC-domains. Binding sites for *S. aureus* surface proteins ClfA, ClfB, FnBPA, FnBPB and the *S. epidermidis* SdrG protein are indicated.

and B. The globular αC-domains can interact with each other and the central E domain via fibrinopeptide B (Litvinov *et al.* 2007).

Cleavage of fibrinopeptides A and B from the N termini of the Aα and Bβ chains by thrombin initiates fibrin assembly. Associations between the αC-domains are eliminated and these regions are then able to participate in intermolecular interactions in which they promote lateral aggregation of fibrin (Medved *et al.* 1985). The αC-domains also contribute to fibrin clot stability by activating transglutaminase factor XIII which cross-links fibrin clots (Lorand *et al.* 1981; Gorkun *et al.* 1994; Collet *et al.* 2005). The interactions between staphylococcal surface proteins and fibrinogen are summarized in Figure 1.2. Adhesins that are involved in bacterial adherence to the host extracellular matrix (ECM) and blood components such as fibrinogen are called MSCRAMMS (microbial surface components recognizing adhesive matrix molecules).

1.4.1.1 Clumping Factor A

Clumping factor A (ClfA) was the first fibrinogen-binding staphylococcal surface protein to be characterized and described in detail (McDevitt *et al.* 1997). The 92 kDa protein is expressed primarily in the stationary phase of growth from a SigB dependent promoter. Weaker *clfA* expression has also been observed in the exponential phase of growth depending on transcription from a SigA-dependent promoter. ClfA is the archetype of the serine-aspartate dipeptide repeat (Sdr) family of proteins, characterised by the presence of a serine-aspartate dipeptide (SD)-repeat stalk region and similar structural organisation. ClfA consists of an N-terminal signal sequence followed by a fibrinogen-binding region (A) and an SD-repeat region that can vary in length between strains (Figure 1.3). The C-terminus of the protein consists of a wall-spanning region, membrane-spanning region and an LPDTG motif involved in anchoring and sorting to the peptidoglycan layer. ClfA binds to a flexible unfolded peptide at the C-terminus of the γ-chain of fibrinogen and binding is inhibited by the presence of Ca^{2+} and Mn^{2+} (O'Connell *et al.* 1998).

The A domain of ClfA can be further sub-divided into three regions called N1, N2 and N3. The fibrinogen-binding region of the A domain has been

localised to the N2N3 subdomains, with each adopting an IgG-like fold. The crystal structure of ClfA in complex with a synthetic peptide corresponding to the C-terminal region of the fibrinogen γ-chain has been solved and the protein was demonstrated to bind fibrinogen using a variation of the "dock, lock and latch" mechanism which is discussed in detail in section 1.4.1.2.1.

ClfA is the main surface protein responsible for platelet activation by *S. aureus*. The ClfA binding site in the γ-chain of fibrinogen is the same region that is recognised by the integrin GPIIb/IIIa on platelets which is necessary for platelet aggregation (Farrell *et al.* 1992; Hettasch *et al.* 1992). Bacteria expressing ClfA stimulate platelet activation by forming a fibrinogen bridge between the bacterium and GPIIb/IIIa. ClfA-specific immunoglobulin is also required to interact with the platelet immunoglobulin Fc receptor (FcγRIIa) for platelet activation to occur (Loughman *et al.* 2005).

The role of ClfA as a virulence factor has been demonstrated in several infection models. In a model of infective endocarditis, mutants deficient in ClfA were less infective than their parental strains (Moreillon *et al.* 1995). In addition, function blocking antibodies to ClfA sterilized vegetations on heart valves when administered with vancomycin (Vernachio *et al.* 2003). ClfA is also a virulence factor in murine models of septic arthritis (Josefsson *et al.* 2001; Palmqvist *et al.* 2005). Active immunization with recombinant ClfA or passive immunization with polyclonal anti-ClfA antibodies protected mice from arthritis and sepsis-induced death (Josefsson *et al.* 2001; McAdow *et al.* 2011).

1.4.1.2 Clumping Factor B

The MSCRAMM ClfB has similar structural organisation to ClfA (Figure 1.3). The signal sequence and wall anchoring domains are 36% and 41% identical respectively, whereas the ligand-binding regions are only 26% identical (Ni Eidhin and Foster 1998). It is expressed in the early exponential phase of growth and is absent from cells in the late exponential and stationary phase.

The N-terminus of ClfB consists of a signal sequence followed by is its binding domain, region A (Ni Eidhin and Foster 1998). This is a 540 amino-

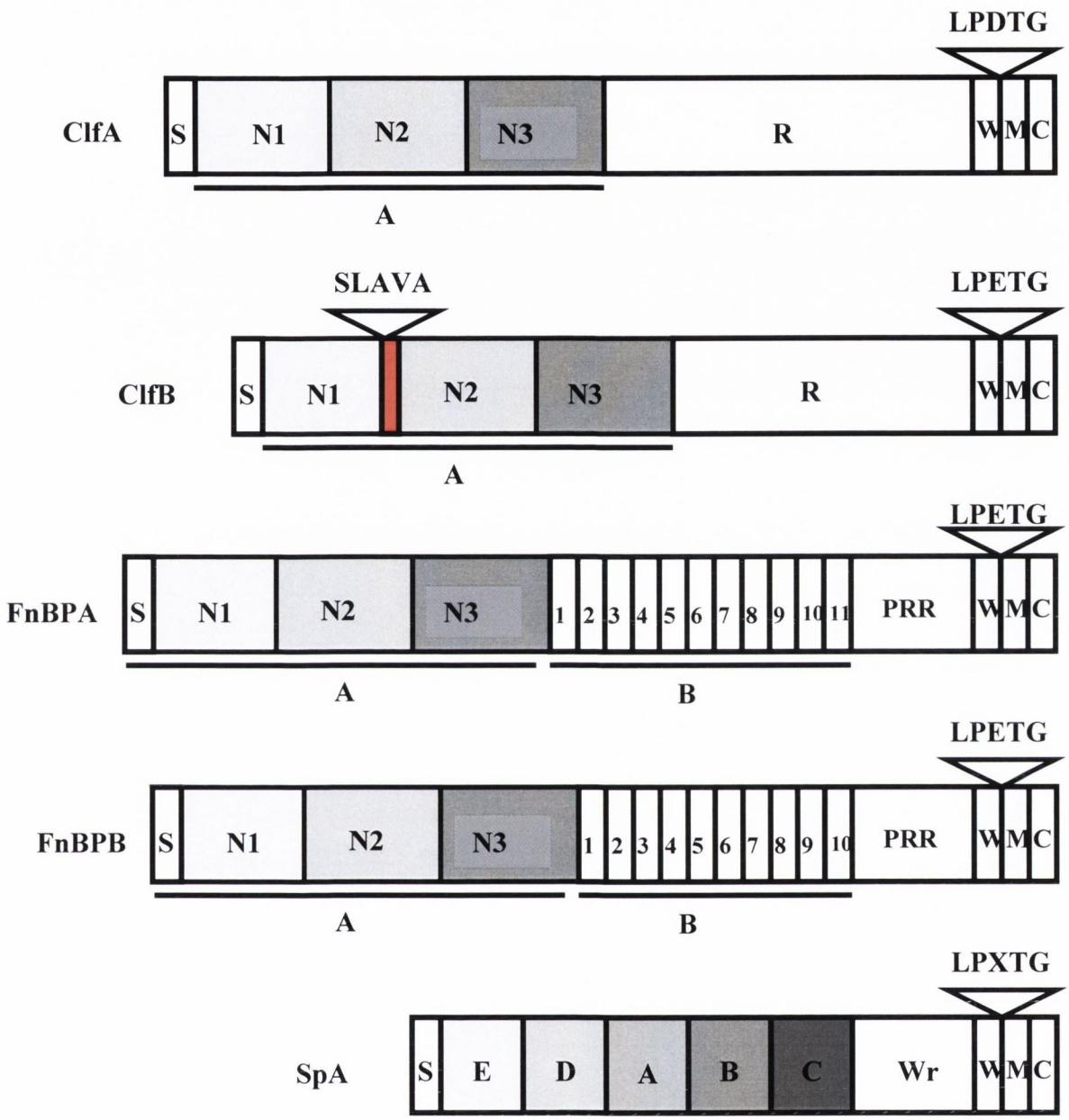

Figure 1.3. Staphylococcal surface proteins. Structural organisation of surface proteins from *S. aureus.* The A domains of ClfA, ClfB, fnPBA and FnBPB are ligand binding domains. Spa domains E, D, A, B and C are homologous ligand-binding repeats. Signal sequence (S), A domain (A), B-repeat region (B), SD-repeat region (R), proline-rich regions (Xr, PRR), wall/membrane/cytoplasmic spanning regions (WMC) and LPXTG sortase A recognition motifs are indicated.

acid-long segment containing 3 independently folded subdomains, N1, N2 and N3 (Perkins *et al.* 2001). N1 is separated from N2N3 by a metalloprotease recognition sequence, SLAVA (McAleese *et al.* 2001). Similarly to ClfA, the ligand-binding region of ClfB has been localised to the N2N3 domain of region A. The N1 domain has no known binding function (Perkins *et al.* 2001). Following the A region is region R, a 270 amino acid region containing a variable number of SD repeats. This repeat region causes the protein to extrude from the cell wall and connects the ligand-binding region to a cell wall-spanning domain and an LPXTG motif.

Studies on the expression of ClfB revealed that transcription of *clfB* ceased at the end of the exponential phase of growth. Surface-bound protein is then proteolytically cleaved by the staphylococcal metalloprotease aureolysin at the SLAVA motif, removing the N1 domain and abolishing ligand-binding activity. ClfB is also lost from the surface of the cell through shedding by autolysis and diluting of the remaining surface-bound ClfB molecules during the final cell division events leading into stationary phase (McAleese *et al.* 2001). While the Agr and Sar global regulators were shown not to be directly involved in regulation of ClfB, SarA represses expression of aureolysin which cleaves ClfB. Increased expression of aureolysin in *sarA* mutant strains results in the presence of the truncated, non-functional form of ClfB on the cell surface earlier in the exponential growth phase (McAleese *et al.* 2001; McAleese & Foster, 2003).

The repressor of toxins, Rot, belongs to the SarA family of regulatory proteins. Rot is a global regulator which represses expression of secreted toxins and enzymes, while also activating certain cell-associated proteins expressed in the exponential growth phase including ClfB (McNamara *et al.* 2000; McAleese and Foster 2003; Said-Salim *et al.* 2003). Transcription of Rot occurs throughout all growth phases. However, in the post-exponential growth phase when the Agr system is active, Rot expression is inhibited by Agr RNAIII post-transcriptionally by promoting cleavage by RNase at Rot-RNAIII mRNA duplexes (Geisinger *et al.* 2006; Boisset *et al.* 2007). This leads to increased exotoxin production and repression of cell-associated factors such as ClfB. This

also leads to decreased expression of SarA resulting in the expression of aureolysin. By promoting the expression of adhesins, Rot is believed to contribute to the early stages of infection and colonisation.

ClfB was initially recognised for its ability to promote clumping of exponential phase cells in a solution of fibrinogen and to promote *S. aureus* adherence to fibrinogen *in vitro* (Ni Eidhin and Foster 1998). Similarly to ClfA, ClfB-dependent adherence to fibrinogen was shown to be inhibited by the presence of Ca^{2+} and Mn^{2+}. The ClfB-binding site within fibrinogen was later localised to the C-terminus of the αC-chain, a region containing 10 tandem repeats. ClfB was found to bind repeat region 5 (Walsh *et al.* 2008). The fibrinogen-binding ability of ClfB plays a role in ClfB-mediated platelet activation by *S. aureus*, which is thought to contribute to the development of infective endocarditis. ClfB has been shown to contribute to the pathogenesis of experimental endocarditis in rats and patients recovering from the infection have elevated titres of anti-ClfB antibodies (Entenza *et al.* 2000; Rindi *et al.* 2006).

Although a role for ClfB in platelet activation has been identified, the main function of ClfB may be to promote nasal colonisation by *S. aureus*. A defective colonization phenotype of a ClfB-deficient mutant of *S. aureus* has been shown *in vivo* in murine and human models. A ClfB-deficient strain of *S. aureus* displayed reduced colonisation compared to a wild-type strain in mice and also in Wistar rats (Schaffer *et al.* 2006). Furthermore, a study carried out in the Netherlands in 2008 expanded upon *in vivo* model studies and demonstrated the requirement of ClfB for *S. aureus* nasal colonisation in humans (Wertheim *et al.* 2008). Following decolonisation, volunteers were recolonised with either a wild-type strain of *S. aureus* or a ClfB-deficient strain. After 10 days only the wild-type strain of *S. aureus* was retained in their noses. To date, ClfB is the only staphylococcal surface protein shown to play a major role in nasal colonisation in humans. Transcriptional analyses of *S. aureus* colonising the nares of cotton rats and humans showed that *clfB* expression is upregulated in the later stages (Burian *et al.* 2010; Burian *et al.* 2010). This echoes previous studies that proposed that WTA is essential for the initial stages of nasal

colonisation whereas surface-expressed proteins play a role in *S. aureus* persistence in the nares (Weidenmaier and Peschel 2008).

ClfB-promoted adherence to human desquamated epithelial cells has been observed and cytokeratin 10 (K10) has been implicated as a potential ligand for ClfB on the surface of squames (O'Brien *et al.* 2002; Clarke *et al.* 2006; Corrigan *et al.* 2009). K10 is described in detail in section 1.7.1. The ClfB-binding region within K10 was localised to the hypervariable glycine and serine-rich tail region of the protein, specifically the omega loop-forming sequence YGGGSSGGGSSSGGGY, known as the "YY loop" (Walsh *et al.* 2004). Recent studies have shown that ClfB binds fibrinogen and K10 using the "dock, lock and latch" mechanism which is discussed in section 1.4.1.2.1. An interaction between ClfB and cytokeratin-8 has also been reported, although its role in nasal colonisation and squame adherence is unknown (Haim *et al.* 2010). Cytokeratin-8 is principally expressed in simple epithelial cells rather than keratinocytes, so its interaction with ClfB may have some other biologically relevant role in the interaction between *S. aureus* and the host.

1.4.1.2.1 The "dock lock and latch" mechanism

The "dock, lock and latch" mechanism of binding was first described for the *S. epidermidis* fibrinogen binding surface protein SdrG (Ponnuraj *et al.* 2003). The ligand-binding A region of SdrG shares structural similarities to ClfA, ClfB and FnBPA, namely an IgG-like fold adopted by the N2 and N3 domains. The crystal structure of SdrG as an apo-protein and also in complex with a synthetic peptide ligand corresponding to the SdrG-binding site within the fibrinogen β-chain was solved. The apo-protein was shown to fold as an open structure containing a ligand-binding trench formed between the N2 and N3 subdomains of the A region. Upon ligand binding, the trench was no longer exposed and the protein-peptide complex structure adopted a closed conformation. These results led to the proposal of the "dock, lock and latch" mechanism (Figure 1.4 A).

In the "dock, lock and latch" mechanism, the ligand peptide enters the exposed binding trench between the N2 and N3 regions of the ligand-binding

domain (Figure 1.5 A). This interaction induces a redirection of a C-terminal extension in the N3 domain, known as the latching peptide. This extension covers the bound ligand, locking it in place, followed by a final latching event where a short segment C-terminal of the locking residues inserts through a β-strand complementation in a trench on the surface of the N2 subdomain. This mechanism was proven experimentally for SdrG which showed that hydrophobic interactions that occurred between the N3 extension and the ligand peptide helped to secure the ligand in place and stabilized the closed conformation of the protein-peptide structure (Bowden *et al.* 2008).

The crystal structure of ClfA as an apo-protein and also in complex with a synthetic fibrinogen γ-chain peptide confirmed that ClfA also employs a variant of the "dock, lock and latch" mechanism (Ganesh *et al.* 2008). Recombinant ClfA forced into a closed, "lock latch" conformation by introducing Cys substitutions into the binding region retained the ability to bind a fibrinogen peptide, indicating that in contrast to SdrG, an open conformation may not be required by ClfA for ligand binding (Figure 1.4 B). Furthermore, when compared to the SdrG protein-peptide closed complex, it was observed that the orientation of the bound ligand is reversed in the ClfA-ligand closed complex. The C-terminal residues of the Fg ligand were found to be docked between the N2 and N3 in ClfA making a parallel β-sheet complementation with the N3 extension domain, whereas in SdrG, the N-terminal residues of the ligand were docked between the N2 and N3 domains to form an anti-parallel β-sheet. It was therefore surmised that ClfA uses a variant of the "dock, lock and latch" mechanism called "latch and lock" (Figure 1.5 B), where the C-terminal region of the Fg peptide is bound by the ClfA ligand binding trench and the remaining residues are threaded into the binding cavity formed in a stable, closed conformation.

Due to the structural similarities between ClfB, SdrG and ClfA, it had been assumed that ClfB also binds its ligand using the "dock, lock and latch" mechanism (Figure 1.4 C). Solving the crystal structure of the ClfB N2N3 region as an apo-protein and in complex with peptides corresponding to the ClfB-binding regions in fibrinogen and K10 confirmed this assumption (Ganesh

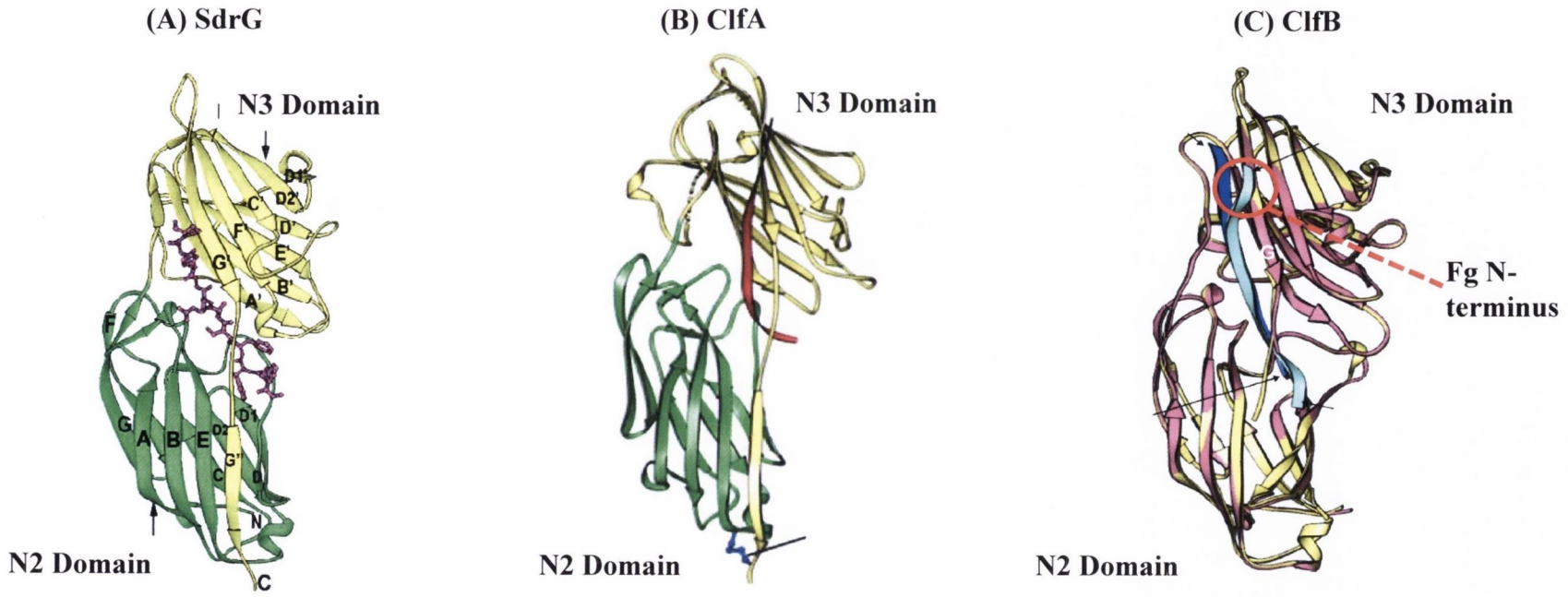

Figure 1.4. Crystal structures of domains N23 of ClfA, ClfB and SdrG in complex with peptides

Ribbon diagrams of the N2N3 domains of ClfA, ClfB and SdrG. (**A**) Fibrinogen β-chain in complex with SdrG is shown in ball and stick form (pink). Ligand binding occurs in a trench formed between the N2 and N3 domains. Upon ligand binding, the latching peptide (G") is redirected across the ligand and forms a β-sheet with the N2 domain by β-strand complementation (taken from Ponnuraj *et al.*, 2003). **(B)** Fibrinogen γ-chain C-terminal region (red) in complex with ClfA. (taken from Ganesh et al, 2008). **(C)** Comparison of fibrinogen α-chain (cyan) and K10 "YY loop" (dark blue) in complex with ClfB. The "kink" that occurs in the fibrinogen peptide is indicated (taken from Ganesh et al, 2011).

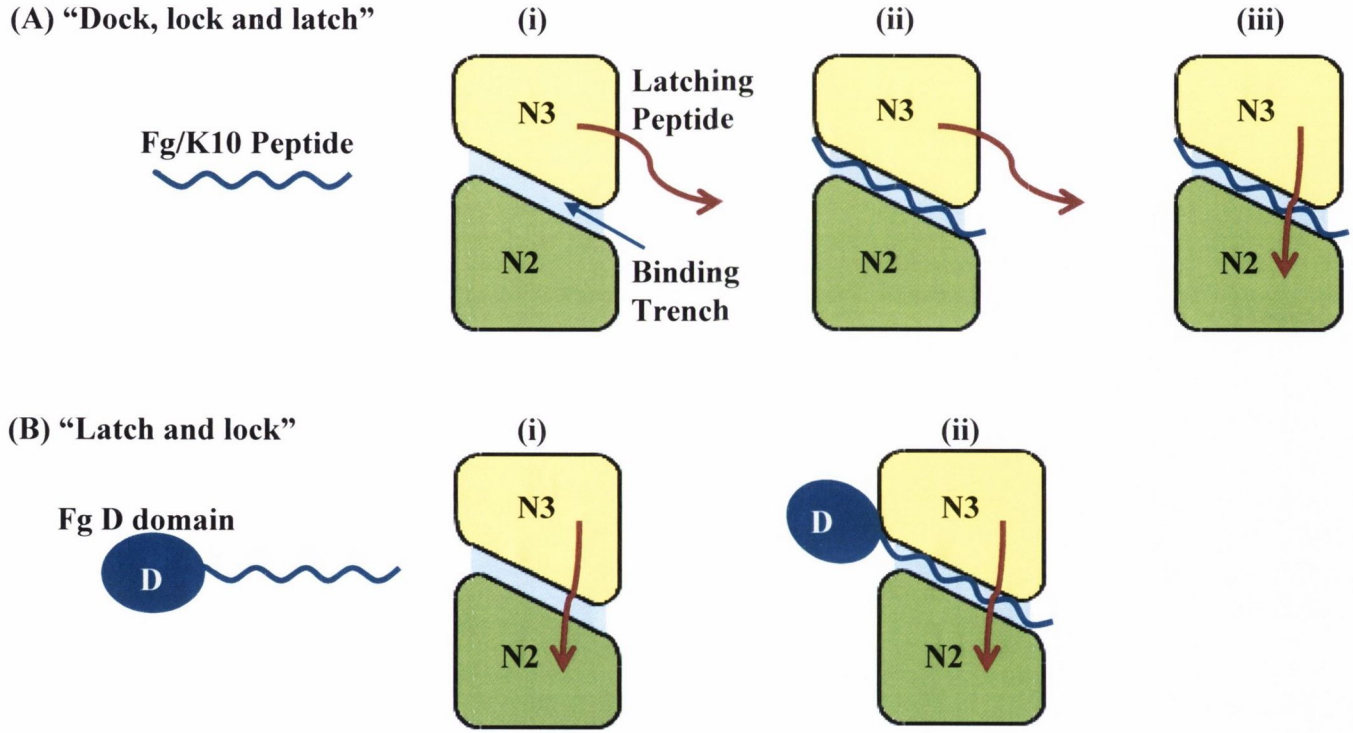

Figure 1.5 Schematic diagram of the "dock, lock and latch" and "latch and lock" mechanisms.

N2 and N3 regions are indicated. The binding trench is highlighted in light blue. The latching peptide is indicated by a red arrow. (A) The "dock, lock and latch" mechanism is used by SdrG and ClfB. (i) The N2N3 region is in an open conformation. Docking of the ligand (ii) triggers conformational changes in the C-terminus of the ClfB N3 region. The C-terminus of ClfB N2N3 runs across the ligand and latches it in place (iii), generating a β-strand that forms a parallel β-sheet with a β-strand in the N2 domain. (B) The "latch and lock" mechanism is used by ClfA. (i) ClfA is capable of binding fibrinogen in a closed conformation. (ii) The C-terminal region of the Fg peptide is bound by the ClfA ligand binding trench and the remaining residues are threaded into the binding cavity formed by the stable, closed conformation of the N2N3 binding domain.

et al. 2011). ClfB N2N3 in complex with fibrinogen or K10 showed that unlike ClfA, an open conformation is most likely adopted by the protein. However, similarly to ClfA, ligand binding induces a parallel β-sheet complementation formed by the interaction between the latching peptide and the N2 region, unlike the anti-parallel β-strand formed in the SdrG protein-peptide complex.

Many important hydrophobic interactions that occurred between ClfB and each ligand in the binding trench were reported, including an interaction with Q_{235}, W_{522} and N_{526}. N_{526} was shown to point inward and line the binding pocket and was proposed to be critical for the locking event. W_{522} was shown to be essential for binding and anchoring peptides in the binding pocket. A stretch of similar residues (GSSGXG) in both ligands were observed to bind to the same residues in the ClfB binding region indicating that a conserved ligand motif is recognised by ClfB. However significant differences were also found between the two ligand binding mechanisms. A kink in the N-terminus of the Fg peptide (Figure 1.4 C) indicated that a weaker interaction may occur between backbone atoms in the Fg peptide and the binding trench compared to ClfB and K10 in complex (Ganesh *et al.* 2011).

Many of the interactions observed between ClfB and its ligands in complex were confirmed by a later study, the results of which strongly supported a "dock, lock and latch" mechanism of ClfB-binding (Xiang *et al.* 2012). However, a similar but more specific ligand motif for ClfB-binding (G_1-S_2-S_3-G_4-G/S/T_5-G_6-X_7-X_8-G_9) was proposed and was supported by the interactions observed between ClfB and its ligands in the binding trench. With this new evidence, a "dock, lock and latch" mechanism for ClfB-ligand interactions was put forward. The ligand docks into the ClfB N2N3 binding trench and residue interactions in the trench lock the ligand in place. Docking of the ligand triggers conformational changes in the C-terminus of the ClfB N3 region, generating a β-strand that forms a parallel β-sheet with a β-strand in the N2 domain. The C-terminus of ClfB N2N3 runs across the ligand and latches it in place. This mechanism was reported for fibrinogen but the final formation of a β-strand in the C-terminus of ClfB N3 (the "latching" event) was not observed in the ClfB-K10 complex. However, the K10 ligand was still shown to be

"locked" in by the N-terminus of the N3 strand, indicating that the "dock, lock and latch" mechanism is used.

1.4.2 Fibronectin binding proteins

Fibronectin (Fn) is a multifunctional extracellular matrix glycoprotein found in blood plasma at high concentrations. It is composed of two covalently linked 220 kDa polypeptides. It contains several distinct domains capable of binding to cell surfaces and many compounds including collagen, fibrin, heparin, DNA and actin. It contributes to a number of cell processes including adhesion, migration, opsonisation, wound repair and the maintenance of the cell shape (Pankov and Yamada 2002).

Two Fn binding proteins (FnBPs) have are expressed on the cell surface of the majority of *S. aureus* strains. FnBPA and FnBPB are expressed during the exponential phase of growth and share highly similar structural features (Figure 1.3). They each contain structurally similar N-terminal A domains that mediate binding to the C-terminus of the fibrinogen γ-chain (similarly to ClfA) and to elastin. Strain-specific variability has been demonstrated in the A domain of FnBPA and FnBPB. Seven different allelic variants have been identified (Loughman *et al.* 2008; Burke *et al.* 2010). This type of allelic variation may play a role in evasion of the host immune system.

The FnBP fibrinogen-binding A domains can be further subdivided into N1, N2 and N3 regions. Fibrinogen binding has been localised to the N2N3 region and binding may occur using the "dock, lock and latch" mechanism (described in section 1.4.1.2.1). The Fn-binding region has been localised to a tandemly arrayed repeat region in each protein (Figure 1.3). FnPBA contains 11 Fn-binding repeats whereas FnBPB contains 10. FnBPs interact with Fn by a tandem β-zipper mechanism. Recently the crystal structure of two Fn-binding repeats of FnBPA in complex with peptides corresponding to the type I modules of Fn has been solved (Bingham *et al.* 2008). The Fn-binding repeats form anti-parallel strands along four adjacent type 1 modules of Fn. The disordered nature of the Fn-binding repeats is thought to facilitate the formation of large intermolecular interfaces allowing one FnBP molecule to bind up to 9 molecules

of fibronectin (Matsuka *et al.* 2003; Bingham *et al.* 2008). The A-domain of the seven isoforms of FnBPB but not FnBPA also bound to Fn by an unknown mechanism (Burke *et al.* 2011).

FnBPs play a role in immune evasion by mediating bacterial adherence to and invasion of endothelial and epithelial cells (Dziewanowska *et al.* 1999; Edwards *et al.* 2010) through the formation of a Fn-bridge between *S. aureus* and integrins on host cells (Sinha *et al.* 1999; Fowler *et al.* 2000). They are also involved in platelet activation and aggregation (Fitzgerald *et al.* 2006), and are responsible for *S. aureus* adhesion to Fn-coated medical implant devices (Vaudaux *et al.* 1993; Arrecubieta *et al.* 2006). Heart valve colonisation and subsequent invasion of the surrounding epithelium was promoted by FnBPs in experimental endocarditis models (Que *et al.* 2005). Furthermore FnBPs are also involved in the intracellular accumulation phase of biofilm formation by some MRSA strains (O'Neill *et al.* 2008).

As well as promoting internal infection, expression of FnBPs has been associated with increased adhesion of *S. aureus* to the skin of individuals suffering with atopic dermatitis (AD) which contributes to the severity of the disease. Higher levels of Fn are found in the stratum corneum of AD sufferers. Mutants lacking both FnBPs displayed reduced adherence to atopic skin compared to normal skin, indicating that these proteins are involved in skin colonisation of AD sufferers (Cho *et al.* 2001). Furthermore, IgG-reactive antigens against FnBPs were isolated from AD patients and recombinant FnBP was shown to be an IgE-reactive protein (Reginald *et al.* 2011). In the same study, FnBP was proposed to require antigen presentation to induce specific cellular responses, as well as inducing the release of pro-inflammatory cytokines such as IL-6, IFN-γ and TNF-α in cultured peripheral blood mononuclear cells from AD patients. FnBP also induced an IgE-mediated allergic response in FnBP-sensitized mice (Reginald *et al.* 2011).

1.4.3 IgG-binding protein A

Surface protein A (SpA) is expressed by at least 95% of *S. aureus* strains (Forsgren and Nordstrom 1974) and was the first *S. aureus* cell wall protein to be characterized (Oeding *et al.* 1964). The surface-exposed N-terminal region of Spa contains five homologous repeats designated as E, D, A, B and C (Figure 1.3). Each subdomain is 58 – 62 amino acids in length and consists of three anti-parallel α-helices that form helical bundles stabilized by hydrophobic interactions in the bundle interior. Each repeat is capable of binding many ligands including the Fc region of IgG, the Fab heavy chain of V_H3 on IgM (Hillson *et al.* 1993), tumour necrosis factor receptor-1 (TNFR-1) and von Willebrand factor (vWF) (Hartleib *et al.* 2000; O'Seaghdha *et al.* 2006). The N-terminal domain is followed by a proline-rich repeat region (Xr domain) (Moks *et al.* 1986).

SpA-mediated binding to the Fc region of IgG leads to coating of the bacterial cell with IgG molecules in an incorrect orientation. This prevents recognition by neutrophil Fc receptors, inhibiting phagocytosis and stimulation of complement fixation by the classical pathway (Foster 2009). Binding of SpA to the Fab region of V_H3-class IgM molecules on B-cells is believed to cause their activation, proliferation and subsequent apoptotic destruction (Silverman 1992) and is potentially immunosuppressive. Binding of SpA to vWF contributes to bacterial adhesion to platelets under shear conditions which may contribute to bloodstream infection (Hartleib *et al.* 2000).

The pro-inflammatory effect of SpA has been demonstrated through the interaction with TNFR-1 on many cell types including osteoblasts, airway epithelial cells and keratinocytes (Gomez *et al.* 2004; Claro *et al.* 2011; Classen *et al.* 2011; Claro *et al.* 2013). SpA acts as a ligand mimicking TNF-α, activating TNFR-1 and causing subsequent pro-inflammatory signalling. It stimulates cleavage of TNFR-1 from the surface of epithelial cells and macrophages, which serves to limit TNF-α signalling (Gomez *et al.* 2006; Gomez *et al.* 2007). Recognition of TNFR-1 by SpA induces the expression of inflammatory chemokines such as interleukin-8. As well as contributing to the severity of osteomyelitis and promoting *S. aureus* virulence in a murine

pneumonia infection model, SpA-mediated adhesion and activation of keratinocytes through an interaction with TNFR-1 is likely to be linked to the severity of AD disease. Furthermore, SpA can induce AD in experimental animals when used in conjunction with subclinical concentrations of detergent (Terada *et al.* 2006).

1.4.4 SasX

The mobile genetic element-encoded staphylococcal surface protein SasX has been identified as a critical factor promoting nasal colonisation, immune evasion and virulence in MRSA strains linked to hospital infections in the far east (Li *et al.* 2012). The *sasX* gene has been found in 3 sequence type (ST) 239 MRSA clones, a predominant ST present in China and most Asian countries, but is absent from other *S. aureus* genomes and other global MRSA strains. The gene is thought to be a horizontally-acquired virulence factor and is predominantly associated with hospital infections. The *sasX* gene encodes a secreted, cell wall-anchored surface-expressed protein (SasX) of 15 kDa. SasX promoted *S. aureus* adherence to human nasal epithelial cells compared to a SasX-deficient strain. SasX-deficient strains also displayed a significantly reduced ability to colonise the nares of mice compared to wild-type strains. Moreover, SasX was also shown to play a role in immune evasion as well as promoting virulence in murine skin abscess and lung infection models. SasX represents a rare but novel determinant of nasal colonisation as well as virulence and immune evasion in MRSA clones.

1.4.5 Iron regulated surface determinant proteins

Bacteria require iron for survival and growth inside the human host. However in humans the majority of iron is sequestered by haem-containing proteins and is unavailable to invading pathogens. In response to iron-limited conditions, *S. aureus* expresses a subset of staphylococcal genes under the control of the ferric uptake response (Fur) transcriptional regulator (Skaar and Schneewind 2004). The iron-regulated surface determinant (*isd*) locus encodes three surface-expressed proteins (IsdA, IsdB, IsdH) containing a LPXTG sorting signal (Figure 1.6). IsdC is also expressed from the locus and is sorted by the

SrtB pathway based on its atypical NPQTN motif which is discussed in section 1.3.3 (Mazmanian *et al.* 2002). It is partially buried in the cell wall. Other *isd* gene products (IsdD, IsdE, IsdF) form an ABC transporter in the bacterial membrane. Expression of Isd proteins is inhibited by Fur in the presence of Fe^{3+}.

IsdA, IsdB, IsdC and IsdH contain variable numbers of a conserved haem-binding domain known as the NEAT (near iron transporter) domain. NEAT domains adopt a conserved structure forming IgG-type beta sandwich folds of 7 or more β-strands in 2 β-sheets. Three-dimensional analysis of the IsdH NEAT 1 domain showed that it is organised into a β sandwich fold composed of two five-stranded antiparallel beta sheets. Based on sequence comparisons, all NEAT domains were predicted to form folds (Pilpa *et al.* 2006; Krishna Kumar *et al.* 2011). They are also multifunctional and recognise other host ligands.

The Isd proteins acquire haem by binding human haemoproteins and removing the haem molecule. Initially, host haemoglobin is released from erythrocytes through the action of secreted cytolytic toxins such as α-, β-, γ- or δ-toxins. The toxic haemoglobin is collected by the host haemoglobin carrier molecule, haptoglobin. IsdH binds haemoglobin or the haptoglobin-haemoglobin complex, strips it of haem and passes it to IsdB and/or IsdA. From here, the haem is passed to IsdC and then to the ABC transporter formed by IsdDEF. Alternatively, IsdB can bind directly to haemoglobin and pass the released haem to IsdA or directly to IsdC. The haem is imported through the plasma membrane into the cytoplasm where it is degraded by haemoxygenases (Liu *et al.* 2008; Muryoi *et al.* 2008; Zhu *et al.* 2008; Grigg *et al.* 2010; Haley and Skaar 2012).

IsdA, IsdH and IsdB are known to have other functions in *S. aureus* infection and colonisation. A role for IsdH in the evasion of phagocytosis has been observed. An *S. aureus* IsdH-deficient strain was engulfed more readily by human neutrophils, survived poorly in fresh whole human blood and was less virulent in a mouse model of sepsis (Visai *et al.* 2009; Smith *et al.* 2011). This protective mechanism could be due to the ability of IsdH to bind to and activate

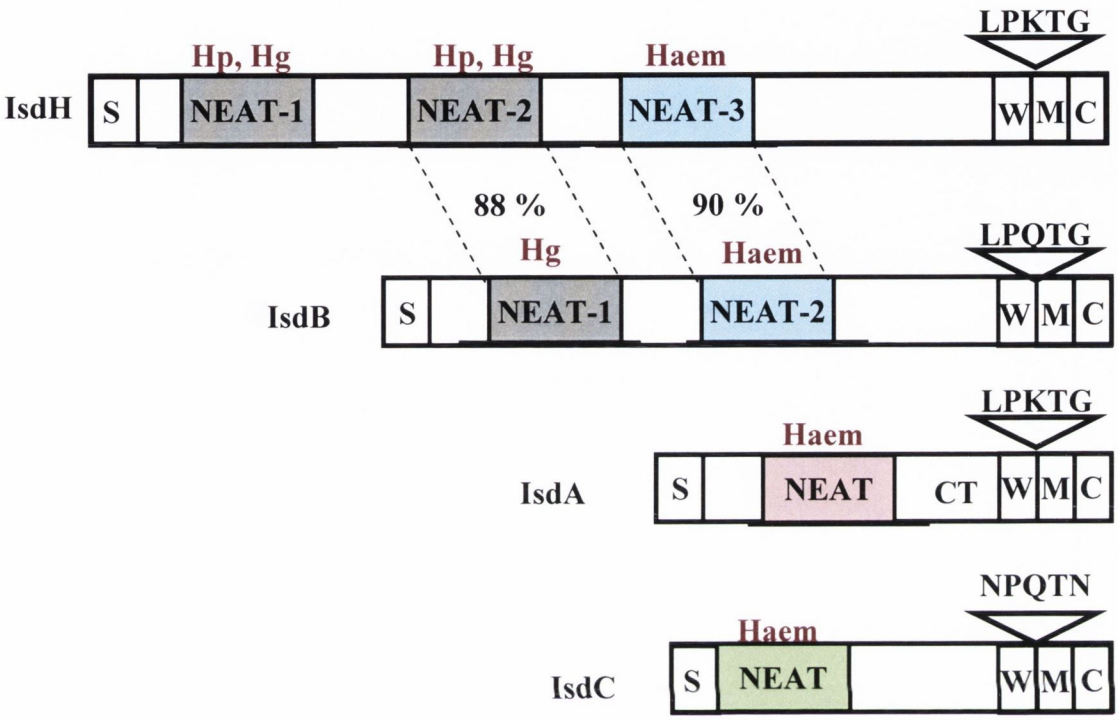

Figure 1.6. The cell-wall associated Isd proteins of *S. aureus*. The surface exposed Isd proteins have variable numbers of NEAT domains. NEAT domains are shown in grey, blue, pink and green. NEAT domains 2 and 3 of IsdH are highly homologous to NEAT domain 1 and 2 of IsdB. The C terminal LPXTG SrtA recognition motifs are indicated for IsdH, IsdB and IsdA. IsdC has an atypical NPQTN motif which is recognised by SrtB. NEAT domains that bind haptoglobin (Hp), haemoglobin (Hg) and haem are indicated. The C-terminal hydrophilic domain of IsdA (CT) is responsible for decreased cellular hydrophobicity rendering *S. aureus* resistant to bactericidal human skin fatty acids and peptides .

complement factor I, which accelerates degradation of the serum opsonin C3b. IsdB is directly involved in platelet activation by binding to platelets via the platelet integrin GPIIb/IIIa (Miajlovic *et al.* 2010) and binds other β3-containing integrins promoting invasion of epithelial cells (Zapotoczna *et al.* 2012). IsdA promotes adherence to squames. It has been implicated in nasal colonisation as well as survival on the skin by conferring resistance to innate immune defences. The different roles of IsdA are described in Chapter 6.

1.4.6 SasG and Pls

S. aureus surface protein G (SasG) exhibits sequence similarity to the type-1 SCC*mec* mobile genetic element-associated plasmin sensitive cell surface protein (Pls) and the accumulation associated protein (Aap) from *S. epidermidis* (Roche *et al.* 2003). The domain organisation of SasG is typical of a member of the LPXTG family of proteins, consisting of an N-terminal secretion signal and A domain, followed by an extended region made up of 128-residue B repeats and a C-terminal sorting sequence. Each repeat element in the B-repeat region is referred to as a G5 domain and is followed by a 50-residue sequence (E). High-level expression of SasG from *S. aureus* strains inhibited adherence to extracellular matrix proteins fibrinogen and fibronectin as well as K10 (Corrigan *et al.* 2007). This was found to be due to the extension of the protein from the cell surface by the B repeats and indicated that the protein may function to mask binding of other adhesins to extracellular matrix ligands, possibly as a method of dissemination into other tissues during certain stages of infection. A role for SasG in the attachment phase of biofilm formation has also been identified and this interaction has been localised to the B repeats of the protein (Geoghegan *et al.* 2010). The interaction was shown to be mediated by the presence of Zn^{2+}. Zinc-dependent self-association events between stretches of tandem G5 domains in opposing molecules occur, leading to extensive contact between two cells and subsequent cell-cell accumulation. This is known as a "zinc zipper" mechanism (Conrady *et al.* 2008). Furthermore, the crystal structure of the B domains of SasG has been solved and showed that identical repeats can form highly extended structures on the surface of the cell (Gruszka *et al.* 2012).

SasG has been shown to mediate bacterial adherence to desquamated epithelial cells, indicating that it may also play a role of attachment of *S. aureus* to the nasal epithelium (Roche *et al.* 2003; Corrigan *et al.* 2009). The A region of the protein inhibited SasG-mediated bacterial attachment to squames, which indicates that this region is responsible for adherence. However the host ligand for this interaction is unknown. Pls shares significant sequence identity to SasG (Roche *et al.* 2003). Pls has also been shown to promote bacterial adherence to human epithelial cells and the recombinant form of the A region of the protein also inhibited SasG-mediated adhesion to squames. Expression of Pls can also mask other MSCRAMMs and can prevent bacterial adherence to fibrinogen, fibronectin and IgG (Savolainen *et al.* 2001; Juuti *et al.* 2004). Pls seems to be able to promote binding to keratinocyte lipids including ganglioside GM3 and other lipids (Huesca *et al.* 2002) but this could not be confirmed (Roche *et al.* 2003). These results indicate that these proteins may bind a common receptor in the nose as part of the process of nasal colonisation.

1.4.7 The Sdr proteins

The Sdr proteins belong to the structurally-related Sdr-Clf family of cell wall proteins. Three proteins (SdrC, SdrD and SdrE) are encoded from the *sdr* locus which comprises a tandemly arranged *sdr*CDE gene. However not all three genes are present in all strains (Josefsson *et al.* 1998). The *sdr* region is separated into three transcriptional units and expression is likely based on different stress factors such as osmotic shock, changes in temperature or the presence of divalent cations (Sitkiewicz *et al.* 2011). Furthermore, SdrD was highly expressed during bacterial growth in human blood. These different expression profiles may indicate dissimilar functions for each protein.

SdrE plays a role in the virulence of *S. aureus*. It has been shown to be involved in bacteraemia, sepsis and kidney abscess formation. This is most likely because it can capture the complement regulator factor H which catalyzes opsonin C3b degradation. An allelic variant of SdrE has been previously identified as a bone-sialoprotein-binding protein and may play a role in bone infections (Tung *et al.* 2000). However this binding ability has not been confirmed (M. Hook and T.J. Foster, unpublished). SdrD has been shown to be

crucial in abscess formation (Cheng *et al.* 2009) but the mechanism is not known. Immunization with recombinant SdrD and SdrE in combination with IsdA and IsdB provided high level of protection in a murine renal infection model (Stranger-Jones *et al.* 2006).

SdrC and SdrD may be involved in nasal colonisation by facilitating bacterial attachment to nasal epithelial cells. Both proteins promote bacterial adherence to human squames (Corrigan *et al.* 2009). However neither protein could facilitate nasal colonisation in mice (Schaffer *et al.* 2006). The binding partner on the surface of squames for each protein is not known, although SdrC has been previously shown to bind the neuronal cell surface protein β-neurexin 1 and promotes attachment to cell types expressing this ligand (Barbu *et al.* 2010).

1.5 Other Staphylococcal factors involved in nasal colonisation

1.5.1 Catalase and alkyl hydroperoxide reductase

Catalase (KatA) and Alkyl hydroperoxide reductase (AhpC) are encoded by the *katA* and *ahpC* genes, respectively, in *S. aureus*. They play compensatory roles in *S. aureus* resistance to stress caused by reactive oxygen species such as H_2O_2 produced as a by-product of bacterial growth (Cosgrove *et al.* 2007). Reactive oxygen species produced by NADPH oxidase inside host neutrophils during infection also have a role in the host defence system. H_2O_2 has the ability to oxidise cysteine and methionine residues which may lead to protein inactivation. Toxicity due to H_2O_2 is mainly due to the reduction of H_2O_2 by Fe(II) leading to the formation of hydroxyl radicals. Sensitivity to H_2O_2 increases the presence of excess iron due to the Fenton reaction, which can lead to DNA damage due to the association of Fe(II) with nucleic acids. KatA is a part of the peroxide response regulator (PerR) regulon and is indirectly regulated by Fur in a Fe(II)-dependent manner. High levels of Fe(II) cause an increase in KatA expression which reduces the level of H_2O_2 and prevents the formation of toxic hydroxyl radicals.

AhpC is a member of the peroxiredoxin family of enzymes, which have activity against H_2O_2, organic peroxides, and peroxynitrite. It is also regulated by PerR, a homologue of Fur. Repression of this regulator is relieved in the

presence of Fe(II) and/or peroxides. Both KatA and AhpC prevent DNA damage in *S. aureus* by scavenging H_2O_2 and have been shown to play roles in resistance against organic hydroperoxide. KatA has been shown to have a role in glucose-starvation survival and roles have also been proposed for both enzymes in desiccation survival. *S. aureus* mutants deficient in each enzyme had an attenuated ability to colonise cotton rat nares compared to a wild-type strain (Cosgrove *et al.* 2007). Although the role of each enzyme in virulence has not been proven, KatA and AhpC may be required for survival and persistence in the nares. As well as protecting against reactive oxygen species produced by the host defence system, KatA and AhpC may play a role in resistance to transient desiccation that may be a factor in the harsh nasal environment.

1.5.2 SceD

Autolysins in *S. aureus* hydrolyse specific bonds in bacterial cell wall peptidoglycan and assist in the expansion and turnover of the cell wall, growth and cell separation. The staphylococcal autolysin SceD is a putative peptidoglycan hydrolase (Stapleton *et al.* 2007). The recombinant form of SceD displayed cell wall hydrolytic activity and had the ability to cleave peptidoglycan. Furthermore, *sceD* was prominently expressed by *S. aureus* strains carried in the nares of humans and was shown to be expressed in both the early and later stages of *S. aureus* nasal colonisation in the cotton rat (Burian *et al.* 2010; Burian *et al.* 2010). *sceD* is a target gene for the essential 2-component regulatory system WalKR, the master regulator of adaptive gene expression in the nose during the onset of nasal colonisation.

Expression of SceD was greatly increased in the presence of salt and an increase in salt sensitivity was observed when *sceD* was inactivated (Stapleton *et al.* 2007). Furthermore, SceD was shown to be required for nasal colonisation in the cotton rat. The significantly reduced ability of a SceD-deficient strain of *S. aureus* to colonise cotton rat nares was the first example of a role for a staphylococcal autolysin in nasal colonisation. It has been speculated that lytic transglycosylase activity may be necessary to make the small changes to the structure of peptidoglycan needed for survival in various environmental conditions in the host, such as those in the nares. Moreover, SceD may play a

role in the establishment and maintenance of *S. aureus* in a high salt environment such as the nasal cavity, due to its role in salt tolerance. Therefore whereas other staphylococcal determinants for nasal colonisation are primarily involved in host-ligand interactions, a role for SceD may be necessary for bacterial adaptation and establishment in different niches in the host.

1.6 The cornified envelope of human skin cells

1.6.1 Formation of desquamated epithelial cells

Nasal desquamated epithelial cells (squames) are dead keratinized cells that slough off the outermost layer of the squamous epithelium. They have fully undergone a process of keratinisation that begins in the basal layers of the epithelial membrane. The outermost layer of these cells comprises a cornified envelope (CE) which replaces the cytoplasmic membrane during the cornification process. The CE is composed of a layer of crosslinked proteins coated with covalently bound lipids. The proteins include keratins such as surface-exposed cytokeratin 10 (K10), loricrin, involucrin and other structural proteins such as filaggrin and small proline-rich proteins all highly crosslinked to form a waterproof layer (Jarnik *et al.* 1998; Nemes Z 1999; Candi *et al.* 2005).

Keratinocytes in the basal layer of the skin (Figure 1.7 (A)) continuously undergo differentiation to replace squamous cells of the stratum corneum which are lost during desquamation. When epidermal differentiation is initiated, the keratin 5 and 14 network present in the proliferating basal keratinocytes begins to change as keratins 1 and 10, as well as other structural proteins, fatty acids and ceramides are synthesized in the spinous layers (Figure 1.7 (B)). The cell loses all mitotic activity. In the granular layer (Figure 1.7 (C)), keratins 1 and 10 begin to aggregate into tight bundles, aided by interfilamentous proteins such as filaggrin, promoting the collapse of the cell into the characteristic flattened shape of a corneocyte in the cornified layer (Figure 1.7 (D)). The cell begins to form a lipid envelope as lipids crosslink covalently to the scaffold created by keratin and structural proteins, including involucrin (Nemes Z 1999; Candi *et al.* 2005). Loricrin, a 26kDa protein, is expressed and stored in keratohyalin

granules, and is released to the granular layer. Loricrin monomers become heavily crosslinked to each other and to small proline-rich proteins (SPRs) by isopeptide bonds through the action of transglutaminase-3. These are then crosslinked to the lipid-protein scaffold by transglutaminase-1 and become the main protein re-enforcement on the cytoplasmic face of the cell. Further crosslinking of structural proteins occurs during desquamation (Candi *et al.* 2005).

The extracellular surface of the cornified envelope contains a lipid layer consisting of ω-OH-ceramide, cholesterol and long fatty acid chains. The outermost part of the CE is thought to be rich in exposed glutamate which provides a carboxyl surface for ceramide attachment. The structural protein involucrin is particularly rich in Glu and ceramide hydroxyl groups are bound by ester linkages to the carboxyl group in this residue. Furthermore, it has been speculated that free fatty acids present in the CE attach covalently to structural proteins such as loricrin via Ser residues present in the protein (Lopez *et al.* 2007). Corneocytes are tightly attached to each other by corneodesmosomes which are modified desmosomal structures. These are proteolytically degraded in the uppermost layers of the cornified layer to allow desquamation.

1.7 Host proteins involved in nasal colonisation

1.7.1 Keratin

Keratin intermediate filaments are obligate heteropolymers that constitute the major differentiation products of the epidermis (Steinert and Roop 1988; Steinert and Liem 1990). Most epithelial cell types express a particular pair of Type I and Type II keratins such as K5/K14 in basal epithelial cells and K1/K10 in corneocytes (Eichner *et al.* 1986). All keratin intermediate filament proteins share common structural features including a central α-helical rod domain of conserved secondary structure and flanking amino- and carboxy-terminal end domains (Figure 1.8). Classification of keratins into types I (acidic) and types II (basic/neutral) is based on particular sequence properties in these domains and the structure of the genes that encode them (Steinert and Roop 1988). The central rod domain is made up of four α-helical segments (1A,

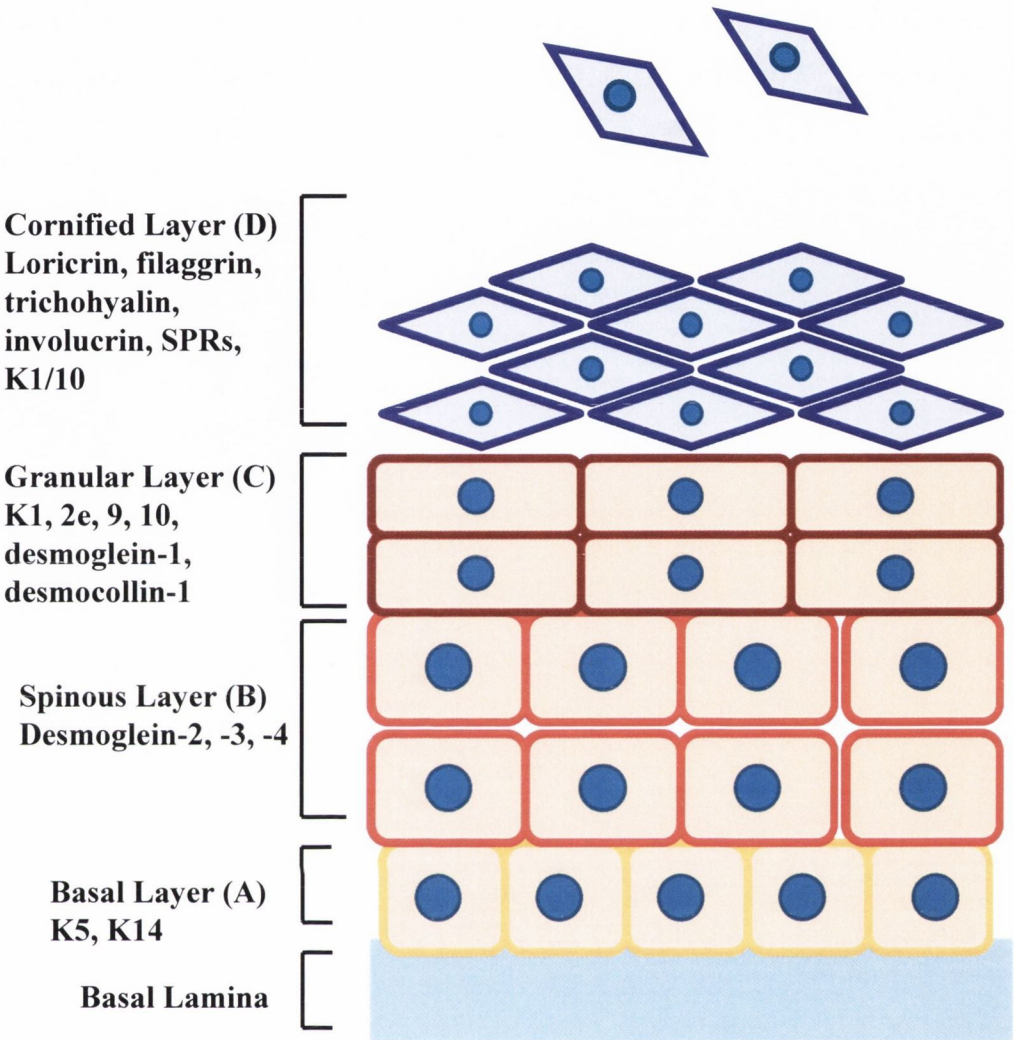

Figure 1.7. Cell differentiation in the epidermis. Cell differentiation begins as cells migrate from the basal layer (A) to suprabasal layers (B), (C). Proteins present in the cell membrane/wall in each layer are listed. Cells in the cornified layer (D) are terminally differentiated and are sloughed off the surface of the epithelium. Adapted from Candi et al, 2005. K – keratin, SPR – small proline-rich protein.

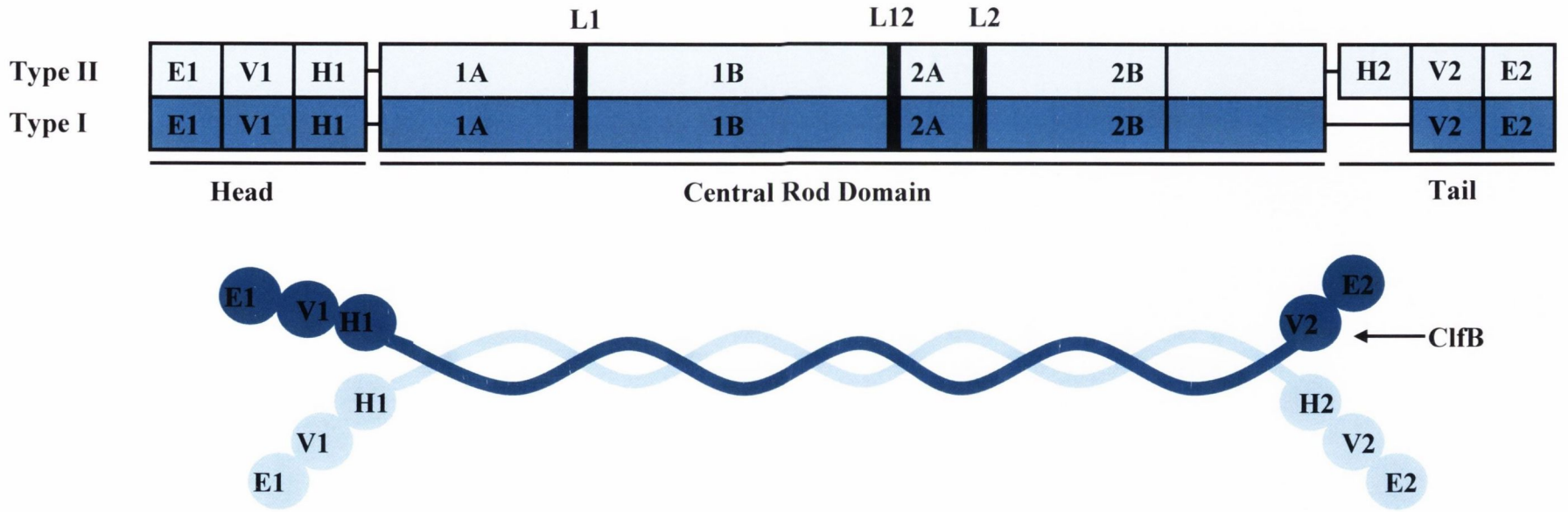

Figure 1.8. Structure of Keratin 1/Keratin 10.

The keratin 1/10 heteroprotein is composed of a type I keratin (K10) and a type II keratin (K1). The central rod domain is divided into four regions (highlighted) and contains three linker regions (L1, L12, L2). The keratin 10 tail region differs from the keratin 1 tail region as it does not contain an H2 domain. The central rod regions interact to form a coiled-coil structure. The ClfB binding region in the K10 tail is indicated. Adapted from Steinert, 1993.

1B, 2A, 2B) that possess a repeating heptad amino acid motif that has potential to form a two-chain coiled-coil. The central rod domain may specify the way in which type I and type II keratin chains associate to form keratin intermediate filaments (Steinert 1993).

The non α-helical end domains are known as head and tail regions and can each be further separated into subdomains. The N-terminal tail regions in epidermal keratins such as K1 and K10 consist of a glycine-serine-rich V2 domain and a conserved E2 domain. Quasi peptide repeats (T-(G/S)*n*) in the V2 regions can adopt an omega-loop structure sometimes referred to as a "glycine loop" (Zhou *et al.* 1988; Steinert *et al.* 1991). These loop regions are made up of a series of hypervariable repeats where hydrophobic residues in the sequence associate and force the glycine stretches into loop structures, resulting in a compact, highly flexible, rosette-like conformation. Polymorphisms with regard to amino acid sequence are highly common in the V2 region (Korge *et al.* 1992; Korge *et al.* 1992). The head and tail regions of keratins determine functional specificity and the V2 domains of the tail of K1 and K10 have a role in supramolecular keratin IF organization and epithelial barrier formation (Sprecher *et al.* 2001; Whittock *et al.* 2002).

K10 is expressed and synthesized in the spinous layers of differentiating epithelial cells and is paired with K1 to form intermediate filaments. It acts as a scaffold for other structural proteins in the process of skin cell cornification and is essential for the cornified cell, eventually making up approximately 10% of the mass of the CE (Jarnik *et al.* 1998). K10 was shown to be surface-expressed and was identified as a potential ligand for ClfB on the surface of squames (O'Brien *et al.* 2002). The ClfB-binding region of K10 was localised to the tail region of the protein, specifically a glycine-serine-rich sequence known as the "YY" loop (YGGGSSGGGSSSGGGY) (Walsh *et al.* 2004). However the cDNA cloned in the study underwent a deletion that eliminated other loops, so ClfB may also bind other loops in the tail region. The crystal structure of ClfB in complex with a peptide corresponding to the YY loop was solved and confirmed the interaction between this peptide sequence and the N2N3 binding-domain of ClfB (Ganesh *et al.* 2011; Xiang *et al.* 2012).

1.7.2 Loricrin

Loricrin is a major component of the cornified cell envelope. It is expressed in the granular layer during skin cell cornification (Mehrel *et al.* 1990) as a late-differentiation product where it is initially localised in discrete keratohyalin granules intermixed with profilaggrin. Loricrin becomes integrated into the CE through many cross-linking interactions by disulfide and N-(γ-glutamyl)lysine isodipeptide bonds which cause loricrin to become highly insoluble (Hohl 1991).

Although loricrin was originally thought to be present only on the cytoplasmic side of the CE, studies have provided evidence for the presence of loricrin on the extracellular and cytoplasmic faces of the cornified cell (Lopez *et al.* 2007). Extensive cross-linking occurs between loricrin monomers before incorporation into the CE. The protein may also be crosslinked to a protein-scaffold created by the other structural components of the CE such as involucrin and cystatin A that are synthesized earlier in the cornification process (Robinson *et al.* 1997). Loricrin-keratin crosslinking and loricrin-filaggrin crosslinking has also been observed. Small proline rich proteins are also crosslinked to loricrin and may act as cross-bridging proteins between loricrin molecules (Candi *et al.* 1999). Crosslinking events such as these have been speculated to be the final step in envelope formation. Epidermal transglutaminases (TG) have been implicated in the loricrin crosslinking process by inter-chain and intra-chain crosslinking using available Glu and Lys residues. TG3 may function to oligomerize and compress loricrin and has also been implicated in loricrin-SPRP crosslinking. Both TG3 and TG1 may play a role in crosslinking loricrin to the protein scaffold following oligmerization (Candi *et al.* 1995). However, multiple TGs may be required for crosslinking *in vivo*. Loricrin is further crosslinked during desquamation, and a minimal concentration of monomeric loricrin is maintained in the keratinized cell (Hohl 1991). Loricrin eventually comprises up to 70% of the cornified envelope.

The loricrin protein consists of 3-4 unstructured domains which are rich in glycine and serine (Hohl 1991). These regions form omega loops similar to those in the tail region of CK10 (Figure 1.9 A). Between these loops and also at

the C- and N-termini of the protein are regions that contain Glu- and Lys-rich TG-recognition sites employed during cornification. The protein also has a high cysteine content which suggests a high amount of disulfide bond formation in the native structure. The combination of transglutamination and disulfide bond formation results in a globular 3-D rosette structure, whereby the internal and terminal regions of the protein are heavily crosslinked and the loops are exposed (Hohl 1991; Candi *et al.* 2005).

The loricrin gene is a part of the epidermal differentiation complex, a cluster of genes at human chromosome 1q21 that encodes late-envelope proteins involved in the various stages of skin cell cornification (Marshall *et al.* 2001). Analysis of the *lor* gene uncovered the presence of multiple natural polymorphisms. One such polymorphism causes a 4-amino acid deletion in the second major unstructured loop domain. As a result of this, different size and sequence variants of the loricrin molecule can exist (Yoneda *et al.* 1992). Single nucleotide polymorphisms within the other loop regions of loricrin have also been reported (Giardina *et al.* 2004).

1.7.2.1 The loricrin back-up system

Although loricrin encompasses the majority of protein mass in the CE, it is not essential and a viable loricrin knockout ($Lor^{-/-}$) mouse has been generated. The loricrin knockout mutation is the result of a homologous recombination event in which the loricrin gene is replaced with a neomycin-resistance cassette (Koch *et al.* 2000). Successful embryonic stem cell clones that had undergone homologous recombination were introduced into C57Bl/6J blastocysts and successful $Lor^{-/-}$ animals were produced. The loricrin mutation was then backcrossed into the FVB mouse inbred strain. As a pup, the skin of the $Lor^{-/-}$ mouse is more permeable than that of wildtype mice of the same genetic background. Pups are runted and have shiny, translucent skin. However, this phenotype disappears as the mice reach maturity and eventually the knock-out mutant and wildtype mouse become indistinguishable.

Immunogold labelling of cornified epidermal tissue indicated a 3-fold increase in the expression of small proline-rich proteins in $Lor^{-/-}$ mice compared

to wild-type mice, possibly as a compensatory mechanism for the lack of loricrin. Analysis of the amino acid composition and cell density of cornified cell tissue from $Lor^{-/-}$ mice indicated that similar amounts of protein are produced in the $Lor^{-/-}$ and wildtype mouse, but the compensatory protein is less glycine serine-rich than loricrin. The structural protein repetin has been implicated as a possible substitute in this backup system, as increased expression was seen in $Lor^{-/-}$ embryos (Jarnik *et al.* 2002). Repetin is rich in glycine and serine, but to a lesser degree than loricrin (Huber *et al.* 2005).

1.7.2.2 Diseases associated with loricrin defects.

Skin diseases associated with mutations in the *lor* gene include Vohwinkels syndrome (keratoderma hereditarium mutilans) and progressive symmetric erythrokeratodermia (PSEK). Vohwinkels syndrome is an inherited autosomal-dominant disease resulting from frameshift mutation caused by a single nucleotide deletion in the *lor* gene. A mutant protein with an extended terminal region is expressed and many important Lys and Glu crosslinking sites are lost. Characteristics of the disease include thickening of the skin caused by an increase thickness of the CE (hyperkeratosis) at the palms and soles and constricting bands that encircle fingers and toes, which may lead to auto-amputation (Maestrini *et al.* 1996).

PSEK is also caused by a frameshift mutation in the *lor* gene generated by a single nucleotide insertion mutation (Ishida-Yamamoto *et al.* 1997). Patients suffer from widespread erythematous plaques and abnormal thickening of the skin on the palms and soles.

1.7.3 Other corneocyte proteins involved in bacterial interactions.

The CE constituents filaggrin and involucrin have been associated with staphylococcal skin disease and nasal colonisation, respectively. Filaggrin is an interfilamentous protein that is produced when its phosphorylated precursor,

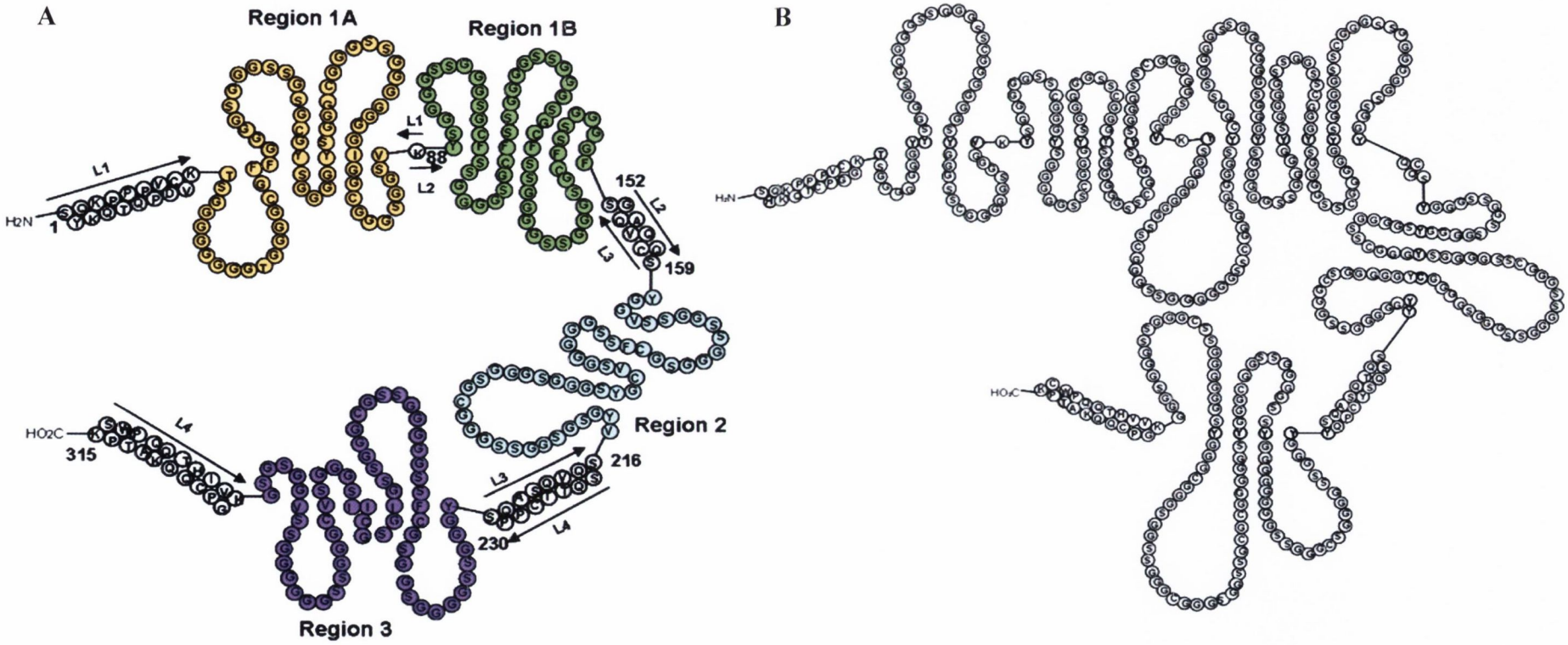

Figure 1.9. Structure of Loricrin. Models of human (A) and murine (B) loricrin depicting N- and C- terminal as well as internal transglutaminase regions and glycine-serine-rich loop regions. Loop regions 1A, 1B, 2, and 3 in human loricrin are highlighted in orange, green, blue and purple, respectively and are described in detail in Chapters 3 and 4. Markers are included to indicate the beginning and end of each synthesized region (L1 - L4). Adapted from Hohl et al, 1991.

profilaggrin, is release into the cornified cell from keratohyalin granules and is dephosphorylated and proteolytically cleaved. Up to 12 individual filaggrin molecules are released which are then crosslinked to the CE. Filaggrin causes keratin intermediate filaments to aggregate into tight bundles and contributes to the structure and flattened shaped of the cornified cell (Candi *et al.* 2005). It is degraded in the cell into hygroscopic amino acids including urocanic acid (UCA) and pyrrolidone carboxylic acid (PCA). These contribute to the natural moisturizing factor of the skin and have been proposed to play a role in skin pH regulation (O'Regan *et al.* 2008).

Loss-of-function mutations in the filaggrin gene results in decreased levels of UCA and PCA on the skin (Kezic *et al.* 2008). These mutations lead to an impaired barrier function and are a major risk factor for the skin disease AD (Palmer *et al.* 2006; O'Regan and Irvine 2008). Recent studies demonstrated that *S. aureus* grown in the presence of UCA and PCA resulted in a reduced growth rate due to acidification of the medium. Furthermore, at the lower pH, reduced expression of secreted and cell wall–associated proteins involved in nasal colonisation and immune evasion, including ClfB, FnBPA and SpA was observed (Miajlovic *et al.* 2010). These studies suggest that AD patients with loss-of-function filaggrin mutations may have an increased susceptibility to *S. aureus* skin colonisation due to changes in pH on the surface of the skin.

Involucrin is an early component in the assembly of the cornified envelope and undergoes extensive crosslinking with other CE structural proteins. It is expressed on the outermost surface of the CE and may interact with lipids and ceramides on the surface of the cornified layer through covalent attachments. Previous studies have indicated that involucrin may function as a host ligand on the surface of squames by interacting with IsdA (Clarke *et al.* 2009). Involucrin was shown to be bound by IsdA *in vitro* and may represent a ligand for this adhesin in the nares.

1.8 Innate immune evasion in the nasal cavity

The mucosal immune system consists of a protective physical barrier and innate immune factors. In order to persist in the nasal cavity, *S. aureus* has

developed methods of resistance to innate immune defences. The fluid that coats the nasal cavity contains several antimicrobial proteins and peptides such as lysozyme, lactoferrin, Secretory Leukocyte Protease Inhibitor (SLPI), beta-defensins and cathelicidins (Cole *et al.* 2002). Furthermore, free fatty acids, glycerolipids, sphingolipids and sterols have been detected in human nasal fluid and many have antimicrobial activity (Do *et al.* 2008). Lysozyme hydrolyses the glycosidic linkages in peptidoglycan. Lactoferrin can sequester free iron and the C-terminus of the protein exhibits antimicrobial activity. *S. aureus* can express factors to counteract the effects of these proteins. A membrane-bound O-acetyltransferase modifies muramic acid and confers lysozyme resistance to peptidoglycan (Bera *et al.* 2005). The surface protein IsdA binds lactoferrin and neutralizes its anti-bacterial activity on the skin and may also bind lactoferrin in nasal secretions (Clarke and Foster 2008).

Antimicrobial peptides and fatty acids also play a role in immune defence on the skin and in the nasal cavity. Sebum fatty acids bind the bacterial cell surface by hydrophobic interactions. Expression of IsdA makes the *S. aureus* cell surface hydrophilic and confers resistance to lipids and cationic antimicrobial peptides. This activity was localised to the C terminal domain of IsdA (Clarke *et al.* 2007). IsdA was required for survival of *S. aureus* on the skin of healthy human volunteers and may also play a similar role in the nasal cavity. *S. aureus* is also protected from antimicrobial peptides on the surface of skin by modifications to teichoic acids and phosphatidyl glycerol. D-alanine and L-lysine modifications on WTA reduce the negative charge at the cell surface and promote resistance to defensins (Peschel *et al.* 1999; Collins *et al.* 2002). WTA also confers protection against sebum fatty acids and lysozyme (Peschel *et al.* 2001; Collins *et al.* 2002; Weidenmaier *et al.* 2005; Weidenmaier *et al.* 2005).

Antimicrobial peptides such as human beta-defensin-1 (HBD-1) are constitutively expressed in the airway fluid, while the expression of HBD-2 and -3 are induced upon pathogenic recognition. HBD-3 is most effective against *S. aureus* (Schutte and McCray 2002). The secreted protein staphylokinase is transcribed during nasal colonisation and can bind α-defensin, thereby inhibiting

bactericidal activity. Multiple antimicrobial factors in nasal fluid may act synergistically in the nasal cavity. Beta-defensins, human cathelicidin (LL-37), and lysozyme displayed synergistic anti-staphylococcal activity in cystic fibrosis patients when administered intranasally (Chen *et al.* 2005). Alterations in expression of one or more innate immune factors may predispose an individual to persistent colonisation. This is in agreement with studies proposing that reduction in the expression of anti-microbial peptides in nasal secretions such as human β-defensin-3 affect colonisation status (Zanger *et al.* 2011). Furthermore, it was reported that intrinsic antimicrobial activity for *S. aureus* was impaired in healthy nasal carriers (Cole *et al.* 2001).

1.9 Treatment for the eradication of *S. aureus* from the nose

Carriage of *S. aureus* in the nares has been proven to be a risk factor for *S. aureus* disease, particularly in a hospital setting. Therefore, decolonisation strategies can help to reduce the risk of nosocomial *S. aureus* infections in patients who are carriers. The use of topical creams containing antibiotics such as mupirocin have been successful in temporarily eliminating *S. aureus* from the nares of individuals at risk for *S. aureus* infection (Peacock *et al.* 2001; von Eiff C 2001). Mupirocin belongs to the monoxycarbolic class of antibiotics and is produced by *Pseudomonas fluorescens*. It inhibits isoleucyl-tRNA synthetase activity which decreases or abolishes bacterial protein synthesis by preventing the incorporation of isoleucine into nascent peptides (Hughes and Mellows 1980; Wuite *et al.* 1985).

Mupirocin treatment has been successful in the prevention of nosocomial infections in patients undergoing dialysis or surgery (Yu *et al.* 1986; Boelaert *et al.* 1993; Kluytmans *et al.* 1996). Eradication has proven to be temporary as re-colonisation from extra-nasal carriage sites has been observed (Wertheim *et al.* 2004). Furthermore, both low level and high level staphylococcal resistance to mupirocin is emerging (Cookson *et al.* 1990; Chatfield *et al.* 1994; Dawson *et al.* 1994; Patel *et al.* 2009). High level resistance is caused by the acquisition of a plasmid-encoded second isoleucyl-tRNA synthetase (Gilbart *et al.* 1993).

Lysostaphin is a glycylglycine endopeptidase which specifically cleaves the pentaglycine crossbridges found in staphylococcal peptidoglycan. Decolonisation treatments in animals involving the use of lysostaphin cream have indicated that lysostaphin may be a novel alternative to mupirocin treatment. Lysostaphin cream administered to intranasally-colonised cotton rats completely eradicated *S. aureus* nasal carriage (Kokai-Kun *et al.* 2003). Furthermore, a single dose of lysostaphin cream was more effective at clearing *S. aureus* from the cotton rat nose than mupirocin. Lysostaphin has also been shown to disrupt *S. aureus* and *S. epidermidis* biofilm formation on artificial surfaces (Wu *et al.* 2003) and inhibited growth of *S. aureus* nasal isolates *in vitro* (von Eiff *et al.* 2003). However, resistance to lysostaphin has been reported *in vitro* and *in vivo* (Dehart *et al.* 1995; Stranden *et al.* 1997; Thumm and Gotz 1997; Climo *et al.* 1998).

1.10 Vaccines

1.10.1 Candidates for vaccination against *S. aureus* infection

S. aureus has developed resistance to every antibiotic introduced into clinical practice (Chambers and Deleo 2009). Effective vaccination strategies are under development as effective treatment of *S. aureus* infections may soon be limited.

StaphVax® was the first developed vaccine candidate against *S. aureus* infection and was produced by NABI Pharmaceuticals. This vaccine contained capsular polysaccharide types 5 and 8 conjugated to the protein carrier *Pseudomonas* exotoxoid A. Results from an initial clinical trial carried out on dialysis patients showed that the vaccine provided some protection against infection approximately 40 weeks after immunization. However subsequent trials were not successful (Shinefield *et al.* 2002).

A vaccine candidate using the surface protein IsdB was developed by Merck after patients recovering from *S. aureus* infection displayed a high antibody response to the protein. After proving immunogenic in mice and rhesus monkeys, the vaccine was due to undergo Phase II/III clinical trials in adults scheduled for elective cardiac surgery (Kuklin *et al.* 2006). However this

was halted in April 2011 when preliminary data was inspected. Little or no protection was evident and in some cases an increase in mortality was observed. This is possibly due to the use of haem-bound IsdB purified from *E. coli*. Another Isd-based vaccine consisting of IsdA, IsdB, SdrD and SdrE is currently under preclinical evaluation (Kim *et al.* 2010).

ClfA has been developed as a vaccine candidate in two separate studies by Inhibitex. The vaccine Veronate® consisted of an anti-ClfA and anti-SdrG immunoglobulin preparation (Vernachio *et al.* 2003). This vaccine was aimed at neonates due to their increased risk of *S. aureus* invasive infection. Elevated antibody levels against both proteins were observed. However it was unsuccessful in Phase III trials due to insufficient protection (Kaufman 2006). The monoclonal anti-ClfA antibody Aurexis® (tefibazumab) was raised against the A domain of the protein. It was protective against an intravenous challenge in a rabbit model of infective endocarditis and demonstrated some efficacy against relapse and complications in adult bacteraemia patients (Bubeck Wardenburg and Schneewind 2008). Currently, a 4-component vaccine consisting of conjugated CP-5 and CP-8, ClfA and Manganese transporter C is in phase I/II trials in America. Initial studies on the ClfA component of this vaccine revealed that immune sera from vaccinated volunteers could displace *S. aureus* adherence to fibrinogen, suggesting that the ligand-binding activity of ClfA can be neutralised by vaccination (Hawkins *et al.* 2012).

LTA has been investigated as a possible candidate for vaccine development. A monoclonal antibody was developed (pagibaximab) but showed no significant decrease in staphylococcal sepsis. A passive monoclonal anti-LTA antibody by Biosynexus is currently under development (Daum and Spellberg 2012). Other vaccine candidates incorporating factors such as Panton-Valentine leukotoxin and α-haemolysin are undergoing preclinical evaluation (Goodyear and Silverman 2005; Stranger-Jones *et al.* 2006). Moreover, a bivalent conjugate vaccine composed of ClfA and deacetylated poly-N-β-(1-6)-acetyl glucosamine (dPNAG) was highly immunogenic in mice, rabbits, goats and rhesus monkeys. The vaccine elicited functional anti-adhesive antibodies

and opsonic/protective antibodies against ClfA and dPNAG, respectively (Maira-Litran *et al.* 2012).

1.10.2 Candidates for vaccination against *S. aureus* nasal colonisation

Vaccinations that reduce *S. aureus* nasal colonisation may provide a means of reduction or control of *S. aureus* infection. Animal nasal colonisation models have provided evidence of the protective effect of vaccination against nasal carriage. Mucosal immunization with exponentially-grown killed *S. aureus* resulted in significantly fewer *S. aureus* CFU present in mouse nares after challenge with a heterologous *S. aureus* strain (Schaffer *et al.* 2006). Moreover, systemic and intranasal immunization with recombinant ClfB significantly reduced levels of *S. aureus* colonisation in mice after a subsequent challenge. In addition, cotton rats that had undergone systemic immunization with recombinant IsdA had significantly lower rates of colonisation compared to control animals. In the same study, both IsdA and IsdH-specific antibodies were implicated in protection against nasal colonisation in humans, as non-carriers displayed significantly higher antibody titres against each protein compared to carriers (Clarke *et al.* 2006).

An initial preclinical trial using a capsular polysaccharide conjugate vaccine was attempted in humans to assess the effects of vaccination against nasal carriage. No statistically significant reduction in colonisation compared to pre-colonisation rates was observed, despite an increase in humoral antibody concentrations against type 5 capsule and type 8 capsule (Creech *et al.* 2009). Moreover, it has been reported that natural antibody responses detected in infants against staphylococcal surface proteins do not protect against subsequent carriage a year later (Prevaes *et al.* 2012).

1.11 Rationale for this study

S. aureus nasal colonisation is a known risk factor for subsequent infection. Nasal carriage can be transiently eradicated by topical administration of the antibiotic mupirocin but this is compromised by the development of resistance. Alternative strategies for reducing nasal carriage are required which

will involve a detailed understanding of the molecular basis of interactions between the host and the bacterium that underlie the process.

ClfB is a major determinant of nasal colonisation and has been extensively proven to play an essential role in bacterial attachment to squames and in colonisation of the nares. Cytokeratin 10 has been implicated as a potential ligand for ClfB on the surface of human squames. The ClfB-binding site in K10 has been localised to the glycine-serine-rich tail region of the protein, specifically to a sequence capable of forming omega loop structures. Unpublished evidence (E. Walsh and T.J. Foster) has suggested that ClfB may also interact with the structural protein loricrin. Given that loricrin is almost completely comprised of the same type of glycine-serine-rich sequences present in the tail region of K10 and is present in much higher abundance in the cornified envelope of squames, it may represent another potential target for ClfB on the surface of the CE.

IsdA mediates *S. aureus* adherence to squames and has been proven to play a crucial role in *S. aureus* nasal colonisation *in vivo*. Furthermore, *in vitro* studies indicate that it may interact with cornified envelope proteins including loricrin. Therefore loricrin may also serve as a ligand for IsdA in the nares, explaining why it may act as a major determinant of nasal colonisation by *S. aureus*.

1.12 Aims and objectives

The initial aims of this study were to examine the interaction between ClfB and loricrin and to compare this interaction to ClfB-fibrinogen and ClfB-K10 binding in order to indicate whether loricrin is bound by the same mechanism and with the same affinity as fibrinogen and K10. Another objective was to localise any ClfB-binding sites within loricrin and to determine the highest affinity ClfB-binding site present within the protein. The interaction between loricrin and ClfB was analysed further by investigating the ability of loricrin to facilitate ClfB-mediated attachment to human desquamated epithelial cells, in order to establish whether loricrin can act as a viable ligand for *S. aureus* on the surface of squames. Finally, transgenic loricrin-deficient mice

were used in a model of *S. aureus* nasal colonisation in order to study the interaction between ClfB and loricrin *in vivo*.

IsdA has also been implicated as a binding partner for loricrin. Therefore another aim was to assess the nature of the interaction between IsdA and loricrin, in order to confirm that loricrin can act as a ligand for IsdA during nasal colonisation. IsdA-mediated attachment to human desquamated epithelial cells was also studied in order to determine whether loricrin can inhibit IsdA-promoted bacterial adhesion to squames. Finally, a study of IsdA-loricrin interactions *in vivo* in a model of nasal colonisation was performed in order to investigate whether loricrin plays a role in IsdA-mediated nasal colonisation *in vivo*.

Chapter 2
Materials and Methods

2.1 Bacterial Strains and Growth Conditions

The bacterial strains used in this study are listed in Table 2.1. *E. coli* strains were used as hosts for cloning. They were grown with shaking (200 rpm) in Luria (L) broth or on L-agar at 37 °C. *S. aureus* strains were grown to exponential or stationary phase with shaking (200 rpm) in tryptic soy (TS) broth or on TS agar at 37 °C. *L. lactis* strains MG1363 (Gasson 1983) and NZ9800 were grown statically in brain heart infusion (BHI) broth or agar at 28°C. Antibiotics were added as follows: streptomycin (Sm) at 500 μg/ml, ampicillin (Amp) at 100 μg/ml, chloramphenicol (Cm) at 10 μg/ml, erythromycin (Erm) at 10 μg/ml and anhdrotetracycline (AnTc) at 1 μg/ml

2.1.1 Growth of bacteria in iron-limited conditions

In order to mimic *in vivo* growth conditions, *S. aureus* strains were grown to late exponential or stationary phase in RPMI 1640 medium (Sigma). RPMI medium is an iron deficient medium which was originally designed for the culture of human leukocytes (Moore *et al.* 1967). Starter cultures were grown overnight at 37 °C in 10 ml RPMI and then diluted in 20 ml RPMI to an OD of 0.05. Strains were then grown at 37 °C with shaking (200 rpm). Sterile plastic vessels were used to eliminate the presence of iron that might leak from glass.

2.1.2 Growth and induction of *L. lactis* strains carrying pNZ8037 derivatives

Nisin is an antimicrobial peptide produced by certain *L. lactis* strains. The gene that encodes nisin, *nisA* is found on the conjugative transposon Tn*5276*. Nisin is an autoregulator and through interaction with the two-component regulatory system NisKR can activate transcription of *nisA* (Kuipers *et al.* 1995). *L. lactis* strain NZ9800 is defective in nisin production so expression of genes cloned in-frame with the *nisA* start codon can be induced by addition of extracellular nisin (de Ruyter 1996). The nisin-controlled expression system of *L. lactis* can therefore be utilised to control levels of protein expression and also to study *S. aureus* surface proteins in isolation. *L. lactis* strains carrying pNZ8037 derivatives were grown and induced with nisin as

follows. Starter cultures of *L. lactis* strain NZ9800 (pNZ8037) were diluted $^{1}/_{100}$ into 5 ml of fresh BHI medium containing 10 µg/ml Cm and grown to OD_{600} of 0.5. Nisin (Sigma) was added to exponential phase cultures at final concentrations that ranged between 150 and 1000 ng/ml. Induced cultures were grown at 28 °C for 16 h.

2.2 Plasmids

The plasmids used in this study are listed in Table 2.2.

2.3 DNA Manipulation

DNA manipulations were performed using standard methods (Sambrook 1989). Restriction endonucleases were purchased from New England Biolabs and Roche and were used according to the manufacturers' instructions. DNA ligase was purchased from Roche. Confirmatory DNA sequencing was carried out by MSC Operon or GATC-Biotech.

2.3.1 Preparation of plasmid and genomic DNA

Plasmid DNA was isolated using the Wizard® Plus SV Miniprep kit (Promega) according to the manufacturer's instructions. DNA purification was carried out using the Wizard® SV Gel and PCR Clean-up System (Promega). Genomic DNA was prepared using Bacterial Genomic DNA purification kit (Edge BioSystems). Plasmid and genomic DNA extracts from *S. aureus* required the addition of 200 µg/ml of lysostaphin to digest cell wall peptidoglycan.

2.3.2 Polymerase Chain Reaction

Polymerase Chain Reaction (PCR) amplification was carried out in a DNA thermal cycler (Techne). Reactions were typically carried out in 50 µl volumes using 1 U Phusion™ Hot Start DNA polymerase in Phusion HF buffer (Finnzymes). Plasmid DNA (10 ng) or genomic DNA (20 ng) were used as templates for PCR. Primers and dNTPs (Bioline) were used at final

Table 2.1 Bacterial strains

Strain	Relevant Characteristics	Source/ Reference
E. coli		
XL1-Blue	Host for cloning	Stratagene
DC10B	Universal staphylococcal cloning host. Δ*dcm* derivative of DH10B	Monk *et al*, 2012
Topp10	Expression host for recombinant proteins. Protease deficient strain.	Stratagene
S. aureus		
Newman	NCTC 8178.	Duthie and Lorenz, 1952
Newman Δ*clfB*	Newman derivative deficient in ClfB. Allelic replacement of *clfB* in Newman with pIMAY Δ*clfB*	This study
Newman Δ*isdA*	Newman derivative deficient in IsdA. Allelic replacement of *isdA* in Newman with pIMAY Δ*isdA*	This study
Newman Δ*clfB*Δ*isdA*	Newman derivative deficient in ClfB and IsdA. Allelic replacement of *IsdA* in Newman Δ*clfB* with pIMAY Δ*isdA*	This study
RN4220	Restriction-deficient derivative of 8325-4	Kreiswirth *et al.*, 1983
SH1000	8325-4 with repaired defect in *rsbU*	Horsburgh *et al.*, 2002

Table 2.1 Bacterial strains, continued

Strain	Relavant Characteristics	Source/ Reference
SH1000 Δ*clfB*	SH1000 derivative deficient in ClfB. Allelic replacement of *clfB* in SH1000 with pIMAY Δ*clfB*	This Study
L. lactis		
MG1363	Derivative of NCD 0712, plasmid-free	Gasson, 1983
NZ9800	Derivative of MG1363 containing nisin-sucrose conjugative transposon *Tn5276*, Δ*nisA*	Kuipers *et al.*, 1995

Table 2.2 Plasmids

Plasmid	Relevant Characteristics	Source/ Reference
pCU1*clfB*	pCU1 encoding full length ClfB. Amp^R/Cm^R	E. Walsh
pQE30	*E. coli* expression vector, polyhistidine-tagged. Amp^R	Qiagen
pQE30*clfB* $N2N3_{201-542}$	pQE30 excoding the N2N3 region of ClfB A domain 201-542. Amp^R	This Study
pQE30*clfB* $N23_{201-521}$	pQE30 excoding the N2N3 region of ClfB A domain 201-521. Amp^R	This Study
pQE30*clfB* $N23_{201-526}$	pQE30 excoding the N2N3 region of ClfB A domain 201-526. Amp^R	This Study
pQE30 $A\alpha_{1-625}$	pQE30 encoding Aα-chain of fibrinogen 1-625. Amp^R	E. Walsh
pUC57$Hlor_{1-315}$	*E. coli* expression vector encoding gene expressing human loricrin 1-315. Amp^R	Genscript Corporation
pUC57$Mlor_{1-480}$	pUC57 encoding gene expressing murine loricrin 1-480. Amp^R	Genscript Corporation
pUC57 Hlor $1A_{1-88}$	pUC57 encoding gene expressing human loricrin region 1-88. Amp^R	Genscript Corporation
pUC57 Hlor $1B_{88-159}$	pUC57 encoding gene expressing human loricrin region 88-159. Amp^R	Genscript Corporation
pUC57 Hlor $2_{152-230}$	pUC57 encoding gene expressing human loricrin region 152-230. Amp^R	Genscript Corporation
pUC57 Hlor $3_{216-315}$	pUC57 encoding gene expressing human loricrin region 216-315. Amp^R	Genscript Corporation
pUC57 Hlor $D2_{159-176}$	pUC57 encoding gene expressing human loricrin region 159-176. Amp^R	Genscript Corporation
pUC57 Hlor $D2_{187-209}$	pUC57 encoding gene expressing human loricrin region 187-209. Amp^R	Genscript Corporation
pUC57 $HK10_{544-563}$	pUC57 encoding gene expressing human keratin region 544-563. Amp^R	Genscript Corporation

Table 2.2 Plasmids, continued

Plasmid	Relevant Characteristics	Source/ Reference
pUC57 $MK10_{454-570}$	pUC57 encoding gene expressing murine keratin region 454-570. Amp^R	Genscript Corporation
pET11a*lor*	pET11a encoding human loricrin cDNA clone	Candi *et al* 1995
pGEX-4T2	*E. coli* expression vector, glutathione-S-transferase-tagged. Amp^R	GE Lifesciences
pGEX-4T2 $Hlor_{1-315}$	pGEX-4T2 encoding gene expressing human loricrin 1-315. Amp^R	This Study
pGEX-4T2 $Mlor_{1-480}$	pGEX-4T2 encoding gene expressing murine loricrin 1-480. Amp^R	This Study
pGEX-4T2 Hlor $1A_{1-88}$	pGEX-4T2 encoding gene expressing human loricrin region 1-88. Amp^R	This Study
pGEX-4T2 Hlor $1B_{88-159}$	pGEX-4T2 encoding gene expressing human loricrin region 88-159. Amp^R	This Study
pGEX-4T2 Hlor $2v_{152-226}$	pGEX-4T2 encoding gene expressing human loricrin region 152-226. Cloned from pET11a. Amp^R	This Study
pGEX-4T2 Hlor $3_{216-315}$	pGEX-4T2 encoding gene expressing human loricrin region 216-315. Amp^R	This Study
pGEX-4T2 Hlor $2_{152-230}$	pGEX-4T2 encoding gene expressing human loricrin region 159-176. Amp^R	This Study
pGEX-4T2 Hlor $D2_{187-209}$	pGEX-4T2 encoding gene expressing human loricrin region 187-209. Amp^R	This Study
pGEX-4T2 Hlor $D2v_{187-205}$	pGEX-4T2 encoding gene expressing human loricrin region 187-205. Amp^R	This Study
pGEX-4T2 $HK10_{544-563}$	pGEX-4T2 encoding gene expressing human keratin region 544-563. Amp^R	This Study
pGEX-4T2 $MK10_{454-570}$	pGEX-4T2 encoding gene expressing murine keratin region 454-570. Amp^R	This Study
pGEX-4T2 $\alpha C_{316-367}$	pGEX-4T2 encoding gene expressing fibrinogen αC region 316-367. Amp^R	This Study

Plasmid	Relevant Characteristics	Source/ Reference
pIMAY	pIMC5 with tetracycline; inducible *secY* antisense from pKOR1. Cm^R / Erm^R	Monk *et al.*, 2012
pIMAY Δ*clfB*	pIMAY carrying *clfB* deletion construct consisting of 500bp upstream and downstream regions of *clfB*. Amplified from Newman. Cm^R / Erm^R	This Study
pIMAY Δ*isdA*	pIMAY carrying *isdA* deletion construct consisting of 500bp upstream and downstream regions of *isdA*. Amplified from Newman. Cm^R / Erm^R	This Study
pNZ8037	*L. lactis* expression vector, *nisA* nisin-inducible promoter . Cm^R	De Ruyter *et al.*, 1996
pNZ8037*clfB*	pNZ8037 containing full length *clfB* gene. Cm^R	Miajlovic *et al*,. 2007
pNZ8037*clfB* Q235A	pNZ8037*clfB* with point mutation at Q235A. Cm^R	Miajlovic *et al*,. 2007
pNZ8037*isdA*	pNZ8037 containing full length *isdA* gene. Cm^R	E. Walsh
pKS80	*L. lactis* expression plasmid. Erm^R	Hartford *et al.*, 2001
pKS80*clfB*	pKS80 containing full length *clfB* gene. Erm^R	H. Miajlovic

concentrations of 0.2 mM and 200 μM, respectively. Primers were purchased from Integrated DNA Technologies or Sigma-Aldrich and are listed in Table 2.3. Initial denaturation was carried out at 98 °C (30 s) followed by 30-35 cycles of denaturation (10 s) at 98 °C, 20 s annealing (temperature dependent on primer used) and extension at 72 °C. When amplifying plasmid DNA, a 15 s extension time per 1kb DNA was used. For high complexity genomic DNA a longer extension time was used (30 s per kb). A final extension step was carried out at 72 °C for 5 min. PCR products were purified using Wizard SV gel and PCR clean-up system (Promega).

2.4 Transformation

Chemically competent *E. coli* were prepared using $CaCl_2$ treatment. An overnight culture of *E. coli* was used to inoculate 400 ml fresh L-broth in a 2L flask. This culture was grown until an OD_{600nm} of 4.0-5.0 was reached. Cells were chilled on ice for 1 h and then harvested. Cells were resuspended in $MgCl_2$ (100 mM) and were harvested again. Cells were washed twice in ice cold buffer (60 mM $CaCl_2$, 10 mM PIPES, 15% (v/v) glycerol, pH 8) before being aliquoted. Cells were snap-frozen in liquid nitrogen and were stored at -70°C. Thawed aliquots were incubated with 2 ng of plasmid or 20 ng of DNA ligation reactions for 10 min on ice. Samples were heated to 42 °C for 2 min and then chilled on ice for 2 min. One ml of L-broth was added and the mixture was incubated for 1h at 37°C with shaking before plating onto L-agar containing the appropriate antibiotic. Plates were incubated for 16-24 h. *E. coli* transformants were screened for the presence of recombinant plasmids using a rapid colony screening procedure (Le Gouill and Dery 1991).

2.4.1. Preparation and electroporation of *E. coli* DC10B.

pIMAY was introduced into the *E. coli dcm* mutant strain DC10B by electroporation (Monk 2012). Electrocompetent cells were prepared by inoculating L-broth (1 L in a 5 L baffled flask) with 10 ml overnight culture of *E. coli* DC10B. The culture was incubated at 37 °C with shaking until an OD_{600nm} of 0.7 was reached. The culture was divided into smaller volumes and was chilled on ice for 10 min. Cells were harvested at 7000x*g* for 10 min at 4

°C and were resuspended in 250 ml sterile 10% (v/v) glycerol. This was repeated twice. Cells were then harvested twice more and were resuspended in 50 ml 10% (v/v) glycerol. Cells were harvested again and re-suspended in 3 ml 10% (v/v) glycerol. Aliquots (40 µl) were snap-frozen in liquid nitrogen and were stored at -70 °C.

Cells were thawed for 5 min on ice before adding up to 5 µg plasmid in a volume of 5 µl. Cells were then left on ice for 1 min before being added to pre-chilled 0.1 cm electroporation cuvettes (Biorad). The exterior of the cuvettes were dried and were then pulsed at 1.5 kV/cm, 200 Ω and 25 uF. Cells were immediately resuspended in SOC medium (10 ml SOB with 100 µl of 2M glucose and 100 µl of 1M $MgSO_4$/1M $MgCl_2$) and were incubated for 1 h at 28 °C with shaking. Cells were then plated onto L-agar containing the appropriate antibiotic. Transformants were screened by PCR and restriction mapping.

2.4.2 Preparation and electroporation of *S. aureus*.

Plasmids isolated from *E. coli* DC10B were introduced into *S. aureus* by electroporation. Electrocompetent cells were prepared by diluting an overnight culture of *S. aureus* Newman or *S. aureus* SH1000 to an OD_{578nm} of 0.5 in 50 ml pre-warmed TSB. The culture was reincubated at 37 °C for 30 min, until an OD_{578nm} of 0.8-0.9 was reached. The culture in its vessel was then placed in an ice-water slurry for 10 min. Cells were harvested at 3,900x*g* for 10 minutes at 4°C. The supernatant was discarded and the pellet was resuspended in 50 ml sterile filtered ice-cold water. Cells were harvested again and the pellet was then resuspended in sterile ice-cold 10% (v/v) glycerol (5 ml). The cells were harvested again two more times, first resuspending in 1 ml sterile ice-cold 10% (v/v) glycerol and then 250 µl sterile ice-cold 10% (v/v) glycerol. Aliquots (50 µl) were snap-frozen in liquid nitrogen and stored at -70 °C.

Aliquots were thawed on ice for 5 min and then at room temperature for 5 min. Cells were harvested at 5,000x*g* for 1 min and were re-suspended in sterile 10% (v/v) glycerol / 500 mM sucrose (50 µl). Up to 5 µg of plasmid was added to the cells in a volume of 5 µl. The cells were mixed by gentle flicking and were then added to a 0.1 cm electroporation cuvette (Biorad). The cells

Table 2.3 Primers

Primer	Sequence (5'-3')[a]
ClfB$_{201-542}$ F	GGGGGATCCGCTGAACCGGTAGTAAATG
ClfB$_{201-542}$ R	GGGAAGCTTATTTACTGCTGAATCACCATC
ClfB$_{201-526}$ F	GGGGGTACCTGAAAGCTTATTTAGCTG
ClfB$_{201-526}$ R	GGGGGTACCTAAATTCTCATTATTCCAACC
ClfB$_{201-521}$ F	GGGGGTACCCTTAATTAGCTGAGC
ClfB$_{201-521}$ R	GGGGGTACCTAAGAAAATACTGTAGTC
Δ*clf*B (A)	CCCGTCGACACAGTTTTTAACTATTCAACTCATGAG
Δ*clf*B (B)	CAAAAATATTACTCCATTTCAATTTCTAGA
Δ*clf*B (C)	AATTGAAATGGAGTAATATTTTTGTAAATACTTTTTTAGGCCGAA TAC
Δ*clf*B (D)	CCCGAATTCCCATATCCTCCCATAGAGTGACCT
Δ*clf*B OUT F	ATACGATCAAGATGAATTTTATGAAATCAA
Δ*clf*B OUT R	CCTTGTGTTAATGCAAATTTAATTGTG
Δ*isd*A (A)	CCCGTCGACGTTGGCAGTGTTTTTACTAATAATATTTTC
Δ*isd*A (B)	GTTGTTTTCCTCCTAAGGATACAA
Δ*isd*A (C)	TATCCTTAGGAGGAAAACAACATCATCGTCACACTCATAACT
Δ*isd*A (D)	CCCGAATTCTTCTTTTGTTTCAGAAGTAGGGGCCTC
Δ*isd*A OUT F	TTCAGAAGTGCGTTCATCTTTGGCAGT
Δ*isd*A OUT R	CTTAGGGGCTTTAACTTCTTTAACTTC
L2vF	GGGGGATCCTCCTCGGGCCAGGCGGTCCAG
L2v R	GGGGAATTCTTAGACCTGCTGCGAGGAGAC

[a] Restriction endonuclease cleavage sites are underlined

Table 2.3 Primers, continued

Primer	Sequence (5'-3')[a]
Fg $A\alpha_{316-367}$ F	GGGGGATCCTGGAAACCTGGGAGCTCT
Fg $A\alpha_{316-367}$ R	GGGGAATTCCCAGTGCCCAGCACTTC
*rps*L F	ATGCCAACTATTAACCAATTA
*rps*L R	ATTGTTTTTAGGTTTCTTAGT
rpsL OUT F	AGGAGGACATATCACATG
*rps*L OUT R	TTTAAGATTTAATTAAAAACTAAATTC
pIMAY MCS-F	TACATGTCAAGAATAAACTGCCAAAGC
pIMAY MCS-R	AATACCTGTGACGGAAGATCACTTCG

[a] Restriction endonuclease cleavage sites are underlined

were pulsed at 21 kV/cm, 100 Ω and 25 uF. A time constant of 2.2-2.4 ms was achieved. The cells were immediately resuspended in sterile TSB / 500 mM sucrose (1 ml) and were incubated for 1.5 h at 37 °C with shaking. Cells were then plated out on TSA containing the appropriate antibiotic. Transformants were screened by PCR, restriction mapping and Western immunoblotting.

2.4.3 Screening of transformants

Colonies intended for screening were toothpicked onto the appropriate agar. Half a toothpicked colony was resuspended in 40 µl TE buffer (1 mM EDTA / 10 mM Tris-HCl, pH 7.8, autoclaved) until a milky suspension was achieved. The suspension was then boiled at 100 °C for 10 min and then centrifuged at 6000 rpm for 10 min. Supernatant (2 µl) was used as a template for PCR using Phire polymerase.

2.5. Strain Construction

2.5.1 Isolation of streptomycin resistant mutants of *S. aureus*

Streptomycin resistant mutants of *S. aureus* were isolated by growth in 200 mL TSB overnight at 37 °C with shaking. Concentrated 1 mL amounts were plated onto TSA containing Sm (500 µg/ml) and grown overnight at 37 °C. Colonies were subcultured onto fresh TSA plates containing Sm (500 µg/ml). DNA was isolated from mutants and parental strains and the *rpsL* gene was amplified by PCR using primers *rpsL* OUT F and *rpsL* OUT R (Table 2.3). PCR constructs were sequenced using primers *rpsL* F and *rpsL* R. Each construct was compared to its parental strain in terms of growth rate and to ensure haemolytic activity had not been altered during strain construction.

2.5.2 Allelic replacement mutagenesis of *clfB* and *isdA*

S. aureus Δ*clfB*, *S. aureus* Δ*isdA* and *S. aureus* Δ*clfBisdA* were constructed by allelic exchange using pIMAY (Monk 2012). Primers were designed to amplify 500 bp of DNA located upstream and downstream of *clfB* or *isdA* to delete the entire gene leaving only the start and stop codons (Δ*clfB* cassette A, B, C, D, Δ*isdA* A, B, C, D, Table 2.3). Genomic DNA from *S.*

aureus strains Newman (Duthie and Lorenz 1952) and SH1000 (Horsburgh *et al.* 2002) were used as template and the resulting PCR products were denatured, allowed to reanneal via the complementary sequences in primers B and C and then amplified using primers A and D, resulting in a 1000 bp fragment in each case consisting of linked sequences upstream and downstream of the gene (Δ*clfB* cassette, Δ*isdA* cassette). The amplimer was ligated to pIMAY between EcoRI and SalI restriction sites (Figure 2.1).

The plasmid was transformed into *E. coli* DC10B and then transformed into electrocompetent streptomycin resistant *S. aureus*. Cells were plated on TSA containing chloramphenicol (10 μg/ml) and incubated at the permissive temperature of 28 °C for 48 h. Putative positive colonies were streaked out and grown overnight at 28 °C on TSA containing Cm (10 μg/ml). Clones were screened with primers designed to amplify the multiple cloning site (MCS) of pIMAY to confirm the presence of replicating plasmid. In order to promote plasmid integration, a single colony was vortexed in 200 μl of TSB and then diluted to 10^{-3}. Dilutions were plated on TSA containing Cm (10 μg/ml) and incubated overnight at 37 °C. Well isolated large colonies were picked and subcultured on TSA containing Cm (10 μg/ml) at 37 °C overnight. Plasmid integration was confirmed by colony PCR using the MCS primers. Positive integrants were screened with a second set of primer pairs (OUT F/D, OUT R/A, Table 2.3) to ascertain the side of integration.

To encourage plasmid excision, one colony was inoculated into 10 ml TSB and grown overnight at 28 °C with shaking (200 rpm). The broth was diluted to 10^{-6} and 50 μl aliquots of the dilutions of 10^{-5} and 10^{-6} were plated onto TSA containing 1 μg/ml AnTc. Plates were incubated at 28 °C for 48 h. Large colonies were streaked onto TSA containing 1 μg/ml AnTc and TSA Cm (10 μg/ml) and incubated at 37 °C overnight. Cm sensitive colonies were screened by colony PCR with the OUT primers, with the PCR extension time allowing for the amplification of the wild type product. Genomic DNA was isolated from putative mutants and the OUT PCR repeated with Phire polymerase.

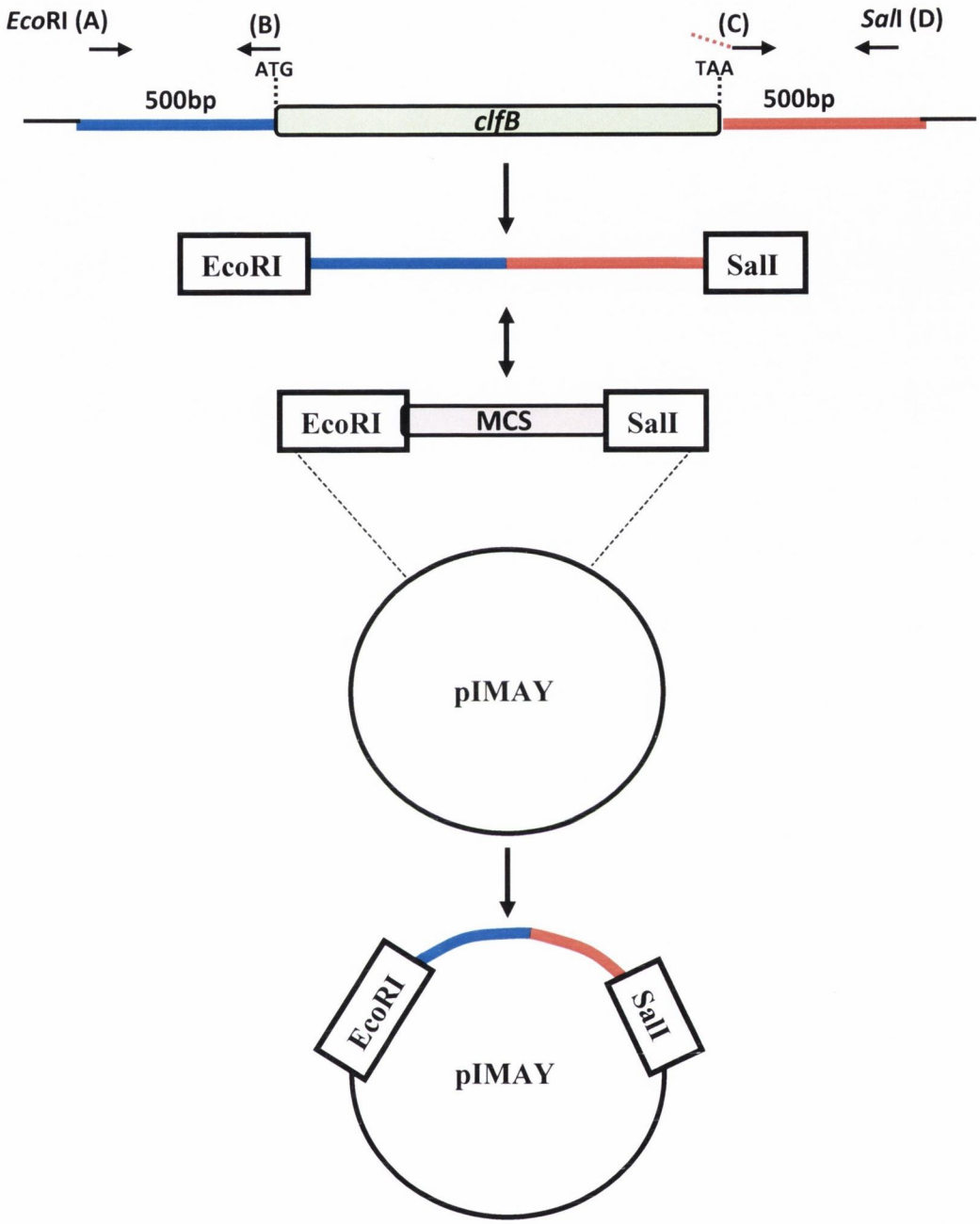

Figure 2.1 Schematic representation of pIMAY *clfB*. Primers were designed to amplify 500 bp regions directly upstream and downstream of the *clfB* gene. EcoRI and SalI restriction endonuclease sites were incorporated into primers (A) and (D) in order to facilitate directional cloning into the multiple cloning site (MCS) of pIMAY. The amplimer was ligated to pIMAY to create pIMAY *clfB*.

2.5.3 Complementation of the *clfB* mutation

S. aureus Newman Δ*clfB* was complemented with pCU1 carrying the full length *clfB* gene (Ni Eidhin and Foster 1998). Plasmid pCU1:*clfB* was transformed into *E. coli* DC10B and then transferred to Newman Δ*clfB*.

2.6 Isolation of cell wall-associated proteins

Cell wall-associated proteins were prepared as previously described (Hartford *et al.* 2001; Roche *et al.* 2003). Exponential phase cultures of *S. aureus* were harvested, washed twice in phosphate-buffered saline (PBS) and resuspended to an OD_{600} of 10 in 250 µl lysis buffer (50 mM Tris-HCl, 20 mM $MgCl_2$, pH 7.5) supplemented with 30% (w/v) raffinose and complete EDTA-free protease inhibitors (40 µl/ml, from a 10x stock, Roche). Cell wall proteins were solubilised by incubation with lysostaphin (200 µg/ml) for 10 min at 37 °C. Protoplasts were removed by centrifugation at 12,000x*g* for 10 min and the supernatant containing solubilised cell wall proteins was aspirated and used in SDS-PAGE or stored at -20 °C.

2.7 Electrophoresis

2.7.1 Agarose electrophoresis

Gels containing 1-1.5 % agarose which was dissolved by boiling in TAE buffer (Invitrogen), and cooled to 65 °C were cast in mini trays (Life Technologies). DNA samples in loading buffer containing an elecrophoretic dye were pipetted into wells along with DNA size markers (Bioline). Electrophoresis of samples was routinely performed at 90 V. Gels were bathed in ethidium bromide for 10 min, washed and viewed under UV light. Gel images were analysed using Alpha Imager™ software.

2.7.2 SDS-PAGE

Protein samples were diluted 2-fold in final sample buffer (125 mM Tris-HCl, pH 6.8, 4% (w/v) SDS, 20% (v/v) glycerol, 10% (v/v) β-mercaptoethanol and 0.002% (w/v) bromophenol blue) and boiled for 5 min. 20 µl volumes of the diluted protein samples were loaded onto acrylamide gels (4.5% stacking and

10-12.5% separating gel) and separated by SDS-PAGE. Electrophoresis was carried out at 120 V after which proteins were visualised by Coomassie blue staining or electroblotted onto PVDF membranes (Roche) for Western immunoblotting.

2.8 Immunoblotting

2.8.1 Western Immunoblotting

Proteins were electroblotted onto PVDF membranes (Roche) for 1h at 100 V using a wet transfer cell (Bio Rad). Membranes were incubated for 1 h at 4 °C in TS buffer (10 mM Tris-HCl, pH 7.4, 150 mM NaCl) containing 10 % (w/v) skimmed milk (Marvel) to block non-specific interactions. Primary antibodies diluted in 10 % (w/v) Marvel/TS buffer were incubated with the membranes for 1 h at room temperature with shaking. Antibodies and their working dilutions are described in Table 2.4. Unbound antibody was removed by three 10 min washes with TS buffer. When necessary, secondary antibodies diluted in 10 % (w/v) Marvel/TS buffer were incubated with the membranes for 1 h at room temperature with shaking. Unbound secondary antibody was removed by washing three times with TS buffer. Chemiluminesent substrate LumiGlo (New England Biolabs) was used according to manufacturers' instructions. Blots were exposed to X-Omat autoradiographic film (Kodak) and visualised using manual development with developer and fixer solutions (Kodak). Alternatively, blots were developed and visualised using ImageQuant TL software (GE). The intensity of protein bands resulting from equal loadings of bacterial cell-wall extracts or purified proteins was assessed visually or by ImageQuant TL software.

2.8.2 Whole cell dot immunoblotting

Bacterial cells in exponential or stationary phase, or human squamous epithelial cells were washed twice in PBS and were resuspended to an OD_{600nm} of 1.0 or 1 x 10^5 cells/ml, respectively. Collection of nasal epithelial cells is described in section 2.9. Doubling dilutions (5 µl) were spotted onto a nitrocellulose membrane (Protran). The membrane was allowed to dry and was then blocked for 1 h with 10 % (w/v) skimmed milk powder (Marvel) in TS

Table 2.4 Antibodies

Antibody	Relevant features	Working dilution/ concentration	Source/ Reference
Rabbit anti-murine loricrin IgG	Raised against a peptide sequence derived from the C-terminus of the mouse loricrin protein	1:500, 1:1000	Covance
Rabbit anti-murine K10 IgG	Raised against recombinant full length murine cytokeratin $10_{1\text{-}570}$	1:500	Bioresources Unit, Trinity College Dublin
Rabbit anti-ClfB A region IgG	Raised against the N123 region of ClfB A domain	1:1000	Bioresources Unit, Trinity College Dublin
Rabbit anti-IsdA	Raised against full length recombinant protein	1:5000	P. Speziale
Rabbit anti-IsdB	Raised against full length recombinant protein	1:2500	P. Speziale
HRP-conjugated anti-His IgG	Secondary antibody raised against proteins containing the epitope tag sequence	1:500	Roche
Swine anti-rabbit IgG	Secondary antibody, FITC-conjugated	1:20	Dako
Protein A-peroxidase	Secondary antibody, HRP-conjugated	1:500	Sigma
Goat anti-GST IgG	Immobilized onto CM5 chip for SPR	30 µg/ml	GE Healthcare
Chicken anti-GST	Chicken IgY, HRP-conjugated	1:500	Gallus Immunotech
Goat anti-rabbit IgG	Secondary antibody, HRP-conjugated	1:2000	Dako

Table 1.1 Functions of *S. aureus* WTA and LTA

Function	Teichoic Acid (TA)	References
Resistance to cationic antimicrobial peptides and antibiotics	D-ala of TAs	(Peschel *et al.*, 1999, Peschel *et al.*, 2000, Collins *et al.*, 2002)
Resistance to lysozyme	WTA	(Bera *et al.*, 2007)
Resistance to antimicrobial fatty acids	WTA	(Kohler *et al.*, 2009)
Resistance to low osmolarity	LTA	(Oku *et al.*, 2009)
Adherence to epithelial and endothelial cells	WTA	(Weidenmaier *et al.*, 2004, Weidenmaier *et al.*, 2005, Weidenmaier *et al.*, 2008)
Attachment to biomaterials and biofilm formation	LTA, WTA	(Gross *et al.*, 2001, Fedtke *et al.*, 2007)

buffer. Primary antibodies were diluted in 10 % (w/v) Marvel/TS buffer and incubated with the membrane for 1 h at room temperature with shaking. Three 10 min washes with TS buffer were performed to remove unbound antibody. Secondary (HRP-conjugated) antibody was diluted in 10 % (w/v) Marvel/TS buffer and incubated with the membrane for 1 h at room temperature with shaking. Unbound secondary antibody was removed by washing three times with TS buffer. The membrane was developed in the dark using the chemiluminescent substrate LumiGlo as described in section 2.8.1.

2.9 Flow cytometry

Nasal desquamated epithelial cells were harvested from the anterior nares of healthy human volunteers by vigorous swabbing. Swabs were agitated in 3 ml sterile PBS and were harvested by centrifugation at 3000x*g* for 8 min. After washing once in PBS, cells were counted using a haemocytometer. A concentration of 10^5 cells in 100 µl was incubated with anti-loricrin IgG (1:500) for 1 h at room temperature. The cells were washed once in PBS and were centrifuged at 3000x*g* for 8 min. The cells were then incubated with FITC-conjugated swine anti-rabbit IgG secondary antibody in a volume of 100 µl for 1 h at room temperature. The cells were washed again and were resuspended in 600 µl PBS/ 2% (v/v) paraformaldehyde before analysis by fluorescent activated cell sorting (FACS) using a BD FACSCalibur II.

2.10 Protein construction and purification

2.10.1 Construction and purification of Histidine-tagged recombinant proteins

In order to construct the minimal binding region of the ClfB A domain, the sequence of ClfB A region was analysed and primers were designed to amplify a ~1000bp region spanning the N2N3 subdomains comprising amino acids 201-542. Plasmid pCU1:*clfB* (Ni Eidhin and Foster 1998) was used as template for PCR amplification. Recognition sequences for BamHI and HindIII were incorporated into the amplicon during PCR to facilitate directional cloning.

PCR amplification was carried out in using Phusion DNA polymerase (Finnzymes). Reactions were carried out according to manufacturers' instructions, using a 10 s denaturation step at 98 °C, a 30 s annealing step at 50 °C and a 30 s extension step at 72 °C. This cycle was repeated 30 times, followed by a final 5 min extension step at 72 °C. A 1 kb fragment was amplified from pCU1 carrying full length *clfB*. This was cloned into pCR-blunt-II-TOPO (Invitrogen) following manufacturer's instructions and was then subsequently isolated and digested to obtain a higher yield of product for cloning. The *clfB* fragment was ligated to pQE30 using T4 DNA ligase (Roche).

In order to construct Δlock-latch mutants of the ClfB N2N3 domain, primers were designed to amplify pQE30 encoding the *clfB* A region without the N-terminus of the A domain from residues 201-526. KpnI sites were incorporated into the forward and the reverse primer. PCR amplification was carried out using Phusion DNA polymerase (Finnzymes) and using pQE30 carrying ClfB $N23_{201\text{-}542}$ as a template. Reactions were carried out using a 10 s denaturation step at 98 °C, a 20 s annealing step at 40 °C and a 1 min elongation period at 72 °C. This cycle was repeated 30 times followed by a 5 min final extension step at 72 °C. The PCR product was digested with DpnI and purified. The PCR product was cut with KpnI and then ligated to itself. Another ClfB N23 truncate was constructed using the same procedure, with primers designed to amplify pQE30 encoding the *clfB* A region without the N-terminus of the A domain from residues 201-521, removing an extra 5 amino acids from the N3 domain.

Recombinant ClfB protein was expressed from pQE30 with an N-terminal hexa-histidine (His) affinity tag to allow purification by nickel affinity chromatography. The pQE30 vector contains an IPTG-inducible promoter for controlled expression of recombinant proteins. The vector is designed with sequences located 5' to the MCS that encode 6 x His residues. The pQE30 constructs were transformed into *E. coli* XL1-Blue. Cultures were grown to OD_{600} nm of 0.5-0.6 and then induced with 1 mM IPTG for 3 h at 37 °C with shaking. Cells were harvested by centrifugation and resuspended in 30 ml PBS containing protease inhibitors (Roche) prior to breakage in a French pressure

cell. The lysate was centrifuged at 17 000 *g* for 20 min. DNase was added to the supernatant followed by filtration through a 0.45 µm filter (Whatman).

A HiTrap™ Chelating HP column (5 ml; GE Healthcare) was used according to the manufacturer's instructions with the flow rate controlled using a peristaltic pump. The column was equilibrated in binding buffer (5 mM imidazole, 0.5 M NaCl, 20 mM Tris-HCl, pH 7.9) and then charged with 150 mM Ni^{2+}. The filtered, cleared cell lysate was applied to the column. The column was washed with binding buffer until the A_{280} nm of the eluate was < 0.001. Bound protein was eluted from the column with a continuous linear gradient of imidazole (5-100 mM; total volume of 100 ml) in 0.5 M NaCl and 20 mM Tris-HCl (pH 7.9). Eluted protein was collected in 5 ml fractions. Elution was monitored by measuring the A_{280} nm of the eluate using a Nanodrop™ 1000 spectrophotometer. Positive fractions were analysed by SDS-PAGE. A volume of 10 µl of each fraction was separated on 10 % acrylamide gels and visualized by Coomassie blue staining. Fractions containing the purified recombinant protein were dialysed against PBS for 16 h at 4 °C. Protein concentrations were determined using the BCA assay kit (Pierce) and by measuring absorbance at 280 nm using a Nanodrop™ 1000 spectrophotometer.

2.10.2 Construction and purification of GST-tagged recombinant proteins

DNA encoding full length human and murine loricrin, a human K10 peptide, a murine K10 peptide and human loricrin subdomains (1A, 1B, 2v, 3, D3, D3v) was codon optimised for *E. coli* and synthesised commercially (Genscript Corporation). Recognition sites for BamHI and EcoRI were incorporated at the 5' and 3' regions of each sequence. DNA was received in the vector pUC57 and was subcloned between the BamHI and EcoRI sites of the expression vector pGEX-4T2 (GE Lifesciences). DNA encoding human loricrin subdomain 2 was amplified by PCR using plasmid pET11a carrying the full length cDNA clone encoding human loricrin (Candi *et al.* 1995) as template and primers designed to amplify DNA encoding the 5' and 3' flanking regions of the loop domain (Table 2.3). The PCR product was ligated to pGEX-4T2 between BamHI and EcoRI sites. Similarly, DNA encoding the ClfB-binding region of fibrinogen (residues 316-367) was amplified by PCR using pQE30 carrying

DNA encoding the fibrinogen α-chain (residues 1-625). BamHI and EcoRI sites were incorporated into the 5' and 3' regions of the sequence, respectively, and the fragment was ligated to pGEX-4T2.

Recombinant proteins were expressed from pGEX-4T2 with an N-terminal glutathione-S-transferase (GST) IPTG-inducible affinity tag. The constructs were transformed into *E. coli* XL1-Blue or TOPP10 strains for large-scale purification. Cultures were grown to OD_{600nm} of 0.5-0.6 and then induced with 1 mM IPTG for 3 h at 37 °C with shaking. Cells were harvested by centrifugation and resuspended in 30 ml PBS containing protease inhibitors (Roche) prior to breakage in a French pressure cell. The lysate was centrifuged at 17 000 *g* for 20 min. DNase was added to the supernatant followed by filtration through a 0.45 μm filter (Whatman).

A GSTrap™ FF column (5 ml; GE Healthcare) was used according to the manufacturer's instructions with the flow rate controlled using a peristaltic pump. The column was equilibrated using PBS. The filtered, cleared cell lysate was applied to the column. The column was washed with PBS and bound protein was eluted from the column using reduced glutathione elution buffer (50 mM Tris-HCl, 10 mM reduced glutathione, pH 8.0). Eluted protein was collected in 2 ml fractions. Elution was monitored by measuring the A_{280} nm of the eluate using a Nanodrop™ 1000 spectrophotometer. Positive fractions were analysed by SDS-PAGE as described in section 2.10.1. Fractions containing the purified recombinant protein were dialysed against PBS for 16 h at 4 °C. Protein concentrations were determined using the BCA assay kit (Pierce) and by measuring absorbance at 280 nm using a Nanodrop™ 1000 spectrophotometer.

Recombinant GST and GST-tagged loricrin L2v were also purified under endotoxin-free conditions in order to be used in a murine nasal colonisation model. Each recombinant protein was purified as described in section 2.10.2 except endotoxin-free water and PBS (Lonza) were used as well as sterile plastic vessels.

2.10.3 Purification of untagged recombinant human loricrin

Untagged human loricrin was purified from pET11a carrying cDNA encoding the full length *lor* gene in *E. coli* XL1-blue (Candi *et al.* 1995). Cultures were grown to OD_{600} nm of 0.5-0.6 and then induced with 1 mM IPTG for 3 h at 37 °C with shaking. Cells were harvested, lysed and DNase-treated as described in section 2.10.2. The protein lysate was dialysed for 16 h at 4 °C three times against 25 mM sodium citrate buffer (pH 3.6). Loricrin is soluble at this pH whereas over 90% of other proteins present in the lysate are not. At each change of dialysis buffer, precipitated proteins were removed from the lysate by centrifugation at 10,000 x *g* for 10 min.

Loricrin was purified from the lysate by chromatography using a HiTrap™ SP FF column (3 x 1ml; GE Healthcare), used according to the manufacturer's instructions with flow adjusted using a peristaltic pump (Amersham). Bound protein was eluted from the column using a gradient of 0–1.0 M NaCl in the citrate buffer. Loricrin eluted at about 0.2 M salt. Elution was monitored as described in section 2.10.2.

2.11 ELISA

2.11.1 Solid phase binding assays

Microtitre plates (96-well, Nunc) were coated with equimolar amounts of His-tagged human fibrinogen α chain, GST-tagged $Fg\alpha_{316-367}$, GST-tagged mouse K10, GST-tagged human K10 YY loop, GST-tagged full length human loricrin or the GST-tagged loricrin loop subdomains in sodium carbonate buffer (15mM Na_2CO_3, 35mM $NaHCO_3$, pH 9.6) and were incubated for 16 h at 4 °C. Wells were washed three times with PBS and were incubated for 2 h at 37 °C in 5% (w/v) Marvel/PBS to block non-specific binding. Wells were washed again and serial dilutions of recombinant ClfB constructs or recombinant His-tagged IsdA in PBS were added. Following a 2 h incubation at 37 °C, wells were washed 3 times with PBS to remove any unbound protein. HRP-conjugated rabbit anti-His IgG in 10 % (w/v) Marvel/PBS buffer were used to detect bound recombinant protein. Plates were incubated for 1 h at room temperature with shaking. After washing, 100 µl of a chromogenic substrate solution (1 mg/ml

tetramethylbenzidine and 0.006% H_2O_2 in 0.05 M phosphate citrate buffer pH 5.0) was added, and plates were developed for 10-30 min in the dark. The reaction was stopped by the addition of 2 M H_2SO_4 (50 µl/well), and plates were read at 450 nm in an ELISA plate reader (Labsystems). Data was plotted and analysed using Prism Graphpad 5 software.

2.11.2 Inhibition studies

Microtitre plates (Nunc) were coated with GST-tagged human loricrin or GST-tagged HK10 in sodium carbonate buffer and were incubated for 16 h at 4 °C. Wells were washed 3 times with PBS and were blocked with 5% skimmed milk proteins in PBS at 37 °C for 2 h. Serial dilutions of recombinant GST, HK10 or Loricrin L2v were pre-incubated with recombinant ClfB $N23_{201-542}$ in PBS at room temperature for 1 h. The protein mixture was added to loricrin-coated microtitre wells and was incubated for 1 h at 37°C. Any unbound protein was removed by washing with PBS, and plates were incubated with HRP-conjugated rabbit anti-His IgG in 1% skimmed milk / PBS for 1 h at room temperature with shaking. 100 µl of a chromogenic substrate solution (1 mg/ml tetramethylbenzidine and 0.006% H_2O_2 in 0.05 M phosphate citrate buffer pH 5.0) was added, and plates were developed for 10 min in the dark. The reaction was stopped by the addition of 2 M H_2SO_4 (50 µl/well), and plates were read at 450 nm in an ELISA plate reader (Labsystems). Percentage inhibition was calculated from the amount of bound protein detected in the absence of inhibitor.

2.11.3 Adherence of bacteria to recombinant ligands

Microtiter plates (Nunc) were coated with serial dilutions of recombinant protein in carbonate buffer and incubated overnight at 4 °C. Wells were washed 3 times with PBS and blocked with filtered 5 % (w/v) bovine serum albumin (BSA) for 2 h at 37 °C. The plates were washed three times with PBS. A bacterial cell suspension (OD_{600} = 1.0 in PBS) was added (100 µl per well) and the plates were incubated for 2 h at 37 °C. After washing, bound cells were fixed with formaldehyde (25% v/v, 100 µl per well) for 20 min and stained with crystal violet (0.5% v/v, 100 µl per well) for 1 min. Following washing with PBS, acetic acid (5% v/v) was added to each well and incubated for 5 min at

room temperature with shaking. The absorbance was measured at 570nm in an ELISA plate reader (Labsystems).

2.11.4 Inhibition of bacterial adhesion to ligands

Microtitre plates (Nunc) were coated with equimolar amounts of GST-tagged human loricrin or GST-tagged HK10 in sodium carbonate buffer and were incubated for 16 h at 4 °C. *S. aureus* cells (1 x 10^8 colony-forming units) were pre-incubated with serial dilutions of recombinant GST, HK10 or Loricrin L2v in PBS at room temperature for 30 min. Following three washes with PBS, the cell-peptide mixture was added to microtiter wells and incubated for 90 min at room temperature. Wells were washed with PBS, and adherent cells were fixed with formaldehyde (25% v/v, 100 µl per well) for 20 min and stained with crystal violet (0.5% v/v, 100 µl per well) for 1 min. After washing, acetic acid (5% v/v) was added to each well and incubated for 5 min at room temperature with shaking. The absorbance was measured at 570 nm as described above. Percentage inhibition was calculated from the amount of adherent cells detected in the absence of inhibitor.

2.12 Surface plasmon resonance

Surface plasmon resonance (SPR) was performed using the BIAcore X100 system (GE Healthcare). Goat anti-GST IgG (30 µg/ml; GE Healthcare) was diluted in 10 mM sodium acetate buffer (pH 5.0) and immobilized on CM5 sensor chips using amine coupling as described by the manufacturer. Recombinant GST-tagged protein (10 - 30 µg/ml) in PBS was passed over the anti-GST surface of one flow cell while recombinant GST (10 - 30 µg/ml) was passed over the other flow cell to provide a reference surface. Increasing concentrations of rClfB in PBS were passed in succession over the surface of the chip without regeneration (Onell and Andersson 2005; Karlsson *et al.* 2006). All sensorgram data were subtracted from the corresponding data from the reference flow cell. The response generated from injection of buffer over the chip was also subtracted. Data was analysed using the BIAevaluation software version 3.0. A plot of the level of binding (response units) at equilibrium against concentration of rClfB was used to determine the K_D.

2.13 Bacterial adherence to desquamated epithelial cells

Nasal desquamated epithelial cells were harvested from the anterior nares of healthy human volunteers by vigorous swabbing. Swabs were agitated in 3 mL sterile PBS and were harvested by centrifugation at 3000x*g* for 8 min. After washing once in PBS, cells were counted using a haemocytometer and were adjusted to 1 x 10^5 cells/ml. *S. aureus* was grown to exponential phase, washed with PBS and adjusted to 1 x 10^8 cells/ml. A suspension of bacterial cells (150 µl) were harvested by centrifugation and resuspended in recombinant GST (30 µM), recombinant loricrin L2v-GST (30 µM) or an equivalent volume of PBS and were then incubated at room temperature for 30 minutes. Volumes (100 µl) of bacterial cell-peptide mixtures were then mixed with 100 µl nasal cells for 1 h at 37 °C with occasional shaking before being captured on 12 µm isopore polycarbonate filters, washed with PBS, fixed and stained with 5% (w/v) crystal violet for 45 s. The filters were mounted onto glass slides and the number of bacteria per 100 squames was counted using light microscopy. Percentage inhibition was calculated from the amount of bound bacterial cells detected in the absence of inhibitor.

2.14 Murine nasal colonisation

Specific pathogen-free female FVB wildtype and FVB loricrin-deficient ($Lor^{-/-}$) mice were housed in groups of 5 animals. Wild-type FVB mice were obtained from Harlan UK. $Lor^{-/-}$ mice have been previously described (Koch *et al.* 2000) and were obtained from Dr. Dennis Roop, University of Colorado Anschutz Medical Centre, Colorado, USA and were bred in-house at Trinity College, Dublin.

Frozen batches of inocula were prepared. Bacterial cells were grown for 18 h on the appropriate solid medium. Cells were harvested from plates by scraping into sterile PBS. Cells were washed using PBS and were re-suspended in PBS containing 5% (w/v) BSA and 20% (v/v) DMSO before being snap-frozen in small aliquots and stored at -80 °C. A single sample was thawed and cells were washed in PBS prior to inoculation.

2.14.1 *S. aureus* nasal colonisation

Mice (8-12 weeks) were given sterile distilled water containing 500 μg/ml Sm 24 hours prior to nasal inoculation and for the duration of the experiment. Mice were inoculated intranasally with 2 x 10^8 CFU (10 μl per nostril) of *S. aureus* Newman or SH1000 wild-type and ClfB-deficient strains. At specific time points post inoculation mice were euthanized. The area surrounding the nose was wiped with 70% ethanol and the nose was excised and homogenised in 500 μl PBS. Lungs were also excised and homogenised in 5 ml PBS. Blood was extracted by cardiac puncture using a 25-gauge needle. Blood and homogenates were plated onto 5% horse blood agar (HBA) or 5% sheep blood agar (SBA) plates to obtain a total count of the nasal flora, and onto TSA containing 500 μg/ml Sm to obtain the number of *S. aureus* CFU present in blood, nose and lung samples. The viability of each inoculum was confirmed by plating onto TSA containing 500 μg/ml Sm.

2.14.2 Nasal colonisation model with *L. lactis*

Mice (8-12 weeks) were given sterile distilled water containing Erm (10 μg/ml) 24 h prior to inoculation and for the duration of the experiment. The mice were inoculated with *L. lactis* MG1363 (pKS80) or *L. lactis* MG1363 (pKS80:*clfB*) exactly as described above but with a challenge inoculum of 2 x 10^{11} CFU (10 μl per nostril). At 24 hours post inoculation mice were euthanized and tissue was processed for viable counts as described above before plating onto BHI containing Erm (10 μg/ml) to enumerate bacteria. Plasmid retention in *L. lactis* MG1363 (pKS80:*clfB*) strains was confirmed by probing bacteria isolated from mouse nares by whole cell dot immunoblotting using anti-ClfB IgG.

2.14.3 Blocking of *S. aureus* adherence *in vivo*

Mice (8-12 weeks) were given sterile distilled water containing 500 μg/ml streptomycin 24 hours prior to nasal inoculation and for the duration of the experiment. *S. aureus* Newman was adjusted to $2x10^{10}$ and was pre-incubated with recombinant GST or recombinant GST-tagged loricrin region 2v (28 μM, purified under LPS-free conditions) for 30 min at room temperature

before intranasal administration. The bacterial cell-peptide mixture was instilled intranasally as described in section 2.14.1. On days 1 and 2 post inoculation, mice were administered 10 µl of recombinant GST or recombinant GST-tagged loricrin region 2v (28 µM) intranasally. Nasal tissue was then harvested on day 3 to assess the bacterial burden as described in section 2.14.1. Denaturation of recombinant GST and Loricrin L2v at various temperatures was investigated by incubating each protein at room temperature, 4 °C, 30 °C and 37 °C for 24 h and comparing them to freshly thawed protein samples by SDS-PAGE.

2.15 Extraction of loricrin and keratin from murine dorsal and nasal tissue

To extract protein from murine dorsal skin, the hair was removed from the backs of euthanized wildtype and $Lor^{-/-}$ mice. Samples of dorsal skin (3 cm^2) were then excised. Skin samples were homogenized in 500 µl PBS and diluted 2-fold in final sample buffer (Laemmli, Sigma). Samples were heated to 95 °C in final sample buffer for 10 min. 20 µl fractions of each sample were applied to 12.5% acrylamide SDS-PAGE gels and were analysed by Western immunoblotting using rabbit anti-murine loricrin polyclonal IgG followed by HRP-conjugated goat anti-rabbit IgG. Bound antibody was removed from membranes by incubating at 50 °C in stripping buffer (2% (w/v) sodium dodecyl sulfate, 100 mM β-mercatoethanol, 50 mM Tris-HCl, pH 6.8) and then re-probed with rabbit anti-murine K10 IgG followed by HRP-conjugated protein A-peroxidase.

Murine nasal tissue was excised from euthanized mice and was homogenised in 500 µl PBS. The total protein concentration of each nose homogenate was measured using a BCA assay and was normalised to 500 µg/ml. The samples were treated and analysed as described above. Nasal protein samples were also analysed by Coomassie staining to confirm that equal protein concentrations were achieved. Expression levels of loricrin and keratin were measured using densitometric analysis. Data was plotted using Prism Graphpad 5 software.

2.16 *S. aureus* intra-peritoneal infection model.

Groups of wild-type and $Lor^{-/-}$ mice received a single intra-peritoneal injection of *S. aureus* Newman (5 x 10^8 CFU). On day 2 post-challenge mice were euthanized. The peritoneal cavity was lavaged with sterile PBS. Blood was collected by cardiac puncture. The kidneys, liver and spleen were excised and homogenised in 500 µl PBS. Tissue homogenates, blood and peritoneal lavage fluid were serially diluted and were plated onto TS agar plates containing 500 µg/ml Sm to obtain the number of *S. aureus* CFU/ml for each sample.

2.17 Ethics Statement

Experiments on mice were conducted under Irish Department of Health guidelines with ethical approval from the Trinity College Dublin ethics committee. Collection of squames from healthy human volunteers was ethically approved by the Health Science Faculty Ethics Committee, Trinity College. Informed consent was given by each volunteer.

2.18 Densitometric Analysis

Densitometry was performed using ImageQuant TL imaging software (GE Corporation).

2.19 Statistical Analysis

Statistical analysis was performed using Prism Graphpad 5 software. Adherence and binding was analysed using an unpaired t test or one-way ANOVA. Statistical analysis on nasal colonisation data was performed using a Mann-Whitney test. Multiple pair-wise analyses were performed using a Krustal-Wallis test and Dunns Multiple Comparison test.

Chapter 3
Strain Construction

3.1 Introduction

The development of genetic manipulation techniques in order to isolate engineered mutations in staphylococcal genes has been an important tool in the study of virulence and pathogenesis in *Staphylococcus aureus*. The production of isogenic mutant strains of *S. aureus* has established the roles of several individual staphylococcal proteins, both surface-expressed and secreted, in the virulence mechanisms employed by the organism. Assessing the virulence of specific isogenic mutants in comparison to their wild-type parental strains *in vitro* and *in vivo* has led to the identification of multiple important factors involved in infection by *S. aureus*. Furthermore, cloning, expression and purification of recombinant staphylococcal proteins has become a helpful method to define the *in vitro* interactions between bacterial and host proteins involved in virulence. In this study, many genetic manipulation techniques were utilized in order to prepare recombinant host and bacterial proteins as well as isolate isogenic mutant strains of *S. aureus*.

Several methods have been developed for the construction of isogenic mutant strains in *S. aureus*. These include transposon mutagenesis, directed plasmid integration and allelic replacement. The use of transposable elements as mutagenic tools allows for the generation of ordered or random insertion mutant libraries without the need of prior knowledge of the target gene. This is followed by a phenotypic screen in order to characterize the phenotypic properties of the constructed mutants. A high transposition frequency and a lack of site-specificity during insertion into the chromosome are both necessary for successful transposon mutagenesis.

Due to the increased availability of genome sequences for *S. aureus* strains, site-specific mutations can now be generated in any sequenced gene using directed plasmid integration and allelic replacement. Directed plasmid integration can be achieved using a number of methods. The introduction of suicide plasmids, carrying a site of shared homology to the gene of interest, to the chromosome can result in a single cross-over event leading to integration of the plasmid and disruption of the target gene. Directed plasmid integration can also be achieved by generating a transcriptional reporter fusion to the target

gene. For example, the plasmid pAZ106 carries a promoterless β-galactosidase gene (*lacZ*). The plasmid integrates at a shared site of homology with the gene of interest and causes transcription of *lacZ* in its place (Kemp *et al.* 1991).

Allelic replacement is an important tool for the generation of chromosomal site-specific mutations. Initially, a deletion construct is produced in a multi-copy plasmid in *E. coli* by cloning regions 5' and 3' to the target gene. A drug-resistance determinant is then inserted between the fragments using a specific restriction site, generating a deletion-substitution mutation construct. The construct is then introduced into *S. aureus* and is integrated onto the chromosome by homologous recombination. Alternatively, primer pairs can be designed to construct a deletion cassette encoding the immediate 5' and 3' regions of the target gene in order to create an in-frame chromosomal deletion. This type of deletion construct is typically used in conjunction with temperature-sensitive plasmids in *S. aureus*.

Temperature-sensitive (TS) plasmids are conditionally-replicating vectors that contain a temperature-controlled origin of replication. Two thermosensitive replicons used for *S. aureus* TS plasmids are derived from pC194 (Horinouchi and Weisblum 1982) and pT181 (Khan and Novick 1983). They can replicate in *S. aureus* at a permissive growth temperature (typically 28 °C), but replication functions become inactive at a higher restrictive temperature which can range from 37-42 °C. These vectors provide a simple procedure for producing unmarked, in-frame deletion mutants carrying no exogenous DNA. The plasmid construct carrying the deletion cassette is introduced into host *S. aureus* cells (Figure 3.1). The transformed cells are propagated at the permissive temperature with selection for the plasmid. Subsequent incubation in selective medium at the restrictive temperature selects for single cross-over integrants. To induce a double-crossover event by homologous recombination, single-crossover variants are incubated at the permissive temperature for replication in non-selective medium (Biswas *et al.* 1993). The plasmid is then eliminated from the bacterial population by growth at the restrictive temperature and either a wild-type or mutant product is obtained, depending on where the second cross-over event has occurred. TS plasmid constructs can be transferred

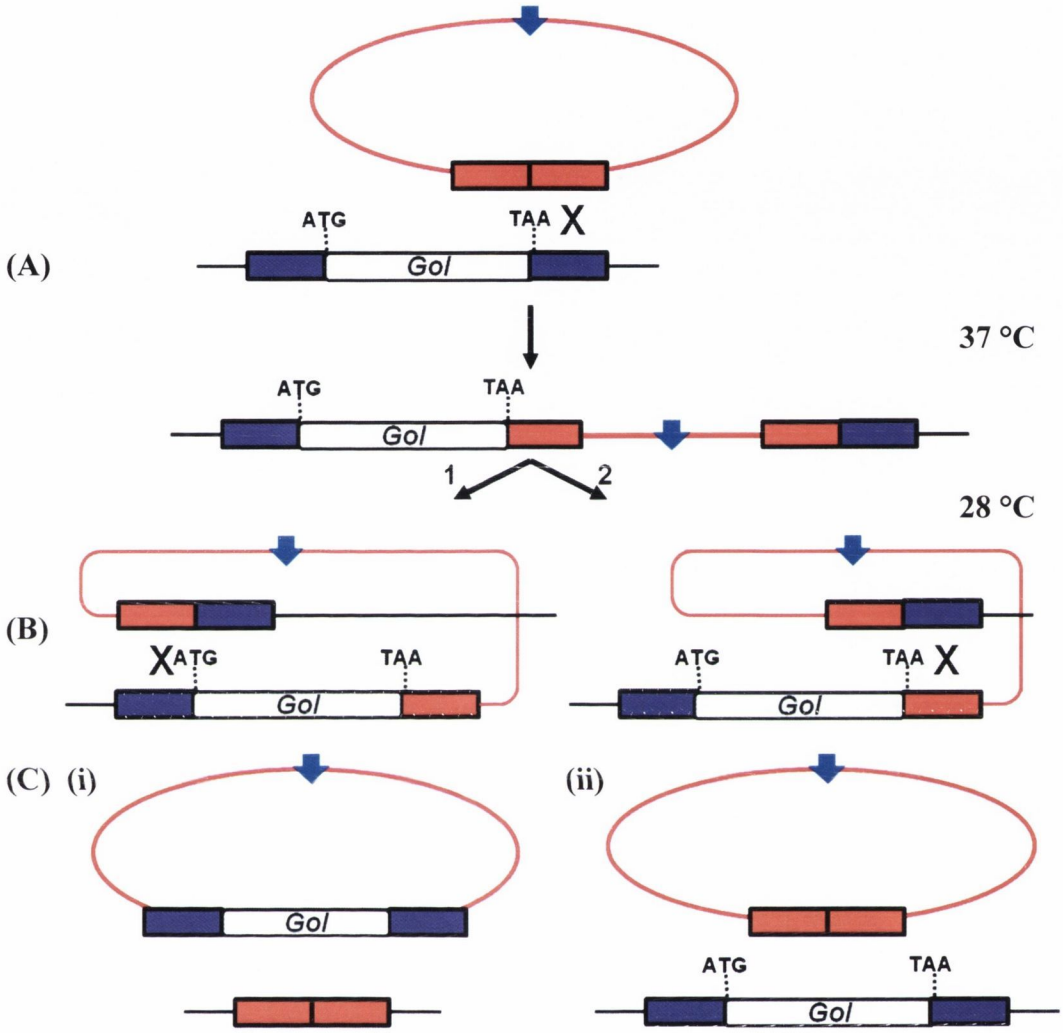

Figure 3.1 Schematic representation of plasmid integration and excision

(A) Plasmid integration at the chromosomal locus by single cross-over event on one side of the mutation. **(B)** A second recombination event allows plasmid excision via an intermediate. **(C) (i)** A second cross-over on the opposite side to the first causes removal of the wild-type gene, resulting in successful allelic replacement. **(ii)** A second cross-over on the same side of the mutation as the first causes removal of the mutation to the plasmid.

between strains at the permissive growth temperature allowing allelic exchange in different backgrounds using the same method.

TS plasmids developed for use in *S. aureus* include pMAD, pKOR1 and pIMAY. pMAD carries a constitutively expressed transcriptional fusion with the *bgaB* gene which encodes a thermostable β-galactosidase enabling staphylococci to cleave the chromogenic substrate X-Gal resulting in blue colonies (Arnaud *et al.* 2004). Expression of *bgaB* provides a blue-white screening tool for detecting the excision and loss of the plasmid, as colonies lacking the plasmid will have a normal colour on X-Gal. Plasmids pKOR1 and pIMAY employ antisense secY RNA inducible counter-selection (Bae and Schneewind 2006; Monk 2012). SecY is a component of the SecYEG translocase that transports signal peptide bearing proteins across the cytoplasmic membrane (Manting and Driessen 2000). Protein secretion and SecY expression are essential for bacterial growth. Expression of secY antisense RNA inhibits staphylococcal growth on agar plates (Ji *et al.* 2001). Anhydrotetracycline-inducible expression of antisense secY RNA selects for plasmid loss and excision.

The 5743bp vector pIMAY was constructed by combining the tetracycline-inducible antisense secY region of pKOR1 with the vector pIMts (Monk 2012). pIMts was constructed by combining the low copy *E. coli* origin of replication (p15A), the multiple cloning site (pBluescript) and the highly expressed cat gene from pIMC (Monk *et al.* 2008) with the temperature-sensitive Gram-positive bacterial replication genes from pVE6007 (Maguin *et al.* 1992). The resulting plasmid, pIMAY, replicates normally in *E. coli* strains but is highly temperature-sensitive in *S. aureus*, with a restrictive temperature of 37 °C. This lower restrictive temperature eliminates the likelihood of secondary mutations that may arise from higher, more stressful restrictive temperatures used by other temperature-sensitive vectors.

The isolation of spontaneous mutations in *S. aureus* has previously been utilized in animal studies in order to easily produce an isogenic strain marked with antibiotic resistance (Kiser *et al.* 1999; Schaffer *et al.* 2006; Park *et al.* 2011). Chromosomal gene mutations in *S. aureus*, as a result of selection

pressure, have led to resistance to many classes of antibiotics. Plating on the aminoglycoside streptomycin can isolate a single-site nucleotide substitution mutation in the *rpsL* gene of many bacterial species including *E. coli* (Gill and Amyes 2004) and *H. pylori* (Torii *et al.* 2003). As a result, the ribosomal S12 protein encoded by *rpsL* contains a single amino-acid substitution which confers resistance to streptomycin. This type of mutation has been isolated previously for use in animal nasal colonisation studies in order to distinguish the organism of interest from the natural nasal flora and to reduce the normal flora prior to inoculation.

Transformation of foreign DNA directly into many staphylococcal strains has previously been unachievable due to the strong restriction barrier present in this species (Waldron and Lindsay 2006; Veiga and Pinho 2009; Corvaglia *et al.* 2010). Previously, DNA from wild-type *E. coli* required passage through the restriction-deficient staphylococcal mutant RN4220 before being subsequently transferred to closely related wild-type S. aureus isolates (Kreiswirth *et al.* 1983). This inability to take up foreign DNA is due to the activity of Type I restriction-modification system and the Type IV restriction endonuclease, SauUSI (Waldron and Lindsay 2006; Corvaglia *et al.* 2010; Xu *et al.* 2011). The substrate for SauUSI is cytosine methylated DNA. It was observed that plasmids isolated from strains of *E. coli* containing a *dcm* mutation causing a lack of cytosine methylation were capable of bypassing the restriction barrier presented by *S. aureus*. A *dcm* deletion mutant of the high-efficiency cloning strain *E. coli* DH10B, known as DC10B, has been engineered and can be used to transfer *E. coli* derived plasmid DNA directly into *S. aureus* (Monk 2012). Other *S. aureus* strains carry additional systems. Whereas strains 8325-4 and Newman carry a single Type I restriction-modification system and a Type IV endonuclease, some strains can have two Type I restriction-modification systems and two Type IV endonucleases. Furthermore, strains in clonal complex CC30 can have an additional Type II restriction-modification system.

The ability to express and purify recombinant protein is a useful tool for the analysis of protein-protein interactions and the identification of protein-binding motifs. In order to generate sufficient protein, DNA encoding the

desired protein can be inserted into an expression vector in *E. coli* followed by induction of protein expression and protein purification using affinity purification. These types of expression systems can produce high levels of the protein. Many expression vectors are commercially available for the production of recombinant proteins in *E. coli.* Expression vectors may contain bacteriophage RNA polymerase promoters, such as the T5 promoter in pQE30 (Bujard *et al.* 1987) or the T7 promoter in the pET expression system (Studier and Moffatt 1986), or hybrid promoters such as the tac promoter in pGEX vectors (de Boer *et al.* 1983). These promoters are coupled to a *lac* operator element that encodes LacI, a strong repressor of expression from the promoter. Addition of IPTG to the bacterial culture inactivates LacI repression, allowing IPTG-inducible control of expression of the promoter that achieves expression of the recombinant protein. Addition of affinity tags results in hexa-histidine or glutathione-S-transferase fusion proteins that are easier to purify and detect in *in vitro* interactions.

This chapter describes the construction and validation of *S. aureus* mutant strains and the preparation of recombinant bacterial and human proteins as follows: (i) construction of variants of the N2N3 region of ClfB, full length human and murine loricrin and the individual omega loop domains of human loricrin, as well as fibrinogen and human and murine keratin protein constructs expressed as His-tagged and GST-tagged fusion proteins (ii) the generation of spontaneous streptomycin resistant mutants of *S. aureus* strains Newman and SH1000, (iii) generation by allelic replacement using the TS plasmid, pIMAY, and validation of an isogenic deletion mutation of the *clfB* gene in *S. aureus* strains Newman and SH1000 and the *isdA* gene of *S. aureus* strain Newman.

3.2 Results

3.2.1 Construction, expression and purification of recombinant His-tagged ClfB region $N2N3_{201-542}$

In order to analyse the interaction between ClfB and loricrin *in vitro*, the minimal binding region of the *clfB* gene was PCR-amplified, cloned into pQE30 and expressed with a N-terminal hexahistidine tag as a recombinant ClfB protein. Recent studies on the crystal structure of the ligand-binding region of ClfB have demonstrated that the N2N3 portion of region A spans amino acids 212-542 (Ganesh *et al.* 2011; Xiang *et al.* 2012). Prior to these findings, the minimal ligand-binding region of ClfB was first defined as the N2N3 domain of region A spanning amino acids 197-542 (Perkins *et al.* 2001). The ClfB minimal binding construct designed in this study is based upon the latter (Figure 3.2 A). Plasmid pCU1 carrying the full length *clfB* gene was used as a template for PCR-amplification of the sequence encoding the N2N3 region of the protein. Primers were designed to amplify DNA encoding a region beginning at the codon for A_{201}, the last residue in the SLAVA protease-recognition motif dividing the formerly defined N1 and N2 regions, and ending at the codon for residue N_{542}, which is the last residue in the latching peptide at the C-terminus of the N3 domain (Figure 3.2 B). The resulting PCR product was ligated to the plasmid pQE30 (Figure 3.2 C). Recombinant ClfB N23 expressed in *E. coli* from plasmid pQE30 consisted of the N2 and N3 domains of the A region of ClfB with an N-terminal 6-histidine extension.

The resulting minimum ligand binding region lacks the metalloprotease recognition sites contained in the SLAVA motif located between N1 and N2. Previous studies have shown that metalloproteases can cleave the full length A region (N123) at the protease-recognition site present in the SLAVA motif (McAleese *et al.* 2001). The exclusion of this motif results in a more stable recombinant protein. The addition of an N-terminal His-tag may prevent a conformational change in the binding region that likely occurs when N1 is cleaved from N2N3 by a metalloprotease. Protein expression from pQE30 was achieved by the addition of IPTG. The protein was first induced on a small scale

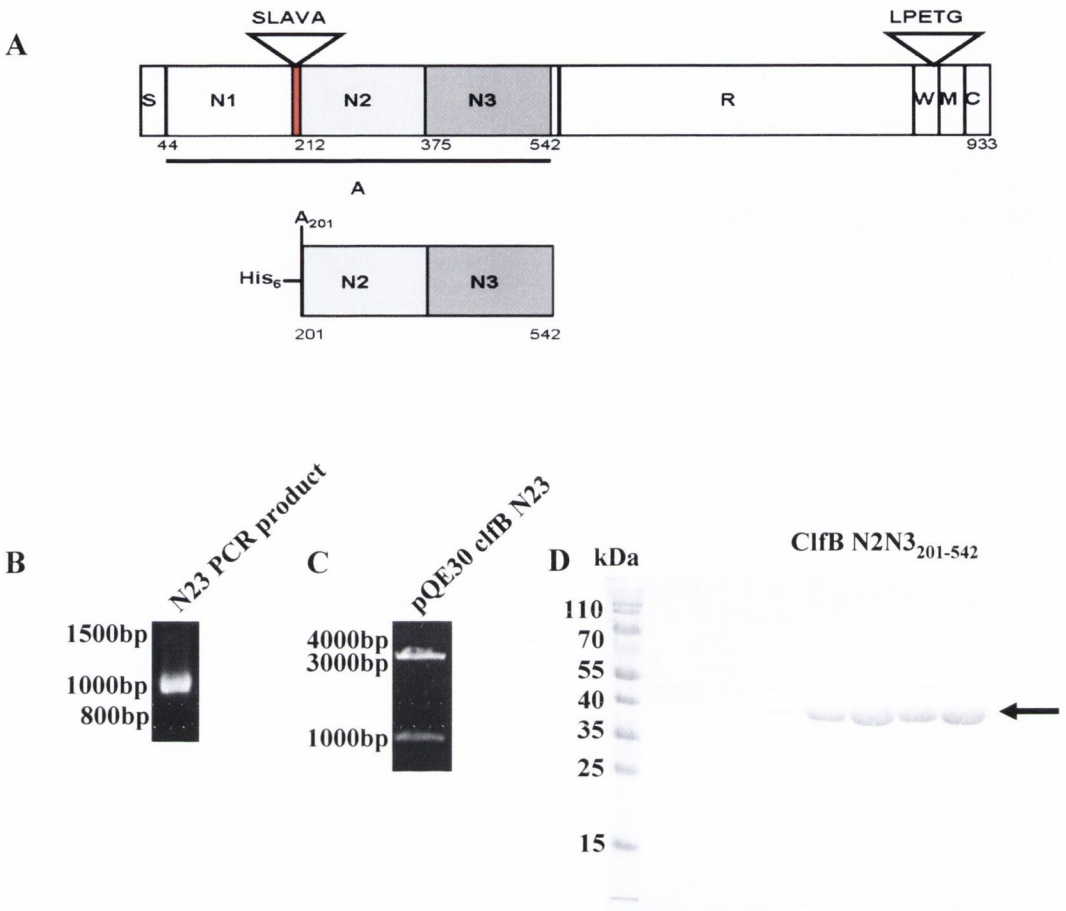

Figure 3.2. Recombinant ClfB $N2N3_{201-542}$. **(A)** Schematic representation of full length ClfB protein and the recombinant N2N3 construct used in this study. The signal sequence (S), SLAVA motif, binding region A with subdomains (N1, N2, N3), SD-repeat region (R), wall-spanning region (W), LPETG motif, membrane anchor (M) and cytoplasmic domain (C) are depicted. Recombinant N2N3 spans amino acids 201-542 and contains an N-terminal his-tag as indicated. **(B)** DNA encoding ClfB N2N3 was PCR-amplified from plasmid pCU1 carrying full length *clfB* and was visualized on a 1% (w/v) agarose gel. **(C)** Restriction analysis of pQE30 carrying the ClfB N2N3 construct. **(D)** Recombinant ClfB N2N3 was purified on a nickel affinity column and was visualized on a 12% acrylamide SDS-PAGE gel stained with Coomassie blue. The recombinant protein is highlighted by a black arrow.

to ensure adequate expression. The protein was then expressed on a large scale giving a high yield followed by purification to homogeneity (Figure 3.2 D).

3.2.2 Construction, expression and purification of recombinant ClfB N2N3 "Δlock-latch" mutants.

In order to determine whether ClfB uses the "dock, lock and latch" mechanism when interacting with its ligands, recombinant ClfB N2N3 domains lacking the lock region and latching peptide involved in the dock, lock and latch mechanism were constructed. The structure of ClfB N23 was analysed using UCSF Chimera molecular modelling software (Figure 3.3 A). From this model, it was concluded that the residues V_{527}-N_{542} at the C-terminus of the N3 domain represented the lock-latch region of ClfB. In order to delete the DNA encoding this region, primers were designed to amplify pQE30 carrying the sequence encoding the ClfB A region without the N-terminus of the A domain and lacking the lock-latch region from residues 201-526. KpnI sites were incorporated into the forward and the reverse primer to facilitate circularization of the PCR product (Figure 3.3 C, E).

The residue W_{522}, present in the N3 domain of the ClfB a region, has been previously shown to play an important role in the ClfB ligand-binding mechanism. Substitution of this amino acid has abolished ligand-binding by ClfB. Another ClfB N23 truncate was constructed using the same procedure, with primers designed to amplify residues 201-521, thus removing an extra 5 amino acids from the N3 domain, including W_{522} (Figure 3.3 B, D). Both mutants were transformed into *E. coli* XL-1 blue and were sequenced in order to validate the mutation. Each protein was expressed abundantly and purified to homogeneity (Figure 3.3 F, G).

3.2.3 Construction, expression and purification of recombinant GST-tagged loricrin and its omega-loop regions

In order to define the interaction between loricrin and ClfB in detail, full length recombinant human and murine loricrin was required. Furthermore, in order to identify ClfB-binding sites within loricrin, recombinant proteins corresponding to individual omega-loop domains within loricrin were also

constructed and purified. Loricrin is composed of three Gly-Ser-rich regions capable of forming omega loops. Region 1 was divided at K_{88} in order to make two separate constructs designated 1A and 1B. The full length human loricrin protein and its four individual loop regions (loop regions 1A, 1B, 2 and 3, Figure 1.9) were amplified from a loricrin cDNA clone template on pET11a. Regions 2 and 3 are separated by short stretches rich in glutamine, where transglutamination reactions occur. The N- and C-termini of the protein also comprise short Glu-rich stretches. Loricrin DNA was amplified by PCR using primers designed to recognize the extreme 5' and 3' ends of the coding sequence. Primers for each loop region were designed to recognise DNA encoding the internal or terminal Glu-rich domains flanking each glycine-serine rich omega-loop region. PCR products were of the expected size, but after cloning into pGEX-4T2, DNA sequencing revealed mutations causing substitutions in the repeat domains of the loop regions. The resulting clones were not suitable. Only DNA for human loricrin loop region 2 was amplified successfully and cloned into the IPTG-inducible vector pGEX-4T2.

In order to obtain wild-type DNA sequences, DNA encoding the full length human and murine loricrin protein and each loop region from human loricrin was synthesized commercially. Each DNA sequence was received on pUC57 and included 5' and 3' restriction sites BamHI and Eco RI, respectively, to facilitate directional cloning (Figure 3.4 A). Each construct was subcloned into the IPTG-inducible vector pGEX-4T2, resulting in expression of glutathione-S-Transferase fusion proteins encompassing a 26 kDa GST-tag (Figure 3.4 B). Loop region 1A began at residue S_1 and terminated at residue K_{88}. Loop region 1B began at K_{88} and terminated at S_{159}. Loop region 2 began at residue G_{152} and terminated at S_{230}. Human loricrin undergoes allelic variation, resulting in both size and sequence variants in loop region 2. Two different size variants of loop region 2 were prepared in order to determine whether this polymorphism has any affect on ClfB binding. One variant of the second loop region (loop region 2v), which corresponds to an allelic variant of the *lor* gene (a 12 base pair deletion), that results in a loop that is 4 residues shorter, was also expressed (G_{152}-S_{226}), as well as the previously constructed larger loop region 2. Loop region 3 spanned amino acids S_{216}-K_{315}.

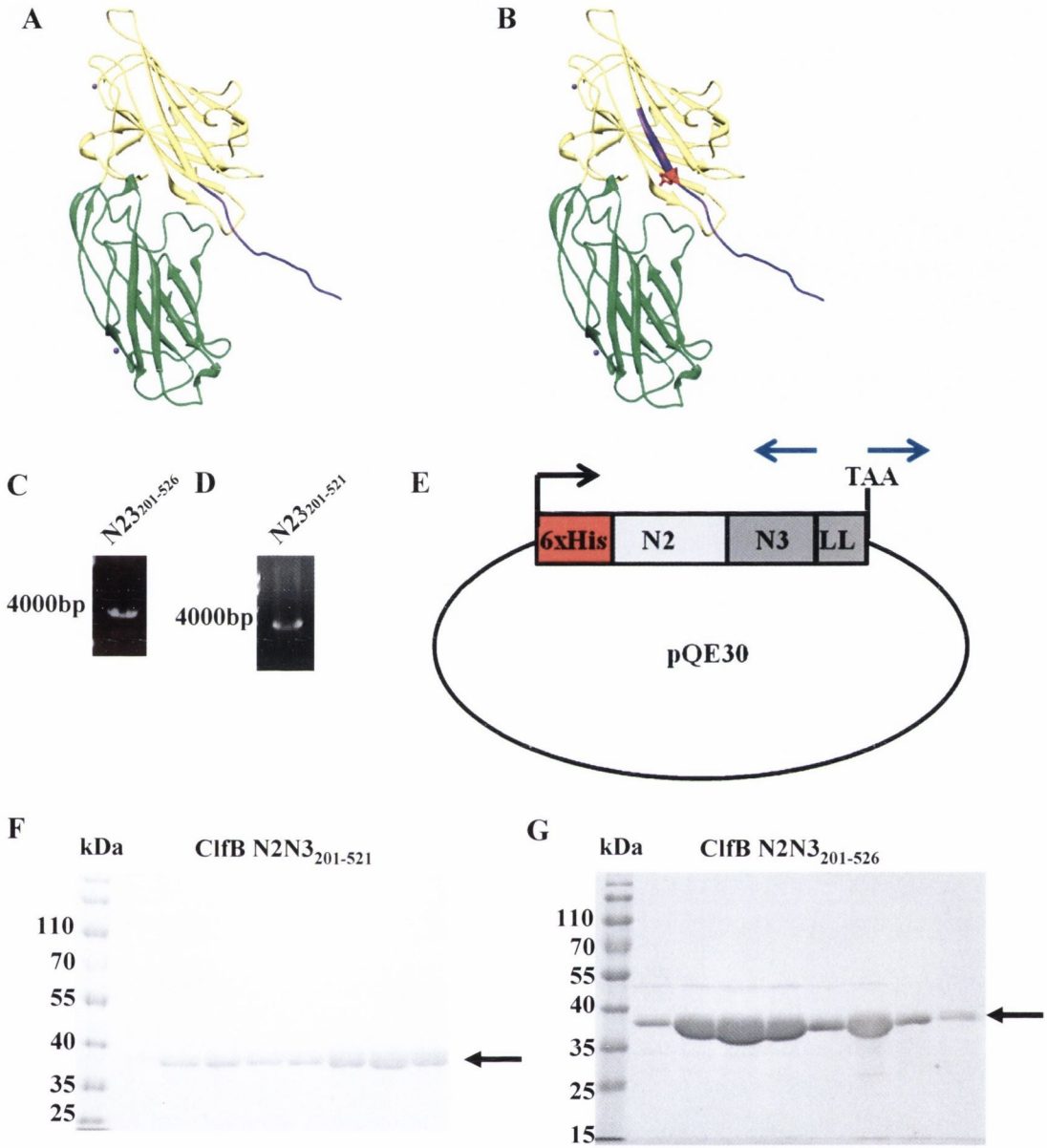

Figure 3.3. Construction of ClfB N2N3 Δlock-latch mutants. ClfB N2 and N3 regions (highlighted in green and yellow, respectively) were visualized and the lock-latch region determined using Chimera software. ClfB regions $N2N3_{201\text{-}526}$ **(A)** and $N2N3_{201\text{-}521}$ **(B)** were both visualized (highlighted in purple). N256 is highlighted (red). DNA encoding pQE30 carrying ClfB $N2N3_{201\text{-}526}$ **(C)** and $N2N3_{201\text{-}521}$ **(D)** were amplified by inverse PCR **(E).** $N2N3_{201\text{-}521}$ **(F)** and $N2N3_{201\text{-}526}$ **(G)** were purified on a large scale and were visualized on 12% SDS-PAGE acrylamide gels stained with Coomassie blue. Proteins are highlighted by a black arrow.

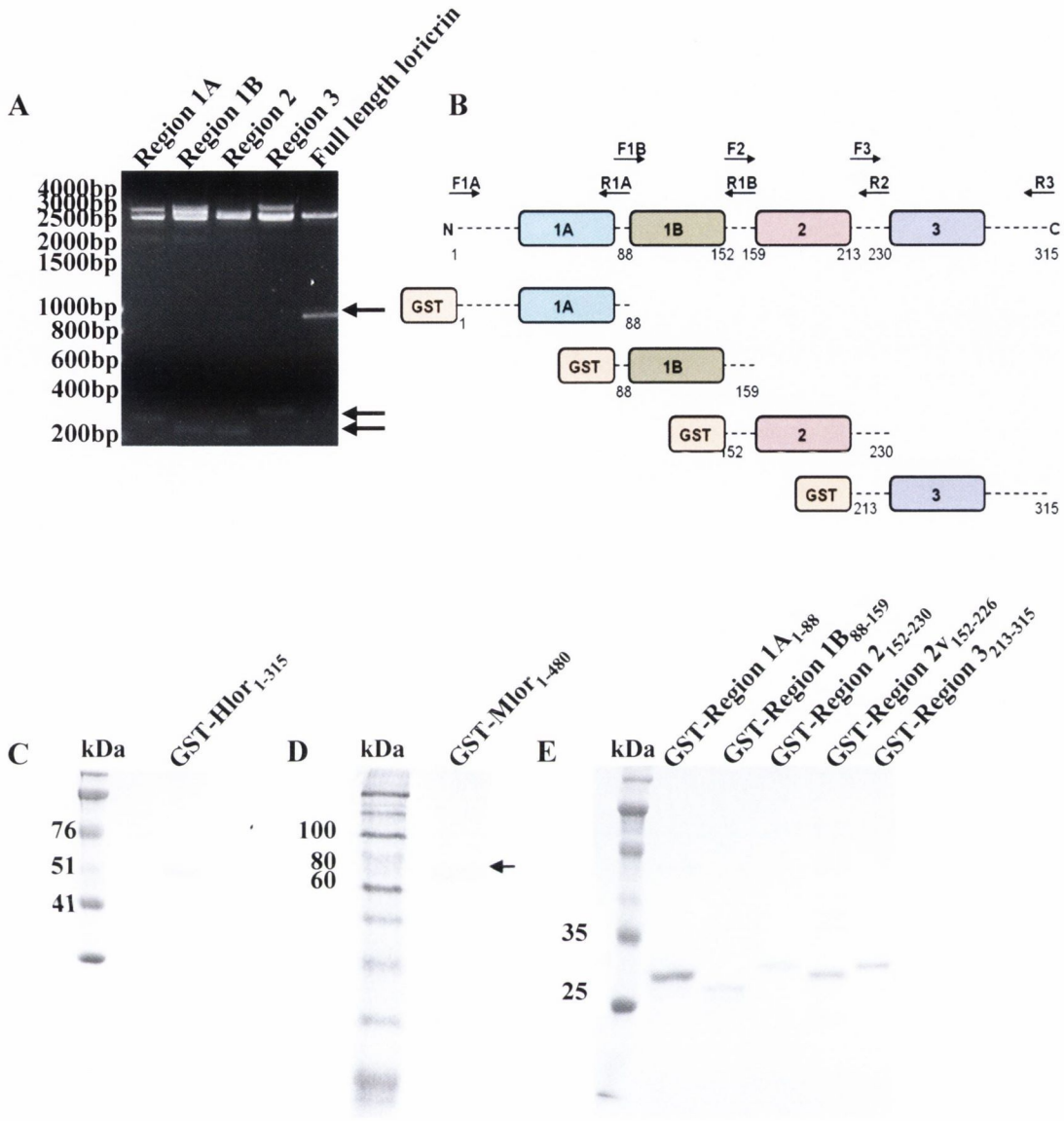

Figure 3.4. Construction of full length loricrin and omega loop domains. (A) DNA encoding full length human loricrin and each omega loop region was synthesized commercially and was isolated from pUC57. The figure shows the DNA cleaved with BamHI and EcoRI to release the insert (indicated by arrows). **(B)** Schematic diagram of human loricrin depicting the starting and finishing locations of each omega loop region produced in this study. The location of the original primers used are indicated by black arrows. GST-tagged and purified recombinant human loricrin **(C)**, mouse loricrin **(D)** and loop region proteins **(E)** are shown on 12% SDS-PAGE gels stained with Coomassie blue. Murine loricrin is indicated by a black arrow.

Recombinant GST-tagged human and murine loricrin were expressed with a high level of purity but at a low yield (Figure 3.4 C, D). Previous studies have suggested that high amounts of loricrin may be toxic to *E. coli* cells, resulting in low yields of purified protein. Also, loricrin has limited solubility at physiological pH (Candi *et al.* 1995). Each GST-tagged omega-loop domain was expressed at a high yield and a high level of purity (Figure 3.4 E).

3.2.4 Construction, expression and purification of recombinant GST-tagged cytokeratin 10 and fibrinogen

In order to compare binding of loricrin by ClfB to known ClfB-binding ligands and also to determine the nature of the ClfB-binding mechanism using *in vitro* recombinant studies, recombinant cytokeratin 10 (K10) and fibrinogen ClfB-binding regions were constructed and expressed. Recombinant human and murine K10 has previously been constructed and expressed as a histidine-tagged protein in order to define its interaction with ClfB (Walsh *et al.* 2004). Due to the GC-rich and repetitive nature of K10 DNA, the cloning methods used in this previous study led to deletions in the resulting recombinant constructs, particularly in the omega-loop-rich tail regions of the proteins. Furthermore, the insoluble nature of K10 meant that it was very poorly expressed and easily degraded. Consequently, the amino acid deletions in the tail region of the human K10 construct led to the discovery of the single "YY loop" within the tail region of keratin to which ClfB binds.

In this study, the construction of recombinant K10 was repeated in order to produce a stable, highly expressed recombinant protein. Due to the problems experienced previously with PCR-amplification of keratin DNA, DNA encoding previously-defined ClfB-binding regions within human and murine keratin was synthesized commercially. The "YY loop" ClfB-binding region in the human K10 tail, spanning amino acids 544-563, and the murine K10 tail region (spanning amino acids 454-570) were chosen as appropriate ligand regions. Restriction sites were incorporated into codon-optimized DNA in order to clone the constructs into the IPTG-inducible vector pGEX-4T2. Each protein was then expressed as a glutathione-S-Transferase fusion protein encompassing a 26 kDa GST-tag. Protein expression was induced on a small scale from *E. coli* strain

XL1-Blue, indicating that each GST-tagged construct was expressed at a high level. The recombinant proteins were then expressed and purified on a large scale. A high yield and high level of purity was obtained for each protein (Figure 3.5 A, B).

The ClfB-binding site within the alphaC-region of fibrinogen has been previously localised to the glycine- and serine-rich tandem repeat region 5 (Walsh *et al.* 2008). In order to produce a GST-tagged ClfB-binding region for *in vitro* studies, DNA encoding this repeat region, which spans amino acids 316-367, was PCR-amplified using primers designed to recognise the 5' and 3'ends of the coding sequence, using the cloned full length fibrinogen α-chain gene as a template. The PCR product was ligated to pGEX-4T2 using restriction sites that were incorporated during PCR-amplification. The resulting construct sequence was verified and expression of the recombinant protein was induced using IPTG. GST-tagged $Fg_{\alpha 316-367}$ was expressed at a high level (Figure 3.5 C).

3.2.5 Construction and validation of streptomycin resistant mutants of *S. aureus* strains Newman and SH1000

Murine nasal colonisation models have employed the use of spontaneous streptomycin-resistant (Sm^R) strains of *S. aureus* (Kiser *et al.* 1999; Schaffer *et al.* 2006; Park *et al.* 2011). The use of a Sm^R mutant enables rapid isolation of the organism from the nose post-colonisation and also allows the use of streptomycin in drinking water to reduce interference by normal flora. Spontaneous Sm^R mutants of *S. aureus* strains Newman and SH1000 were produced in this study. The mutation was isolated by growth overnight in TSB followed by plating onto TSA plates containing streptomycin (500 μg/ml). Single site mutations in the *rpsL* gene often result in high level streptomycin resistance. Genomic DNA was isolated from Newman and SH1000 mutants and parental strains and the *rpsL* gene was amplified by PCR using primers designed to recognise 20-30 base pairs 5' prime and 3' of the gene sequence. The *rpsL* PCR products were sequenced using primers designed to recognize the 5' prime and 3' regions of the gene. Sequencing revealed a single nucleotide substitution (T165A) in strain Newman that resulted in a single site amino acid substitution (K55T) in the S12 protein of 30S ribosomal subunit. A similar single site amino

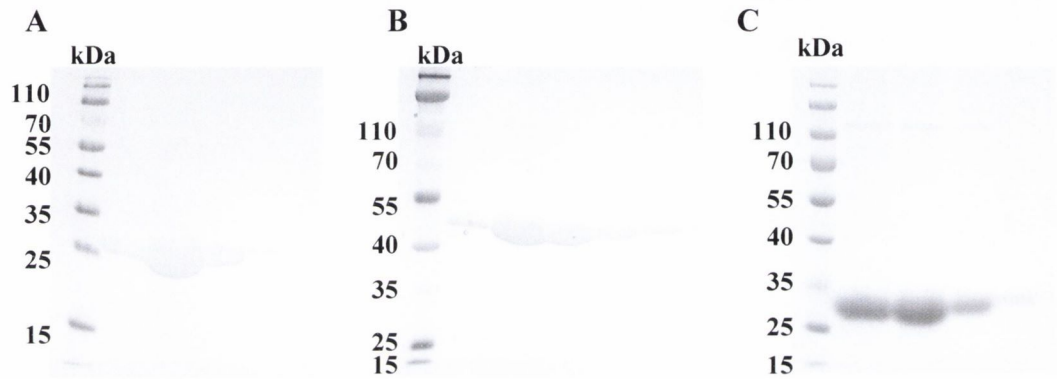

Figure 3.5. Construction of ClfB-binding regions of keratin and fibrinogen. DNA encoding the ClfB-binding "YY loop" of human keratin and the tail region of murine keratin was synthesized commercially and then subcloned into pGEX-4T2. Purified HK10-GST **(A)** and MK10-GST **(B)** are shown on 12.5% SDS-PAGE gels stained with Coomassie blue. DNA encoding the ClfB-binding region in the αC-domain of human fibrinogen was PCR-amplified from pQE30:Fg$\alpha_{1\text{-}625}$ and cloned into pGEX-4T2. The purified protein is shown on a 12% SDS-PAGE gel **(C)**.

acid substitution (K55N) was present in the corresponding SH1000 protein (Figure 3.6).

Each strain was tested for delta toxin production in order to assess *agr* function. Spontaneous *agr* mutations can occur at high frequency in bacteria under stress (Traber and Novick 2006; Traber *et al.* 2008). These mutations may affect expression of virulence factors and alter fitness due to a lower growth rate. δ-haemolysin is a short peptide that is translated from RNAIII, a transcript from the Agr two-component system. It has weak activity on sheep blood agar but is strongly synergistic with β-haemolysin, producing a zone of clear haemolysis where they interact. Sm^R Newman and its parental strain were cross-streaked against RN4220, which produces only β-haemolysin (Tegmark *et al.* 2000). A similar zone of clear haemolysis was observed for each strain, indicating normal *agr* function (Figure 3.7 A). A similar result was observed for SH1000 Sm^R. The growth rate of Sm^R Newman and Sm^R SH1000 was examined. Each mutant exhibited a minor reduction in growth rate when compared to its parental strain (Figure 3.7 B, C). As Sm^R Newman was required for use in *in vitro* adherence assays, the ability of Sm^R Newman to adhere to recombinant K10 was investigated in comparison to its parental strain. Both Sm^R Newman and its parental strain displayed a similar level of adherence to K10, indicating that the single site mutation does not affect the strain significantly (Figure 3.7 D).

3.2.6 Construction and validation of a *clfB* null mutation in *S. aureus* strains Newman and SH1000

S. aureus Newman Sm^R Δ*clfB* was constructed by allelic exchange using pIMAY (Figure 3.8 A). Two sets of primers were designed to amplify 500 bp of DNA located upstream and downstream of the *clfB* gene. Primers A and B recognised the 5' and 3' regions of the 500bp upstream region of *clfB*. Primers C and D recognised the 5' and 3' regions of the 500bp downstream region of *clfB*. Restriction sites EcoRI and SalI were incorporated into primers A and D, respectively, to allow for directional insertion into pIMAY. Primer C was designed to include a 5' extension complementary to the nucleotide sequence of primer B. Genomic DNA was isolated from strain Newman and was used as

template. The resulting PCR products were denatured, allowed to reanneal via the complementary sequences in primers B and C and then amplified using primers A and D, resulting in a 1000 bp fragment consisting of linked sequences upstream and downstream of the *clfB* gene (Δ*clfB* cassette, Figure 3.8 B). The amplimer was cloned into pIMAY between EcoRI and SalI restriction sites (Figure 3.8 C). Deletion of the *clfB* gene was achieved by allelic exchange. To allow for allelic replacement, pIMAY containing the Δ*clfB* cassette was transferred to electrocompetent Newman. Following a temperature shift to the restrictive temperature (37 °C), cells were plated onto TSA containing chloramphenicol to select for a single crossover event leading to integration. The side of integration was determined by PCR screening using primers designed to recognise 500bp sequences upstream and downstream of the deletion construct (OUT primers, Table 2.3). In order to induce plasmid excision, successful integrants were grown at the permissive temperature (28 °C). The same Δ*clfB* cassette was used to construct SH1000 Δ*clfB*.

The deletion was confirmed in both strains by amplification of the Δ*clfB* cassette from genomic DNA (Figure 3.8 D). The same OUT primers were used to screen genomic DNA isolated from possible mutants and their parental strains. If the mutation construct was retained in the chromosome then PCR-amplification would yield a 1000bp product from Newman Δ*clfB* and SH1000 Δ*clfB*, but not their parental strains. As predicted, a 1000bp product was amplified from Newman Δ*clfB* and SH1000 Δ*clfB* whereas the parental strain of each yielded the wild-type product.

The resulting ClfB-deficient strains were validated. Each strain was compared to its parental wild-type strain for expression of δ-toxin in order to assess *agr* function (Figure 3.9 A). The delta-haemolytic profile of Newman Δ*clfB* and SH1000 Δ*clfB* compared to its wild-type strain suggests a normally functioning Agr system. Each mutant displayed a similar growth rate compared to its corresponding wild-type strain (Figure 3.9 B). Lack of expression of ClfB was verified by Western immunoblotting using anti-ClfB IgG (Figure 3.9 C). The functionality of SH1000 was assessed using single-point-binding bacterial adherence assays (Figure 3.9 D). SH1000 Δ*clfB* displayed a reduced ability to

Figure 3.6. Validation of the *rpsL* single site mutation in *S. aureus* Newman and SH1000. The *rpsL* gene was amplified from each mutant and its parental strain. Each product was sequenced and compared using ClustalW software to confirm the amino acid substitution caused by a single site mutation (highlighted in blue box).

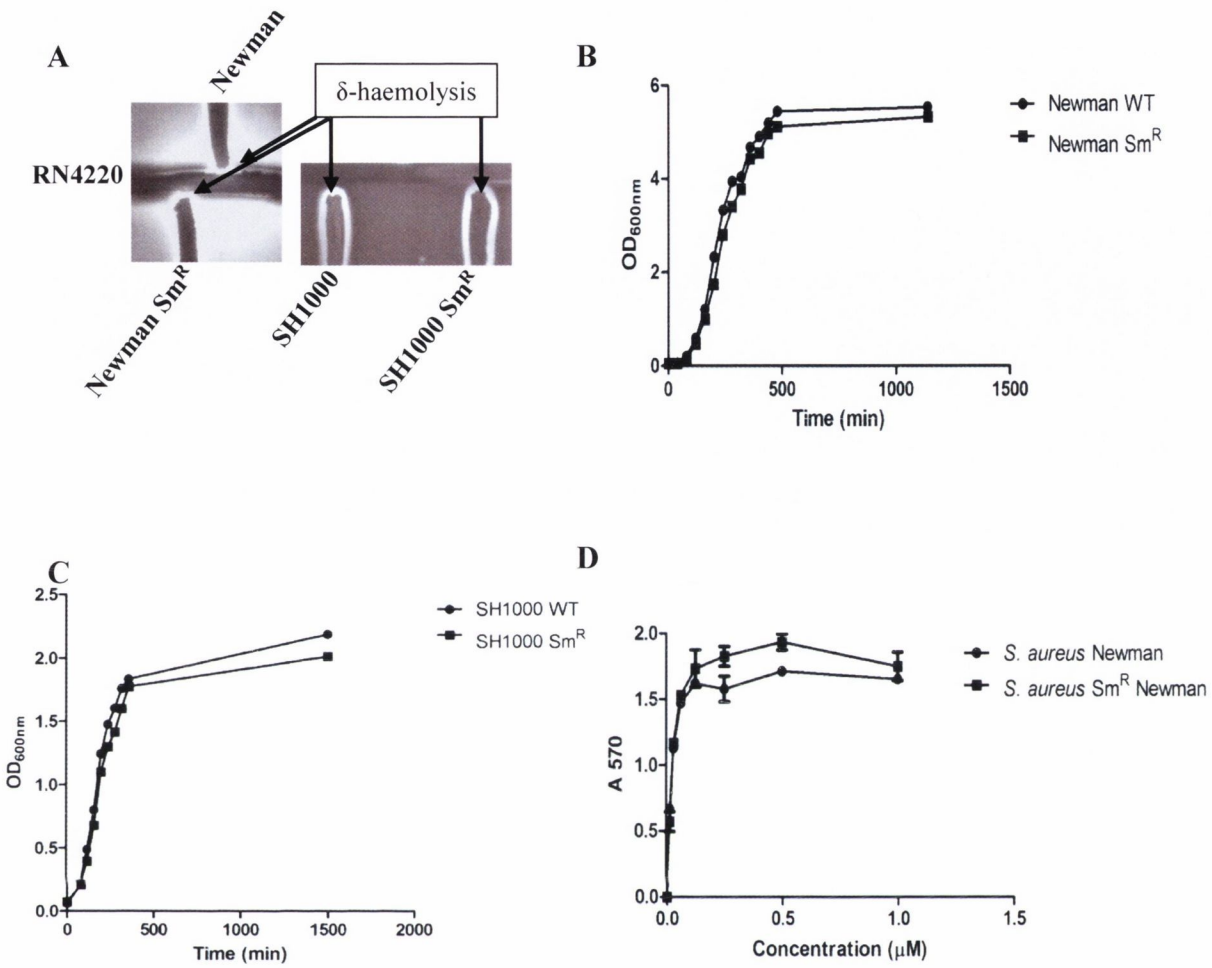

Figure 3.7. Validation of streptomycin resistant mutants of *S. aureus* strains Newman and SH1000. **(A)** Sm^R Newman and its parental strain were cross-streaked against RN4220 in order to compare the haemolytic pattern. Haemolysis is indicated by black arrows. The growth rate of Sm^R Newman **(B)** and SH1000 **(C)** were examined compared to their parental strains. **(D)** The ability of Sm^R Newman to adhere to recombinant GST-K10 was investigated compared to its parental strain. Bacteria were added to wells coated with different concentrations of K10. Bacterial adherence was measured by staining with crystal violet and measurement of the absorbance at 570nm. Each point represents the mean ± SD of triplicate wells. The results shown are representative of three separate experiments.

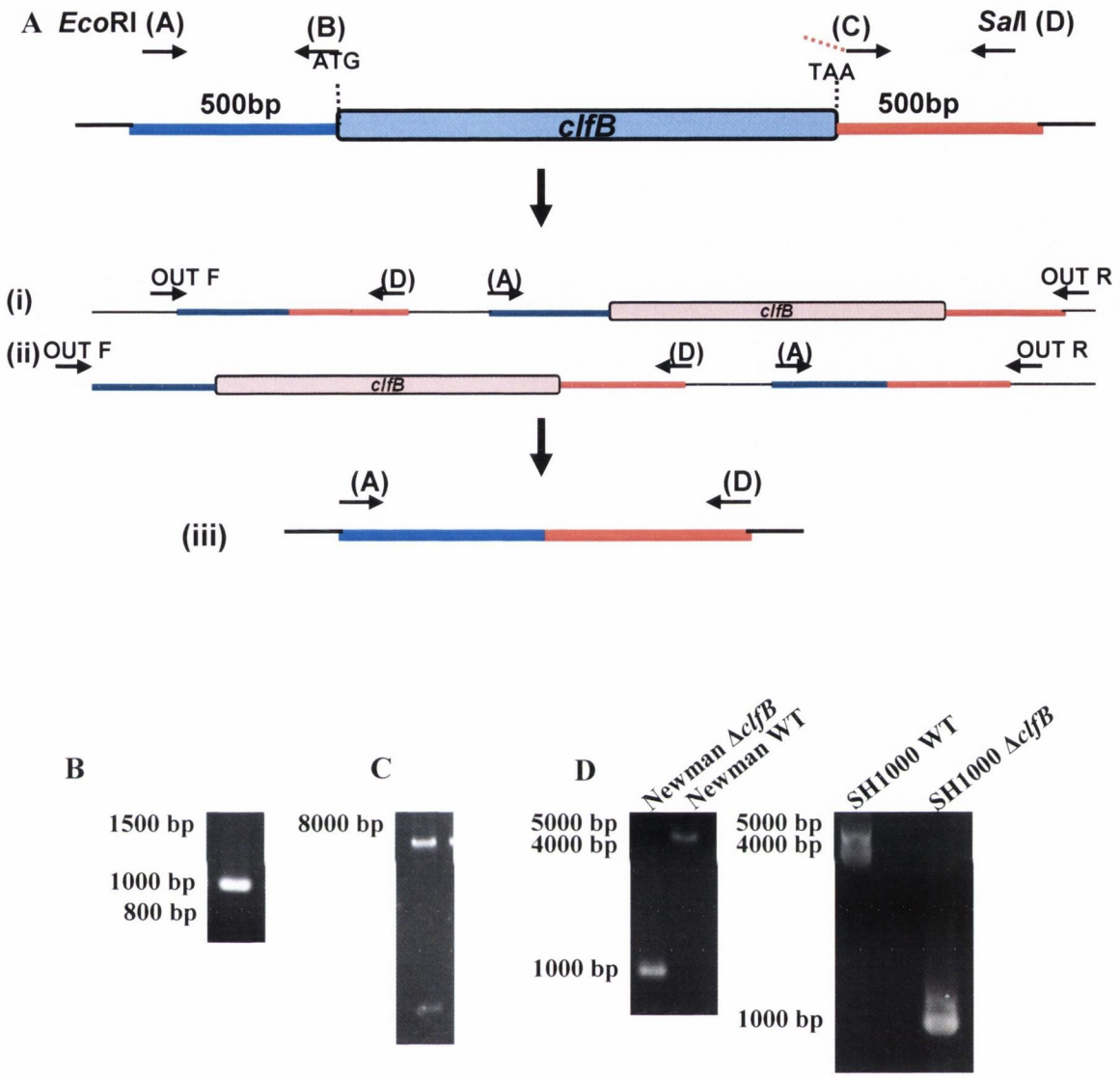

Figure 3.8. Construction of pIMAY Δ*clfB*. **(A)** Schematic representation of the *clfB* mutation. 500 bp regions upstream and downstream of the *clfB* gene were amplified by PCR and were joined to form a *clfB* mutation construct. The construct was cloned into pIMAY and was then introduced into *S. aureus* Newman and SH1000. The side of integration on the chromosome can be determined by PCR-amplification of the regions using OUT primers **(i, ii)**. The plasmid is then excised, leaving the deletion construct on the chromosome **(iii).** **(B)** PCR amplification of the 1000bp *clfB* deletion construct. **(C)** Restriction analysis of pIMAY carrying the *clfB* deletion construct. **(D)** The deletion was confirmed by PCR-amplifying the deletion and comparing it to the wild-type product from *S. aureus* Newman and SH1000 genomic DNA.

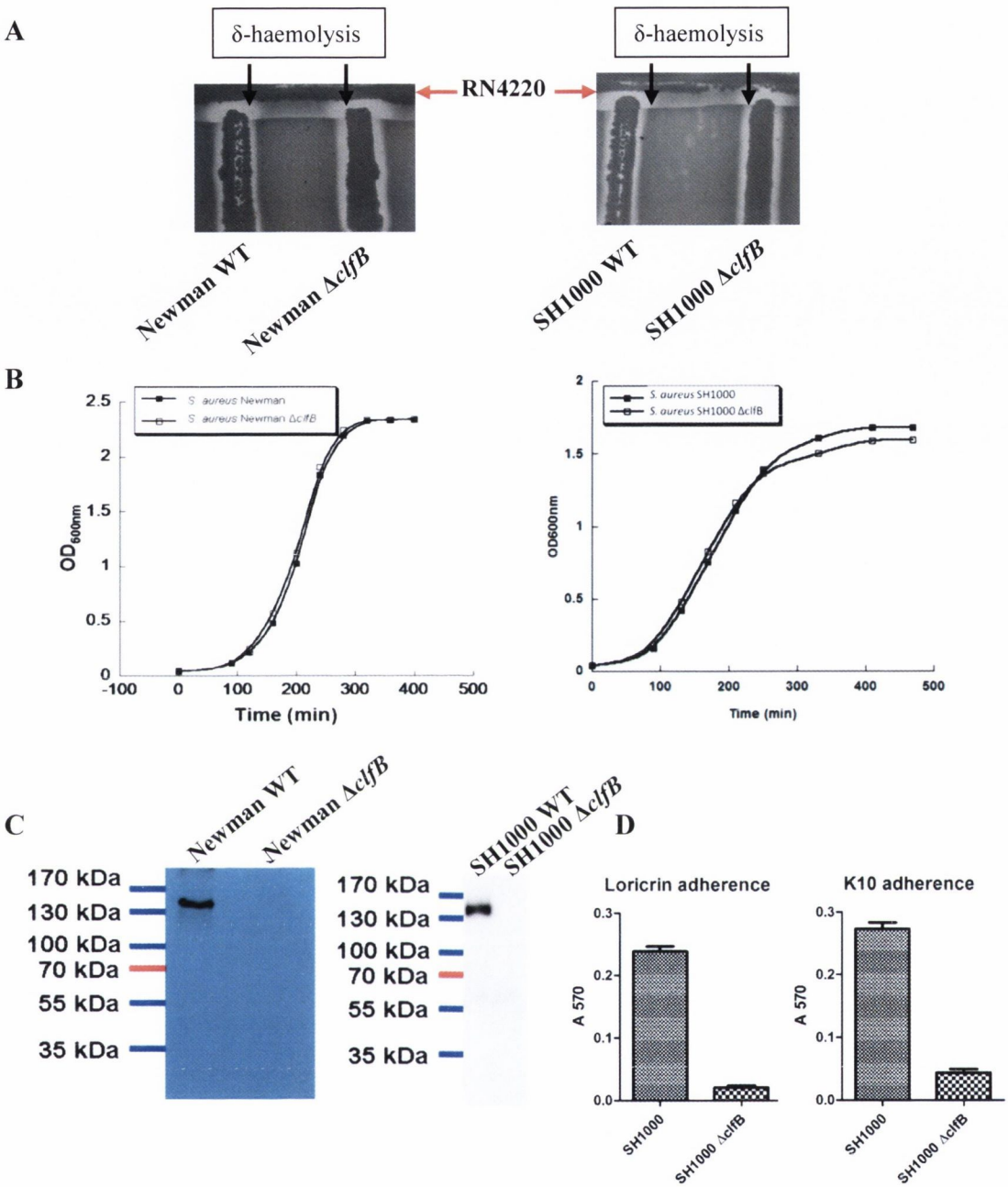

Figure 3.9. Validation of the *clfB* mutants of *S. aureus* Newman and SH1000. **(A)** *S. aureus* Newman parental strain and *S. aureus* Δ*clfB* were cross-streaked against RN4220 in order to compare the haemolytic pattern. Enhanced haemolysis due to δ-toxin is indicated by black arrows. Growth rates of mutant Newman and SH1000 strains were compared to their parental strains **(B).** Expression of ClfB was analysed by Western immunoblotting of cell wall proteins that had been solubilized by lysostaphin during protoplast formation, separated on a 12% SDS-PAGE gel and probed with anti-ClfB IgG **(C).** The functionality of *S. aureus* SH1000 Δ*clfB* was analysed by testing for adherence to recombinant loricrin and cytokeratin 10 (0.5 μm) **(D)**.

adhere to recombinant loricrin and recombinant K10 compared to its wild-type parental strain, indicating that ClfB-mediated adherence to these ligands has been abolished.

3.2.7 Construction and validation of *isdA* null mutations in *S. aureus* strains Newman and Newman Δ*clfB*.

S. aureus Δ*isdA* and Δ*clfB*Δ*isdA* were constructed by homologous recombination using pIMAY, following the same protocol used for the construction of *S. aureus* Δ*clfB*. Primer pairs recognising the 500bp upstream and downstream regions of the proteins were designed and a 1000bp deletion construct was produced (Figure 3.10 A) and cloned into pIMAY (Figure 3.10 B). Deletion of *isdA* was achieved by allelic exchange and the resulting strain was validated. PCR-amplification using specific OUT primers for the *isdA* deletion region produced a 1000bp product from genomic DNA isolated from each mutant (Figure 3.10 C), confirming that the mutation was introduced into the chromosome. Bacteria were grown in iron restricted medium RPMI and the absence of IsdA protein was confirmed using Western immunoblotting (Figure 3.10 D). Anti-IsdB antibodies were also included in order to ensure that the *isd* operon was still expressed. *S. aureus* Δ*isdA* and *S. aureus* Δ*clfB*Δ*isdA* were phenotypically identical to their parental strains in terms of growth rate in TSB (Figure 3.10 F) and in RPMI (data not shown) and the haemolytic profile of each strain indicated that Agr is intact (Figure 3.10 G).

3.2.8 Validation of nisin-inducible expression of staphylococcal proteins in *Lactococcus lactis*

Whole cell dot immunoblots were carried out to compare expression of staphylococcal proteins on the surface of *L. lactis*. *L. lactis* strains containing plasmids pNZ8037 *clfB*, pNZ8037 *clfB* Q235A and pNZ8037 *isdA* were grown with concentrations of nisin ranging from 0 ng/ml to 1000 ng/ml. Serial dilutions of washed, induced bacterial cells were spotted onto nitrocellulose membranes and probed with anti-ClfB (Figure 3.11 A) or anti-IsdA IgG (Figure 3.11 B). The level of expression of staphylococcal proteins by *L. lactis* was proportional to the amount of nisin added to the growth medium. There was no

noticeable difference in the levels of expression of the wild type and non-fibrinogen binding ClfB proteins.

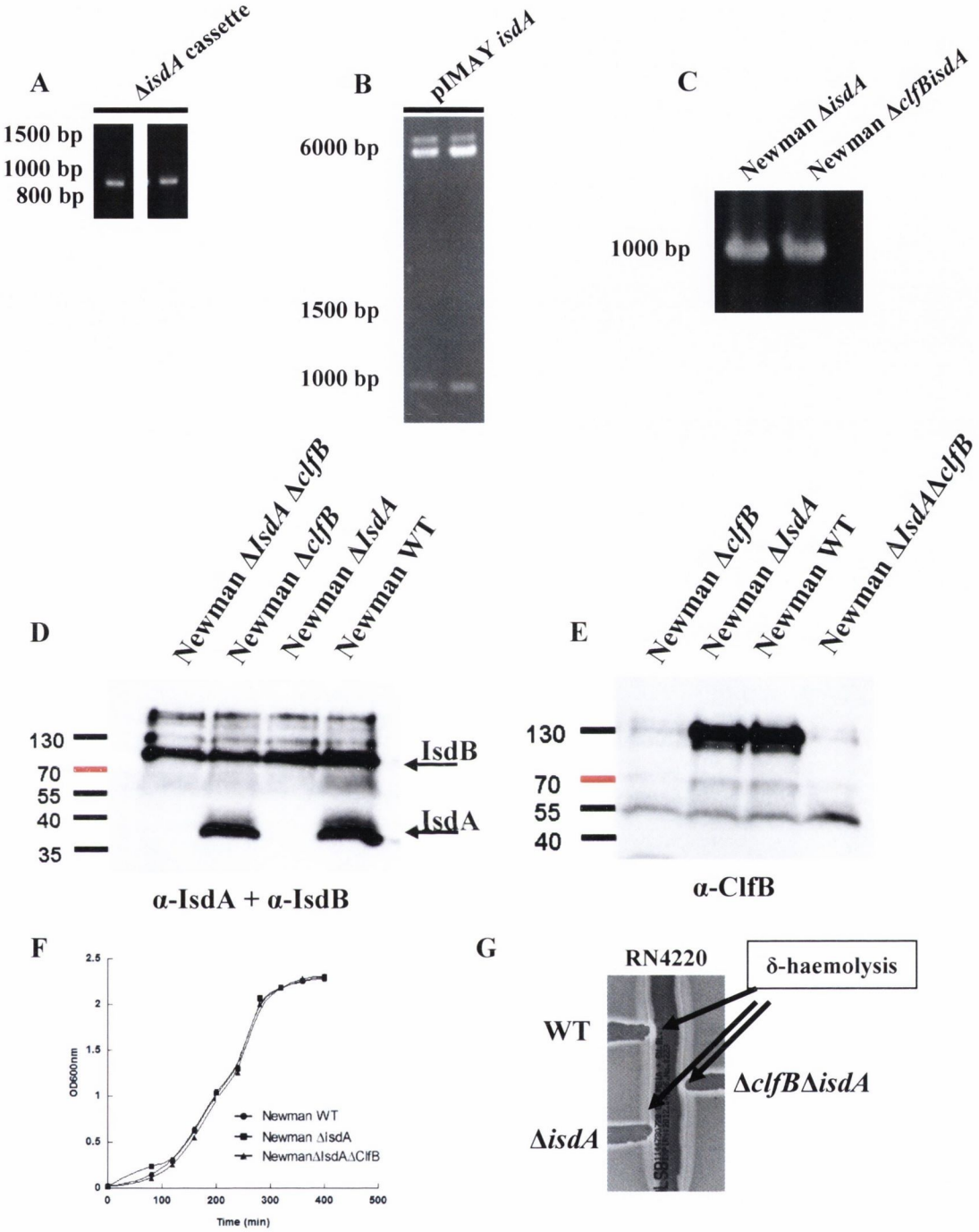

Figure 3.10. Construction and validation of *isdA* mutation in *S. aureus* Newman and *S. aureus* Newman *clfB*. The *isdA* mutation construct (Δ*isdA* cassette) was amplified **(A)** and cloned into pIMAY (pIMAY *isdA*) **(B).** The mutation was confirmed by PCR-amplification of the mutation construct from genomic DNA **(C),** Western immunoblotting of cultures grown in RPMI using anti-IsdA IgG, anti-IsdB IgG **(D)** and anti-ClfB IgG **(E),** growth rate in TSB **(F)** and haemolytic profile on 5% sheep blood agar **(G).** Haemolysis is indicated by black arrows.

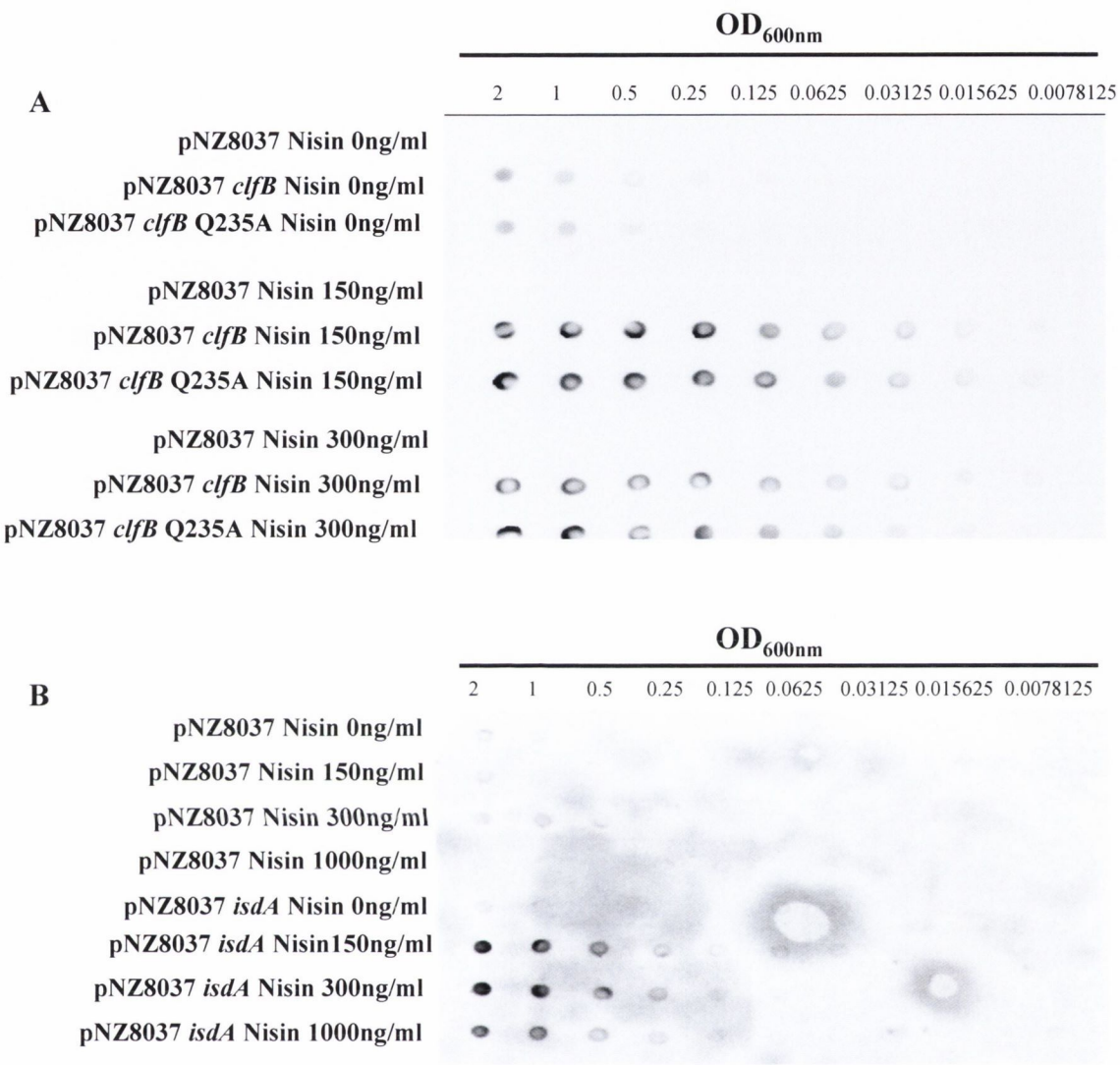

Figure 3.11. Validation of nisin-inducible expression of proteins from *Lactococcus lactis*. The expression of ClfB **(A)** and IsdA **(B)** from the nisin-inducible vector pNZ8037 in *L. lactis* was verified by whole cell dot immunoblotting. Bacteria incubated with increasing concentrations of nisin were dotted onto nitrocellulose membranes and were compared to an empty vector control. Each membrane was probed with anti-ClfB IgG **(A)** or anti-IsdA IgG **(B)** followed by protein A-peroxidase.

3.3 Discussion

The study of *S. aureus* virulence mechanisms requires the generation of isogenic mutations in chromosomal genes and the production of recombinant bacterial and host proteins, in order to identify important virulence factors and to define their interaction with host ligands. This chapter describes the construction and production of recombinant affinity-tagged proteins in order to perform *in vitro* analysis of the interaction between ClfB and loricrin and to define the mechanism involved in comparison to other ligands. Furthermore, a spontaneous streptomycin resistant mutant was isolated and validated in *S. aureus* strains Newman and SH1000 for use in animal studies. Finally, this chapter describes the isolation and validation of deletion mutations in the *clfB* and *isdA* genes of *S. aureus* Newman and SH1000 by allelic replacement using the temperature-sensitive plasmid pIMAY.

The production of recombinant proteins using expression systems in *E. coli* enables *in vitro* analysis of protein-ligand interactions, and identification of the mechanisms and binding motifs involved between bacterial and host proteins. The minimal ligand-binding region of ClfB has previously been identified using recombinant studies (Perkins *et al.* 2001). In this chapter, a more stable recombinant variant of the minimal binding region of ClfB was constructed and purified in order to perform *in vitro* analysis of the interaction between ClfB and its potential ligand, loricrin. Furthermore, two truncated variants of ClfB lacking the lock region and latching peptide were produced in order to analyse the binding mechanism involved during the interaction between ClfB and its ligands. This interaction and mechanism is analysed in detail in Chapter 4.

The human cornified envelope protein loricrin has been identified as a potential ligand for ClfB on the surface of squames. In order to define this interaction, recombinant human loricrin was produced. Previously human loricrin has been purified from the vector pET11a carrying human loricrin cDNA using a method of purification involving repeated dialysis of the crude *E. coli* lysate at a pH where only loricrin is soluble (Candi *et al.* 1995). This method was time-consuming and the resulting untagged protein was obtained at

a low yield and at varying levels of purity. In order to produce large amounts of loricrin at a higher level of purity using a simple method of purification, the *lor* gene was synthesized commercially and was subcloned into a pGEX expression vector. Previous attempts to amplify the gene from *lor* cDNA resulted in many substitution mutations, possibly due to the GC-rich and repetitive nature of *lor* DNA. This was rectified by commercially acquiring DNA that was codon-optimized for expression in *E. coli*. The resulting recombinant protein was produced more easily at a higher level of purity. However, the protein was not expressed at a high yield, possibly due to the insoluble nature of the protein or because it is toxic to the *E. coli* cell (Candi *et al.* 1995). Individual omega-loop regions of loricrin were also constructed as well as human and murine keratin constructs.

ClfB has previously been implicated in adherence to squames and in nasal colonisation by *S. aureus* (Clarke *et al.* 2006; Schaffer *et al.* 2006; Corrigan *et al.* 2009). In order to investigate ClfB-mediated bacterial attachment to recombinant loricrin *in vitro*, to human squames *ex vivo* and in a murine model of nasal colonisation, an isogenic *clfB* deletion mutant was generated in *S. aureus* by allelic replacement using pIMAY. This validated, stable deletion allowed the identification of the role played by ClfB and loricrin in nasal colonisation discussed in detail in Chapter 4 and 5.

Nasal colonisation is a multifactorial process in which many proteins have been shown to play a role. The role of the multi-ligand binding protein IsdA in nasal colonisation has been demonstrated *in vivo* in a cotton rat model (Clarke *et al.* 2006). It also facilitates adherence to squames and binds to recombinant loricrin (Clarke *et al.* 2006; Clarke *et al.* 2009). In order to investigate the interaction between loricrin and IsdA *in vivo*, an isogenic *isdA* deletion mutant was introduced in *S. aureus* by allelic replacement using pIMAY. Furthermore, a double *ΔclfBΔisdA* deletion mutant was constructed in *S. aureus* Newman using the same method, in order to assess the relative contributions of IsdA and ClfB in *S. aureus* adherence to loricrin and to human squames. This is discussed in detail in Chapter 6.

Spontaneous mutations in the *agr* locus may occur when bacteria are subjected to stressful conditions, such as the temperature shift involved when using temperature-sensitive plasmids in mutagenesis studies. These secondary mutations can be detected by assessing δ-haemolysin production by the organism. *S. aureus* produces four types of haemolysin, namely α-, β-, δ- and γ-toxins. α-, β- and δ-haemolysin production can each be detected by zones of lysis on sheep blood agar (SBA). δ-haemolysin is strongly upregulated by the accessory gene regulator (Agr) two-component quorum-sensing system. The Agr system is a global regulator of proteins associated with virulence in *S. aureus*. It is activated in the late-exponential phase of growth. The *agr* locus produces two divergent transcripts known as RNAII and RNA III, initiated from the P2 and P3 promoters, respectively (Novick *et al.* 1993; Novick *et al.* 1995). RNAIII functions as the regulatory signal of the Agr system and regulates the transcription of many target genes. It also encodes δ-haemolysin.

δ-haemolysin produces a weak zone of haemolysis on SBA, but is highly synergistic with β-haemolysin. The mutant strains described in this chapter were cross-streaked against *S. aureus* strain RN4220 along with their corresponding parental strains, in order to assess δ-haemolysin production. RN4220 only produces β-haemolysin, which forms a turbid zone of incomplete lysis around growth of the organism on sheep blood agar. A pronounced zone of clear haemolysis was observed where β-haemolysin and δ-haemolysin interact, due to the synergistic nature of the two toxins. All mutants produced the same level of δ-haemolysin as their parental strains, indicating that no secondary *agr* mutations were present.

Previous staphylococcal nasal colonisation studies have shown that the administration of streptomycin prior to inoculation results in more consistent levels of colonisation by reducing interference from the endogenous nasal flora (Kiser *et al.* 1999; Park *et al.* 2011). In this study, spontaneous streptomycin resistant mutants of *S. aureus* Newman and SH1000 were isolated prior to any subsequent genetic manipulation. This single-site mutation was validated and shown to be stable. The acquired resistance to streptomycin allows easy selection of bacterial inoculum retained in the nose.

Chapter 4

Analysis of the interaction between clumping factor B and loricrin

4.1 Introduction

The surface protein ClfB plays a critical role in squame adhesion and nasal colonisation by *S. aureus* (Clarke *et al.* 2006; Schaffer *et al.* 2006; Corrigan *et al.* 2009). ClfB is a member of a family of proteins that are structurally related to clumping factor A (ClfA), the archetypal fibrinogen (Fg) binding protein of *S. aureus*. It is attached covalently to peptidoglycan in the cell wall by sortase. The N-terminal 542 residues comprise the ligand-binding A domain followed by a flexible stalk formed by repeats of the dipeptide serine-aspartate. The A domain is composed of three separately folded subdomains N1, N2 and N3, the last two of which are the minimum region of the protein required for binding to fibrinogen (Fg) and cytokeratin 10 (K10) (Perkins *et al.* 2001; Ganesh *et al.* 2011; Xiang *et al.* 2012).

The first ligand discovered for ClfB was the blood glycoprotein Fg. The binding site for ClfB in Fg is a single repeat (number 5) in the αC region of the α-chain (Walsh *et al.* 2008). In addition, ClfB binds to the C-terminus of cytokeratin 10 (K10), a region composed of quasi repeats of the amino acid sequence $Y[GS]_nY$ (O'Brien *et al.* 2002). This type of Glycine-serine-rich sequence can form omega loops, resulting in the GS sequences protruding as loops forming rosette-like structures (Leszczynski and Rose 1986; Zhou *et al.* 1988). One such omega loop sequence (YGGGSSGGGSSSGGGY) was shown to bind to recombinant ClfB A domain with a K_D in the low micromolar range (Walsh *et al.* 2004).

Omega loops can be defined as segments of a polypeptide that change direction over the course of 6 or more residues, and where the ends of the segment are close together in 3-dimensional space. The protein segment follows a lariat or loop pattern, similar to the Greek letter Ω. They are found almost exclusively at the protein surface, often clustered at one part of the protein molecule (Leszczynski and Rose 1986). Typical Ω loops are 6-16 residues in length and have few hydrophobic residues within the putative loop. However tryptophan is commonly found at the beginnings and ends of loops (Pal and Dasgupta 2003). Amino acids most commonly found in omega loops include glycine, cysteine, serine and proline. Tyrosine is also present but not as

frequently. Hydrophobic residues such as phenylalanine and methionine are much less common (Leszczynski and Rose 1986). Omega loops have been shown to play a role in protein function by acting as substrate recognition sites, as inhibitors or ligand-binding sites. They can confer substrate specificity in certain enzymes and can serve as ligand-binding sites in specific protein interactions. Omega loops can also act as "lids" over active sites, with the ability to block or expose the site by becoming mobile. Omega loop involvement in protein folding has been widely reported (Fetrow 1995).

In vitro studies have identified K10 as an important ligand for ClfB (O'Brien *et al.* 2002; Walsh *et al.* 2004). These results have been extrapolated to assume that an interaction between ClfB and K10 on the desquamated epithelial cells facilitates *S. aureus* nasal colonisation. However, this remains only an association and has not been proven unambiguously. To date the host ligand targeted by ClfB to facilitate its interaction with the nasal epithelium *in vivo* remains to be established. K10 constitutes approximately 13% of the cornified envelope of squames and has been determined to be surface-exposed (Steven and Steinert 1994; O'Brien *et al.* 2002). The cornified envelope (CE) protein loricrin encompasses up to 80% of the cornified envelope and has been revealed to be surface-exposed on human cornified epithelial cells (Lopez *et al.* 2007) and on squames in this study (Chapter 5). Moreover, the structure of loricrin consists of 3 major omega loop regions, similar to those found in the tail region of K10. Located between the loop domains and also at the N- and C-termini are stretches rich in glutamate and cysteine residues that form covalent links to other proteins in the CE by transglutamination and disulfide bond formation (Yoneda *et al.* 1992; Candi *et al.* 1995). The omega loop-rich structure of loricrin and its high occurrence in the CE of desquamated epithelial cells identifies it as a potentially important target for ClfB binding during *S. aureus* nasal colonisation. Furthermore, unpublished data from Walsh and Foster provided evidence of an *in vitro* interaction between ClfB and loricrin, suggesting that it is another potential target for ClfB.

The human loricrin gene can undergo natural polymorphisms resulting in size and sequence variants of the protein. One polymorphism has been localised

to the second major loop region. This 12bp nucleotide deletion results in a 4-amino acid deletion in the loop region, causing size variation in the protein and sequence variation within loop region 2. Size alleles segregate by normal Mendelian processes and an individual may carry both alleles at one time. The carboxy terminus of human cytokeratin is similarly polymorphic (Yoneda *et al.* 1992).

Recently the X-ray crystal structures of both the apo form of ClfB N2N3 and the protein in complex with peptides mimicking the binding domains in Fg and K10 were solved (Ganesh *et al.* 2011; Xiang *et al.* 2012). These studies demonstrated that the two seemingly disparate proteins contain related peptides that can bind in a hydrophobic trench located between the separately folded N2 and N3 domains. These studies confirmed earlier predictions that ClfB bound its ligands by the "dock, lock and latch" mechanism first defined for the Fg binding proteins SdrG and ClfA (Ponnuraj *et al.* 2003; Bowden *et al.* 2008). After the peptide inserts into the ligand-binding trench between the N2 and N3 domains, a C-terminal extension of domain N3 undergoes a conformational change, covers the inserted peptide and binds residues in N2 by β-strand complementation which locks the peptide in place.

In this chapter, the binding affinity of ClfB for its ligands was measured using an analytical technique called surface plasmon resonance (SPR). The phenomenon of SPR occurs in thin conducting films placed between two media of differing refractive indices. In the Biacore system, a thin gold layer on the sensor chip acts as the conducting film between the sample on the sensor chip (ligand) and the sample in solution (analyte). When polarised light is focused on this gold surface at a certain angle, it excites electrons in the gold film forming surface plasmons, accompanied by a drop in the intensity of reflected light off the gold surface. An interaction between the ligand and analyte causes a change in mass on the chip surface, causing the angle of light at which SPR occurs to shift due to a change in refractive index on the surface of the chip. This shift is measured and depicted in a sensorgram, where one response unit (RU) corresponds to 0.0001° shift in SPR angle.

In SPR, affinity and kinetics can be measured in two ways, using a multi-cycle approach or a single-cycle approach. In a multi-cycle kinetics assay, doubling dilutions of analyte are passed over the ligand-coated chip. Each concentration cycle has its own association and dissociation phase. The ligand has to be captured on the chip before each concentration cycle and the chip has to be regenerated after each concentration cycle. Single-cycle kinetics allows kinetic analysis when it is difficult to find optimal regeneration conditions. In this type of assay, 5 concentrations of analyte can be passed over the chip in a single cycle. The ligand is captured on the chip only once, the chip is only regenerated once and there is only one dissociation phase. Ligand capture levels on the chip remain constant because there is no repeated capture and regeneration step between different concentrations of analyte (Onell and Andersson 2005; Karlsson *et al.* 2006).

The advantage of SPR analysis is that the response for an interaction is measured in real time rather than obtaining a result from the end-point of an ELISA-based binding assay. SPR also measures a more accurate affinity between binding partners for many reasons. Firstly, tagged ligands captured on a chip will not be subject to steric hindrance in SPR analysis. Secondly, fast or slow association rates are not accounted for in solid phase binding assays. For example, an accurate affinity measurement will not be obtained in a solid phase binding assay if the association between binding partners is very slow, whereas in SPR analysis the assay can be optimized to account for this and a reliable result can be achieved. Finally, SPR analysis provides the opportunity to perform kinetic analysis on ligand-analyte binding interactions.

In this chapter, an interaction between ClfB and loricrin was determined and examined in detail. Adherence of *S. aureus* and *L. lactis* expressing ClfB to immobilized human and murine loricrin were tested. The affinity of recombinant ClfB for human and murine loricrin for K10 and Fg was measured by SPR. Several putative ClfB-binding regions were identified within loricrin and the affinity of each loop was measured. A lock-latch mutant was isolated and tested for binding to loricrin, K10 and fibrinogen, to determine whether the "dock, lock and latch" mechanism is responsible for ligand binding.

Furthermore, inhibition studies were performed to determine if loricrin and K10 are bound by the same region of ClfB.

4.2 Results

4.2.1 *S. aureus* adherence to human and murine loricrin is ClfB-dependent.

In order to determine whether *S. aureus* interacts with human loricrin and whether this depends on expression of ClfB, *S. aureus* Newman and ClfB-deficient mutant Newman Δ*clfB* were tested for adhesion to immobilized recombinant human and murine loricrin (HLor, MLor) and to human and murine K10 peptides (HK10, MK10). *S. aureus* Newman adhered avidly and dose-dependently to all ligands (Figure 4.1 A, B). *S. aureus* Newman Δ*clfB* did not adhere detectably to HLor and MLor, indicating that adherence to loricrin is facilitated by ClfB. To establish if ClfB alone can promote bacterial adhesion to immobilized loricrin, adhesion assays were performed using *L. lactis* MG1363 carrying a plasmid that expressed ClfB (pKS80:*clfB*) and compared to *L. lactis* carrying the empty vector. *L. lactis* (pKS80:*clfB*) adhered strongly to each of the proteins indicating that ClfB alone is sufficient for promoting bacterial adhesion to loricrin.

In order to compare adhesion of *S. aureus* to each ligand, single-point binding of *S. aureus* to each ligand was tested (Figure 4.2). Again, *S. aureus* adhered strongly to HLor, MLor, HK10 and MK10. *S. aureus* Δ*clfB* did not adhere detectably to HLor and MLor, and displayed significantly reduced adherence to HK10 and MK10. This is in agreement with a previous observation that Newman appears to have a second, albeit less potent, K10 adhesin (O'Brien *et al.* 2002). Complementation of *S. aureus* Newman Δ*clfB* with pCU1:*clfB* restored adherence to HLor (Figure 4.3). These data show that loricrin is a ligand for ClfB.

4.2.2. Recombinant ClfB N2N3 binds to recombinant human loricrin.

In order to demonstrate a direct interaction between ClfB and loricrin, recombinant ClfB was tested for binding to recombinant loricrin in ELISA-type binding assays. Previous studies have indicated that the minimum Fg and K10 binding region of ClfB comprises the N2 and N3 subdomains. Recombinant ClfB $N2N3_{201\text{-}542}$ was constructed and expressed with an N-terminal hexahistidine tag. Doubling concentrations of rClfB were incubated with

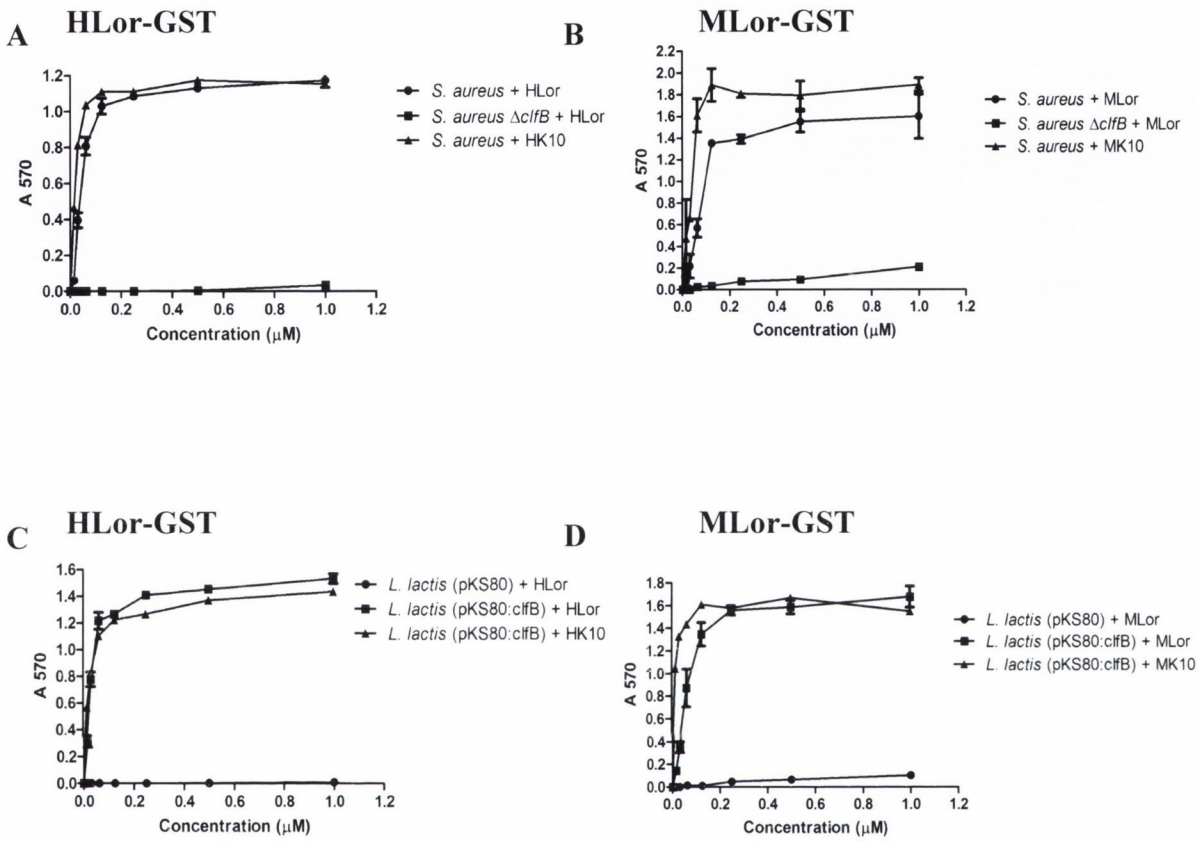

Figure 4.1 Bacterial adherence to loricrin. *S. aureus* Newman, Newman Δ*clfB* (A, B), *L. lactis* MG1363 (pKS80) and *L. lactis* MG1363 (pKS80:*clfB*) (C, D) were tested for binding to ligands immobilized on 96-well plates. Bacteria were added to wells coated with doubling dilutions of immobilized GST-tagged recombinant human loricrin (Hlor, A, C) and murine loricrin (Mlor, B, D). Human K10 peptide (HK10) and murine K10 peptide (MK10) were used as positive controls. Bacterial adherence was measured by staining with crystal violet and measurement of the absorbance at 570nm. Values represent the mean ± SD of triplicate wells. The data shown is representative of three individual experiments.

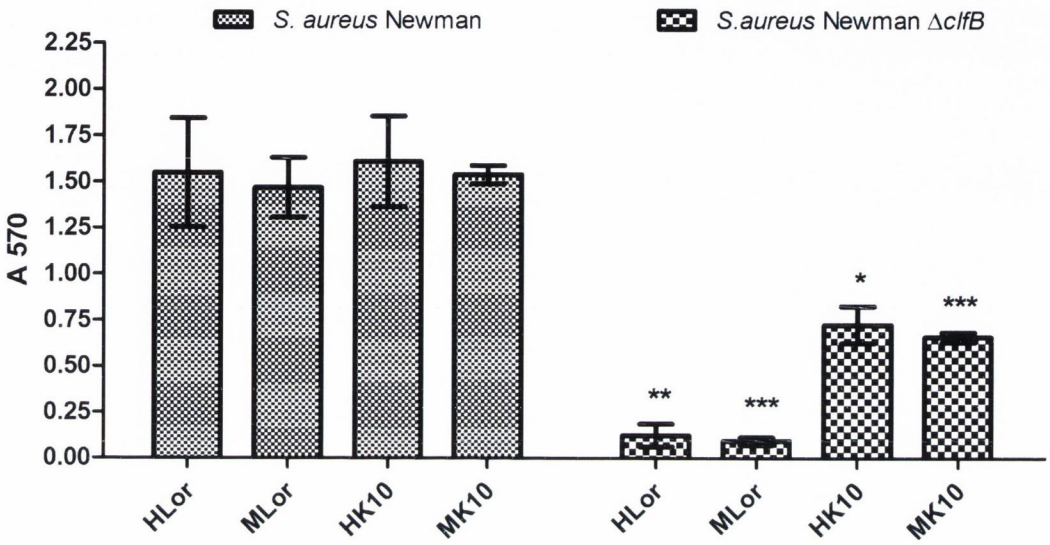

Figure 4.2 ClfB-promoted adherence of *S. aureus* Newman to loricrin and keratin. *S. aureus* Newman and Newman Δ*clfB* were tested for binding to ligands immobilized on 96-well plates. Bacteria were added to wells coated with immobilized GST-tagged recombinant human loricrin (Hlor), murine loricrin (MLor)) human K10 peptide (HK10) and murine K10 peptide (MK10)) (1μM). Bacterial adherence was measured by staining with crystal violet and measurement of the absorbance at 570nm. Values represent the mean ± SD of triplicate wells. The data shown is representative of two individual experiments. Statistical analysis was performed using an unpaired t test. * $p<0.05$, ** $p<0.005$, ***$p<0.0005$ versus binding of ClfB-expressing bacteria.

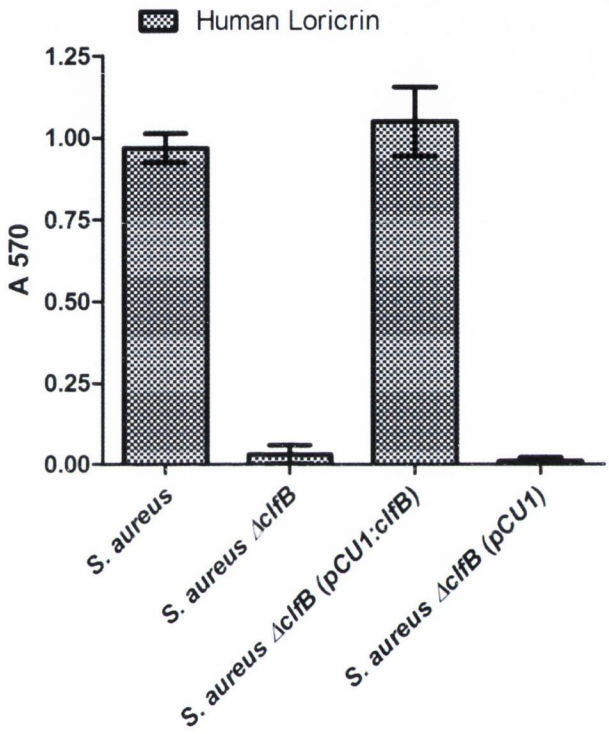

Figure 4.3 Complementation of the *clfB* mutation. *S. aureus* Newman, Newman Δ*clfB*, Newman Δ*clfB* (pCU1:*clfB*) and Newman Δ*clfB* (pCU1) were grown to exponential phase and added to wells coated with immobilized GST-HLor (1 μM). Bacterial adherence was detected by staining with crystal violet and measurement of the absorbance at 570nm. Values represent the mean ± SD of triplicate wells. The data shown is representative of 2 individual experiments.

immobilized HLor, HK10, MK10 and the minimal ClfB-binding region of fibrinogen ($Fg\alpha_{316-367}$) (Figure 4.4). ClfB bound to each ligand in a dose-dependent and saturable manner. The estimated half-maximum binding concentration of ClfB for HLor, HK10, MK10 and Fg were 131nM, 130nM, 220nM and 335nM, respectively. These results indicate that ClfB binds directly to human loricrin with a similar affinity to its other known ligands.

In order to confirm a direct interaction between ClfB and loricrin and to measure the affinity of binding, surface plasmon resonance (SPR) was employed. Initially, SPR analysis was performed using multicycle kinetics. This analysis method is time consuming and stable regeneration conditions were difficult to optimize. Regeneration conditions that are too harsh can damage the chip and lead to reduced ligand-capture levels with each concentration cycle. Furthermore, regeneration conditions that are too mild can cause the chip to not be completely stripped of ligand after each concentration cycle. Both problems with regeneration occurred while using multicycle kinetics analysis for ClfB and the resulting data was unreliable. SPR was repeated using single cycle kinetics analysis. Suitable regeneration conditions were established easily with this method and assays performed using single cycle kinetics produced more reliable results.

HLor was captured on the surface of a sensor chip that had been coated with anti-GST IgG. Increasing concentrations of $rClfB_{201-542}$ were passed over the surface of the HLor-coated chip. $rClfB_{201-542}$ bound to HLor in a concentration-dependent manner (Figure 4.5 A). From analysis of the equilibrium binding data the dissociation constant (K_D) of the interaction between $rClfB_{201-542}$ and loricrin was determined to be 4.33 ± 1.1 μM. Similar experiments carried out with MLor showed that ClfB displayed a slightly lower affinity for this ligand (K_D = 15.66 ± 3.4 μM, Figure 4.5 B). The affinity of $rClfB_{201-542}$ for HK10, MK10 and $Fg\alpha_{316-367}$ was determined by the same method. Again, rClfB bound to each ligand in a concentration-dependent manner (Figure 4.6). rClfB bound HK10 and MK10 with a similar affinity as it did to HLor and MLor (7.89±2.10 μM and 14.38±3.0 μM, respectively). The K_D measured for GST-$Fg\alpha_{316-367}$ was 5.25 μM, in the same low μM range as the

other ligands. These data indicates that ClfB has a similar affinity for loricrin, K10 and the αC-region of Fg.

4.2.3 Localisation of ClfB-binding sites within loricrin.

Loricrin is composed of three major Gly-Ser-rich regions capable of forming omega loops (Hohl 1991; Candi *et al.* 1995). In order to determine whether loricrin contains any ClfB-specific binding sites, DNA encoding each major loop region was synthesized and was cloned into a pGEX vector allowing expression and purification of GST-tagged proteins. Loop regions 1A, 1B, 2, 2v and 3 were each tested for binding by ClfB (Figure 4.7). rClfB bound L2v most avidly, with an estimated half-maximum binding value of 30 nM. It bound L3 and L2 with the next highest affinity displayed approximate half-maximum binding concentrations of 190 nM and 300 nM, respectively. ClfB bound L1A and L1B with the weakest affinity, exhibiting half-maximum binding concentrations of 1.2 μM and 33 μM, respectively. These data indicates that loricrin contains multiple binding sites for ClfB and that ClfB binds most strongly to the second major loop region.

SPR was also used to identify binding sites within human loricrin and to determine the affinity of each interaction. The affinity of ClfB $N2N3_{201\text{-}542}$ for loop regions 1A, 1B, 2, 2v and 3 was measured and the results are summarized in Table 4.1. ClfB bound loop region 2v and 2 with the highest affinity (K_D = 2.21 ± 1.1 μM and 3.31 ± 0.81 μM respectively). Loop region 1B had the lowest affinity for ClfB (34.48 ± 2.70 μM). These data confirm that loricrin contains more than one binding site for ClfB and that the highest affinity binding site is present within loop region 2.

In order to localise a specific ClfB-binding loop region, the ability of rClfB to bind to loop region 2 was further investigated. Loop region 2 can be divided into 2 major sub-loop regions, designated D1 and D2 (Figure 1.9). The size variation that occurs in loricrin has previously been localised to D2. Therefore, two variants of D2 were synthesized to account for the 4-amino acid deletion that occurs in this region and were designated D2 and D2v. D2v contained the 4-amino acid deletion. rClfB was tested for binding to each sub-

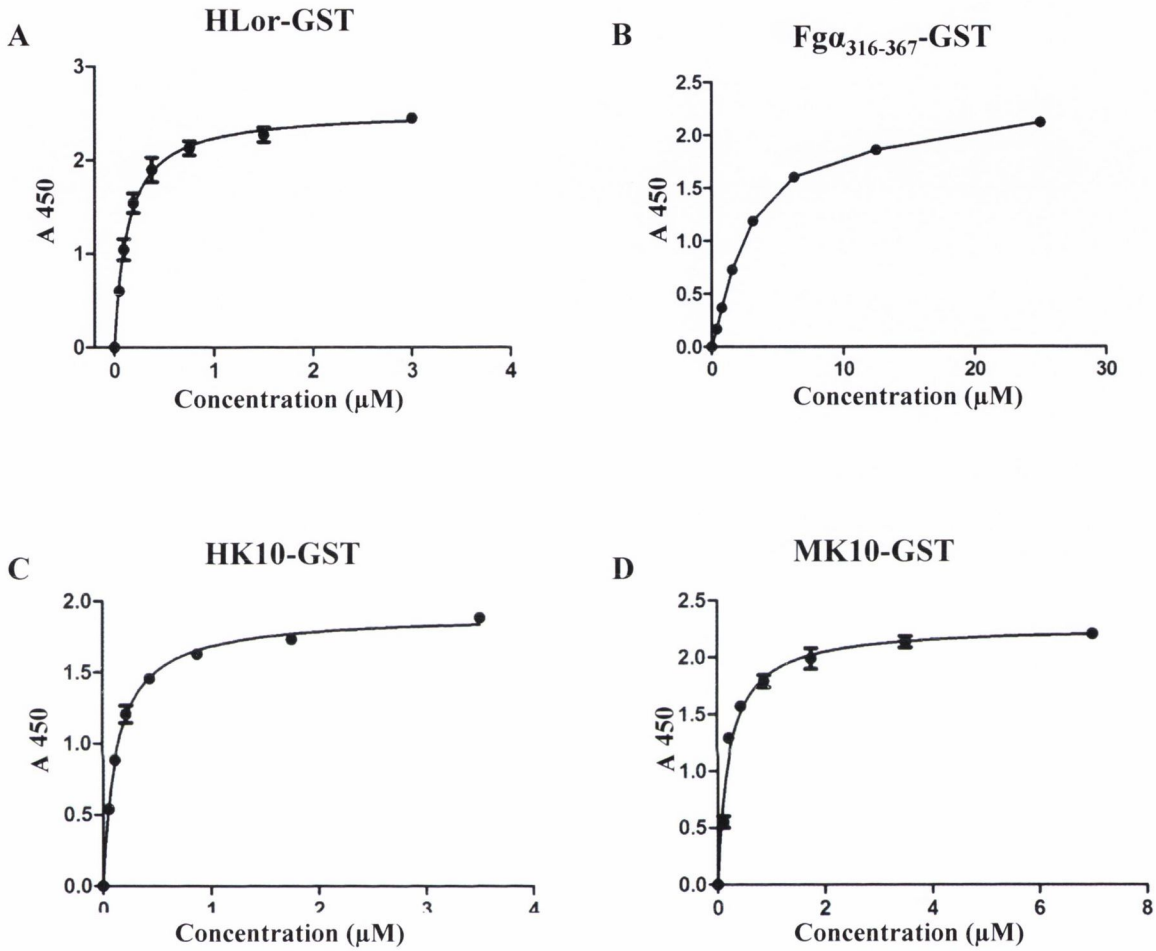

Figure 4.4 Binding of recombinant ClfB $N2N3_{201-542}$ to human loricrin. Increasing concentrations of ClfB $N2N3_{201-542}$ were added to microtitre wells containing immobilized GST-Hlor, (A), GST-Fg316-367 (B), GST-HK10 (C) and GST-MK10 (D) (1μM). PBS was used as a control. Bound ClfB was detected using HRP-labelled anti-His antibody and developed by incubation with a chromogenic substrate. The absorbance at 450 nm was determined. Values represent the mean ± SD of triplicate wells. The data shown is representative of 3 individual experiments.

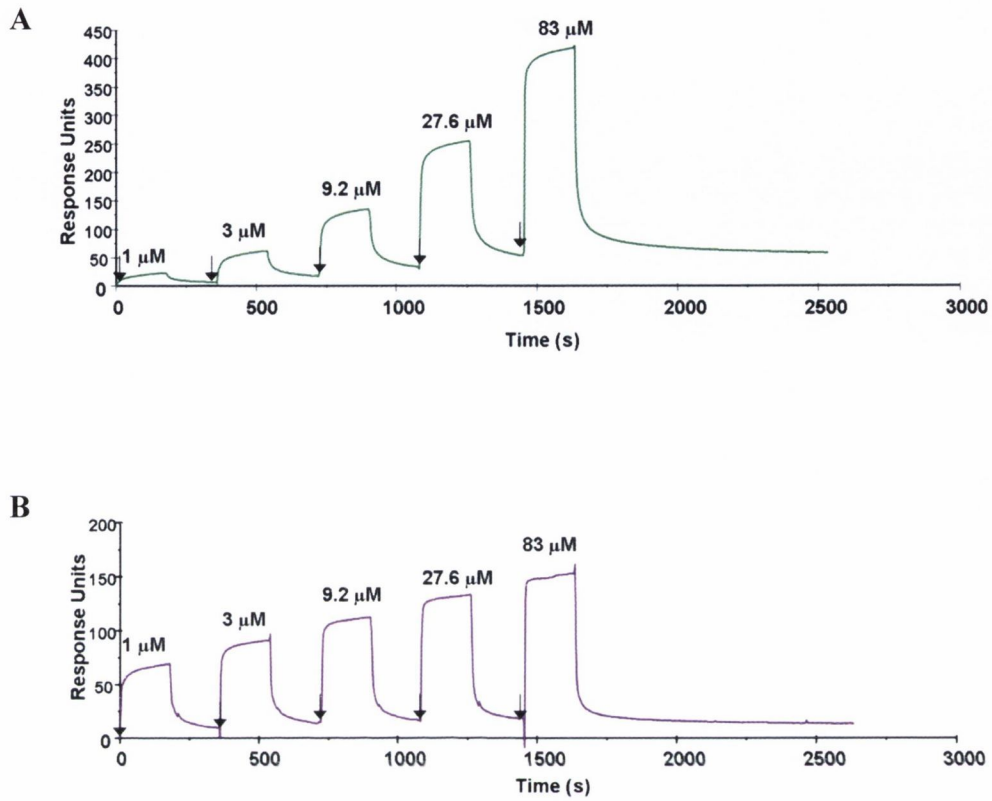

Figure 4.5 Surface Plasmon Resonance analysis of the interaction of ClfB with loricrin. Representative sensorgrams display binding of $rClfB_{201-542}$ to and dissociation from (A) GST-Hlor and (B) GST-MLor in a single cycle kinetics assay. GST-tagged ligands were captured onto a CM5 chip coated with anti-GST IgG and were exposed to increasing concentrations of $rClfB_{201-542}$. Binding is measured as response units (RU) against time. The affinities were calculated from curve fitting to a plot of the RU values against concentrations of $rClfB_{201-542}$. Arrows indicate the time at which $rClfB_{201-542}$ is injected. The data shown is representative of 3 individual experiments.

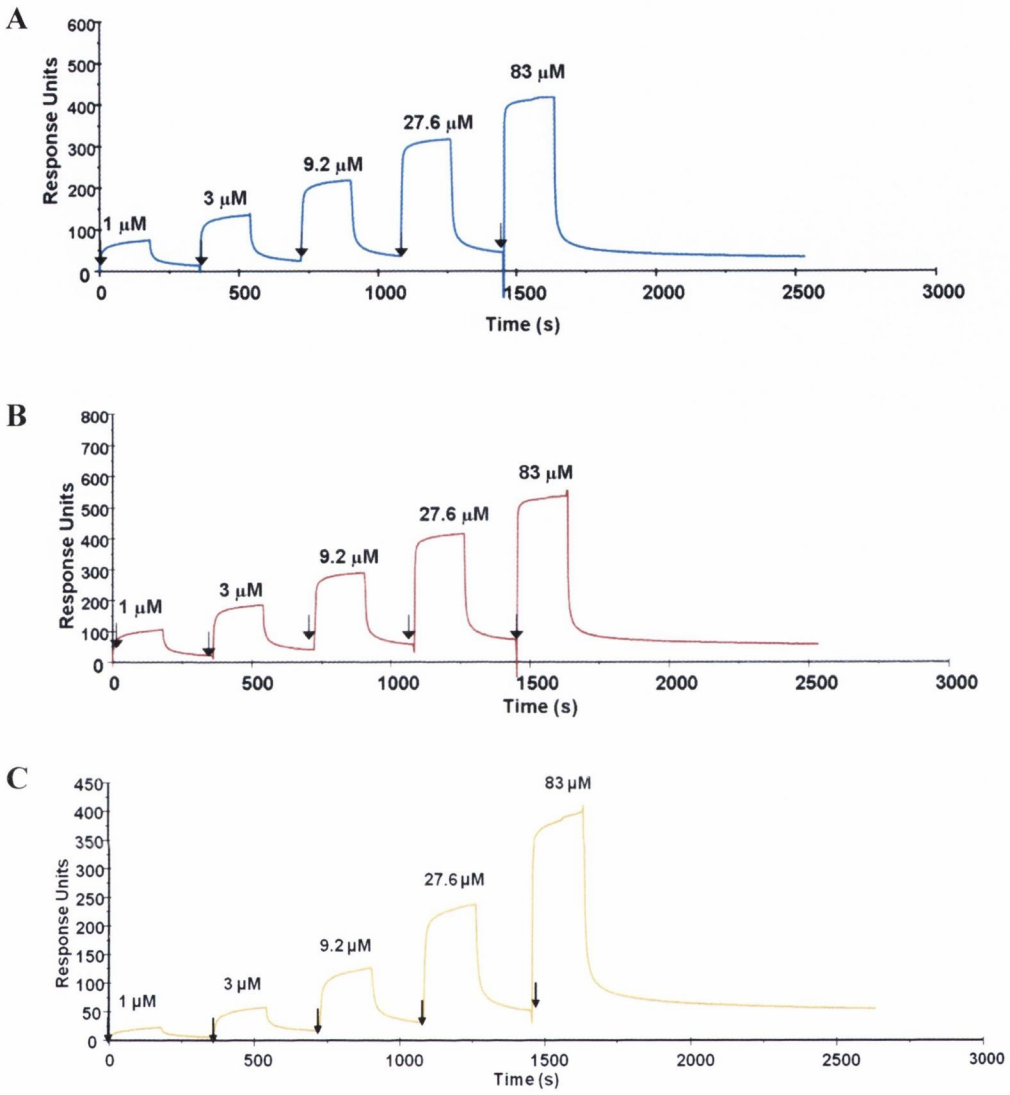

Figure 4.6 Surface Plasmon Resonance analysis of the interaction of ClfB with keratin and fibrinogen. Representative sensorgrams display binding of $rClfB_{201-542}$ to and dissociation from (A) GST-HK10 (B) GST-MK10 and (C) GST-$Fg\alpha_{316-367}$ in a single cycle kinetics assay. GST-tagged ligands were captured onto a CM5 chip coated with anti-GST IgG and were exposed to increasing concentrations of $rClfB_{201-542}$. Binding is measured as response units (RU) against time. The affinities were calculated from curve fitting to a plot of the RU values against concentrations of $rClfB_{201-542}$. Arrows indicate the time at which $rClfB_{201-542}$ is injected. The data shown is representative of 3 individual experiments.

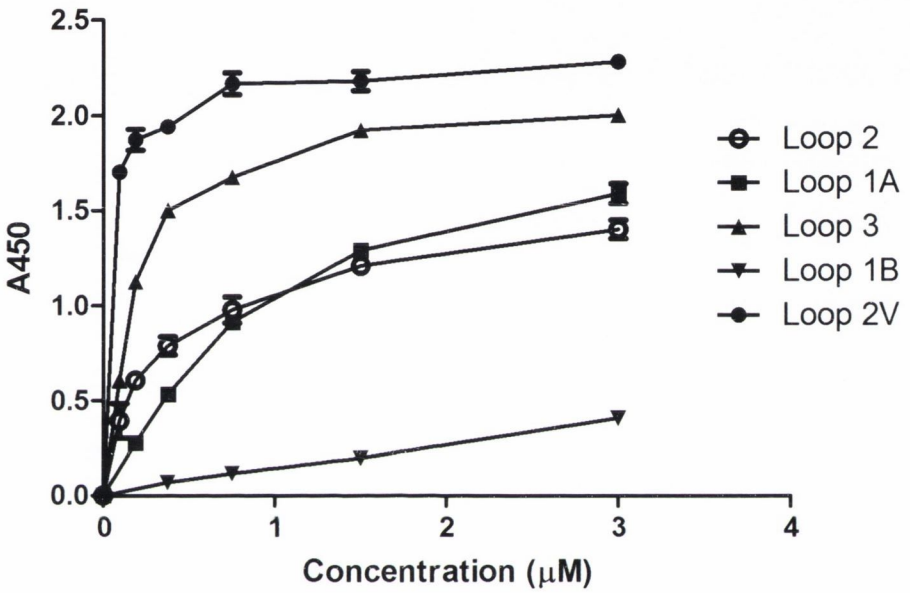

Figure 4.7 ClfB-binding to omega-loop regions within loricrin. Recombinant ClfB $N2N3_{201-542}$ was tested for binding to individual GST-tagged loricrin loop regions 1A, 1B, 2, 2v and 3. Increasing concentrations of rClfB $N2N3_{201-542}$ were added to microtitre wells containing each immobilized ligand (1 μM). Bound ClfB was detected using anti-His IgG and developed by incubation with a chromogenic substrate. Each point represent the mean ± SD of triplicate wells. The data shown is representative of 3 individual experiments.

Table 4.1. Affinities of ClfB $N2N3_{201-542}$ for loricrin, keratin and fibrinogen using surface plasmon resonance.

GST-Tagged Protein	K_D (μM)±SE
HLor	4.33±1.10
MLor	15.66±3.40
HK10	7.89±2.10
MK10	14.38±3.0
$Fg\alpha_{316-367}$	5.25±1.5
Loricrin Loop Region 2v	2.21±1.10
Loricrin Loop Region 2	3.31±0.81
Loricrin Loop Region 3	5.47±1.40
Loricrin Loop Region 1A	16.70±2.30
Loricrin Loop Region 1B	34.48±2.70

domain. Each sub-domain was bound in a dose-dependent manner (Figure 4.8). ClfB appeared to bind D1 with the weakest affinity, with an approximate half-maximum binding value of 28 μM. Although ClfB appeared to bind D2v more strongly than D2, the half-maximum binding concentration was similar for each ligand (225nM, 825nM, respectively). This data indicates that a specific ClfB-binding site within loop region 2 can be localised to the second major loop.

4.2.4 ClfB lock-latch mutants display impaired binding to loricrin, keratin and fibrinogen.

ClfB binds keratin and fibrinogen using the "dock, lock and latch" mechanism (Xiang *et al.* 2012). In order to determine whether ClfB also binds loricrin using this mechanism, two ClfB N23 lock-latch mutants were constructed by inverse PCR. In the first mutant, the amino acids 522-542 were excluded, removing the extended latching peptide and lock region, as well as a 5 amino acid region in the N3 domain (ClfB $N2N3_{201-521}$). W_{522} has been previously shown to make contact with ligands in the ClfB binding trench (Ganesh *et al.* 2011). In the second mutant, amino acids 527-542 were excluded, removing the lock and latching peptide only (ClfB $N2N3_{201-526}$). Different concentrations of each mutant were tested for binding to HLor, $Fg\alpha_{316-367}$, HK10 and MK10. rClfB $N2N3_{201-526}$ bound to each ligand in a dose-dependent manner (Figure 4.9). However, binding was impaired compared to binding by full length wild-type ClfB $N2N3_{201-542}$ for all ligands except HK10. The approximate half-maximum binding concentration for ClfB $N2N3_{201-526}$ binding to HLor, MK10 and Fg was 15 μM, 3.8 μM and 3.5 μM, respectively. This data indicates that ClfB $N2N3_{201-526}$ binds each ligand less avidly than ClfB $N2N3_{201-542}$. There was no observed decrease in binding to HK10 by ClfB $N2N3_{201-526}$ compared to ClfB $N2N3_{201-542}$. ClfB $N2N3_{201-521}$ was unable to bind any of the ligands effectively (data not shown), confirming that the amino acid W_{522} is essential for ClfB binding activity.

The binding ability of ClfB $N2N3_{201-526}$ was further analysed using SPR. Increasing concentrations of ClfB were passed over a chip coated with HLor, HK10, MK10 or Fg. SPR analysis showed that ClfB $N2N3_{201-526}$ bound each ligand with a similar affinity seen using ClfB $N2N3_{201-542}$ (Table 4.2). Together,

the results obtained here indicate that the presence of the latching peptide in ClfB is not essential to facilitate binding to keratin, loricrin and fibrinogen. However it is required for efficient, maximal binding, suggesting that the "dock, lock and latch" mechanism is employed for binding to these ligands.

4.2.5. Inhibition of *S. aureus* adherence and recombinant ClfB binding to loricrin and keratin.

The ClfB-binding HLor region L2v and HK10 were used in inhibition studies in order to provide further evidence that ClfB uses the "dock, lock and latch" mechanism to bind loricrin as well as keratin. *S. aureus* was pre-incubated with increasing concentrations of recombinant HK10 or L2v. Adherence of *S. aureus* pre-incubated with HK10 to loricrin was inhibited dose-dependently (Figure 4.10 A). Similarly, pre-incubation of *S. aureus* with increasing concentrations of L2v caused dose-dependent inhibition of adherence to HK10 (Figure 4.10 C). Each assay was repeated to include GST as a control. Pre-incubation of *S. aureus* with GST alone did not inhibit adherence compared to *S. aureus* pre-incubated with an equal concentration of HK10 or L2v (Figure 4.10 B, D). These results indicate that loricrin and keratin are bound by the same mechanism.

In order to determine whether loricrin and keratin bind the same site within ClfB, recombinant ClfB $N2N3_{201\text{-}542}$ was pre-incubated with either HK10 or L2v and then tested for binding to each ligand. Pre-incubation of recombinant ClfB with HK10 inhibited binding to loricrin in a dose-dependent manner (Figure 4.11 A, B). Similarly, pre-incubation of ClfB with L2v inhibited binding to HK10 (Figure 4.11 C, D). These data indicate that HLor and HK10 bind to the same region in ClfB, providing strong evidence that loricrin is also bound using the "dock, lock and latch" mechanism.

4.2.6 *L. lactis* expressing a ClfB trench mutant cannot adhere to ligands

In order to further investigate whether ClfB binds loricrin by the "dock, lock and latch" mechanism, adhesion assays were performed using *L. lactis* NZ9800 carrying a plasmid which expresses a variant of ClfB (Q235A) that cannot bind Fg or K10. Glu_{235} makes direct contact with ligands in the ClfB

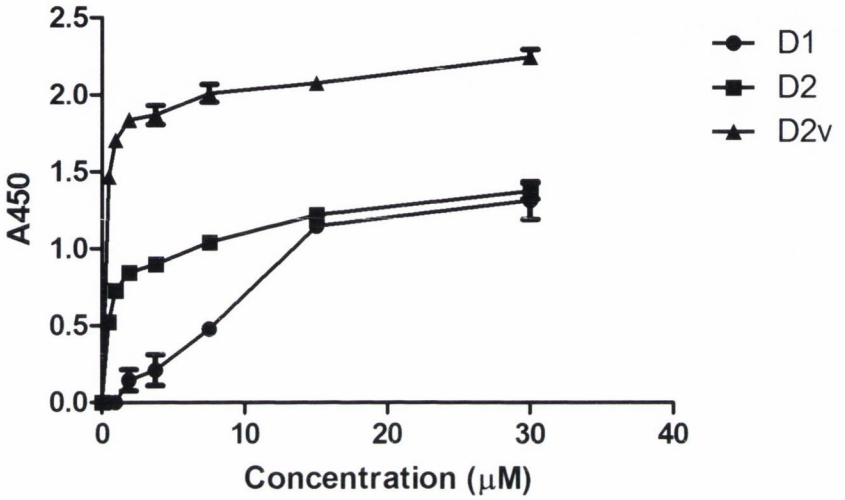

Figure 4.8 The ClfB-binding region of L2v is localised to the largest omega loop. ClfB $N2N3_{201-542}$ was tested for binding to each omega loop stretch within L2v. Increasing concentraions of rClfB were added to microtitre plates coated with GST-tagged D1, D2 and D2v (1μM). Bound protein was detected using anti-His IgG and developed by incubation with a chromogenic substrate. The absorbance was measured at 450nm. Each point represent the mean ± SD of triplicate wells. The data shown is representative of 3 individual experiments.

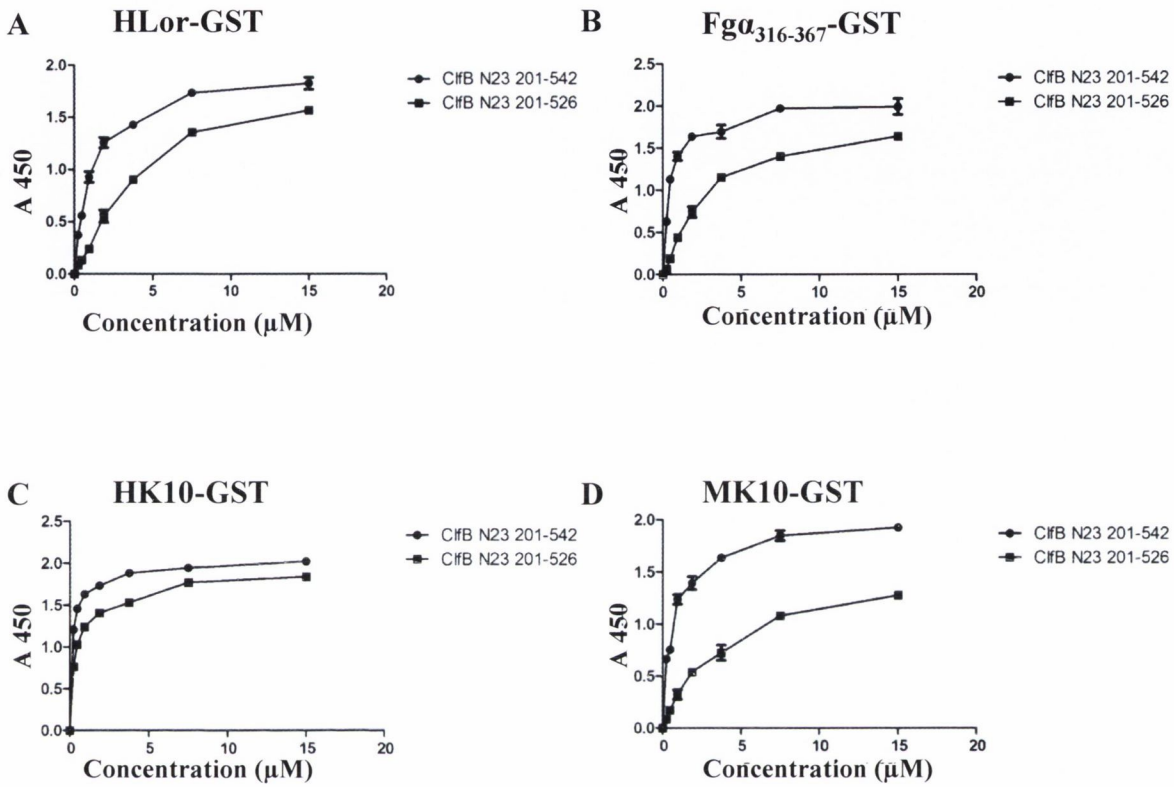

Figure 4.9 Binding of ClfB $N2N3_{201-526}$ to loricrin, keratin and fibrinogen. Recombinant lock-latch mutant ClfB $N2N3_{201-526}$ was tested for binding to GST-tagged ligands HLor (A) Fg $\alpha C_{316-367}$ (B) HK10 (C) and MK10 (D) in comparison to rClfB $N2N3_{201-542}$. Increasing concentrations of ClfB were added to 96-well plates coated with each ligand (1μM). Bound protein was detected using anti-His IgG. Each point represent the mean ± SD of triplicate wells. The data shown is representative of 3 individual experiments.

Table 4.2. Affinities of ClfB $N2N3_{201-526}$ for loricrin, keratin and fibrinogen using surface plasmon resonance.

GST-Tagged Protein	K_D (μM) ± SE ClfB $N2N3_{201-526}$	K_D (μM) ± SE ClfB $N2N3_{201-542}$
HLor	9.2 ± 2.2	4.33±1.10
HK10	8.5 ± 2.3	7.89±2.10
MK10	12.2 ± 1.0	14.38±3.0
$Fg\alpha_{316-367}$	9.3 ± 2.0	5.25±1.5

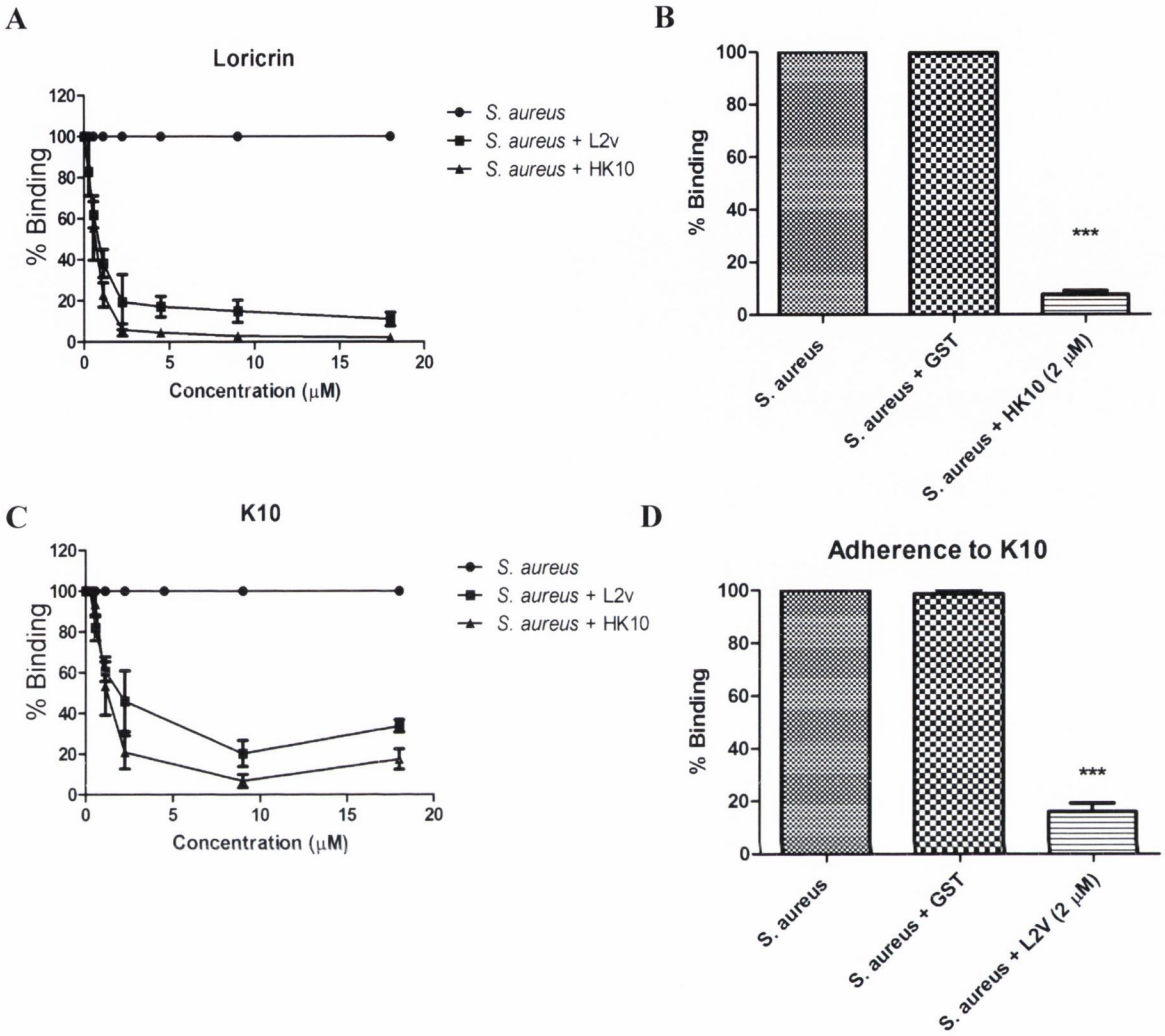

Figure 4.10 Inhibition of *S. aureus* adherence to immobilized ligands by loricrin and keratin. *S. aureus* Newman pre-incubated with increasing concentrations of Hlor or HK10 was added to loricrin-coated (A) and K10-coated (C) microtitre wells (0.5 μM). The pre-incubated bacteria were also added to wells containing single concentrations of HLor (B) and HK10 (D) (2 μM). Recombinant GST was used as a control. Bacterial adherence was measured by staining with crystal violet and measurement of the absorbance at 570nm and was expressed as a percentage of total binding. Values represent the mean ± SD of triplicate wells. The data shown is representative of two individual experiments. Statistical analysis was performed using an unpaired t-test. *** $p<0.0005$ versus pre-incubation with GST.

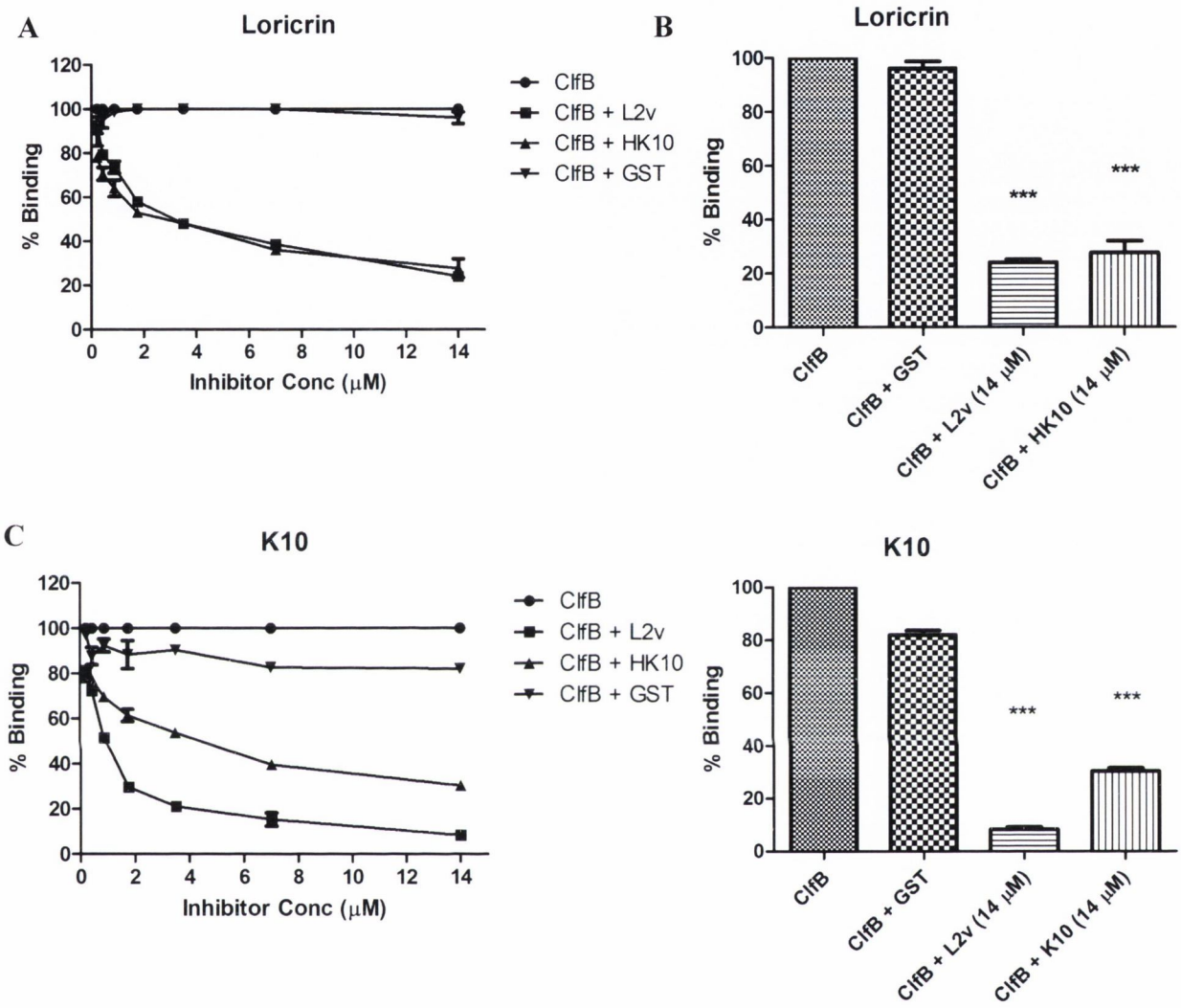

Figure 4.11 Inhibition of binding by recombinant ClfB to loricrin and keratin. Recombinant ClfB $N23_{201-542}$ (30μM) was pre-incubated with increasing concentrations of GST, HK10 or L2v before being added to loricrin-coated (A) or K10-coated (C) microtitre wells (0.5 μM). Pre-incubated ClfB was also added to microtitre wells coated with fixed concentrations of each ligand (B, D, 14 μM). Bound protein was detected using HRP-conjugated anti-his IgG and was expressed as a percentage of total bound protein. Values represent the mean ± SD of triplicate wells. The values shown are representative of 3 individual experiments. Statistical analysis was performed using an unpaired t-test. *** $p<0.0005$ versus pre-incubation with GST.

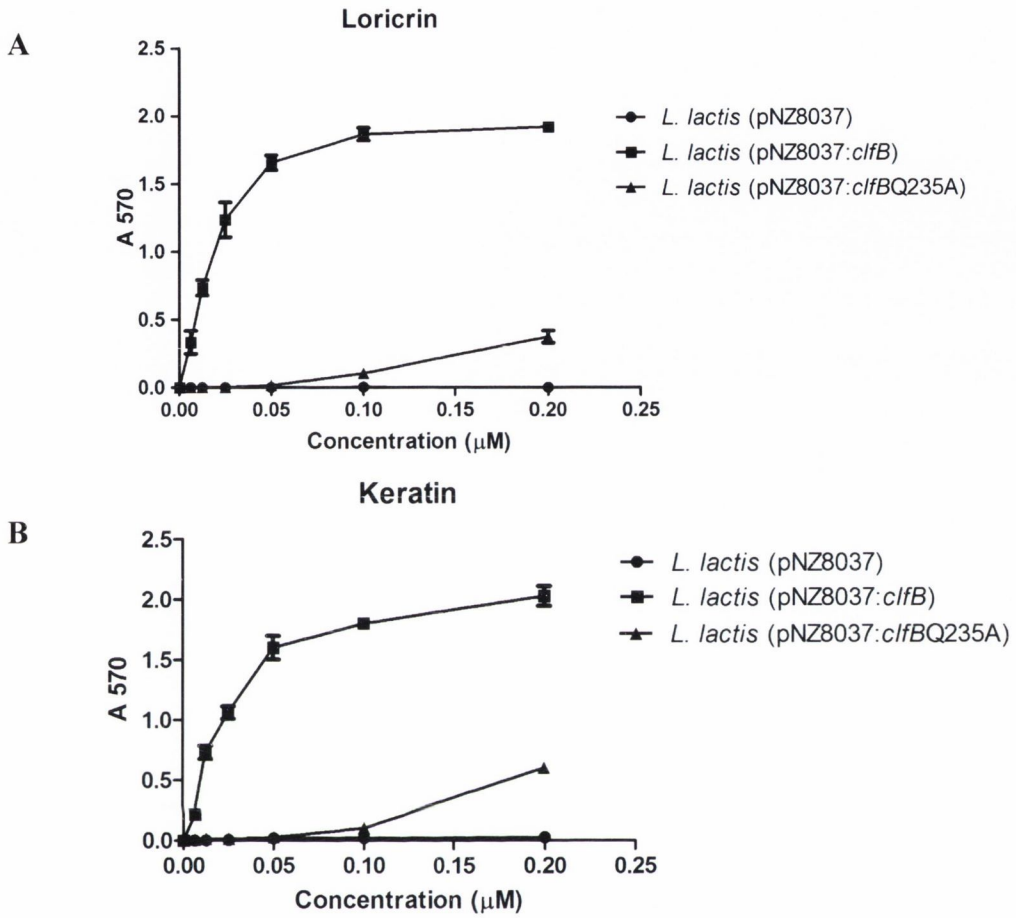

Figure 4.12 Inhibition of bacterial adherence to immobilized ligands. *L. lactis* NZ9800 (pNZ8037), *L. lactis* NZ9800 (pNZ8037:*clf*B) and *L. lactis* NZ9800 (pNZ8037:*clf*BQ235A) were added to wells containing increasing concentrations of immobilized GST-tagged Hlor (A) and HK10 (B). Bacterial adherence was measured by staining with crystal violet and measurement of the absorbance at 570 nm. The data shown is representative of two individual experiments.

binding trench (Ganesh *et al.* 2011). *L. lactis* expressing the mutant ClfB protein (*L. lactis* pNZ8037:*clfB*Q235A) did not adhere detectably to HLor or HK10 in comparison to *L. lactis* expressing wild-type ClfB (*L. lactis* pNZ8037:*clfB*) (Figure 4.12 A, B). When induced with the same concentration of nisin, the expression levels of ClfB and ClfB (Q235A) on the surface of *L. lactis* were found to be equal (Figure 3.11). This further indicates that ClfB binds HLor using "dock, lock and latch".

4.3 Discussion

ClfB has been previously defined as a bi-functional ligand, with the ability to bind the αC region of fibrinogen and more recently the tail region of the cornified envelope protein keratin, with the implication that it is a ligand for ClfB during nasal colonisation by *S. aureus* (O'Brien *et al.* 2002; Walsh *et al.* 2004; Walsh *et al.* 2008). Bacterial adherence assays described here demonstrated that ClfB promotes adherence of *S. aureus* to immobilized loricrin. *S. aureus* Newman grown to exponential phase in TSB adhered strongly to loricrin whereas bacteria lacking ClfB did not adhere. Consistent with previous findings, these results demonstrated that ClfB also promotes adherence of *S. aureus* to cytokeratin 10. Furthermore, ClfB promoted adherence of *L. lactis* to immobilized loricrin. Taken together these results indicate that *S. aureus* adhesion to loricrin is dependent on the expression of ClfB.

ClfB-binding sites have been localised to glycine-serine rich stretches with the capability of forming omega loops. The structural protein loricrin is thought to be comprised almost entirely of omega loop regions similar to those found in the tail region of K10 and is highly abundant in the cornified envelope, making it another viable ligand candidate for ClfB. In this chapter, the affinity of ClfB for loricrin was determined and compared to Fg and K10. ClfB-binding regions within loricrin were localised and analysed using SPR. It has been demonstrated that ClfB uses the "dock, lock and latch" mechanism to bind Fg and K10 (Ganesh *et al.* 2011; Xiang *et al.* 2012). The mechanism used by ClfB for loricrin was assessed. Inhibition studies and assays using recombinant ClfB constructs lacking the latching peptide and adherence assays using *L. lactis* expressing a ClfB trench mutant indicated that loricrin, K10 and Fg are bound by the same region of ClfB and that the MSCRAMM binds loricrin using the "dock, lock and latch" mechanism.

Recombinant ClfB displayed a strong interaction with loricrin in binding assays. SPR was used to demonstrate a direct interaction between recombinant ClfB and loricrin and to measure the affinity of binding. The loricrin binding site is located in the N2N3 subdomains of ClfB. ClfB bound to human loricrin with a K_D of 4.33 ± 1.10 μM, which is similar to the affinities for the ClfB-K10

and ClfB-Fg interactions (7.89 ± 2.10 and 5.52 ± 1.5 μM respectively). The K_D determined here for $rClfB_{201-542}$ binding to GST-HK10 by SPR (7.89 ± 2.10 μM) is similar to the K_D previously determined for rClfB binding to His-tagged $rMK10_{454-570}$ and synthetic HK10 peptides in solution (isothermal titration calorimetry, 1.4 μM, intrinsic tryptophan fluorescence, 1.7 and 5.4 μM, respectively (Walsh *et al.* 2004).

By subdividing the human loricrin molecule into three major loop regions, it was revealed that binding sites for ClfB exist throughout the protein. However the highest affinity ClfB binding site was localised to loop region 2. Previous studies on the human loricrin gene have shown that the major loop region designated loop region 2 contains a polymorphism, and can undergo a 12bp deletion, resulting in a loop region that is 4 amino acids shorter (Yoneda *et al.* 1992; Yoneda *et al.* 1992). More recently, several single nucleotide polymorphisms have been identified in the human loricrin gene (Giardina *et al.* 2004). Two size variants of loop region 2 were synthesized in order to investigate whether this particular polymorphism had an effect on the binding ability of ClfB. Previous studies on omega loop structures suggest that deletions in the loop sequence could cause the omega loop structure to change or fold differently. For example, deletion of 6 amino acids in an omega loop region in the active site of staphylococcal nuclease forces the omega loop into a different conformation, causing an increase in enzyme stability (Poole *et al.* 1991). The SPR results showed that the affinities of ClfB for both loop 2 variants are similar. Nevertheless, it is possible that other sequence variants of loricrin may have an effect on the ability of ClfB to bind.

Recombinant ClfB demonstrated a strong binding affinity in ELISA assays, with half-maximum binding concentrations in the nanomolar range. However, the affinity values measured by SPR were weaker. This difference in affinity could be due to the sensitivity of each detection method. Differences in sensitivity between ELISA-based and SPR detection methods have been reported (Lofgren *et al.* 2007; Hodnik and Anderluh 2009; Heinrich *et al.* 2010). When using a ligand containing multiple analyte-binding sites such as loricrin, SPR will give an average result between the K_D values for each binding site

because complexes corresponding to each affinity can be found in solution, whereas the highest affinity is detected in ELISA-based assays. Therefore different affinity values are determined by ELISA and SPR because each detection method does not observe the interaction in the same way. However the SPR results obtained here for the interaction between ClfB and K10 reflect previous results, and therefore can be considered to be accurate.

The ability of ClfB to recognise murine K10 and loricrin was also tested. ClfB promoted bacterial adherence to MK10 and loricrin in a similar way to the human proteins and rClfB bound to MK10 and loricrin similarly to HK10 and loricrin, albeit with a slightly reduced affinity. There are size and sequence differences between human and murine loricrins, but they have a similar amino acid composition and omega loop region organization (Hohl 1991). In addition, it has been shown using fluorescence spectrometry and circular dichroism that the structures of recombinant human loricrin and *in vivo* murine loricrin are indistinguishable in solution (Candi *et al.* 1995). It can therefore be assumed with confidence that the ClfB-loricrin interactions characterised *in vitro* have *in vivo* relevance in a mouse model.

Recombinant ClfB proteins constructed in this study lacking the C-terminal region of the N3 domain showed that the latching peptide is necessary for efficient binding by ClfB. A previous study using a similar ClfB construct lacking amino acid residues 256-542 showed that this deletion ablated ClfB binding to K10 and Fg peptides and confirmed that N_{526} is crucial for ClfB binding activity (Ganesh *et al.* 2011). This result was confirmed here, as a latch mutant containing N_{526} retained some binding ability. Furthermore, the results obtained here confirm that residues in the region 522-526 are also essential for ligand binding by ClfB. It is also possible that a truncation as large as ClfB $N2N3_{201\text{-}521}$ may change the conformation of the N3 region and alter the binding trench. In all, the results obtained here indicate that the "dock, lock and latch" method is used by ClfB to bind loricrin.

In binding assays using recombinant protein, the impairment in ligand binding by the ClfB latch mutant was observed as a decrease in the estimated half-maximum binding affinity of the interaction compared to the full ClfB

N2N3 region. For loricrin, Fg and MK10, half-max binding values increased from the nanomolar rage to the micromolar range. However, when analysed using SPR, the affinities for the interaction between ClfB $N2N3_{201-526}$ and each ligand did not alter significantly compared to full length ClfB N2N3. This could again be due to the sensitivity of both detection methods used. SPR analysis measures the affinity of the interaction in real time whereas the washing steps used in a binding assay may remove any weakly-bound ClfB latch mutant, which may create a different end result.

When ClfB $N2N3_{201-526}$ was tested for binding to HK10, no difference in binding was observed when compared to the full length ClfB N2N3 region. Previous studies solving the crystal structure of ClfB N2N3 in complex with peptides corresponding to K10 and Fg ClfB-binding domains have demonstrated that, due to a kink in the N-terminus of the Fg peptide, a weaker interaction may occur between backbone atoms in the Fg peptide and the binding trench, compared to ClfB and K10 in complex (Ganesh *et al.* 2011). Docking of the Fg peptide in the ClfB binding trench triggers conformational changes in the C-terminus of the ClfB N3 region, generating a β-strand that forms a parallel β-sheet with a β-strand in the N2 domain. The C-terminus of ClfB N2N3 runs across the Fg peptide and latches it in place, consistent with the "dock, lock and latch" method. However in the ClfB-K10 complex, although the ligand was "docked" and "locked" in place by residue interactions in the binding trench, no evidence of the "latch" event (formation of a β-strand in the C-terminus of ClfB N3) was observed (Xiang *et al.* 2012). Taken together, stronger interactions in the binding trench and the lack of a latching event may explain why binding of a ClfB N2N3 latch mutant to HK10 may not be as impaired as binding to Fg. It is surprising that a similar result was not observed with MK10, but the larger size of the MK10 protein construct may account for this.

Previous studies demonstrated that ClfB containing amino-acid substitution $Q_{235}A$ is defective in K10- and Fg-binding by the "dock, lock and latch" mechanism (Miajlovic *et al.* 2007; Walsh *et al.* 2008; Ganesh *et al.* 2011). Residue Q_{235} is located in the ligand binding trench and makes direct contact with the K10 and the Fg peptide (Ganesh *et al.* 2011). *L. lactis* expressing

$ClfB_{Q235A}$ was unable to adhere to loricrin. Furthermore, pre-incubation of *S. aureus* cells or recombinant ClfB with HK10 inhibited binding to loricrin and vice versa, indicating that both ligands recognise similar sites in ClfB. This is consistent with ClfB binding to loricrin by the "dock, lock and latch" mechanism and is supported by the similarities between the sequences recognised by ClfB in K10, Fg and loricrin. The sequence of the loop region displaying the strongest affinity for ClfB (YSGGGSGCGGGSSGGSGSGY) bares a similarity to the HK10 YY loop (YGGGSSGGGSSSGGGY) and tandem repeat region 5 in Fg (NSGSSGTGSTGNQ). Solving the crystal structure of ClfB in complex with peptides corresponding to binding sites within loricrin will provide further insight into the mechanism of loricrin binding by ClfB.

In summary, this chapter has described a novel interaction between ClfB and the cornified envelope protein loricrin. ClfB was shown to bind loricrin with a similar affinity as its other known ligands K10 and Fg. Multiple ClfB-binding regions were localised within loricrin and the affinity for each interaction was determined. Furthermore, this chapter provides evidence that ClfB also binds loricrin using the "dock, lock and latch" mechanism and confirms that this is the method used for ClfB binding to K10 and Fg.

Chapter 5

The role of clumping factor B and loricrin in nasal colonisation by *Staphylococcus aureus*

5.1. Introduction

The primary habitat for *S. aureus* is the moist squamous epithelium of the anterior nares (Cole *et al.* 2001; Peacock *et al.* 2001). Here, it is known to adhere to human desquamated epithelial cells (squames) (Aly *et al.* 1977; Bibel *et al.* 1982). *S. aureus* is carried persistently by approximately 20% of the population while the remainder act as transient carriers (van Belkum *et al.* 2009). Nasal carriage is a known risk factor for infection resulting in autogenous infection for many patients (von Eiff C 2001; Wertheim *et al.* 2004; Munoz *et al.* 2008). Although their risk for invasive *S. aureus* disease is higher than non-carriers, carriers suffer significantly less from fatalities following *S. aureus* infection, implying that nasal carriage offers a degree of protective immunity (Wertheim *et al.* 2004).

Several *S. aureus* factors have been implicated in nasal colonisation. Surface proteins ClfB, IsdA and more recently SasX, as well as factors such as wall teichoic acid, capsule, alkyl hydroperoxide reductase, catalase and the autolysin SceD, have all been proven to contribute to nasal colonisation *in vivo* (Kiser *et al.* 1999; Weidenmaier *et al.* 2004; Clarke *et al.* 2006; Schaffer *et al.* 2006; Cosgrove *et al.* 2007; Stapleton *et al.* 2007; Li *et al.* 2012). ClfB appears to play an essential role in *S. aureus* nasal colonisation in both human and murine experimental models. In a mouse model, a ClfB-deficient mutant of *S. aureus* displayed an impaired ability to colonise the nares (Schaffer *et al.* 2006). Similarly, when a group of human volunteers were inoculated with either a wild-type strain or a ClfB-deficient strain of *S. aureus* in their noses, the ClfB mutant was eliminated more rapidly than the wild-type strain (Wertheim *et al.* 2008). Both models provide evidence of an important role for ClfB in nasal colonisation by *S. aureus*.

Attachment to squames may be a crucial step in the successful initiation of nasal colonisation. The structural protein loricrin is the most abundant protein of the cornified envelope of squames, representing ~70% of the protein mass (Steven and Steinert 1994). Although loricrin occurs in high abundance in

the cornified envelope, surprisingly it is non-essential. A loricrin knock-out ($Lor^{-/-}$) mouse has been produced (Koch *et al.* 2000) and has provided evidence for the existence of a loricrin back-up system that compensates for the loss of loricrin in the skin (Jarnik *et al.* 2002).

Adherence of *S. aureus* to squames is a multifactorial process in which staphylococcal surface proteins including ClfB, IsdA, SasG, SdrC and SdrD have all been implicated (Clarke *et al.* 2006; Corrigan *et al.* 2009). Previously published *in vitro* evidence has identified cytokeratin 10 as a binding partner for ClfB (O'Brien *et al.* 2002; Walsh *et al.* 2004) while the interaction between ClfB and loricrin has been defined *in vitro* in this study (Chapter 4). Although these results could be extrapolated to assume that these cornified envelope (CE) constituents serve as ClfB-binding partners on the nasal epithelium during colonisation by *S. aureus*, the host ligand targeted by ClfB to facilitate its interaction with the nasal epithelium *in vivo* remains to be established.

Exposure of the CE constituents involved in staphylococcal protein interactions on the surface of squames may be an essential requirement in order to act as viable ligands *in vivo* during bacterial attachment to the epithelium. Confocal microscopy and flow cytometry have been used to show that cytokeratin 10 is present on the surface of human squames (O'Brien *et al.* 2002). Although there is as yet no published evidence of surface exposure of loricrin on squames, previous studies have reported that it is exposed on the extracellular face of other types of human epithelial cell (Lopez *et al.* 2007). Specific gold-labelled loricrin antibodies detected loricrin on the outermost layer of the CE of human corneocytes, indicating that loricrin is accessible at the surface of the CE.

Nasal colonisation by *S. aureus* has previously been successfully achieved in both inbred and outbred mouse strains (Kiser *et al.* 1999; Schaffer *et al.* 2006). However, recent studies involved in *S. aureus* nasal colonisation *in vivo* have demonstrated the effectiveness of the cotton rat as a model for sustained nasal colonisation (Kokai-Kun *et al.* 2003; Clarke *et al.* 2006; Weidenmaier *et al.* 2008; Burian *et al.* 2010). Despite these findings, the mouse remains an effective tool for nasal colonisation. *In vivo* nasal colonisation studies in human volunteers have reflected results previously achieved in the

mouse, lending support to the reliability of the model (Schaffer *et al.* 2006). Furthermore, the murine colonisation model affords the opportunity of genetic manipulation of the host, an option not yet available in the cotton rat model.

This study was directed toward examining the roles of ClfB and loricrin during *S. aureus* nasal colonisation *in vivo*. The availability of loricrin as a surface-exposed ligand on squames was investigated using whole cell dot immunoblotting and flow cytometry. *S. aureus* nasal colonisation was established and optimized in wild-type FVB mice, allowing the effects of a host loricrin-deficiency on *S. aureus* nasal colonisation to be examined *in vivo*. This loricrin-deficiency was validated in $Lor^{-/-}$ mice, and variation observed in the expression of loricrin and keratin 10 in wild-type and $Lor^{-/-}$ mice was examined and correlated to *S. aureus* nasal colonisation using Western immunoblotting and densitometry analysis. Isogenic ClfB-deficient mutants of *S. aureus* strains Newman and SH1000 were utilized in further colonisation studies using wild-type and $Lor^{-/-}$ mice in order to confirm the role of ClfB in *S. aureus* nasal colonisation and to examine the interaction between ClfB and loricrin in the nose. A novel nasal colonisation model using the heterologous host *Lactococcus lactis* was established in order to investigate the specific interaction between loricrin and ClfB in isolation from other *S. aureus* proteins. Finally, *in vivo* and *ex vivo* inhibition studies in the mouse nose and on human squames were used to examine the specificity of the interaction between ClfB and loricrin.

5.2 Results

5.2.1 Loricrin loop region L2v inhibits ClfB-mediated adherence of *S. aureus* to human nasal desquamated epithelial cells.

Previous studies have demonstrated the importance of ClfB in *S. aureus* adherence to squames (Clarke *et al.* 2006; Corrigan *et al.* 2009). To confirm this interaction, *S. aureus* Newman and *S. aureus* Δ*clfB* were tested for adherence to squames. Consistent with previously published studies, the ability of *S. aureus* Δ*clfB* to adhere to squames was significantly reduced (P=0.002) compared to its parental strain (Figure 5.1). In order to determine whether loricrin plays a role in this process, *S. aureus* Newman and *S. aureus* Δ*clfB* were pre-incubated with GST-tagged recombinant loricrin loop region L2v and were then tested for adherence to squames compared to pre-incubation with a GST control. Pre-incubation of *S. aureus* Newman with L2v caused a significant reduction in adherence to squames (P=0.0072) compared to *S. aureus* pre-incubated with GST alone (Figure 5.1 A). This illustrates that an interaction with a ligand on the surface of that recognises the same binding domain in ClfB as loricrin is necessary for efficient *S. aureus* adherence to squames. *S. aureus* Δ*clfB* was pre-incubated in the same manner in order to investigate the specificity of the inhibitory effect of loricrin L2v for ClfB. There was no further reduction in adherence when *S. aureus* Δ*clfB* was pre-incubated with L2v compared to GST alone, indicating that ClfB is the only *S. aureus* factor binding to loricrin on squames under these conditions.

In order to investigate this interaction in nutrient-deficient conditions such as those found in the nasal cavity, *S. aureus* Newman and *S. aureus* Δ*clfB* were grown in the iron-limiting medium RPMI and the inhibition assay was repeated (Figure 5.1 B). Again, there was a significant decrease in squame-binding by *S. aureus* Δ*clfB* compared to *S. aureus* Newman. Similarly, pre-incubation with L2v significantly inhibited adherence of *S. aureus* to squames compared to pre-incubation with GST alone, but not *S. aureus* Δ*clfB*. These results indicate that ClfB is the sole *S. aureus* factor binding to loricrin on the surface of squames under iron-limited conditions.

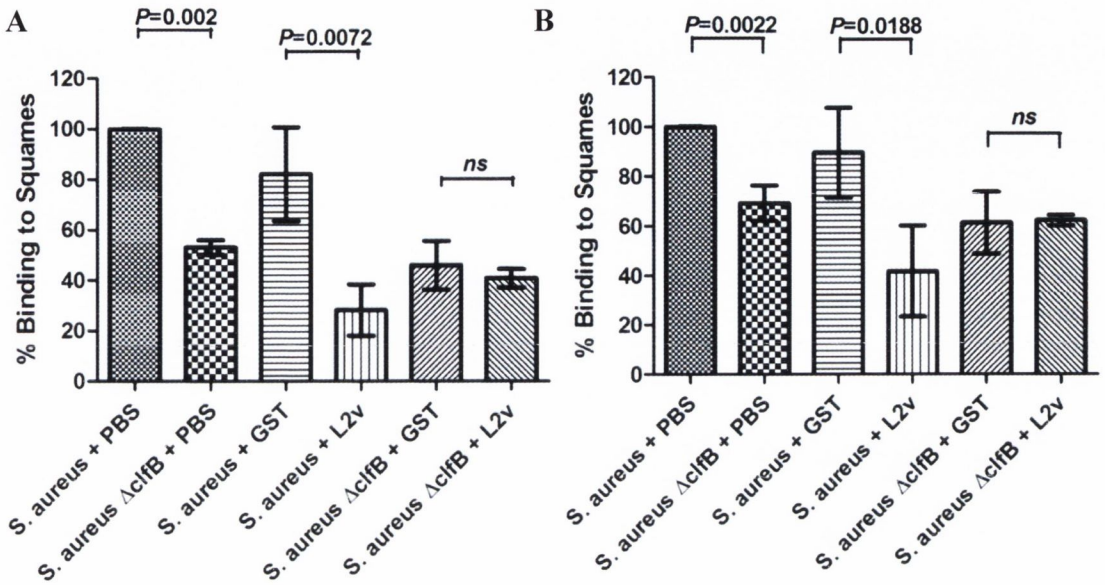

Figure 5.1 ClfB-mediated adherence to human squames is inhibited by loricrin. *S. aureus* strains were grown to exponential phase in TSB **(A)** or RPMI **(B)**. Washed cells were incubated with recombinant GST or recombinant L2V-GST, before being incubated with human nasal squamous epithelial cells. Crystal violet-stained adherent bacteria were enumerated by microscopy and were expressed as a percentage of the positive control. Results are expressed as the mean ±SD of 3 independent experiments. Statistical analysis was performed using a *t* test.

5.2.2 Loricrin is expressed on the surface of squames.

Loricrin has been previously detected on the extracellular surface of human corneocytes (Lopez *et al.* 2007). In order to determine whether loricrin is expressed on the surface of human squames, specific anti-loricrin IgG was used to probe squames obtained from healthy volunteers, using flow cytometry and dot immunoblotting techniques.

Samples of squames were received from healthy volunteers by vigorous swabbing of the anterior nares. Washed squames were adjusted to approximately 1 x 10^5 squames per ml. In order to determine whether loricrin is exposed detectably on the surface of squames, human squamous cell samples were analysed by whole cell dot immunoblotting. Doubling dilutions of squame samples were dotted onto a nitrocellulose membrane and were then probed with anti-loricrin IgG (Figure 5.2 A). The anti-loricrin IgG probe bound to squames on the membrane in a dose-dependent manner, indicating that loricrin is exposed on the surface of squames.

Squame samples were then probed with anti-loricrin IgG followed by a FITC-labelled secondary antibody and the fluorescence intensity was measured by flow cytometry. An increase in fluorescence occurred in squames probed with primary and secondary antibodies, compared to squames probed with secondary antibodies alone (Figure 5.2 B). This confirms that loricrin is surface-exposed on squames.

5.2.3 Optimization of a 10 day colonisation model in FVB mice

The FVB strain of mouse has not previously been used as a model of *S. aureus* nasal colonisation. Successful levels of nasal colonisation have been achieved previously using *S. aureus* in both inbred (BALB/c, C57BL/6) and outbred (ICR) strains of mice (Kiser *et al.* 1999). In order to assess the ability of FVB mice to be colonised nasally, an initial 10-day nasal colonisation study was performed using a spontaneous streptomycin resistant (Sm^R) mutant of *S. aureus* strain Newman. Mice were inoculated with $2x10^8$ CFU per nostril. This inoculum size has resulted in sufficient levels of colonisation in inbred strains of mouse in previous studies. Mice were administered streptomycin in their

drinking water 24 hours prior to inoculation and for the duration of the experiment in order to reduce interference from the commensal bacterial flora. At specific time points after inoculation, nasal tissue was excised and homogenized and the number of CFU per nose was enumerated. The results of this study showed that FVB mice are capable of being nasally colonised by *S. aureus*.

On day 1, all mice were colonised consistently (median = 319 CFU/nose, Figure 5.3 A). On days 3 and 5, a steady increase in colonisation levels was seen (Median = 662, 2657 CFU/nose, respectively) reaching similar levels of colonisation seen previously for inbred mice. This provides evidence that the bacteria are proliferating in the nose. By days 7 and 10, colonisation levels had dropped slightly but were still constant (Median = 1208, 1192, respectively). These results showed that FVB mice can be sufficiently colonised by *S. aureus* for at least 10 days at a level similar to previously published successful murine nasal colonisation models. Total nasal flora counts were performed using 5% sheep blood agar plates (Figure 5.3 B). Similar bacterial counts were observed, suggesting that *S. aureus* instilled into the nose made up the majority of the nasal flora during the experiment. Lung tissue was also excised and homogenised, in order to check for dissemination of the bacteria into the lungs (Figure 5.3 C). On each day, the median value for each group of mice was <10 CFU per lung, implying that minimal systemic dissemination occurred. No bacteria were present in blood samples, confirming that the bacteria did not disseminate from the nose (data not shown). Days 3 and 10 were chosen as suitable days for further colonisation experiments due to the consistent levels of colonisation seen at these time-points.

The effectiveness of using fresh cultures of *S. aureus* to inoculate mice was compared to using a frozen batch culture of the strain. Wild-type FVB mice were inoculated with $2x10^8$ CFU of either a fresh culture of *S. aureus* Newman or a previously prepared frozen stock of the same strain. After 3 days, nasal and lung tissue were excised and the bacterial burden in each was enumerated (Figure 5.4 A). Mice that were inoculated with the frozen culture of *S. aureus* retained bacteria more consistently in their noses (median=2325 CFU/nose) than

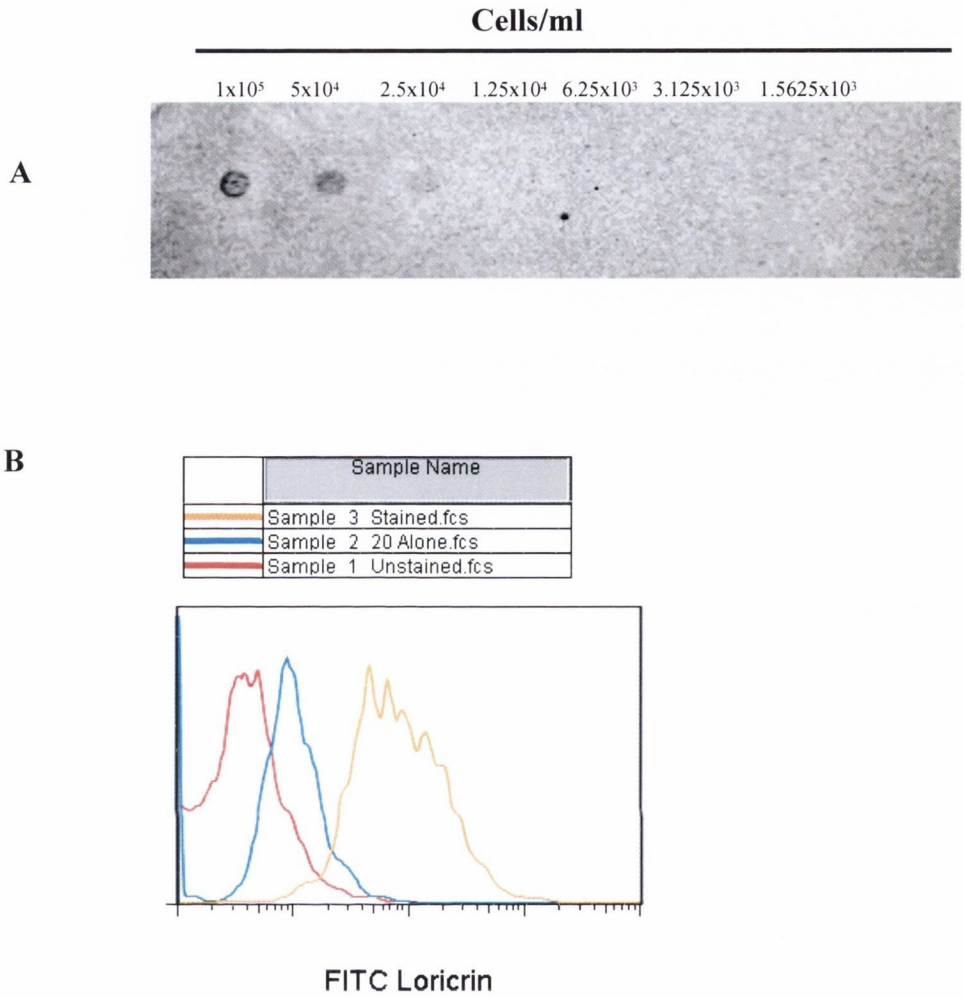

Figure 5.2 Loricrin is exposed on the surface of squames. (A) Whole cell dot immunoblot of squames. Doubling dilutions of squames were spotted onto a nitrocellulose membrane and were probed with anti-loricirn IgG followed by HRP-conjugated swine anti-rabbit IgG. **(B)** Flow cytometry. Fluorescent intensity of human desquamated epithelial cells stained with anti loricirn IgG and FITC-labelled swine anti-rabbit IgG (yellow), compared to the fluorescent intensity of cells stained with FITC-labelled secondary stain only (blue) and unstained cells (red).

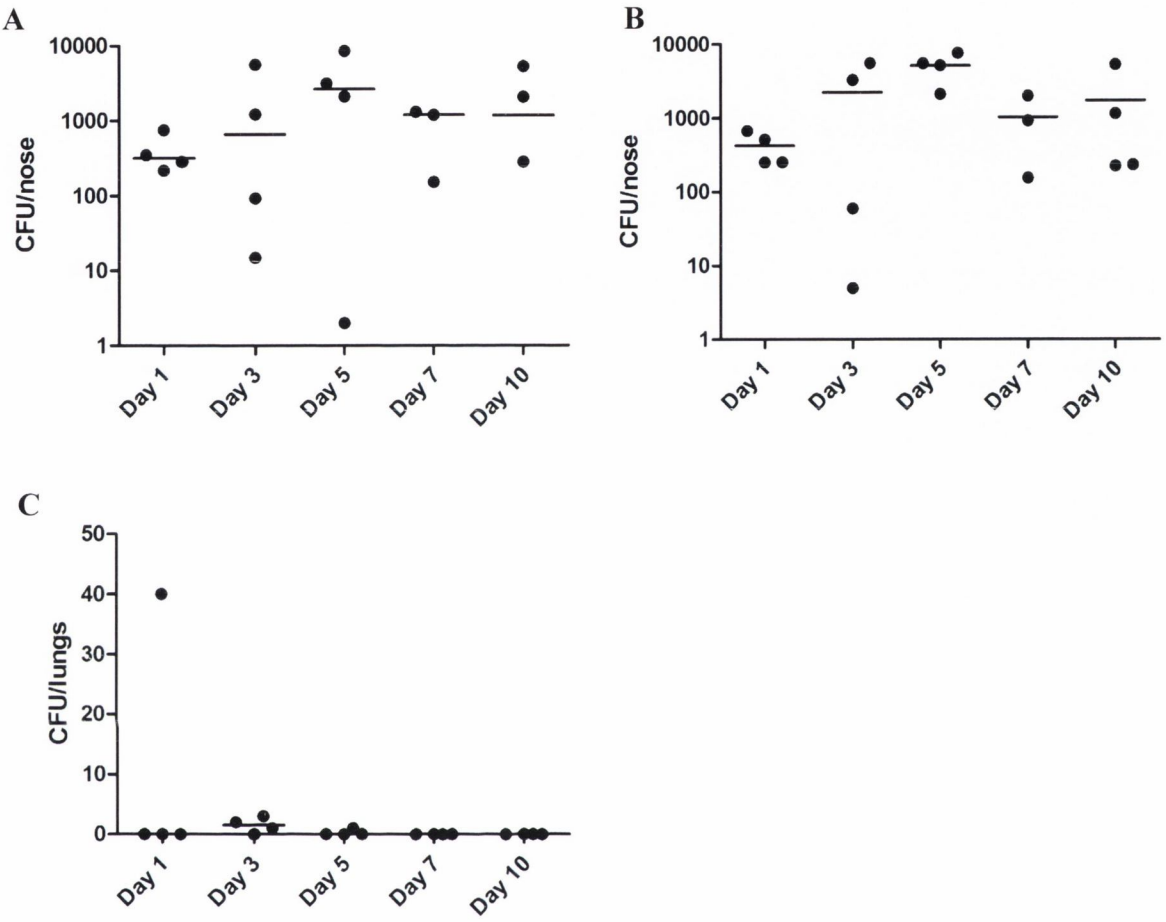

Figure 5.3 10-day nasal colonisation model using FVB mice. Mice were inoculated intra-nasally with *S. aureus* Newman (2 x 10^8 CFU). Mice were euthanized and bacterial burden in the noses was established on days 1, 3, 5, 7 and 10. Nose homogenates were plated onto TSA containing streptomycin to obtain CFU/nose **(A)** and on 5% SBA to obtain a total cell count per nose **(B)**. Lungs were also excised and the bacterial burden established **(C)**. Each dot indicates the number of CFU/nose or lung for a single mouse. Results expressed as median Log CFU per nose (n=4, per group).

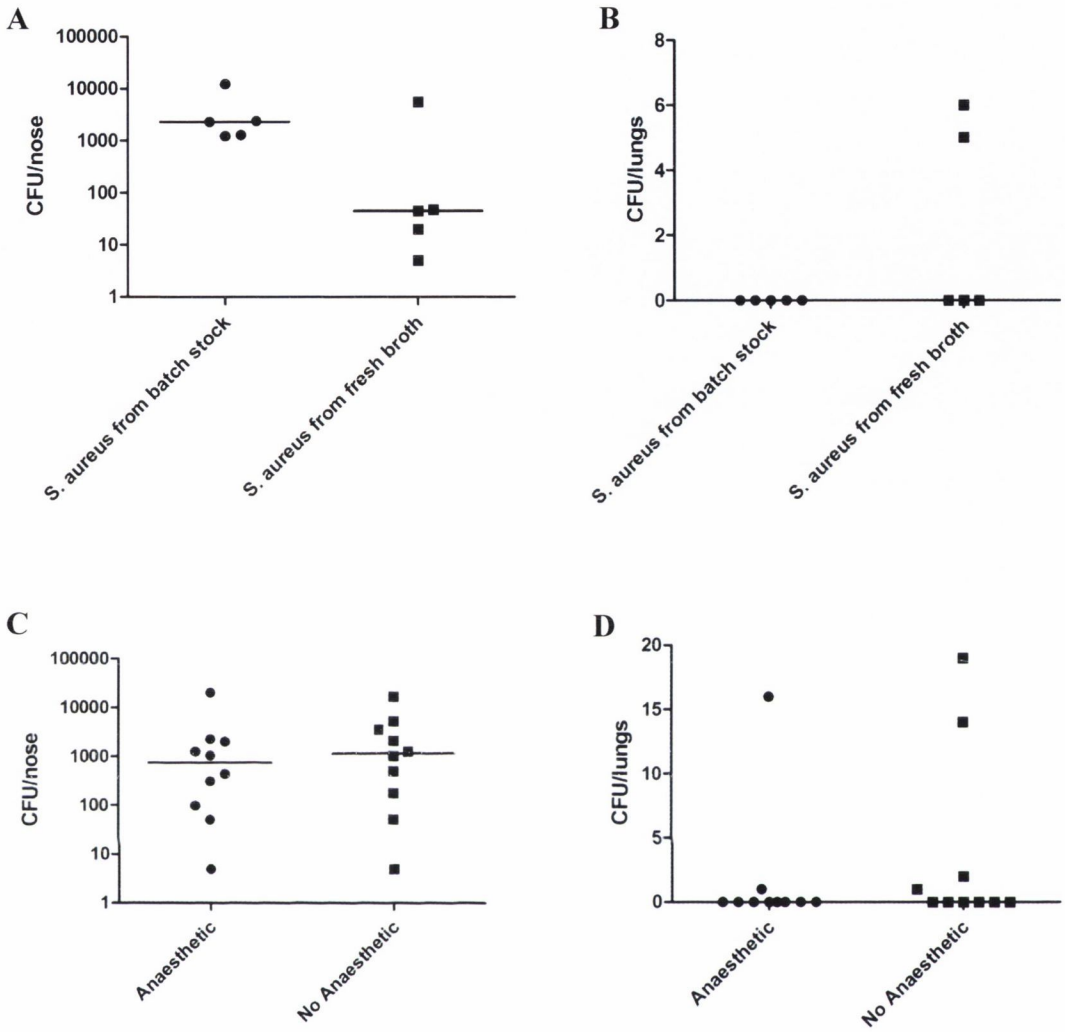

Figure 5.4 Optimization of intranasal inoculation of FVB mice. Mice were inoculated intranasally (2 x 10^8 CFU) with *S. aureus* Newman. Mice were euthanized and the bacterial burden in the noses was established on day 3. Nose homogenates were plated onto TSA containing streptomycin to obtain CFU per nose. **(A)** Mice inoculated with a frozen stock of *S. aureus* Newman were compared to mice inoculated with a fresh culture of the same strain (n=5 per group). **(C)** Mice that were anaesthetized prior to intranasal inoculation were compared to mice inoculated while fully awake (n=10 per group). Lungs were excised and the bacterial burden established **(B, D)**. Each dot indicates the number of CFU/nose or lung of a single mouse. Results are expressed as median Log CFU per nose.

mice inoculated with a fresh culture (median=45 CFU/nose). Very low levels of bacteria were found in the lungs of each group (Figure 5.4 B). This data suggests that inoculation with a frozen bacterial suspension resulted in more consistent and reliable levels of colonisation in wild-type FVB mice. Therefore, a frozen stock culture of *S. aureus* was used for all subsequent mouse experiments.

In order to determine whether the administration of anaesthetic to mice prior to inoculation had an effect on colonisation, wild-type FVB mice intranasally inoculated following anaesthetic isofluorane gas were compared to wild-type FVB mice inoculated intranasally while fully awake. After 10 days, nasal tissue was excised and the bacteria present were quantified (Figure 5.4 C). Mice that were anaesthetized displayed similar levels of colonisation to those inoculated while awake (median=738, 1002 CFU/nose, respectively). Similarly, there was minimal dissemination to the lungs in both groups of mice (Figure 5.4 D). These results imply that administering anaesthetic to mice prior to inoculation had no positive or negative effects on colonisation levels and did not lead to an increase or decrease of systemic dissemination. Nevertheless, this method appeared to be less stressing and injurious to the mice and was therefore applied to the remainder of the mouse experiments.

In order to ensure that no other streptomycin resistant staphylococci were already present in the nasal flora of FVB mice, nasal tissue from mice that had not been previously colonised was excised and homogenised. Homogenates were plated onto TSA containing streptomycin (0.5 mg/ml) and were incubated at 37 °C. After 24 hours, there were no colonies present on plates (data not shown). This indicates that there are no streptomycin-resistant bacteria normally present in the nasal flora of FVB mice.

5.2.4 *S. aureus* nasal colonisation is impaired in loricrin-deficient mice.

The importance of loricrin in *S. aureus* nasal colonisation was investigated. In accordance with the initial colonisation study, mice were treated with streptomycin in their drinking water 24 hours prior to inoculation and for

the duration of the experiment. Nasal tissue, lung tissue and blood samples were taken and the bacterial burden in each was enumerated.

On day 1, wild-type and Lor$^{-/-}$ mice retained similar levels of *S. aureus* Newman in their noses (Figure 5.5). Consistent with the initial colonisation study, wild-type mice remained stably colonised with Newman over a period of 10 days with the number of bacteria increasing slightly during this period. In contrast, there was a significant reduction in the levels of *S. aureus* Newman present in the noses of Lor$^{-/-}$ mice on day 3 (p=0.0355) and day 10 (p=0.0343), indicating that Lor$^{-/-}$ mice were unable to retain *S. aureus* in their noses when compared to wild-type mice (Figure 5.5, Figure 5.6 A, B). By day 21, *S. aureus* Newman had been completely cleared from the noses of Lor$^{-/-}$ mice, while low numbers of bacteria were still detectable in wild-type mice. These results suggest that the absence of loricrin does not impact initial attachment of *S. aureus* to the nasal tissue, but the protein appears to be essential for the maintenance of the bacterium in the nose and for sustained colonisation up to a period of 21 days. Total nasal bacterial counts showed that *S. aureus* made up the majority of the nasal flora during the study (Figure 5.6 C, D). No bacteria were detected in the blood of either wild-type or Lor$^{-/-}$ mice and low levels of bacteria were detectable in the lungs of wild-type and Lor$^{-/-}$ mice at 3 days (median =1 CFU) and 10 days (median <10 CFU) post inoculation (Figure 5.6 E, F), indicating that minimal systemic dissemination of the bacteria occurred.

5.2.5 Nasal expression levels of loricrin and keratin do not affect *S. aureus* nasal colonisation.

In order to confirm the absence of loricrin in Lor$^{-/-}$ mice, dorsal skin samples were extracted from each strain of mouse and were probed for loricrin expression. Protein solubilised from murine dorsal skin homogenates were analysed by Western immunoblotting using specific anti-loricrin IgG (Fig. 5.7 A). A 56 kDa band corresponding to loricrin was detected in FVB mouse homogenates but not in Lor$^{-/-}$ mice. Keratin expression was also analysed using specific murine keratin 10 antibodies. A ~57 kDa band corresponding to keratin was seen in all homogenates, confirming that protein was present. This confirms that loricrin is not expressed in Lor$^{-/-}$ mice.

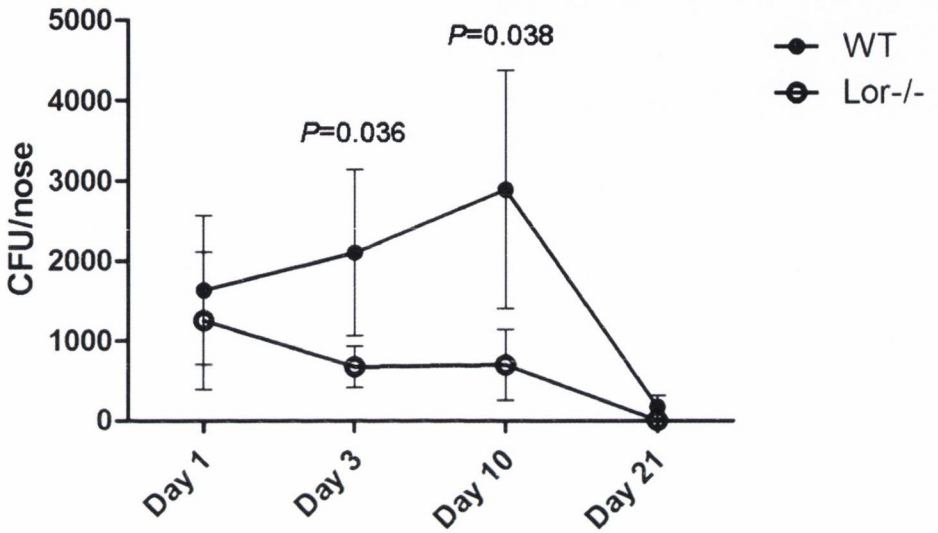

Figure 5.5 Nasal colonisation of *S. aureus* in the FVB wild-type and Lor$^{-/-}$ mouse. Mice were inoculated intranasally with *S. aureus* Newman (2 x 10^8 CFU). Mice were euthanized and bacterial burden in the noses established on days 1, 3, 10 and 21. Results expressed as mean Log CFU per nose (n=15, per group). Statistical analysis was performed using a Mann-Whitney test.

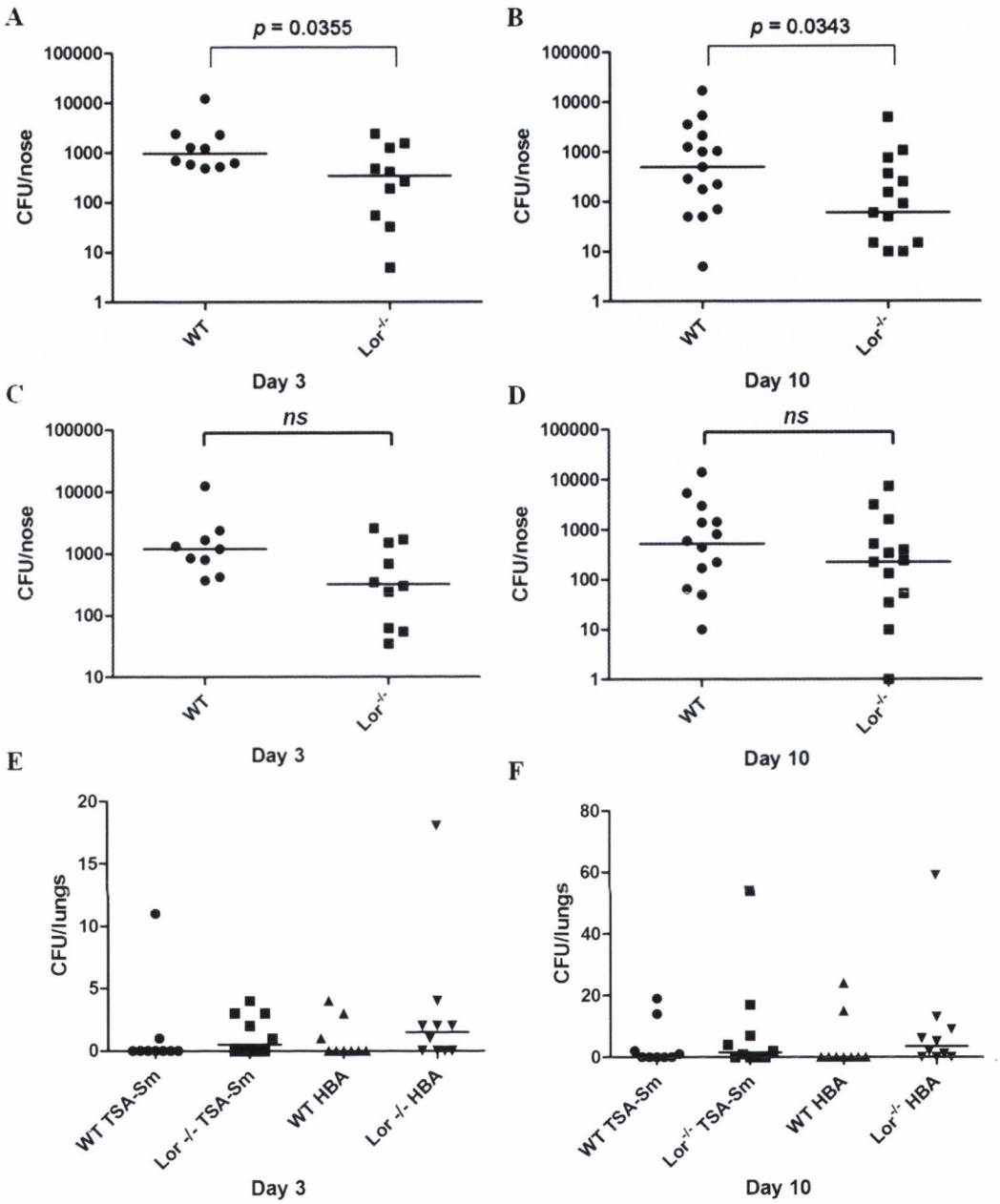

Figure 5.6 Individual data points for nasal colonisation in FVB wildtype and Lor$^{-/-}$ mice on days 3 and 10. Mice were inoculated intranasally with *S. aureus* Newman (2 x 10^8 CFU). Mice were euthanized and bacterial burden in the noses established. Nose homogenates were plated onto TSA containing streptomycin to obtain *S. aureus* CFU/nose **(A, B)** and on 5% SBA to obtain a total cell count per nose **(C, D)**. Lungs were also excised and the bacterial burden established **(E, F)**. Each dot indicates the CFU for an individual mouse. Results expressed as median Log CFU per nose or lung (n=15, per group). Statistical analysis was performed using a Mann-Whitney test.

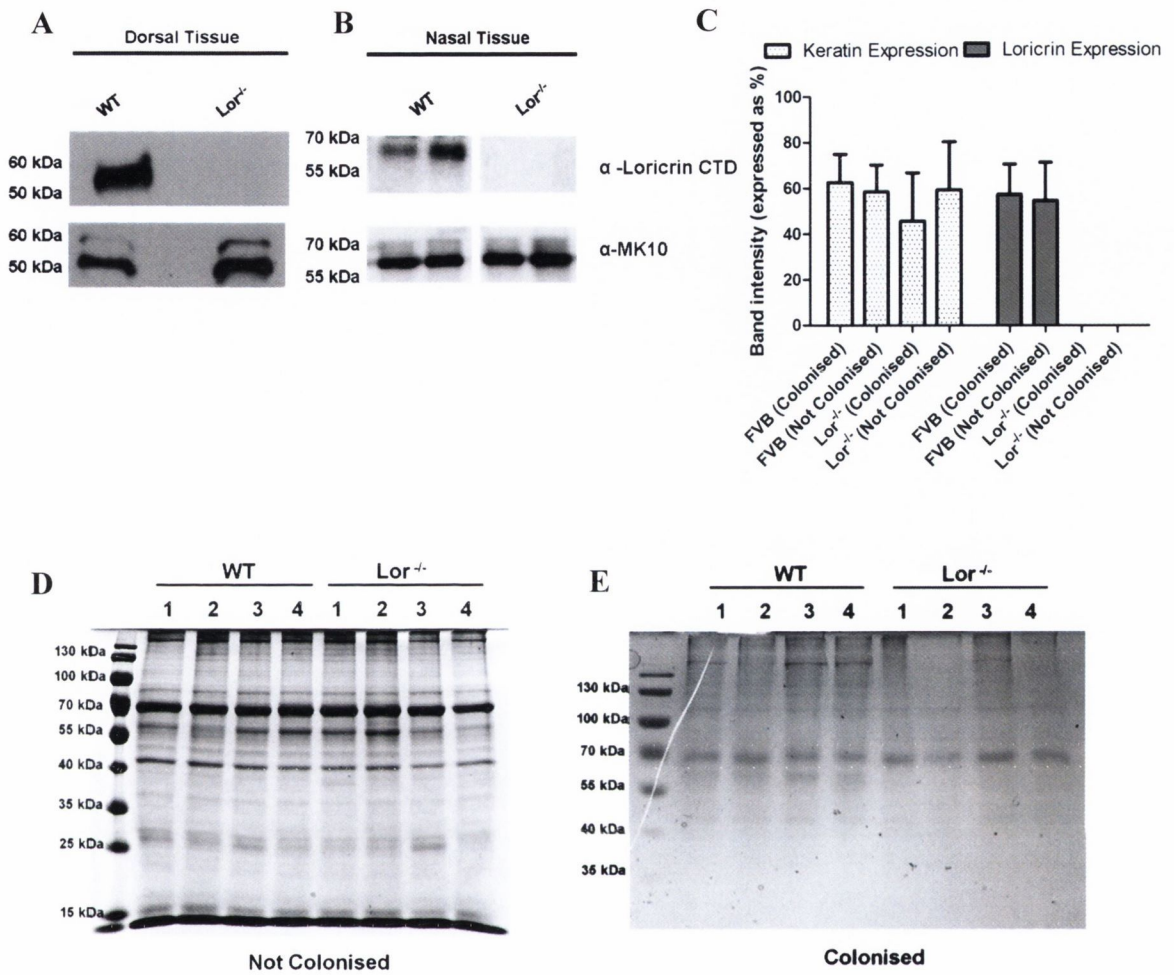

Figure 5.7 Analysis of variation in expression of loricrin and keratin in FVB and Lor$^{-/-}$ mice. Dorsal tissue **(A)** and nasal tissue **(B)** from WT and Lor$^{-/-}$ mice was excised and homogenised in PBS. Soluble proteins were extracted and analysed by Western immunoblotting using rabbit anti-murine loricrin IgG followed by HRP-conjugated goat anti-rabbit IgG. Bound antibody was removed and the filter was re-probed with rabbit anti-murine K10 IgG followed by HRP-conjugated protein A. The band intensity of samples was measured using ImageQuant software and was expressed as a percentage of the highest intensity band **(C).** Data represents mean ±SEM (n=4 mice, per group). Equal protein concentrations of non-colonised **(D)** and *S. aureus*-colonised mice (E) were confirmed by Coomassie staining.

Previous studies have provided evidence of a loricrin back-up system, whereby the expression of other CE proteins is increased to compensate for the lack of loricrin (Jarnik *et al.* 2002). An increase in the expression of keratin in $Lor^{-/-}$ mice was not previously observed. In the murine models performed here, a high level of variability was apparent in the colonisation rates of individual mice. In order to correlate these variable colonisation rates with keratin and loricrin expression in the nose, and also to observe any increase or decrease in the expression of these proteins in individual mice, loricrin and keratin expression in the noses of FVB and $Lor^{-/-}$ mice was compared in the absence of *S. aureus* nasal colonisation and also on day 10 post-colonisation. Nasal tissue was excised from WT and $Lor^{-/-}$ mice. Proteins were then solubilised from nasal tissue homogenates and analysed by Western immunoblotting using specific loricrin and murine keratin antibodies. A ~ 56 kDa band corresponding to loricrin was seen in the nasal tissue from WT but not $Lor^{-/-}$ mice (Fig. 5.7 B).

The band intensity in each nasal homogenate was quantified using densitometric analysis. Concurrent with previously published data, there was no significant difference in K10 expression in $Lor^{-/-}$ mice when compared to wild-type mice, either in the absence or presence of *S. aureus* nasal colonisation (Fig 5.7 C). Similarly, the levels of loricrin expression did not vary significantly in colonised or non-colonised animals. Each nose homogenate was analysed by Coomassie staining to ensure that equal amounts of protein were present in each lane (Fig 5.7 D, E). Although individual samples displayed some variation in loricrin and keratin expression, there was no correlation between the variability of loricrin or keratin expression and the variability seen in *S. aureus* colonisation levels in these mice 10 days after colonisation (Fig 5.8 A, B). Taken together, these data show that keratin expression is not up-regulated in $Lor^{-/-}$ mice and that variation in loricrin or keratin expression has no impact on *S. aureus* nasal colonisation.

5.2.6 *Lactococcus lactis* expressing ClfB facilitated nasal colonisation in wild-type but not loricrin-deficient mice.

To investigate further the importance of ClfB in mediating the interaction between *S. aureus* and loricrin during colonisation, a new model of nasal colonisation was developed using *L. lactis* expressing ClfB. Mice were treated with erythromycin 24 hours prior to inoculation and throughout the experiment. Wild-type and Lor$^{-/-}$ mice were inoculated intranasally with ClfB-expressing *L. lactis* (pKS80:*clfB*) or the empty vector control strain *L. lactis* (pKS80). After 24 hours, lung and nasal tissue was excised and the CFU present in each were enumerated. Significant levels of ClfB-expressing *L. lactis* were recovered from the noses of wild-type mice (median = 50 CFU/nose), whereas there was a ~80% reduction in the levels of ClfB-expressing *L. lactis* colonizing the noses of Lor$^{-/-}$ mice (P=0.048, Figure 5.9 A). The majority of mice did not retain detectable levels (<5 CFU) of the control strain *L. lactis* (pKS80) in their noses. Minimal levels of *L. lactis* were detected in the lungs of each mouse strain (Figure 5.9 B). ClfB-expression by *L. lactis* in the nose was confirmed by whole cell dot immunoblotting of colonies recovered from nasal tissue homogenates, compared to *L. lactis* and *S. aureus* strains expressing and deficient in ClfB (Figure 5.9 C). These results demonstrate that the interaction between ClfB and loricrin alone is sufficient to facilitate nasal colonisation, as well as confirming the important role for ClfB in bacterial attachment to the nares.

5.2.7 *S. aureus* Δ*clfB* exhibited reduced nasal colonisation in wild-type but not Lor$^{-/-}$ mice.

Previous *in vivo* data has been published highlighting the importance of ClfB in *S. aureus* nasal colonisation, in both murine and human models (Schaffer *et al.* 2006; Wertheim *et al.* 2008). In order to confirm this interaction, and also to confirm the importance of the interaction between loricrin and ClfB in *S. aureus* nasal colonisation, a murine nasal colonisation experiment was carried out in FVB wild-type and Lor$^{-/-}$ mice using ClfB-deficient mutants of *S. aureus*.

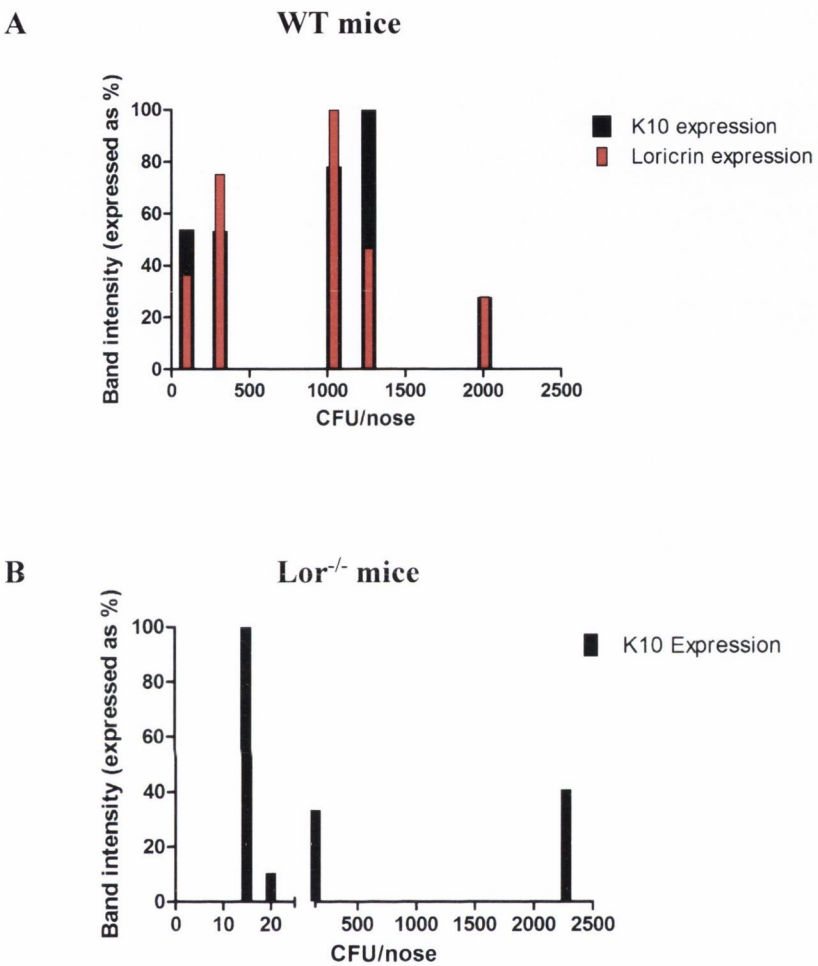

Figure 5.8 Comparison of keratin and loricrin expression to *S. aureus* nasal colonisation in FVB mice. Protein expression levels (measured by band intensity) of individual *S. aureus*-colonised wild-type mice **(A)** and $Lor^{-/-}$ mice **(B)** were compared to CFU counts of each.

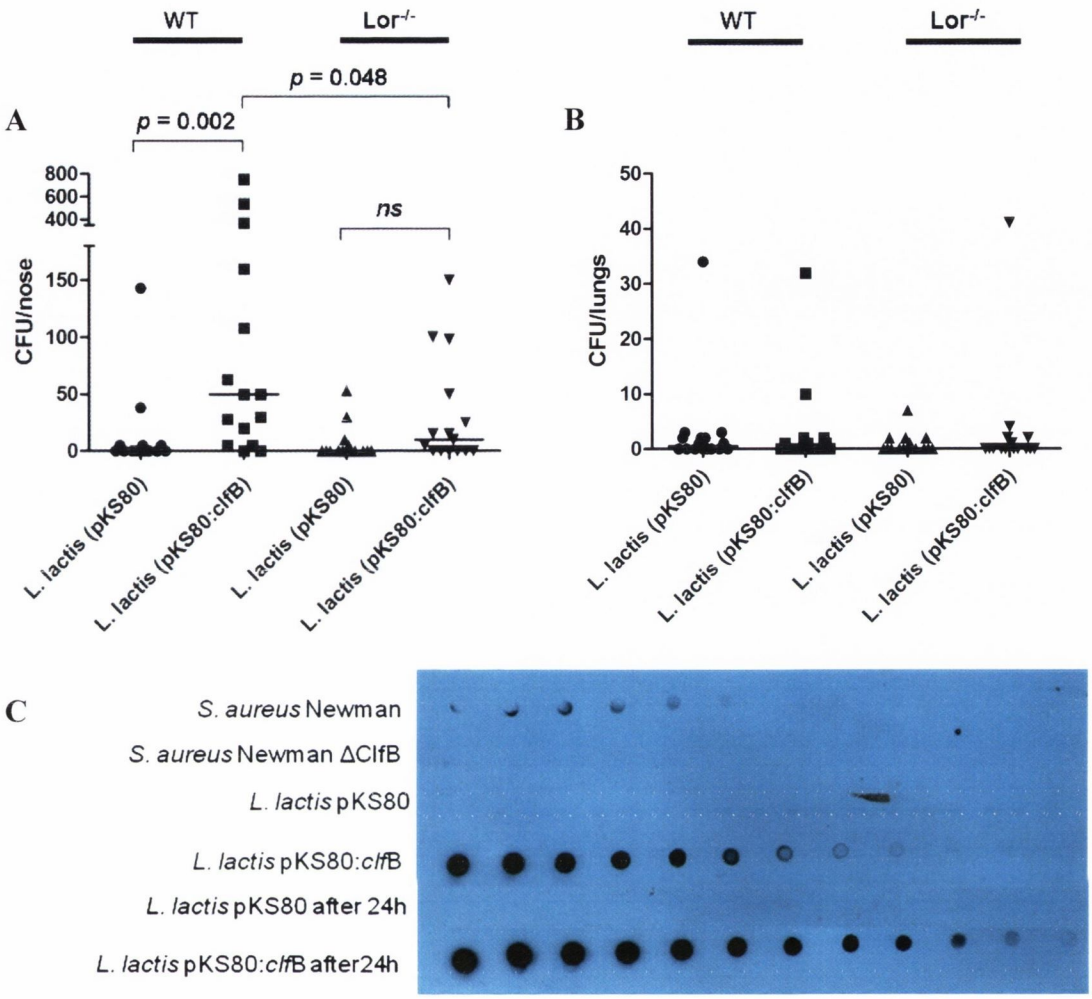

Figure 5.9 Nasal colonisation of *L. lactis* expressing ClfB in FVB wild-type and Lor$^{-/-}$ mice. Mice were inoculated intranasally with *L. lactis* MG1363 (pKS80) or *L. lactis* MG1363 (pKS80:*clf*B) (2 x 10^{11} CFU). Mice were euthanized after 24 hours and the bacterial burden in the nasal tissue **(A)** and lungs **(B)** was established. Each dot indicates the number of CFU/nose or lung for a single mouse. Results were expressed as log CFU per nose,with the median indicated by bar (n=16 per group). Statistical analysis was performed using a Mann Whitney test. **(C)** Whole cell dot immunoblot of *L. lactis* MG1363 (pKS80) and *L. lactis* MG1363 (pKS80:*clf*B) after 24 h in the mouse nose. Doubling dilutions of each strain were spotted onto a nitrocellulose membrane and were then probed with anti-ClfB IgG followed by protein A-peroxidase. *L. lactis* MG1363 (pKS80) and *L. lactis* MG1363 (pKS80:*clf*B) were included as negative and positive controls, respectively, as well as *S. aureus* and *S. aureus* Δ*clfB*.

5.2.7.1 *S. aureus* Newman

FVB wild-type and Lor$^{-/-}$ mice were inoculated intranasally with *S. aureus* Newman or Newman Δ*clfB*. After 10 days, the bacterial burden in nasal and lung tissue was quantified. There was a significant reduction in colonisation of wild-type mice by Newman Δ*clfB* compared to the parental strain (P=<0.005), confirming the role played by ClfB in nasal colonisation (Figure 5.10 A). In contrast, there was no significant difference between colonisation with the parental Newman strain and Newman Δ*clfB* in Lor$^{-/-}$ mice. Both Newman and Newman Δ*clfB* were almost completely cleared from the nares of Lor$^{-/-}$ mice. Comparable to the previous model, minimal levels of bacteria were present in the lungs, indicating that bacterial dissemination did not occur (Figure 5.10 B). This data indicates that loricrin is the primary ligand for ClfB *in vivo* and is required for the maintenance of *S. aureus* during nasal colonisation.

5.2.7.2 *S. aureus* SH1000

In order to confirm the deleterious effect of ClfB-deficiency on nasal colonisation in another strain of *S. aureus*, the 10-day colonisation experiment was repeated using *S. aureus* strain SH1000. A spontaneous Sm^{R} mutant of *S. aureus* SH1000 was selected and an isogenic ClfB-deficient mutant was constructed using pIMAY. FVB wild-type and Lor$^{-/-}$ mice were inoculated intranasally with SH1000 Δ*clfB* or its wild-type parental strain. The nasal bacterial burden in lung and nasal tissue was enumerated 10 days post colonisation. Consistent with data obtained from the previous *S. aureus* Newman Δ*clfB* model, a significant reduction in colonisation of wild-type mice by SH1000 Δ*clfB* was observed (P=<0.05, Figure 5.10 C) compared to the parental strain. Similarly, there was no significant difference between SH1000 and SH1000 Δ*clfB* in Lor$^{-/-}$ mice. Again, low levels of bacteria in lung samples showed that there was minimum dissemination of the bacteria from the nose (Figure 5.10 D). This data confirms that loricrin is the main ligand for ClfB in the nose and is essential for nasal colonisation by *S. aureus*.

5.2.8 *S. aureus* nasal colonisation is inhibited *in vivo* in wild-type mice using recombinant loricrin L2v.

In order to provide further confirmation of the role played by loricrin in mediating nasal colonisation with *S. aureus*, the ability of recombinant loricrin loop L2v to inhibit *S. aureus* nasal colonization *in vivo* in FVB wild-type mice was investigated. *S. aureus* Newman was pre-incubated with recombinant loricrin L2v or recombinant GST prior to inoculation. Mice were then administered recombinant loricrin L2v or recombinant GST intra-nasally 24 h and 48 h post inoculation. A significant decrease in nasal colonisation by *S. aureus* Newman was observed after 3 days in the presence of recombinant loricrin L2v but not GST (Figure 5.11 A). This result indicates that nasal colonisation by *S. aureus* can be inhibited by the presence of loricrin L2v, confirming the importance and necessity of the role of ClfB and loricrin in *S. aureus* nasal colonisation. In order to ensure that the incubation temperature in the mouse nose did not cause breakdown of either protein, samples of GST and L2v were incubated for 24 hours at varying temperatures and were then analysed by SDS-PAGE (Figure 5.11 B). Neither protein displayed any breakdown after incubation compared to a freshly thawed sample, indicating that incubation for 24 h in the mouse nares would not affect protein stability.

5.2.9 The absence of loricrin does not affect *S. aureus* systemic infection in mice.

The absence of loricrin in the nasal passages of $Lor^{-/-}$ mice has a substantial effect on *S. aureus* nasal colonisation. Taking into account that the loricrin-deficiency is present throughout squamous epithelial tissue in the $Lor^{-/-}$ mouse, the role of loricrin during *S. aureus* systemic infection was investigated. WT and $Lor^{-/-}$ mice were challenged by intraperitoneal injection with *S. aureus* Newman ($5x10^8$ CFU). The bacterial burden in the lungs, spleen, liver, blood and peritoneal cavity was quantified. After 3 days, there appeared to be no significant differences in the levels of systemic bacterial infection between WT and $Lor^{-/-}$ mice (Table 5.1), implying that the interaction between loricrin and *S. aureus* is specific to the nasal epithelium and there is no evidence of a role for loricrin is *S. aureus* systemic infection.

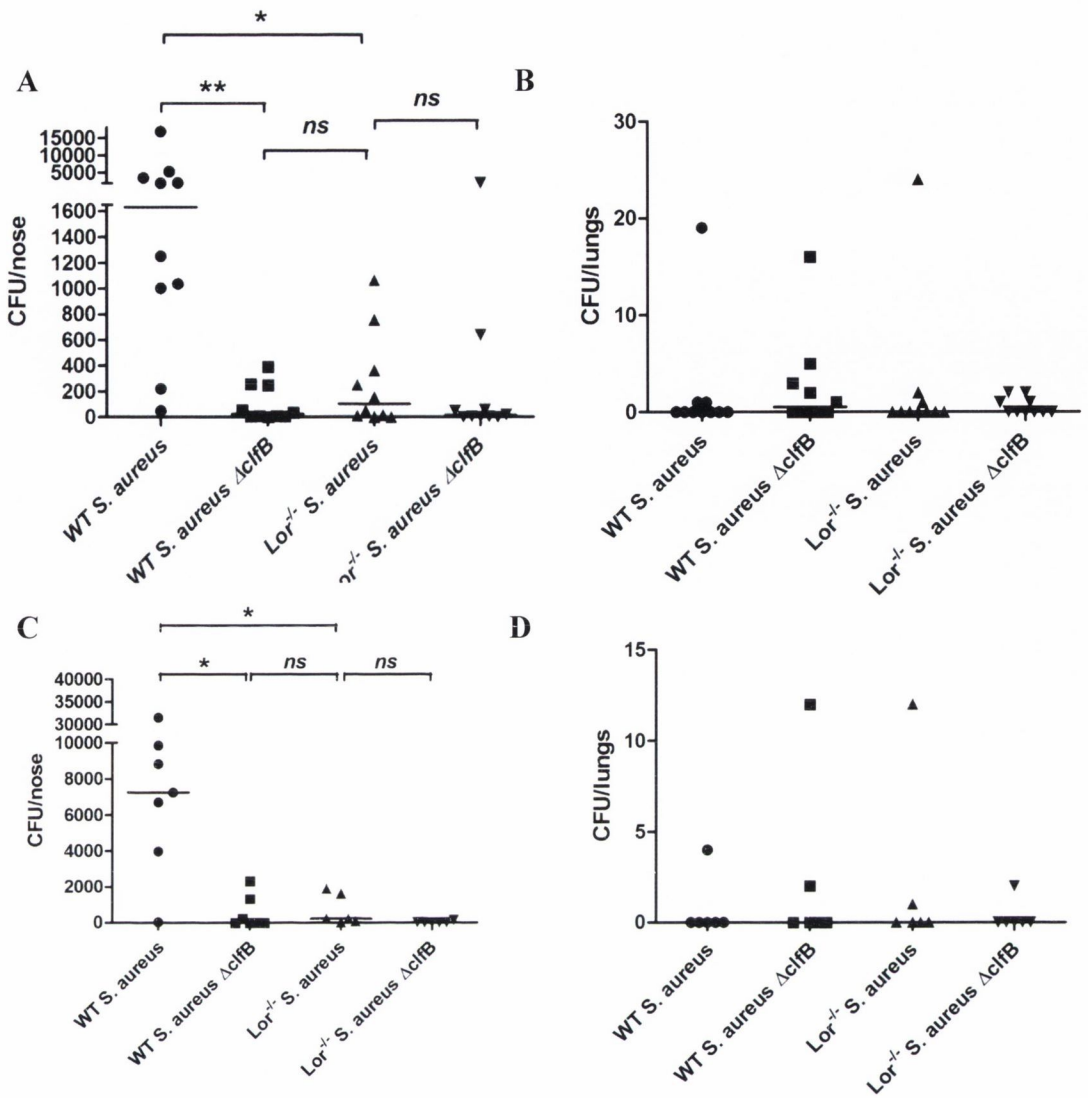

Figure 5.10. Nasal colonisation of *S. aureus* Δ*clfB* in FVB wild-type and Lor$^{-/-}$ mice.

Mice were inoculated intranasally with **(A)** Newman or Newman Δ*clfB* (2x10^8 CFU, n=10 per group) or **(C)** SH1000 or SH1000 Δ*clfB* (2x10^8 CFU, n=6-7 per group). After 10 days, mice were euthanized and the bacterial burden in the nasal tissue was established. Lung tissue was also excised and the bacterial burden was quantified **(B, D).** Each dot indicates the number of CFU/nose or lung for a single mouse. Results are expressed as log CFU per nose with the median indicated by a bar. Statistical analysis was performed using the Krustal-Wallis test and Dunns Multiple Comparisons test.

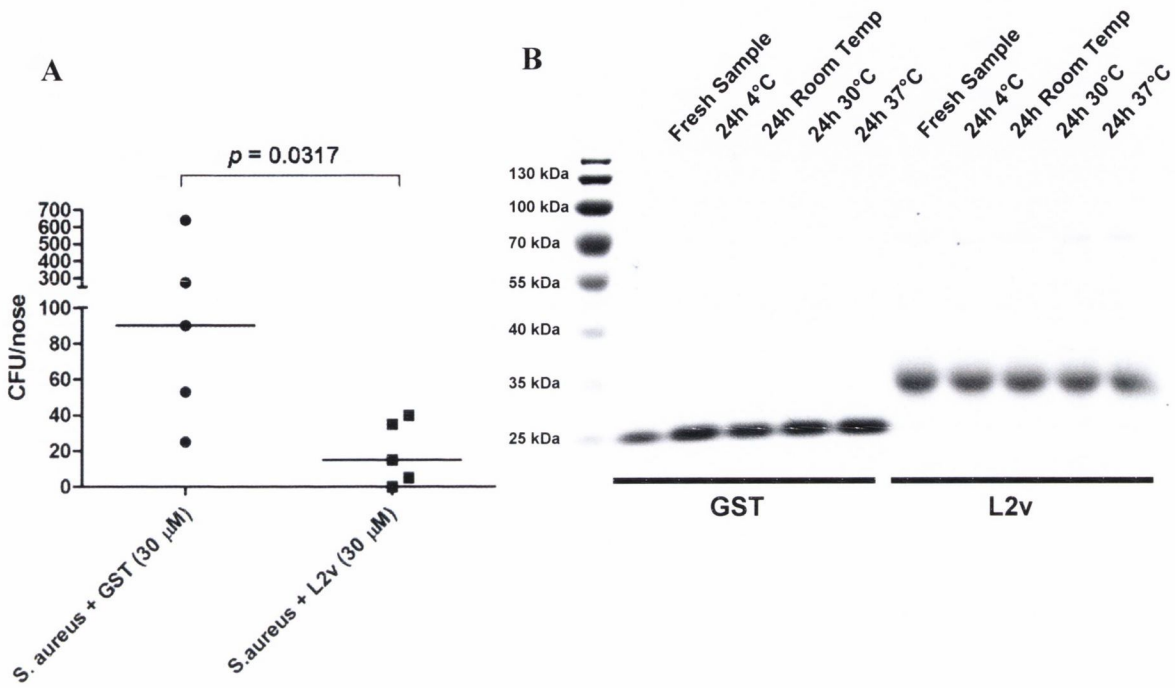

Figure 5.11. ***In vivo*** **blocking of** ***S. aureus*** **with recombinant loricrin L2v in FVB mice. (A)** *S. aureus* Newman was pre-incubated with recombinant GST or recombinant L2V-GST for 30mins before intranasal inoculation (2 x 10^8 CFU). Mice were then treated intranasally with recombinant GST or recombinant L2V-GST on days 1 and 2. Mice were euthanized and the bacterial burden in the noses established on day 3. Each dot indicates the number of CFU/nose for a single mouse. Results expressed as log CFU per nose with the median indicated by a bar (n=5 per group). Statistical analysis was performed using a Mann-Whitney test. **(B)** Recombinant GST and recombinant L2v were purified under LPS-free conditions and were incubated at varying temperatures for 24h. Equal amounts of each protein were analysed by SDS-PAGE and stained with Coomassie blue.

Table 5.1 Systemic infection in Lor$^{-/-}$ mice

	Peritoneal Cavity	Blood	Liver	Kidney	Spleen
WT	3.26 ± 0.52	5.46 ± 0.27	7.24 ± 0.11	5.01 ± 0.12	5.4 ± 0.41
Lor-/-	3.59 ± 1.31	6.24 ± 0.53	6.91 ± 0.30	5.42 ± 0.90	6.25 ±0.65
	P=0.8571	*P*=0.2286	*P*=0.6286	*P*=0.6286	*P*=1

Results expressed as mean log CFU/ml of fluid or homogenised tissue ± SEM, n=4 per group

5.3 Discussion

The ability of *S. aureus* to adhere to desquamated epithelial cells in the nasal cavity is due in part to the expression of clumping factor B. ClfB plays an important role in nasal colonisation and facilitates adherence of *S. aureus* to human nasal desquamated epithelial cells (squames) (Clarke *et al.* 2006; Corrigan *et al.* 2009). The ability of ClfB to adhere to squames is likely due to its capacity to interact with structural proteins exposed on the surface of the cornified envelope (CE). Previous *in vitro* studies have shown that ClfB can bind to cytokeratin 10 (K10), a surface exposed CE structural protein (O'Brien *et al.* 2002; Walsh *et al.* 2004). Furthermore, *in vitro* evidence generated in this study has shown that ClfB binds to the CE protein loricrin. In this chapter, the interaction between loricrin and ClfB *in vivo* was examined. The availability of loricrin as a surface-exposed ligand was assessed and its involvement in ClfB-mediated adherence to squames was investigated. The roles of loricrin and ClfB in nasal colonisation were defined in order to confirm the important role played by ClfB in this process and to establish whether loricrin is the main target for ClfB in the nose.

The mechanism of nasal colonisation by *S. aureus* most likely depends on attachment of the bacterial cell to the nasal epithelium. The ability of *S. aureus* surface proteins such as ClfB and IsdA to promote bacterial adhesion to squames may be the foundation for their importance in nasal colonisation. In this chapter, the ability of ClfB to mediate bacterial adherence to human squames was confirmed and was shown to be dependent on loricrin. Adherence of a ClfB-deficient mutant of *S. aureus* to human squames was significantly reduced compared to its wild-type parental strain, confirming the importance of ClfB in this mechanism. A similar significant reduction in adherence was observed in *S. aureus* pre-incubated with recombinant loricrin loop region 2v (L2v), compared to the same strain pre-incubated with recombinant GST alone. L2v reduced *S. aureus* squame adherence to a similar level as *S. aureus* Δ*clfB*, implying that L2v is inhibiting ClfB-mediated adherence to squames. Consistent with previous studies, adherence to squames was not completely abolished, providing further proof that this is a multifactorial process. No

further reduction in squame adherence was observed after pre-incubation of *S. aureus* Δ*clfB* with L2v, indicating that L2v is not bound detectably by other staphylococcal surface proteins under these conditions. This data provides strong evidence that the interaction between ClfB and loricrin plays a major role in squame adherence.

In order for an interaction to occur between ClfB and loricrin in the nose, loricrin must be exposed on the surface of squames. Loricrin has previously been detected on the surface of skin epithelial cells (Lopez *et al.* 2007). Using whole cell dot immunoblotting and flow cytometry, this study revealed that loricrin is exposed on the surface of squames. Monospecific loricrin antibodies recognizing the C-terminal region of the protein bound to human squames. According to the predicted 3D rosette-like structure of loricrin, this region is heavily modified by transglutaminases and is occluded by the omega loop domains within the protein (Candi *et al.* 1995). Therefore, it is possible that if this region is detectable on the surface of squames then the loop regions of loricrin bound by ClfB are also surface-exposed.

The mouse model used in this study has been previously utilized (Kiser *et al.* 1999; Schaffer *et al.* 2006). Other recent colonisation studies have revealed the effectiveness of the cotton rat as a robust animal model for rapid and sustained *S. aureus* nasal colonisation. Despite the proven superiority of the cotton rat model to achieve higher sustained levels of *S. aureus* nasal colonisation compared to mouse models (Kokai-Kun *et al.* 2003), the use of mice holds a substantial advantage in this field due to the availability of transgenic and knock-out animals. Models such as these provide more in-depth analysis of the host-bacterial interaction, an option not yet obtainable with the cotton rat.

Levels of *S. aureus* colonisation in the mouse may be influenced by factors such as mouse strain, inoculum load and bacterial strain. Using an inbred strain of mouse and a bacterial load of 10^8 CFU per nose, stable levels (10^3 CFU per nose) of nasal colonisation that were comparable to those seen previously in more efficiently colonised outbred mouse strains were achieved in this study for a period up to 21 days. Furthermore, the reliability of the model

was validated by using two different *S. aureus* strains. Both *S. aureus* strains Newman and SH1000 exhibited steady rates of nasal colonisation after 10 days.

The method of inoculation was optimized by investigating the effect of inoculation with a fresh *S. aureus* culture compared to frozen cells on colonisation levels. The use of a frozen bacterial culture, where one batch of bacteria is prepared and separated into fractions, may reduce variability in the model by using identically-treated inocula in successive colonisation experiments. Mice inoculated with a frozen culture of *S. aureus* cells were colonised more reliably than those inoculated with a fresh culture of the organism. Similarly, the effects of inoculating an anaesthetized mouse compared to an alert mouse were analysed. A major drawback of the administration of anaesthetic to mice prior to inoculation is the potential for inhalation of the bacteria into the lungs, possibly leading to systemic dissemination. However, using a bacterial load of 10^8 CFU per nose, no increase in dissemination to the lungs was seen in mice that were given anaesthetic compared to fully alert animals.

In order to analyse the interaction between ClfB and loricrin *in vivo*, nasal colonisation in wild-type and $Lor^{-/-}$ mice was established and compared. Both strains were initially colonised with *S. aureus* to the same extent suggesting that the loricrin-ClfB interaction is not required for initial attachment of bacteria to the nasal tissue. However, a significantly lower level of colonization was observed in $Lor^{-/-}$ mice over time compared to a sustained and increasing level of colonization in the wild-type animals, indicating that loricrin is necessary for efficient proliferation of the bacteria in the nose. A lower level of *S. aureus* colonisation was observed in the $Lor^{-/-}$ mice, presumably due to the ability of ClfB and other *S. aureus* factors to bind alternative receptors.

The variability in colonisation levels of wild-type and $Lor^{-/-}$ mice brings into question the variability of expression of major CE constituents implicated in this process. Previous studies have shown that keratin expression is not increased in $Lor^{-/-}$ mice (Jarnik *et al.* 2002). Using Western immunoblotting and densitometry, this study determined that wild-type and $Lor^{-/-}$ mice express varying but similar levels of keratin. Likewise, loricrin expression in wild-type

mice was variable. However, this did not correlate with the observed variation in colonisation levels. It is possible that the variable colonisation rates observed are due to factors inherent in the colonisation process. Alternatively, variation in the surface exposure of ligand-binding loop regions within loricrin could serve as another explanation. Analysis of the affinity of ClfB for the individual loricrin loop regions (Chapter 4) showed that ClfB bound to different loops with varying affinities. Perhaps variation in the surface exposure of these loricrin loop regions during formation of the CE plays a role in the subsequent strength of bacterial attachment to the squamous cell during colonisation. More knowledge of the organisation of proteins in the CE is required in order to characterise this interaction further.

The specificity of the interaction between ClfB and loricrin *in vivo* was established using a novel murine nasal colonisation model in which mice were inoculated with the surrogate host *L. lactis* expressing ClfB. *L. lactis* is widely used as a tool for surface expression of bacterial factors, and has previously been utilized in nasal administration of pneumococcal vaccines (Medina *et al.* 2010). However, to date, the heterologous expression system has not been used to examine protein-protein interactions in a nasal colonization model. After 24 hours, an 80% decrease in the levels of *L. lactis* ClfB$^+$ colonisation was observed in Lor$^{-/-}$ mice compared to wild-type mice, indicating that loricrin represents the major binding target for ClfB in the nares. This model also demonstrated that expression of ClfB alone is sufficient to promote nasal colonisation, without any dependence on other staphylococcal factors. The low numbers of bacteria recovered from the noses of these mice and the short duration of colonisation is likely due to the fact that *L. lactis* is an avirulent and nutritionally fastidious organism that grows optimally at 28-30°C (Jensen and Hammer 1993). Although these results propose that colonisation in this model is almost entirely due to the interaction between loricrin and ClfB, the residual binding of *L. lactis* ClfB$^+$ observed likely reflects a minimal interaction of ClfB with other CE proteins such as K10.

The specificity of the ClfB-loricrin interaction seen during nasal colonisation was confirmed *in vivo* by investigating the colonisation ability of

ClfB-deficient mutants of *S. aureus* in $Lor^{-/-}$ mice. Consistent with previous studies, a ClfB-deficient mutant of *S. aureus* Newman was significantly impaired in its ability to colonise wild-type mice compared to its parental strain 10 days post inoculation. The role played by ClfB in this significant loss in colonisation levels was confirmed using a ClfB-deficient mutant of *S. aureus* SH1000. Unlike previous studies (Schaffer *et al.* 2006), the colonisation defect seen here was not lost when using a bacterial load of 10^8 CFU per nose. In contrast, a low level of colonisation was achieved when $Lor^{-/-}$ mice were inoculated with either a *clfB* mutant or its parental strain, indicating that the interaction between ClfB and loricrin is crucial for *S. aureus* nasal colonisation.

Previous studies and the *ex vivo* results generated in this chapter indicate that several staphylococcal factors are involved in initial bacterial attachment to squames (Clarke *et al.* 2006; Corrigan *et al.* 2009). However, the *in vivo* data obtained here suggests that the interaction between ClfB and loricrin is crucial for sustained nasal colonisation. This was confirmed again by blocking the ClfB-loricrin interaction *in vivo* using recombinant loricrin L2v. After 3 days, colonisation levels of *S. aureus* pre-incubated with L2v were reduced by a factor of 10 compared to *S. aureus* pre-incubated with GST alone. Taken together, the nasal colonisation data obtained in this chapter demonstrates that in the absence of loricrin, ClfB-expressing bacteria colonise poorly, despite the presence of K10. This suggests that K10 is not an important ligand for ClfB during nasal colonisation. A similar model using a K10-deficient mouse would help to establish the relative contribution of loricrin and K10 in colonisation (Reichelt *et al.* 2001). However, in the absence of K10, it is likely that ClfB expressed by *S. aureus* would still bind to loricrin, which may compensate for the effects of a K10 deficiency. Ideally, a mouse deficient in both K10 and loricrin would be required for a comprehensive study on the interaction between ClfB and its ligands in the nose. However, such a strain currently does not exist and the double mutation may be lethal.

The results obtained in this chapter demonstrate that the absence of loricrin has a marked effect on *S. aureus* nasal colonisation. An *S. aureus* infection study was carried out in order to determine whether a loricrin-

deficiency has a global effect on *S. aureus* interactions with the host. The results showed that the effects of a loricrin-deficiency are limited to the nasal passages and that there is no role for loricrin in infection.

In summary, this chapter has defined loricrin as a major binding partner for ClfB during nasal colonisation. Loricrin was revealed to interact with *S. aureus* on the surface of human squames in a ClfB-mediated process. A previously successful murine model of nasal colonisation was optimized and utilized to characterise the interaction between ClfB and loricrin *in vivo*. ClfB has been confirmed as one of the primary bacterial adhesins involved in nasal colonization and the mechanism by which it interacts with the host has been elucidated. This chapter reveals the role of loricrin as a major determinant of *S. aureus* nasal colonisation and as the primary target for ClfB in the nose.

Chapter 6

Evaluation of the interaction between iron-regulated surface determinant protein A and loricrin

6.1 Introduction

Growth of *Staphylococcus aureus* under iron-limited conditions most likely represents the growth environment during *S. aureus* colonisation and infection *in vivo*. Growth under these conditions elicits the expression of a subset of staphylococcal genes known as the iron-regulated surface determinant (*isd*) genes. Collectively, the products of these genes are responsible for the acquisition of iron from haemoglobin and haem and its transport into the bacterial cell (Dryla *et al.* 2003; Mazmanian *et al.* 2003). Individually, many of the products of this gene set have ligand-binding capabilities that extend beyond haem-uptake to other processes involved in bacterial colonisation and infection.

The surface-expressed haem-binding proteins IsdA, IsdH and IsdB are known to have other functions in *S. aureus* infection and colonisation. IsdH is involved in evasion of phagocytosis due to its ability to bind to and activate complement factor I, which accelerates degradation of the serum opsonin C3b (Visai *et al.* 2009). IsdB has been shown to play a direct role in platelet activation by binding to platelets via the platelet integrin GPIIb/IIIa and triggering activation (Miajlovic *et al.* 2010) and binds other β3-containing integrins promoting invasion of epithelial cells (Zapotoczna *et al.* 2012). IsdA is a multi-ligand binding protein that promotes adherence to squames and nasal colonisation as well as survival on the skin by conferring resistance to innate immune defences.

It has been proposed that IsdA is a multi-ligand binding protein. The recombinant form of IsdA was shown to bind extracellular matrix proteins such as fibrinogen and fibronectin, albeit at a low affinity. It can also interact with the cornified envelope proteins loricrin, involucrin and cytokeratin 10. Atomic force microscopy demonstrated a direct, specific interaction between IsdA and loricrin. In addition, IsdA has been reported to mediate weak bacterial adherence to several ligands, including fibrinogen, fibronectin, loricrin, involucrin and keratin, as adherence appeared to be abolished in an IsdA-

deficient strain under iron-limited growth conditions (Clarke, Wiltshire *et al.* 2004; Clarke, Andre *et al.* 2009).

The role played by IsdA in *S. aureus* nasal colonisation has been established comprehensively. As well as ClfB, IsdA promotes adherence of *S. aureus* to human desquamated epithelial cells. In a cotton rat model of staphylococcal nasal colonisation, a mutant deficient in IsdA was unable to colonise the nares of cotton rats compared to a wild-type strain (Clarke *et al.* 2006). However, unlike ClfB, direct evidence for a role for IsdA in colonising the nares of humans is lacking. In addition, cotton rats immunized with IsdA, and also IsdH, had significantly lower rates of nasal colonisation by *S. aureus*. However dose-dependent vaccination was only observed using IsdA. Furthermore, in a human study, significantly increased cross-reactive anti-IsdA IgG titres were reported in non-carriers compared to healthy carriers, suggesting that IsdA-specific antibodies may have a role in protection against nasal colonisation (Clarke *et al.* 2006). In addition, IsdA has been shown to be an immunological marker of infection as antibodies are raised against it during *S. aureus* disease (Clarke, Brummell *et al.* 2006). Anti-IsdA IgG was also found in serum from patients convalescing from *S. aureus* infections (Clarke *et al.* 2004).

IsdA confers resistance to host innate immune defences and is required for survival on human skin and possibly in the nasal mucosa. Under iron-limited conditions, IsdA was shown to decrease cell surface hydrophobicity causing the bacterial cell to be more negatively charged which confers protection against the bactericidal activity of sebum fatty acids and antimicrobial peptides such as beta-defensin 2. In a human skin colonisation study, significantly lower numbers of an IsdA-deficient mutant of *S. aureus* were recovered from the skin of healthy human volunteers than a wild-type parental strain (Clarke, Mohamed *et al.* 2007). Furthermore, IsdA mutants are more sensitive to killing by the bactericidal host protein lactoferrin (Clarke and Foster 2008).

In this chapter, the ligand binding capability of IsdA was tested and the interaction between IsdA and loricrin was examined *in vivo* and *ex vivo*. *S. aureus* Δ*isdA* and a mutant deficient in both IsdA and ClfB were used in adherence assays in order to assess the ability of IsdA to mediate binding to

loricrin in the presence and absence of ClfB. Similarly, *Lactococcus lactis* expressing IsdA was used to examine the ability of IsdA to promote bacterial adherence to cornified envelope proteins. Purified recombinant IsdA was tested in ELISA-based binding assays and by SPR in order to analyse the interaction between IsdA and loricrin in more detail. Adhesion studies using human desquamated epithelial cells were performed in order to determine whether IsdA interacts with loricrin on the surface of squames *ex vivo*. Finally, a murine nasal colonisation model was established using *S. aureus* Δ*isdA* in $Lor^{-/-}$ mice in order to analyse the interaction between IsdA and loricrin in the mouse nose.

6.2 Results

6.2.1 Adherence of *S. aureus* to recombinant loricrin is not dependent on IsdA under iron-limited conditions.

IsdA has been previously described as a multi-functional adhesin capable of binding to CE proteins loricrin, involucrin and keratin as well as fibrinogen and fibronectin (Clarke, Wiltshire *et al.* 2004; Clarke, Andre *et al.* 2009). In order to evaluate the interaction between IsdA and loricrin, *S. aureus* strains Newman, Newman Δ*isdA*, Newman Δ*clfB* and Newman Δ*isdA*Δ*clfB* were tested for adhesion to immobilized loricrin. All strains were grown in iron-limited conditions in RPMI to induce expression of IsdA.

S. aureus Newman adhered avidly to HLor-GST and MLor-GST (Figure 6.1). However, there was no observed reduction in adherence by *S. aureus* Δ*isdA*. Similar results were generated using untagged recombinant human loricrin (data not shown). In order to assess whether the effects of the IsdA deficiency were masked by ClfB expression, a ClfB-deficient strain of mutant was also tested for adherence. *S. aureus* Δ*clfB* did not adhere detectably to loricrin, indicating that the adherence observed is facilitated only by ClfB and not by IsdA. Furthermore, a double mutant deficient in ClfB and IsdA did not adhere detectably to loricrin, indicating that ClfB alone promotes adhesion to loricrin when bacteria are grown under iron-limited conditions.

Each strain was also tested for adherence to HK10-GST, MK10-GST and commercial fibrinogen (Figure 6.2). There was no detectable reduction in adherence to fibrinogen observed using Newman Δ*clfB* and Newman Δ*isdA*Δ*clfB* compared to the wild-type strain (Figure 6.2 A). This is most likely due to the expression of ClfA by Newman. Newman Δ*isdA* adhered avidly to fibrinogen. Similarly, Newman Δ*clfB* and Newman Δ*isdA*Δ*clfB* displayed reduced adherence to HK10 and MK10 compared to the wild-type strain, whereas Newman Δ*isdA* showed no reduction in adherence compared to its parental strain (Figure 6.2 B, C). These results indicate that under these conditions, adherence to fibrinogen and K10 is not facilitated by IsdA.

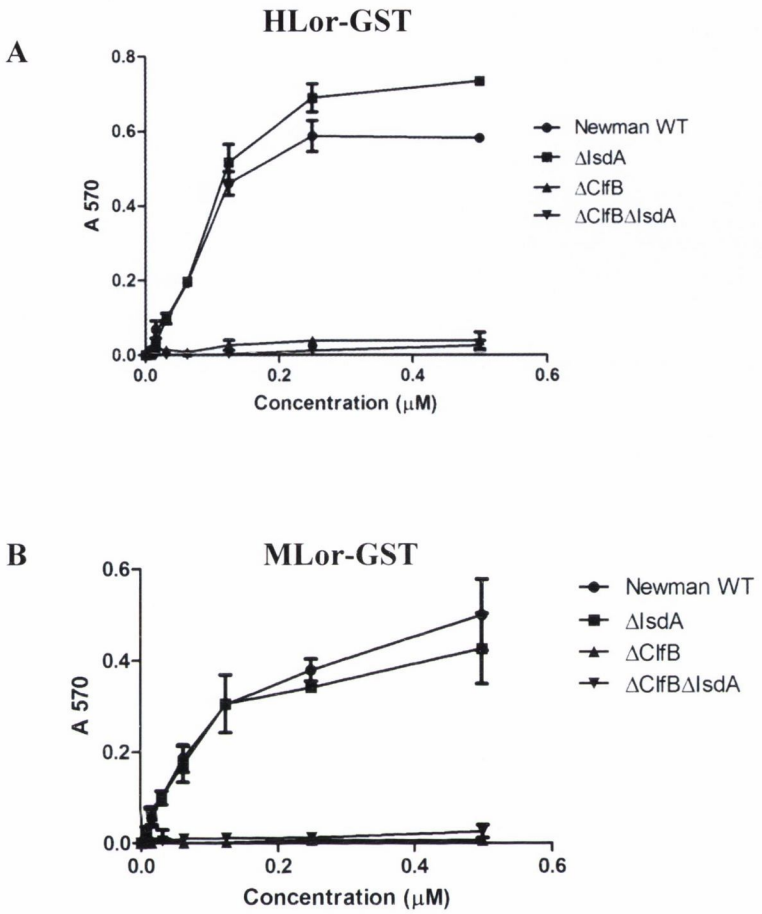

Figure 6.1. Adherence to loricrin by *S. aureus* under iron-limited conditions. *S. aureus* Newman, Newman Δ*isdA*, Newman Δ*clfB*, and Newman Δ*clfB*Δ*isdA* were tested for binding to **(A)** GST-tagged human loricrin and **(B)** GST-tagged murine loricrin (0.5 μM) immobilized on 96-well plates. Bacterial adherence was measured by staining with crystal violet and measurement of the absorbance at 570nm. Values are representative of mean ±SD of triplicate wells. The data shown is representative of three individual experiments.

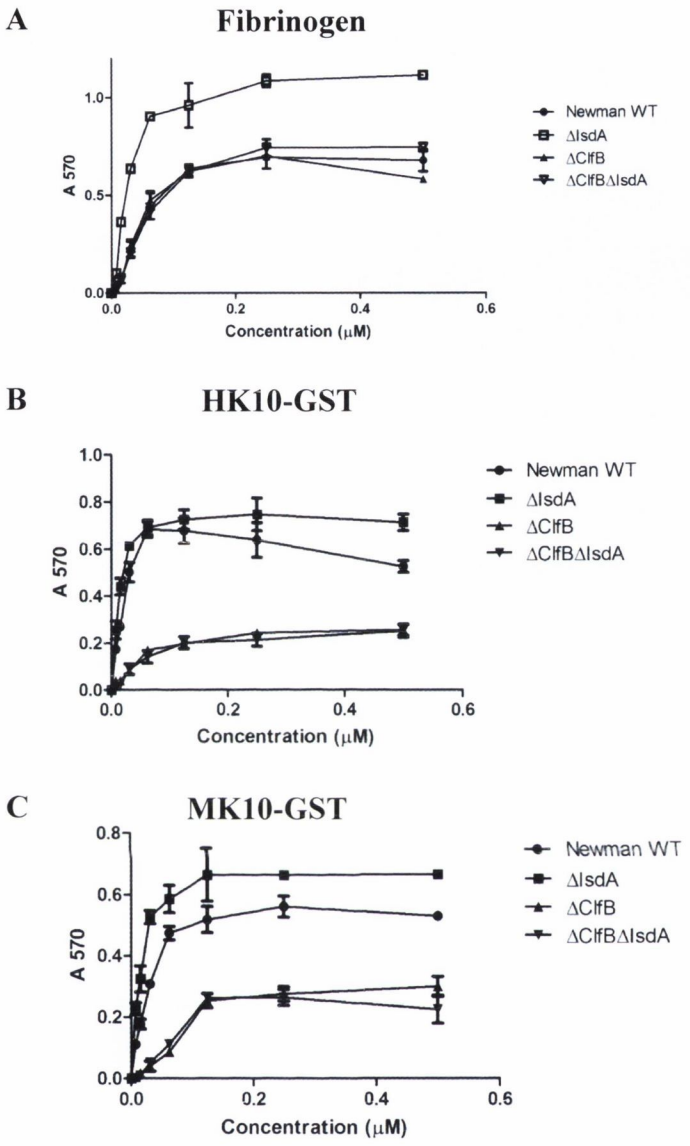

Figure 6.2. Adherence to fibrinogen and keratin by *S. aureus* under iron-limited conditions. *S. aureus* Newman, Newman Δ*isdA*, Newman Δ*clfB*, and Newman Δ*clfB*Δ*isdA* were tested for binding to **(A)** commercial fibrinogen **(B)** GST-tagged HK10 YY loop and **(C)** GST-tagged MK10 tail region (0.5 μM) immobilized on 96-well plates. Bacterial adherence was measured by staining with crystal violet and measurement of the absorbance at 570nm. Values are representative of mean ±SD of triplicate wells. The data shown is representative of three individual experiments.

Lactococcus lactis carrying the plasmid NZ9800 expressing IsdA from a nisin-inducible promoter was tested for adherence to loricrin, keratin and fibrinogen compared to a strain carrying the empty-vector. *L. lactis* expressing IsdA did not adhere detectably to any of the ligands (data not shown), indicating that IsdA expressed on the surface of the cell does not adhere to human or murine loricrin, K10, or to fibrinogen. Whole cell dot immunoblotting using anti-IsdA IgG was performed in order to ensure that IsdA was expressed on the surface of *L. lactis* (Chapter 3 Figure 3.11).

6.2.2 Recombinant IsdA displays weak binding to recombinant loricrin and keratin.

The ability of IsdA to interact directly with loricrin and keratin was investigated using the recombinant form of the protein. Recombinant IsdA was expressed with an N-terminal Histidine-tag from the plasmid pQE30 and was purified (Figure 6.3 A). Doubling concentrations of rIsdA (0.15 μM-20 μM) were added to microtitre plates coated with a fixed concentration of Hlor-GST, MLor-GST, HK10-GST and MK10-GST. rIsdA exhibited low, dose-dependent binding to each ligand (Figure 6.3 B). rIsdA bound HK10 the strongest, whereas the weakest interaction occurred between rIsdA and human loricrin. The estimated concentrations at half-maximum binding for MLor, HK10 and MK10 were 13.24 μM, 9.73 μM, and 40.67 μM, respectively. The concentration at half-maximum binding for HLor could not be determined. This data indicates that recombinant IsdA interacts with loricrin and keratin, albeit very weakly. Increasing the highest concentration of rIsdA to 40 μM did not alter the half-maximum binding concentrations (data not shown).

SPR was also performed in order to assess the ability of rIsdA to bind to recombinant loricrin and keratin. HLor-GST was captured on the surface of a sensor chip that had been coated with anti-GST IgG. Increasing concentrations of rIsdA were passed over the surface of the HLor-coated chip. This experiment did not provide any evidence for an interaction between IsdA and loricrin. Similarly, there was no binding observed by IsdA to a chip coated with MLor, HK10 or MK10 (data not shown), indicating that the recombinant form of IsdA has a very weak affinity for these ligands.

6.2.3 IsdA-mediated adherence of *S. aureus* to human desquamated epithelial cells is not dependent on an interaction with loricrin

IsdA has been shown to play a role in *S. aureus* adherence to squames using bacteria grown under iron-limited conditions and it has also been suggested that it facilitates adherence to recombinant human loricrin *in vitro* (Clarke, Brummell *et al.* 2006; Clarke, Andre *et al.* 2009). However no evidence of this interaction has been observed in this study. In order to establish whether an interaction between IsdA and loricrin promotes bacterial adherence to squames, binding assays were performed using *S. aureus* Newman and *S. aureus* Newman Δ*isdA* grown under iron-limited conditions.

A significant reduction (p=0.0045) in adherence of *S. aureus* Δ*isdA* to squames was observed when compared to a wild-type strain (Figure 6.4). In order to establish a role for loricrin in this interaction, *S. aureus* Δ*isdA* was pre-incubated with L2v and tested for adherence to squames. Pre-incubation of *S. aureus* Δ*isdA* with L2v significantly impaired adherence to squames compared to pre-incubation of *S. aureus* Δ*isdA* with GST alone, most likely by inhibiting the interaction between ClfB and its ligands. A double mutant (*S. aureus* Δ*clfB*Δ*isdA*) demonstrated a similar significantly impaired ability (*P*=0.0322) to adhere to squames, compared to that observed when *S. aureus* Δ*isdA* was pre-incubated with Lv2. Pre-incubation with L2v did not cause any further drop in adherence of *S. aureus* Δ*clfB*Δ*isdA*. Taken together, these results confirm that IsdA contributes significantly to adherence of *S. aureus* to human squames but shows that this does not involve an interaction between IsdA and loricrin loop region L2v.

6.2.4 Nasal colonisation of *S. aureus* Δ*isdA* in FVB wild-type and Lor$^{-/-}$ mice.

A role for IsdA in nasal colonisation has previously been implicated using a cotton rat model (Clarke *et al.* 2006). In order to demonstrate whether an interaction with loricrin is the basis for this role, groups of wild-type and Lor$^{-/-}$ mice were inoculated intra-nasally with Newman or Newman Δ*isdA*. After 10 days, the nasal bacterial burden was quantified (Figure 6.5). There was a significant reduction ($p<0.05$) in colonisation of wild-type mice by Newman

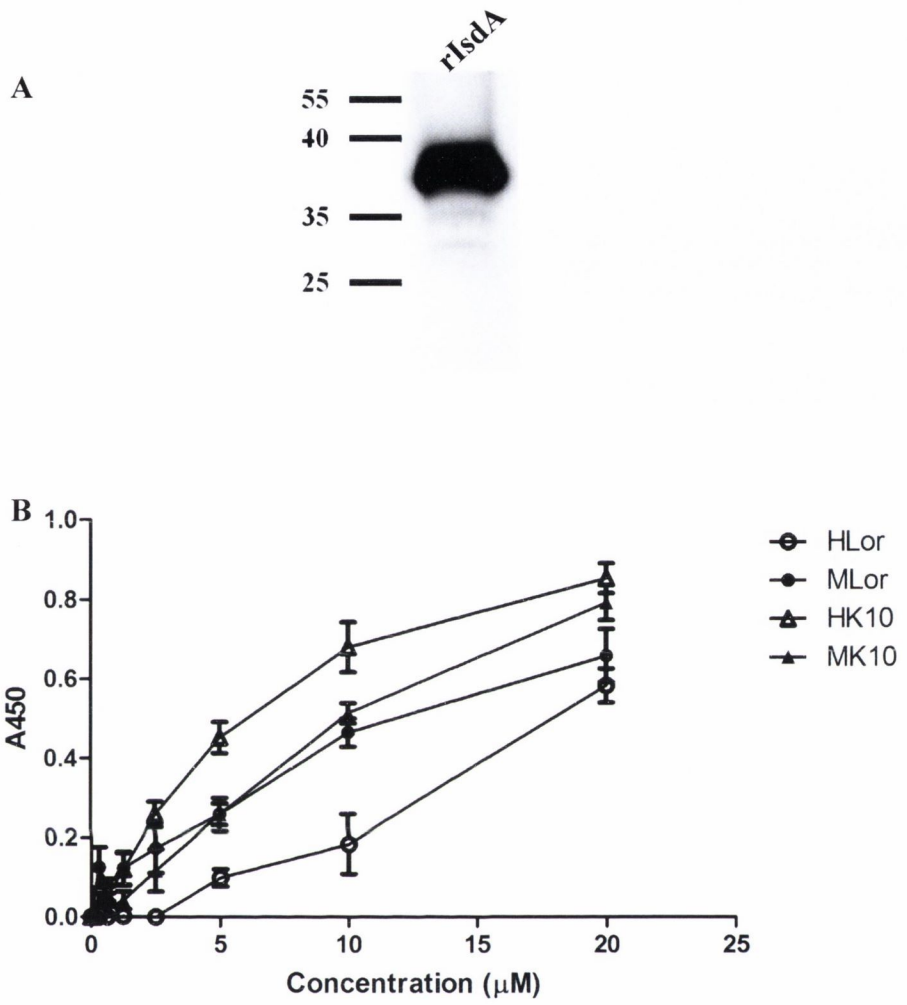

Figure 6.3. Binding of recombinant IsdA to loricrin and keratin. (A) Western blot depicting recombinant His-tagged IsdA. Recombinant IsdA was analysed by SDS-PAGE and was then transferred to a PVDF membrane. The membrane was probed with anti-IsdA IgG. Bound antibody was detected using HRP-conjugated protein A **(B)** Doubling dilutions of recombinant His-tagged IsdA were added to wells containing immobilized Hlor-GST, Mlor-GST, HK10-GST and MK10-GST (0.5 μM). Bound protein was detected using HRP-conjugated anti-His IgG and developed by incubation with a chromogenic substrate. The absorbance at 450 nm was determined. Values represent the mean ± SD of triplicate wells. The values shown are representative of 3 individual experiments.

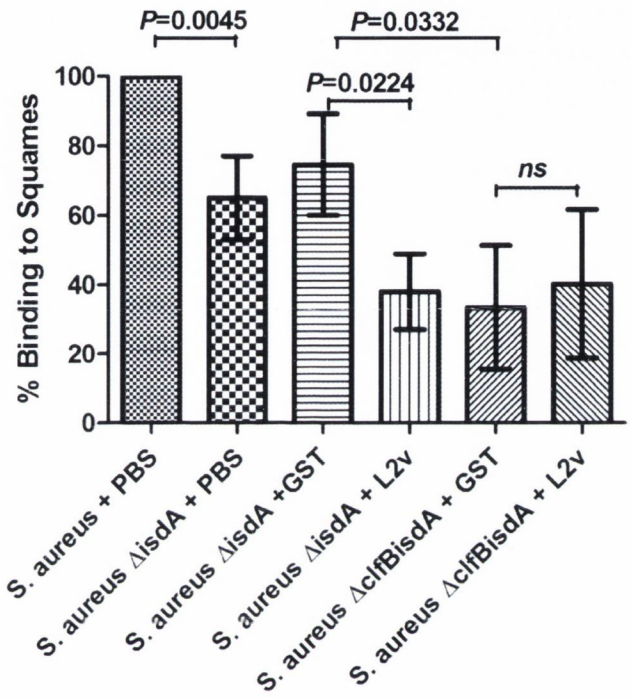

Figure 6.4. IsdA-mediated bacterial adherence to human squames. *S. aureus* Newman Δ*isdA* and Newman Δ*clfB*Δ*isdA* were grown in RPMI. Washed cells were incubated with recombinant GST or recombinant L2v-GST before being incubated with human nasal squamous epithelial cells. Crystal violet-stained adherent bacteria were enumerated by microscopy and were expressed as a percentage of the positive control. Results are expressed as the mean ±SD of 3 independent experiments. Statistical analysis was performed using a *t* test.

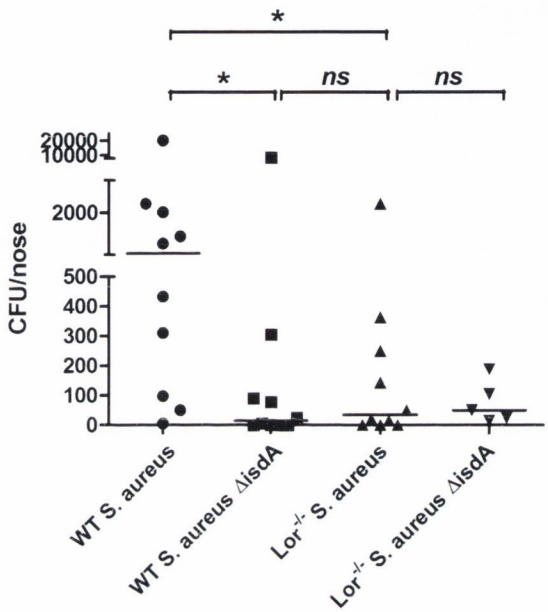

Figure 6.5. Nasal colonisation of *S. aureus* Δ*isdA* in FVB wild-type and Lor$^{-/-}$ mice. Mice were inoculated intranasally with Newman Δ*isdA* ($2x10^8$ CFU, n=5-10 per group). After 10 days, mice were euthanized and the bacterial burden in the nasal tissue was established. Each dot indicates the number of CFU/nose for a single mouse. Results are expressed as log CFU per nose with the median indicated by bar. Statistical analysis was performed using the Krustal-Wallis test and Dunns Multiple Comparisons test. * $P< 0.05$

Δ*isdA* compared to the parental strain, confirming the role played by IsdA in nasal colonisation. In contrast, there was no significant difference between colonisation with the parental Newman strain and Newman Δ*isdA* strain in the $Lor^{-/-}$ mice.

6.3 Discussion

S. aureus nasal colonisation is a multifactorial process in which many staphylococcal surface proteins have been implicated. The surface adhesin IsdA is part of a collection of proteins responsible for extracting haem from haemoglobin and transporting it into the bacterial cell (Dryla *et al.* 2003; Mazmanian *et al.* 2003). It has been clearly demonstrated that IsdA promotes adhesion to human desquamated epithelial cells (Clarke *et al.* 2006; Corrigan *et al.* 2009). Previous studies have suggested that this is due to the ability of IsdA to bind to loricrin, K10 and involucrin. Studies performed in this chapter were designed to confirm the role of IsdA in adhesion to squames and colonisation of the nose and to determine if loricrin is a binding partner for IsdA *in vivo*. IsdA-mediated bacterial adherence to human squames was verified, but was found not to be dependent on an interaction with loricrin loop region L2v. Also in a murine nasal colonisation model, colonisation rates of *S. aureus* Δ*isdA* did not differ significantly in WT or $Lor^{-/-}$ mice. Thus the *in vitro* results presented in this study suggest that it is unlikely that IsdA interacts with loricrin in the nose.

In this chapter the ability of IsdA to mediate bacterial adherence to CE proteins loricrin and keratin, and blood glycoprotein fibrinogen was tested experimentally. ClfB is expressed by *S. aureus* grown to stationary phase in RPMI, unlike TSB or BHI (Miajlovic *et al.* 2010). Therefore in order to observe only IsdA-promoted adhesion, *S. aureus* mutants deficient in ClfB were also used. When grown under iron-limited conditions, *S. aureus* strain Newman deficient in IsdA displayed no detectable reduction in adherence to any ligands either in the presence of or in the absence of ClfB. These results contradict those published previously and may be due to differences in the experimental procedures used. In this study, an isogenic IsdA-deficient mutant of *S. aureus* strain Newman was generated and validated by allelic replacement using the temperature-sensitive vector pIMAY, whereas previous experiments were performed using a *S. aureus* strain SH1000 IsdA-deficient derivative generated using an *isdA:lacZ* reporter gene fusion (Clarke *et al.* 2004). The contradictory results generated here may be due to the use of different strains.

Differences in growth media may account for the differences in results obtained. The previous study used chemically defined metal limitation (CL) medium (Horsburgh *et al.* 2001) in order to create the iron-limited conditions necessary for IsdA expression, whereas the commercial medium RPMI 1640 provided iron-limited conditions for IsdA expression in this study. The difference in the constitution of the two media and the subsequent different growth environments may account for the different results generated. Although these differences may account for the conflicting results obtained using *S. aureus* in adherences assays, the lack of detectable binding of *L. lactis* expressing IsdA in this study cannot be explained. Further studies on the affect of growth medium on ligand-binding facilitated by IsdA may be required to explain conclusively these interactions *in vitro*.

Studies with recombinant IsdA in this chapter agreed with previously published results. Recombinant IsdA bound weakly to loricrin and K10 in ELISA-based binding assays. However, these results could not be confirmed using SPR analysis. The estimated half-maximum binding concentrations for IsdA and MLor, HK10 and MK10 were all in the micromolar range. The estimated half-maximum binding concentration for IsdA and HLor could not be determined from the data generated. These half maximum binding concentrations indicate very weak binding and therefore an interaction may have been too weak to detect using SPR. Previously, SPR analysis was used to display the ability of IsdA to bind to fibrinogen, fibronectin and transferrin (Clarke *et al.* 2004). The method used involved passing increasing concentrations of each ligand over an IsdA-coated chip. In this chapter, a different SPR experimental approach was adopted wherein increasing concentrations of IsdA were passed over ligand-coated chips. It is possible that the difference in experimental technique created unsuitable conditions for the IsdA-ligand interactions seen previously using SPR. Further studies using alternative methods of SPR analysis may be required in order to confirm the nature of the interaction between IsdA and its proposed ligands. An interaction between IsdA and loricrin has been demonstrated using atomic force microscopy (Clarke *et al.* 2009) but no affinity for the interaction was reported.

The ligands used in this study consisted of recombinant GST-fusion variants of proteins found in the CE, namely full length human and murine loricrin, the human keratin YY loop found in the tail region of the protein, and the tail region of murine keratin, as well as commercial fibrinogen. It is possible that a strong interaction was not observed between IsdA and the recombinant keratins because the IsdA-binding site was not present within these protein constructs. Further studies using full length recombinant K10 proteins would determine unambiguously whether IsdA interacts with keratin. Untagged human loricrin as well as the GST-tagged variant yielded the same results in adherence assays, indicating that an IsdA-binding site is not being occluded by the large GST-tag.

Previous studies have shown that IsdA promotes bacterial adhesion to squames (Clarke *et al.* 2006; Corrigan *et al.* 2009) and this may be a basis for its role in nasal colonisation. The results generated in this chapter demonstrate that adherence to human squames by *S. aureus* Δ*isdA* is significantly reduced, confirming that IsdA mediates this process. However, the data implies that IsdA does not interact with loricrin loop region 2v, as pre-incubation of *S. aureus* Δ*isdA* with L2v resulted in further reduction in adhesion to squames compared to *S. aureus* Δ*isdA* pre-incubated with GST alone. This data suggests that although IsdA mediates *S. aureus* adherence to squames, this does not involve an interaction with the second major loop region of loricrin. Adherence to loricrin still occurs in the absence of IsdA but not in the absence of ClfB, suggesting that the main binding partner for loricrin is ClfB rather than IsdA. Further inhibition studies using full length loricrin and other cornified envelope proteins may conclusively reveal IsdA binding partners on the surface of squames.

The role of IsdA in nasal colonisation has been confirmed in this chapter. Furthermore, colonisation rates of *S. aureus* Δ*isdA* did not differ significantly in WT or $Lor^{-/-}$ mice. However IsdA-mediated bacterial adherence to loricrin and keratin *in vitro* has not been verified in this study, suggesting that the colonisation rates obtained *in vivo* do not signify an interaction between loricrin and IsdA. The CE protein involucrin, also previously reported to be a ligand for

IsdA (Clarke, Andre *et al.* 2009), may act as a binding-partner in the nose. The exposure of involucrin on the cell surface has been observed in earlier studies (Lopez *et al.* 2007), suggesting that it may be a viable ligand for IsdA on squames. Moreover, the ability of IsdA to promote evasion from host innate immune defences may also provide an explanation for its role in nasal colonisation.

The nasal cavity is coated in a protective fluid containing several antimicrobial proteins including lysozyme, lactoferrin, secretory leukoprotease inhibitor (SLPI) and cationic antimicrobial peptides (Lehrer and Ganz 1999; Travis *et al.* 2001; Cole *et al.* 2002). As well as this, all major classes of lipids, including free fatty acids, glycerolipids, sphingolipids and sterols have been detected in human nasal fluid and many have displayed antimicrobial activity (Do *et al.* 2008). It is possible that IsdA plays a role in resistance to the antimicrobial peptides and fatty acids found in nasal secretions as part of the nasal colonisation process. The faster elimination of *S. aureus* Δ*isdA* from the nares observed here could be due to enhanced killing by antimicrobial substances rather than reduced adhesion. Furthermore, recent studies have reported that the presence of haemoglobin in human nasal secretions promotes *S. aureus* nasal colonisation (Pynnonen *et al.* 2011). Considering recombinant IsdA has been implicated in haemoglobin binding (Clarke *et al.* 2004), it is tempting to speculate that the presence of haemoglobin in nasal secretions may be a mechanism for IsdA-mediated colonisation.

In summary, this chapter has analysed the role of IsdA as a multi-ligand binding adhesin and has assessed its involvement in nasal colonisation in relation to the CE protein loricrin. IsdA-mediated bacterial adherence to loricrin could not be confirmed here, and it was shown that loricrin is not involved in IsdA-mediated bacterial adherence to squames. However studies with recombinant proteins suggest that a weak interaction with loricrin may occur. Although these conflicting results warrant further study in order to elucidate the function of IsdA as a multi-ligand binding adhesin, this chapter confirms that loricrin is a major determinant in the multi-faceted mechanism of *S. aureus* nasal colonisation.

Chapter 7
Discussion

7.1 Discussion

S. aureus is an opportunistic pathogen that permanently and asymptomatically colonises the anterior nares of 20% of the population. Nasal carriage of *S. aureus* is a known risk factor for subsequent infection and it has been reported that a significant number of systemic infections can be attributed to an endogenous source (von Eiff C 2001; Wertheim *et al.* 2005). Current eradication strategies are limited and rely on the use of topical antimicrobial treatments against which *S. aureus* is becoming increasingly resistant. The development of new therapeutic options for controlling nasal colonisation requires a deeper appreciation of the molecular interactions that occur between the bacterium and the host at the nasal epithelial surface.

It is likely that *S. aureus* nasal colonisation involves a number of different bacterial factors that mediate adherence to the nasal epithelium. *In vitro* studies have characterised the interactions of several surface-expressed staphylococcal proteins (ClfB, IsdA, SdrC, SdrD and SasG) with desquamated epithelial cells (Clarke *et al.* 2006; Corrigan *et al.* 2009). However, only ClfB, IsdA and the surface-exposed anionic glycopolymer wall teichoic acid (WTA) have been shown to play an active role in the colonisation process *in vivo* (Weidenmaier *et al.* 2004; Clarke *et al.* 2006; Schaffer *et al.* 2006; Wertheim *et al.* 2008).

The surface proteins SdrC, SdrD and SasG have each been reported to promote *S. aureus* adhesion to squames (Corrigan *et al.* 2009). However, binding partners for these proteins in the host have not yet been identified and the involvement of each adhesin in nasal colonisation (if any) is unclear. Although SasG has been reported to promote *S. aureus* squame adhesion (Roche *et al.* 2003; Corrigan *et al.* 2007; Corrigan *et al.* 2009), it is not expressed by many strains (Corrigan *et al.* 2007). The type-1 staphylococcal cassette chromosome (SCC) *mec* mobile genetic element-associated plasmin sensitive cell surface protein (Pls) shares significant sequence identity to SasG (Roche *et al.* 2003). Pls has also been shown to promote bacterial adherence to human

epithelial cells and the recombinant form of the protein inhibited SasG-mediated adhesion to squames. These results indicate that both proteins may be a part of a family of proteins that bind a common receptor in the nose. The ability of Pls to promote binding to keratinocyte lipids was demonstrated (Huesca *et al.* 2002) but could not be confirmed (Roche *et al.* 2003). Future research into the mechanism of squame adhesion by these proteins may help to clarify the nasal colonisation process.

Adherence to squames promoted by SdrC and SdrD has been observed *ex vivo* but neither protein was shown to facilitate nasal colonisation in a murine colonisation model (Schaffer *et al.* 2006). SdrC has been previously shown to bind the neuronal cell surface protein β-neurexin 1 and promotes attachment to cells expressing this ligand (Barbu *et al.* 2010). However the binding partner for SdrC on the squamous cell remains unknown. Further *in vitro* and *in vivo* studies are required in order to determine the nature of the involvement of these proteins in nasal colonisation by *S. aureus*.

S. aureus adhesion to desquamated epithelial cells is also promoted by ClfB and IsdA and several ligands on the surface of squames have been suggested for each adhesin (O'Brien *et al.* 2002; Clarke *et al.* 2006; Corrigan *et al.* 2009). In addition, the defective colonisation phenotype of a ClfB-deficient mutant of *S. aureus* has been proven in a murine model (Schaffer *et al.* 2006). Similarly, the colonisation defect of an IsdA-deficient strain of *S. aureus* has been proven in a cotton rat model over 26 days (Clarke *et al.* 2006). The data generated in this study has confirmed the importance of both of these proteins in squame adherence *ex vivo.* In *S. aureus* colonisation *in vivo* the primary binding partner for ClfB in the nares was identified as loricrin. Previous studies have proposed that an interaction between IsdA and loricrin occurs and that this interaction may have implications for the role of IsdA in nasal colonisation (Clarke *et al.* 2009). Although the importance of IsdA in nasal colonisation has been confirmed here, the results of this study suggest that an interaction between IsdA and loricrin is not the basis for IsdA-mediated colonisation of the nares. Further studies on the role of IsdA in nasal colonisation are warranted in order to define conclusively the factors involved in this process.

More recently, the mobile genetic element-encoded staphylococcal surface protein SasX was found to be a critical factor promoting nasal colonisation, immune evasion and virulence in *S. aureus* strains causing hospital infections in the far east (Li *et al.* 2012). SasX-deficient strains of *S. aureus* had a reduced ability to adhere to nasal epithelial cells. Furthermore, recombinant SasX protein inhibited bacterial adhesion to squames. SasX-deficient strains also displayed a significantly reduced ability to colonise the nares of mice compared to wild-type strains. This recent discovery may help to provide a deeper understanding of the complex and multifactorial process of nasal colonisation.

A role in nasal colonisation has been proposed for the surface exposed polymer WTA. A WTA-deficient mutant could not colonize the nares of cotton rats and displayed impaired adhesion to human epithelial cells (Weidenmaier *et al.* 2004). Furthermore, a WTA-deficient mutant was almost completely eliminated from the cotton rat nose after 1 day whereas a strain deficient in sortase A persisted for up to 14 days (Weidenmaier *et al.* 2008), indicating that WTA-mediated attachment is important for the initial stages of colonisation, whereas MSCRAMMs may have a more crucial role in continued colonisation. However, WTA-deficient mutants display reduced growth compared to their parental strains and the effect of WTA-deficiency on MSCRAMM expression has not been assessed comprehensively. Furthermore, a ligand for WTA in the nose has not yet been identified, although an interaction with lectin-like receptors and the scavenger receptor-specific ligand polyinosinic acid has been speculated. A stable *tag*O deletion in *S. aureus* isolated under conditions that eliminate the stress of counter selection during allelic exchange and that is carefully prepared so as to prevent the occurrence of secondary mutations is required in order to provide more conclusive evidence of the role of WTA in nasal colonisation. Moreover, further research is necessary to determine the binding partner for WTA in the nose. In all, these studies infer that ClfB, WTA and IsdA each play a role in the process of staphylococcal nasal colonisation, but the importance of ClfB has been proven most thoroughly due to the evidence of its necessity for nasal colonisation in both rodent and human models and the identification of its binding partner *in vivo*.

Animal models have often provided further insight into the mechanisms employed by *S. aureus* during nasal colonisation. Although use of the mouse has provided satisfactory results in this field that have been emulated in a human study (Schaffer *et al.* 2006; Wertheim *et al.* 2008), the cotton rat represents an excellent model for nasal colonisation. The cotton rat model has already been successfully used for many human respiratory pathogens due to the similar histological properties and similar respiratory disease progression shared by both species (Prince 1994). In addition, its success as a model for *S. aureus* nasal colonisation has been repeatedly demonstrated (Kokai-Kun *et al.* 2003; Weidenmaier *et al.* 2004; Weidenmaier *et al.* 2008). The study of *S. aureus* nasal colonisation would benefit greatly from the development of transgenic cotton rat strains. Although the murine model used in this study has generated similar results to the cotton rat with regard to IsdA, as well as providing strong evidence of an *in vivo* interaction between loricrin and ClfB, a loricrin-deficient cotton rat may provide further insight into the mechanisms involved in loricrin-dependent nasal colonisation by *S. aureus*. Rat loricrin is thought to bear similar structural characteristics to human and murine loricrin (Mehrel *et al.* 1990; Yoneda *et al.* 1992). Furthermore, the histological properties shared by humans and cotton rats including squamous epithelial areas (Prince 1978), indicates that the cotton rat may provide a superior model to study this type of interaction. However to date a transgenic cotton rat strain has not been produced.

Given that nasal colonisation is a known risk factor for subsequent *S. aureus* infection, vaccines that reduce *S. aureus* nasal colonisation may provide a means of reduction of *S. aureus* infection. Eradication of nasal colonisation has been shown to reduce the risk of nosocomial and community-acquired *S. aureus* infections (Kluytmans *et al.* 1996; Lee *et al.* 1999; van Rijen *et al.* 2008). Promising evidence for an effective immunization strategy against nasal colonisation has been reported. Mucosal immunization with exponentially grown killed *S. aureus* resulted in significantly fewer *S. aureus* CFU being present in mouse nares compared to control animals after challenge with a heterologous *S. aureus* strain (Schaffer *et al.* 2006). Moreover, systemic and intranasal immunization with recombinant ClfB significantly reduced levels of *S. aureus* colonisation in mice after a subsequent challenge. In addition, cotton

rats that had undergone systemic immunization with recombinant IsdA had significantly lower rates of colonisation compared to control animals. In a human study, both IsdA and IsdH-specific antibodies were speculated to have a play a role in protection against nasal colonisation, as non-carriers displayed significantly higher antibody titres against each protein compared to carriers (Clarke *et al.* 2006).

However, in a human trial where cohorts received a capsular polysaccharide conjugate vaccine, no statistically significant reduction in colonisation compared to pre-colonisation rates was observed, despite an increase in humoral antibody concentrations against type 5 capsule and type 8 capsule (Creech *et al.* 2009). Moreover, natural antibody responses detected in infants against staphylococcal surface proteins do not protect against subsequent carriage (Prevaes *et al.* 2012). Taken together, limited success has been observed in human vaccine trials, but due to the positive results generated using mucosal and systemic immunization in animal models, the development of a vaccine targeting antigens that are known to be involved in colonisation warrants further investigation.

The use of topical creams containing the antibiotic mupirocin has provided a successful decolonisation strategy for individuals at risk for *S. aureus* infection. Although mupirocin treatment has been successful in eradication of nasal carriage in some patients (Peacock *et al.* 2001; von Eiff C 2001), re-colonisation from extra-nasal carriage sites has been observed (Wertheim *et al.* 2004). Furthermore, staphylococcal resistance to mupirocin is emerging (Cookson *et al.* 1990; Chatfield *et al.* 1994; Dawson *et al.* 1994). Alternative treatments in animals involving the use of lysostaphin cream have generated promising results. Lysostaphin cream administered to intranasally colonised cotton rats completely eradicated *S. aureus* nasal carriage (Kokai-Kun *et al.* 2003). Furthermore, a single dose of lysostaphin cream was more effective at clearing *S. aureus* from the cotton rat nose than mupirocin. In addition, lysostaphin has also been shown to disrupt *S. aureus* and *S. epidermidis* biofilm formation on artificial surfaces (Wu *et al.* 2003) and inhibited growth of *S. aureus* nasal isolates *in vitro* (von Eiff *et al.* 2003). However, resistance to

lysostaphin has been reported *in vitro* and *in vivo* (Dehart *et al.* 1995; Stranden *et al.* 1997; Thumm and Gotz 1997; Climo *et al.* 1998).

Due to the lack of a successful vaccine against nasal colonisation and the emerging resistance of *S. aureus* to topical antibiotics, novel *S. aureus* eradication strategies are required. The design of new therapeutic blocking agents may provide an alternative method of reducing or eradicating *S. aureus* nasal colonisation. The crystal structure of ClfB in complex with peptides corresponding to ClfB-binding partners has uncovered the mechanism involved in ClfB-mediated attachment to ligands in the nares (Ganesh *et al.* 2011; Xiang *et al.* 2012). Findings such as these may lead to the development new therapeutic strategies for eradication of *S. aureus* nasal colonisation and subsequent infection control. In this study, loricrin was shown to be bound by the same method as keratin and fibrinogen. Furthermore, pre-incubation of *S. aureus* Newman with the GST-tagged loricrin L2v peptide inhibited binding of the organism to ligands *in vitro* and significantly reduced squame adherence *ex vivo*. Intranasal inoculation of the *S. aureus* pre-incubated with loricrin L2v and subsequent instillation of the peptide into the mouse nares resulted in a significant reduction in nasal colonisation compared to mice treated with GST alone. As well as this, previous studies demonstrated that WTA pre-instilled in the nares of cotton rats resulted in reduced staphylococcal colonisation compared to control animals (Weidenmaier *et al.* 2004). Based on these results, a small molecule inhibitor may provide a novel effective decolonisation strategy. Further studies into the mechanisms of *S. aureus* nasal colonisation and the discovery of additional ligands is of fundamental importance and could lead to new strategies to reduce nasal carriage and the risk of infection.

As well as its role in several invasive diseases, *S. aureus* has been shown to play an important role in the cutaneous skin diseases eczema and atopic dermatitis (AD). *S. aureus* skin colonisation is a known risk factor in the severity of AD disease (Machura *et al.* 2008; Machura *et al.* 2008) and the release of superantigenic toxins by *S. aureus* has been shown to trigger AD occurrence and to contribute to its severity (Leung *et al.* 1993; Campbell and Kemp 1998; Tomi *et al.* 2005). *S. aureus* nasal colonisation in the first year of

life is associated with the subsequent occurrence of AD in later childhood years (Lebon *et al.* 2009). *S. aureus* transiently colonises 5% of adults with healthy human skin whereas it can be isolated from lesions in 90% of adults with AD (Leyden *et al.* 1974; Hauser *et al.* 1985).

Increased adherence of *S. aureus* to AD skin is associated with the expression of fibronectin-binding proteins A and B, due to higher levels of fibronectin found in the stratum corneum of AD sufferers (Cho *et al.* 2001). The pro-inflammatory effect of staphylococcal protein A (SpA) has been demonstrated through the interaction with tumour necrosis factor receptor-1 (TNFR-1) on many cell types including osteoblasts, airway epithelial cells and keratinocytes (Gomez *et al.* 2004; Claro *et al.* 2011; Classen *et al.* 2011; Claro *et al.* 2013). Recognition of TNFR-1 by SpA induces the expression of inflammatory chemokines such as interleukin-8. SpA-mediated adhesion and activation of epithelial cells through an interaction with TNFR-1 has been linked to the severity of AD disease. Furthermore, SpA can induce AD in animal models when used in conjunction with subclinical concentrations of detergent. Loss-of-function mutations in the gene encoding the structural protein filaggrin are also linked to exacerbated AD symptoms and increased survival of *S. aureus* on the skin (Terada *et al.* 2006; Miajlovic *et al.* 2010). Given that nasal colonisation is a prerequisite for *S. aureus* colonisation of the skin, new therapeutic methods to eradicate nasal colonisation may be effective in delaying the onset of AD symptoms and preventing severe occurrences of the disease. The role of *S. aureus* nasal colonisation warrants further investigation in order to provide insight into its role in the development and occurrence of AD.

Nasal colonisation by *S. aureus* has been proven to be a complex and multifactorial process. This study has characterised the role of ClfB in nasal colonisation and provided novel *in vitro* and *in vivo* evidence of an interaction between the staphylococcal adhesin and the cornified envelope protein loricrin. Further research into the role of other surface-expressed proteins and staphylococcal factors is necessary in order to clarify the mechanisms involved in nasal colonisation, so that new therapeutic strategies can be developed to reduce nasal carriage and prevent subsequent *S. aureus* infection.

References

Aly, R., H. I. Shinefield, W. G. Strauss and H. I. Maibach (1977). "Bacterial adherence to nasal mucosal cells." Infect Immun 17(3): 546-549.

Arnaud, M., A. Chastanet and M. Debarbouille (2004). "New vector for efficient allelic replacement in naturally nontransformable, low-GC-content, gram-positive bacteria." Appl Environ Microbiol 70(11): 6887-6891.

Arrecubieta, C., T. Asai, M. Bayern, A. Loughman, J. R. Fitzgerald, C. E. Shelton, H. M. Baron, N. C. Dang, M. C. Deng, Y. Naka, T. J. Foster and F. D. Lowy. (2006). "The role of *Staphylococcus aureus* adhesins in the pathogenesis of ventricular assist device-related infections." J Infect Dis 193(8): 1109-1119.

Bae, T. and O. Schneewind (2006). "Allelic replacement in *Staphylococcus aureus* with inducible counter-selection." Plasmid 55(1): 58-63.

Barbu, E. M., V. K. Ganesh, S. Gurusiddappa, R. C. Mackenzie, T. J. Foster, T. C. Sudhof and M. Hook (2010). "beta-Neurexin is a ligand for the *Staphylococcus aureus* MSCRAMM SdrC." PLoS Pathog 6(1): e1000726.

Bera, A., S. Herbert, A. Jakob, W. Vollmer and F. Gotz (2005). "Why are pathogenic staphylococci so lysozyme resistant? The peptidoglycan O-acetyltransferase OatA is the major determinant for lysozyme resistance of *Staphylococcus aureus*." Mol Microbiol 55(3): 778-787.

Bibel, D. J., R. Aly, H. R. Shinefield, H. I. Maibach and W. G. Strauss (1982). "Importance of the keratinized epithelial cell in bacterial adherence." J Invest Dermatol 79(4): 250-253.

Bingham, R. J., E. Rudino-Pinera, N. A. Meenan, U. Schwarz-Linek, J. P. Turkenburg, M. Hook, E. F. Garman and J. R. Potts (2008). "Crystal structures of fibronectin-binding sites from *Staphylococcus aureus* FnBPA in complex with fibronectin domains." Proc Natl Acad Sci U S A 105(34): 12254-12258.

Biswas, I., A. Gruss, S. D. Ehrlich and E. Maguin (1993). "High-efficiency gene inactivation and replacement system for gram-positive bacteria." J Bacteriol 175(11): 3628-3635.

Boelaert, J. R., H. W. Van Landuyt, C. A. Godard, R. F. Daneels, M. L. Schurgers, E. G. Matthys, Y. A. De Baere, D. W. Gheyle, B. Z. Gordts and L. A. Herwaldt (1993). "Nasal mupirocin ointment decreases the incidence of *Staphylococcus aureus* bacteraemias in haemodialysis patients." Nephrol Dial Transplant 8(3): 235-239.

Boisset, S., T. Geissmann, E. Huntzinger, P. Fechter, N. Bendridi, M. Possedko, C. Chevalier, A. C. Helfer, Y. Benito, A. Jacquier, C. Gaspin, F. Vandenesch and P. Romby (2007). "*Staphylococcus aureus* RNAIII coordinately represses the synthesis of virulence factors and the transcription regulator Rot by an antisense mechanism." Genes Dev 21(11): 1353-1366.

Bowden, M. G., A. P. Heuck, K. Ponnuraj, E. Kolosova, D. Choe, S. Gurusiddappa, S. V. Narayana, A. E. Johnson and M. Hook (2008). "Evidence for the "dock, lock, and latch" ligand binding mechanism of the staphylococcal microbial surface component recognizing adhesive matrix molecules (MSCRAMM) SdrG." J Biol Chem 283(1): 638-647.

Brickner, S. J., M. R. Barbachyn, D. K. Hutchinson and P. R. Manninen (2008). "Linezolid (ZYVOX), the first member of a completely new class of antibacterial agents for treatment of serious gram-positive infections." J Med Chem 51(7): 1981-1990.

Brown, S., Y. H. Zhang and S. Walker (2008). "A revised pathway proposed for *Staphylococcus aureus* wall teichoic acid biosynthesis based on in vitro reconstitution of the intracellular steps." Chem Biol 15(1): 12-21.

Bubeck Wardenburg, J. and O. Schneewind (2008). "Vaccine protection against *Staphylococcus aureus* pneumonia." J Exp Med 205(2): 287-294.

Bujard, H., R. Gentz, M. Lanzer, D. Stueber, M. Mueller, I. Ibrahimi, M. T. Haeuptle and B. Dobberstein (1987). "A T5 promoter-based transcription-translation system for the analysis of proteins *in vitro* and *in vivo*." Methods Enzymol 155: 416-433.

Burian, M., M. Rautenberg, T. Kohler, M. Fritz, B. Krismer, C. Unger, W. H. Hoffmann, A. Peschel, C. Wolz and C. Goerke (2010). "Temporal expression of adhesion factors and activity of global regulators during establishment of *Staphylococcus aureus* nasal colonization." J Infect Dis 201(9): 1414-1421.

Burian, M., C. Wolz and C. Goerke (2010). "Regulatory adaptation of *Staphylococcus aureus* during nasal colonization of humans." PLoS One 5(4): e10040.

Burke, F. M., A. Di Poto, P. Speziale and T. J. Foster (2011). "The A domain of fibronectin-binding protein B of *Staphylococcus aureus* contains a novel fibronectin binding site." FEBS J 278(13): 2359-2371.

Burke, F. M., N. McCormack, S. Rindi, P. Speziale and T. J. Foster (2010). "Fibronectin-binding protein B variation in *Staphylococcus aureus*." BMC Microbiol 10: 160.

Burton, R. A., G. Tsurupa, L. Medved and N. Tjandra (2006). "Identification of an ordered compact structure within the recombinant bovine fibrinogen alphaC-domain fragment by NMR." Biochemistry 45(7): 2257-2266.

Campbell, D. E. and A. S. Kemp (1998). "Production of antibodies to staphylococcal superantigens in atopic dermatitis." Arch Dis Child 79(5): 400-404.

Candi, E., G. Melino, G. Mei, E. Tarcsa, S. I. Chung, L. N. Marekov and P. M. Steinert (1995). "Biochemical, structural, and transglutaminase substrate properties of human loricrin, the major epidermal cornified cell envelope protein." J Biol Chem 270(44): 26382-26390.

Candi, E., R. Schmidt and G. Melino (2005). "The cornified envelope: a model of cell death in the skin." Nat Rev Mol Cell Biol 6(4): 328-340.

Candi, E., E. Tarcsa, W. W. Idler, T. Kartasova, L. N. Marekov and P. M. Steinert (1999). "Transglutaminase cross-linking properties of the small proline-rich 1 family of cornified cell envelope proteins. Integration with loricrin." J Biol Chem 274(11): 7226-7237.

Chambers, H. F. and F. R. Deleo (2009). "Waves of resistance: *Staphylococcus aureus* in the antibiotic era." Nat Rev Microbiol 7(9): 629-641.

Chatfield, C. A., W. A. O'Neill, R. P. Cooke, K. J. McGhee, M. Issack, M. Rahman and W. C. Noble. (1994). "Mupirocin-resistant *Staphylococcus aureus* in a specialist school population." J Hosp Infect 26(4): 273-278.

Chen, X., F. Niyonsaba, H. Ushio, D. Okuda, I. Nagaoka, S. Ikeda, K. Okumura and H. Ogawa (2005). "Synergistic effect of antibacterial agents human beta-defensins, cathelicidin LL-37 and lysozyme against *Staphylococcus aureus* and *Escherichia coli*." J Dermatol Sci 40(2): 123-132.

Cheng, A. G., H. K. Kim, M. L. Burts, T. Krausz, O. Schneewind and D. M. Missiakas (2009). "Genetic requirements for *Staphylococcus aureus* abscess formation and persistence in host tissues." FASEB J 23(10): 3393-3404.

Cho, S. H., I. Strickland, M. Boguniewicz and D. Y. Leung (2001). "Fibronectin and fibrinogen contribute to the enhanced binding of *Staphylococcus aureus* to atopic skin." J Allergy Clin Immunol 108(2): 269-274.

Clarke, S. R., G. Andre, E. J. Walsh, Y. F. Dufrene, T. J. Foster and S. J. Foster (2009). "Iron-regulated surface determinant protein A mediates adhesion of *Staphylococcus aureus* to human corneocyte envelope proteins." Infect Immun 77(6): 2408-2416.

Clarke, S. R., K. J. Brummell, M. J. Horsburgh, P. W. McDowell, S. A. Mohamad, M. R. Stapleton, J. Acevedo, R. C. Read, N. P. Day, S. J. Peacock, J. J. Mond, J. F. Kokai-Kun and S. J. Foster (2006). "Identification of in vivo-expressed antigens of *Staphylococcus aureus* and their use in vaccinations for protection against nasal carriage." J Infect Dis 193(8): 1098-1108.

Clarke, S. R. and S. J. Foster (2008). "IsdA protects *Staphylococcus aureus* against the bactericidal protease activity of apolactoferrin." Infect Immun 76(4): 1518-1526.

Clarke, S. R., R. Mohamed, L. Bian, A. F. Routh, J. F. Kokai-Kun, J. J. Mond, A. Tarkowski and S. J. Foster (2007). "The *Staphylococcus aureus* surface protein IsdA mediates resistance to innate defenses of human skin." Cell Host Microbe 1(3): 199-212.

Clarke, S. R., M. D. Wiltshire and S. J. Foster (2004). "IsdA of *Staphylococcus aureus* is a broad spectrum, iron-regulated adhesin." Mol Microbiol 51(5): 1509-1519.

Claro, T., A. Widaa, C. McDonnell, T. J. Foster, F. J. O'Brien and S. W. Kerrigan (2013). "*Staphylococcus aureus* protein A binding to osteoblast tumour necrosis factor receptor 1 results in activation of nuclear factor kappa B and release of interleukin-6 in bone infection." Microbiology 159(Pt 1): 147-154.

Claro, T., A. Widaa, M. O'Seaghdha, H. Miajlovic, T. J. Foster, F. J. O'Brien and S. W. Kerrigan (2011). "*Staphylococcus aureus* protein A binds to osteoblasts and triggers signals that weaken bone in osteomyelitis." PLoS One 6(4): e18748.

Classen, A., B. N. Kalali, C. Schnopp, C. Andres, J. A. Aguilar-Pimentel, J. Ring, M. Ollert and M. Mempel (2011). "TNF receptor I on human keratinocytes is a binding partner for staphylococcal protein A resulting in the activation of NF kappa B, AP-1, and downstream gene transcription." Exp Dermatol 20(1): 48-52.

Clement, S., P. Vaudaux, P. Francois, J. Schrenzel, E. Huggler, S. Kampf, C. Chaponnier, D. Lew and J. S. Lacroix (2005). "Evidence of an intracellular reservoir in the nasal mucosa of patients with recurrent *Staphylococcus aureus* rhinosinusitis." J Infect Dis 192(6): 1023-1028.

Climo, M. W., R. L. Patron, B. P. Goldstein and G. L. Archer (1998). "Lysostaphin treatment of experimental methicillin-resistant *Staphylococcus aureus* aortic valve endocarditis." Antimicrob Agents Chemother 42(6): 1355-1360.

Cole, A. M., H. I. Liao, O. Stuchlik, J. Tilan, J. Pohl and T. Ganz. (2002). "Cationic polypeptides are required for antibacterial activity of human airway fluid." J Immunol 169(12): 6985-6991.

Cole, A. M., S. Tahk, A. Oren, D. Yoshioka, Y. H. Kim, A. Park and T. Ganz (2001). "Determinants of *Staphylococcus aureus* nasal carriage." Clin Diagn Lab Immunol 8(6): 1064-1069.

Collet, J. P., J. L. Moen, Y. I. Veklich, O. V. Gorkun, S. T. Lord, G. Montalescot and J. W. Weisel (2005). "The alphaC domains of fibrinogen affect the structure of the fibrin clot, its physical properties, and its susceptibility to fibrinolysis." Blood 106(12): 3824-3830.

Collins, L. V., S. A. Kristian, C. Weidenmaier, M. Faigle, K. P. Van Kessel, J. A. Van Strijp, F. Gotz, B. Neumeister and A. Peschel. (2002). "*Staphylococcus aureus* strains lacking D-alanine modifications of teichoic acids are highly susceptible to human neutrophil killing and are virulence attenuated in mice." J Infect Dis 186(2): 214-219.

Conrady, D. G., C. C. Brescia, K. Horii, A. A. Weiss, D. J. Hassett and A. B. Herr (2008). "A zinc-dependent adhesion module is responsible for intercellular adhesion in staphylococcal biofilms." Proc Natl Acad Sci U S A 105(49): 19456-19461.

Cookson, B. D., R. W. Lacey, W. C. Noble, D. S. Reeves, R. Wise and R. J. Redhead (1990). "Mupirocin-resistant *Staphylococcus aureus*." Lancet 335(8697): 1095-1096.

Corrigan, R. M., H. Miajlovic and T. J. Foster (2009). "Surface proteins that promote adherence of *Staphylococcus aureus* to human desquamated nasal epithelial cells." BMC Microbiol 9: 22.

Corrigan, R. M., D. Rigby, P. Handley and T. J. Foster (2007). "The role of *Staphylococcus aureus* surface protein SasG in adherence and biofilm formation." Microbiology 153(Pt 8): 2435-2446.

Corvaglia, A. R., P. Francois, D. Hernandez, K. Perron, P. Linder and J. Schrenzel. (2010). "A type III-like restriction endonuclease functions as a major barrier to horizontal gene transfer in clinical *Staphylococcus aureus* strains." Proc Natl Acad Sci U S A 107(26): 11954-11958.

Cosgrove, K., G. Coutts, I. M. Jonsson, A. Tarkowski, J. F. Kokai-Kun, J. J. Mond and S. J. Foster (2007). "Catalase (KatA) and alkyl hydroperoxide reductase (AhpC) have compensatory roles in peroxide stress resistance and are required for survival, persistence, and nasal colonization in *Staphylococcus aureus*." J Bacteriol 189(3): 1025-1035.

Creech, C. B., 2nd, B. G. Johnson, A. R. Alsentzer, M. Hohenboken, K. M. Edwards and T. R. Talbot, 3rd. (2009). "Vaccination as infection control: a pilot study to determine the impact of *Staphylococcus aureus* vaccination on nasal carriage." Vaccine 28(1): 256-260.

Cregg, K. M., I. Wilding and M. T. Black. (1996). "Molecular cloning and expression of the spsB gene encoding an essential type I signal peptidase from *Staphylococcus aureus*." J Bacteriol 178(19): 5712-5718.

Dassy, B., W. T. Stringfellow, M. Lieb and J. M. Fournier (1991). "Production of type 5 capsular polysaccharide by *Staphylococcus aureus* grown in a semi-synthetic medium." J Gen Microbiol 137(5): 1155-1162.

Daum, R. S. and B. Spellberg (2012). "Progress toward a *Staphylococcus aureus* vaccine." Clin Infect Dis 54(4): 560-567.

Dawson, S. J., L. F. Finn, J. E. McCulloch, S. Kilvington and D. A. Lewis (1994). "Mupirocin-resistant MRSA." J Hosp Infect 28(1): 75-78.

de Boer, H. A., L. J. Comstock and M. Vasser (1983). "The tac promoter: a functional hybrid derived from the trp and lac promoters." Proc Natl Acad Sci U S A 80(1): 21-25.

de Ruyter, P. G., O. P. Kuipers and W. M. de Vos. (1996). "Controlled gene expression systems for *Lactococcus lactis* with the food-grade inducer nisin. ." Appl Environ Microbiol(62): 3662-3667.

Dehart, H. P., H. E. Heath, L. S. Heath, P. A. Leblanc and G. L. Sloan (1995). "The Lysostaphin Endopeptidase Resistance Gene (epr) Specifies Modification of Peptidoglycan Cross Bridges in *Staphylococcus simulans* and *Staphylococcus aureus*." Appl Environ Microbiol 61(7): 2811.

Do, T. Q., S. Moshkani, P. Castillo, S. Anunta, A. Pogosyan, A. Cheung, B. Marbois, K. F. Faull, W. Ernst, S. M. Chiang, G. Fujii, C. F. Clarke, K. Foster and E. Porter (2008). "Lipids including cholesteryl linoleate and cholesteryl arachidonate contribute to the inherent antibacterial activity of human nasal fluid." J Immunol 181(6): 4177-4187.

Drancourt, M. and D. Raoult (2002). "*rpoB* gene sequence-based identification of *Staphylococcus* species." J Clin Microbiol 40(4): 1333-1338.

Dryla, A., D. Gelbmann, A. von Gabain and E. Nagy (2003). "Identification of a novel iron regulated staphylococcal surface protein with haptoglobin-haemoglobin binding activity." Mol Microbiol 49(1): 37-53.

Duthie, E. S. and L. L. Lorenz (1952). "Staphylococcal coagulase; mode of action and antigenicity." J Gen Microbiol 6(1-2): 95-107.

Dziewanowska, K., J. M. Patti, C. F. Deobald, K. W. Bayles, W. R. Trumble and G. A. Bohach (1999). "Fibronectin binding protein and host cell tyrosine kinase are required for internalization of *Staphylococcus aureus* by epithelial cells." Infect Immun 67(9): 4673-4678.

Edwards, A. M., J. R. Potts, E. Josefsson and R. C. Massey. (2010). "*Staphylococcus aureus* host cell invasion and virulence in sepsis is facilitated by the multiple repeats within FnBPA." PLoS Pathog 6(6): e1000964.

Eichner, R., T. T. Sun and U. Aebi (1986). "The role of keratin subfamilies and keratin pairs in the formation of human epidermal intermediate filaments." J Cell Biol 102(5): 1767-1777.

Emonts, M., A. G. Uitterlinden, J. L. Nouwen, I. Kardys, M. P. Maat, D. C. Melles, J. Witteman, P. T. Jong, H. A. Verbrugh, A. Hofman, P. W. Hermans and A. Belkum (2008). "Host polymorphisms in interleukin 4, complement factor H, and C-reactive protein associated with nasal carriage of *Staphylococcus aureus* and occurrence of boils." J Infect Dis 197(9): 1244-1253.

Endl, J., H. P. Seidl, F. Fiedler and K. H. Schleifer (1983). "Chemical composition and structure of cell wall teichoic acids of staphylococci." Arch Microbiol 135(3): 215-223.

Entenza, J. M., T. J. Foster, D. Ni Eidhin, P. Vaudaux, P. Francioli and P. Moreillon (2000). "Contribution of clumping factor B to pathogenesis of experimental endocarditis due to *Staphylococcus aureus*." Infect Immun 68(9): 5443-5446.

Eriksen, N. H., F. Espersen, V. T. Rosdahl and K. Jensen (1995). "Carriage of *Staphylococcus aureus* among 104 healthy persons during a 19-month period." Epidemiol Infect 115(1): 51-60.

Fahlberg, W. J. and J. Marston (1960). "Coagulase production by *Staphylococcus aureus*. I. Factors influencing coagulase production." J Infect Dis 106: 111-115.

Farrell, D. H., P. Thiagarajan, D. W. Chung and E. W. Davie. (1992). "Role of fibrinogen alpha and gamma chain sites in platelet aggregation." Proc Natl Acad Sci U S A 89(22): 10729-10732.

Fetrow, J. S. (1995). "Omega loops: nonregular secondary structures significant in protein function and stability." FASEB J 9(9): 708-717.

Fischetti, V. A., V. Pancholi and O. Schneewind (1990). "Conservation of a hexapeptide sequence in the anchor region of surface proteins from gram-positive cocci." Mol Microbiol 4(9): 1603-1605.

Fitzgerald, J. R., A. Loughman, F. Keane, M. Brennan, M. Knobel, J. Higgins, L. Visai, P. Speziale, D. Cox and T. J. Foster (2006). "Fibronectin-binding proteins of *Staphylococcus aureus* mediate activation of human platelets via

fibrinogen and fibronectin bridges to integrin GPIIb/IIIa and IgG binding to the FcgammaRIIa receptor." Mol Microbiol 59(1): 212-230.

Flannagan, S. E., J. W. Chow, S. M. Donabedian, W. J. Brown, M. B. Perri, M. J. Zervos, Y. Ozawa and D. B. Clewell (2003). "Plasmid content of a vancomycin-resistant *Enterococcus faecalis* isolate from a patient also colonized by *Staphylococcus aureus* with a VanA phenotype." Antimicrob Agents Chemother 47(12): 3954-3959.

Forsgren, A. and K. Nordstrom (1974). "Protein A from *Staphylococcus aureus*: the biological significance of its reaction with IgG." Ann N Y Acad Sci 236(0): 252-266.

Foster, T. J. (2009). "Colonization and infection of the human host by staphylococci: adhesion, survival and immune evasion." Vet Dermatol 20(5-6): 456-470.

Fowler, T., E. R. Wann, D. Joh, S. Johansson, T. J. Foster and M. Hook (2000). "Cellular invasion by *Staphylococcus aureus* involves a fibronectin bridge between the bacterial fibronectin-binding MSCRAMMs and host cell beta1 integrins." Eur J Cell Biol 79(10): 672-679.

Ganesh, V. K., E. M. Barbu, C. C. Deivanayagam, B. Le, A. S. Anderson, Y. V. Matsuka, S. L. Lin, T. J. Foster, S. V. Narayana and M. Hook (2011). "Structural and Biochemical Characterization of *Staphylococcus aureus* Clumping Factor B/Ligand Interactions." J Biol Chem 286(29): 25963-25972.

Ganesh, V. K., J. J. Rivera, E. Smeds, Y. P. Ko, M. G. Bowden, E. R. Wann, S. Gurusiddappa, J. R. Fitzgerald and M. Hook (2008). "A structural model of the *Staphylococcus aureus* ClfA-fibrinogen interaction opens new avenues for the design of anti-staphylococcal therapeutics." PLoS Pathog 4(11): e1000226.

Gasson, M. J. (1983). "Genetic transfer systems in lactic acid bacteria." Antonie Van Leeuwenhoek 49(3): 275-282.

Geisinger, E., R. P. Adhikari, R. Jin, H. F. Ross and R. P. Novick (2006). "Inhibition of *rot* translation by RNAIII, a key feature of *agr* function." Mol Microbiol 61(4): 1038-1048.

Geoghegan, J. A., R. M. Corrigan, D. T. Gruszka, P. Speziale, J. P. O'Gara, J. R. Potts and T. J. Foster (2010). "Role of surface protein SasG in biofilm formation by *Staphylococcus aureus*." J Bacteriol 192(21): 5663-5673.

Ghuysen, J. M. and J. L. Strominger (1963). "Structure of the Cell Wall of *Staphylococcus Aureus*, Strain Copenhagen. Ii. Separation and Structure of Disaccharides." Biochemistry 2: 1119-1125.

Giardina, E., F. Capon, M. C. De Rosa, R. Mango, G. Zambruno, A. Orecchia, S. Chimenti, B. Giardina and G. Novelli (2004). "Characterization of the loricrin (LOR) gene as a positional candidate for the PSORS4 psoriasis susceptibility locus." Ann Hum Genet 68(Pt 6): 639-645.

Gilbart, J., C. R. Perry and B. Slocombe (1993). "High-level mupirocin resistance in *Staphylococcus aureus*: evidence for two distinct isoleucyl-tRNA synthetases." Antimicrob Agents Chemother 37(1): 32-38.

Gill, A. E. and S. G. Amyes (2004). "The contribution of a novel ribosomal S12 mutation to aminoglycoside resistance of *Escherichia coli* mutants." J Chemother 16(4): 347-349.

Goerke, C., R. Pantucek, S. Holtfreter, B. Schulte, M. Zink, D. Grumann, B. M. Broker, J. Doskar and C. Wolz (2009). "Diversity of prophages in dominant *Staphylococcus aureus* clonal lineages." J Bacteriol 191(11): 3462-3468.

Gomez, M. I., A. Lee, B. Reddy, A. Muir, G. Soong, A. Pitt, A. Cheung and A. Prince (2004). "*Staphylococcus aureus* protein A induces airway epithelial inflammatory responses by activating TNFR1." Nat Med 10(8): 842-848.

Gomez, M. I., M. O'Seaghdha, M. Magargee, T. J. Foster and A. S. Prince (2006). "*Staphylococcus aureus* protein A activates TNFR1 signaling through conserved IgG binding domains." J Biol Chem 281(29): 20190-20196.

Gomez, M. I., M. O. Seaghdha and A. S. Prince (2007). "*Staphylococcus aureus* protein A activates TACE through EGFR-dependent signaling." EMBO J 26(3): 701-709.

Gonzalez-Zorn, B., J. P. Senna, L. Fiette, S. Shorte, A. Testard, M. Chignard, P. Courvalin and C. Grillot-Courvalin. (2005). "Bacterial and host factors implicated in nasal carriage of methicillin-resistant *Staphylococcus aureus* in mice." Infect Immun 73(3): 1847-1851.

Goodyear, C. S. and G. J. Silverman (2005). "B cell superantigens: a microbe's answer to innate-like B cells and natural antibodies." Springer Semin Immunopathol 26(4): 463-484.

Gorkun, O. V., Y. I. Veklich, L. V. Medved, A. H. Henschen and J. W. Weisel (1994). "Role of the alpha C domains of fibrin in clot formation." Biochemistry 33(22): 6986-6997.

Grigg, J. C., G. Ukpabi, C. F. Gaudin and M. E. Murphy (2010). "Structural biology of heme binding in the *Staphylococcus aureus* Isd system." J Inorg Biochem 104(3): 341-348.

Gruszka, D. T., J. A. Wojdyla, R. J. Bingham, J. P. Turkenburg, I. W. Manfield, A. Steward, A. P. Leech, J. A. Geoghegan, T. J. Foster, J. Clarke and J. R. Potts (2012). "Staphylococcal biofilm-forming protein has a contiguous rod-like structure." Proc Natl Acad Sci U S A 109(17): E1011-1018.

Haim, M., A. Trost, C. J. Maier, G. Achatz, S. Feichtner, H. Hintner, J. W. Bauer and K. Onder (2010). "Cytokeratin 8 interacts with clumping factor B: a new possible virulence factor target." Microbiology 156(Pt 12): 3710-3721.

Haley, K. P. and E. P. Skaar (2012). "A battle for iron: host sequestration and *Staphylococcus aureus* acquisition." Microbes Infect 14(3): 217-227.

Hartford, O. M., E. R. Wann, M. Hook and T. J. Foster (2001). "Identification of residues in the *Staphylococcus aureus* fibrinogen-binding MSCRAMM clumping factor A (ClfA) that are important for ligand binding." J Biol Chem 276(4): 2466-2473.

Hartleib, J., N. Kohler, R. B. Dickinson, G. S. Chhatwal, J. J. Sixma, O. M. Hartford, T. J. Foster, G. Peters, B. E. Kehrel and M. Herrmann (2000). "Protein A is the von Willebrand factor binding protein on *Staphylococcus aureus*." Blood 96(6): 2149-2156.

Hauser, C., B. Wuethrich, L. Matter, J. A. Wilhelm, W. Sonnabend and K. Schopfer (1985). "*Staphylococcus aureus* skin colonization in atopic dermatitis patients." Dermatologica 170(1): 35-39.

Hawkins, J., S. Kodali, Y. V. Matsuka, L. K. McNeil, T. Mininni, I. L. Scully, J. H. Vernachio, E. Severina, D. Girgenti, K. U. Jansen, A. S. Anderson and R. G. Donald (2012). "A recombinant clumping factor A-containing vaccine induces functional antibodies to *Staphylococcus aureus* that are not observed after natural exposure." Clin Vaccine Immunol 19(10): 1641-1650.

Heinrich, L., N. Tissot, D. J. Hartmann and R. Cohen (2010). "Comparison of the results obtained by ELISA and surface plasmon resonance for the determination of antibody affinity." J Immunol Methods 352(1-2): 13-22.

Herrick, S., O. Blanc-Brude, A. Gray and G. Laurent (1999). "Fibrinogen." Int J Biochem Cell Biol 31(7): 741-746.

Hettasch, J. M., M. G. Bolyard and S. T. Lord (1992). "The residues AGDV of recombinant gamma chains of human fibrinogen must be carboxy-terminal to support human platelet aggregation." Thromb Haemost 68(6): 701-706.

Hillson, J. L., N. S. Karr, I. R. Oppliger, M. Mannik and E. H. Sasso (1993). "The structural basis of germline-encoded VH3 immunoglobulin binding to staphylococcal protein A." J Exp Med 178(1): 331-336.

Hodnik, V. and G. Anderluh (2009). "Toxin detection by surface plasmon resonance." Sensors (Basel) 9(3): 1339-1354.

Hohl, D. e. a. (1991). "Characterization of Human Loricrin." J Biol Chem 266(10): 6626-6636.

Horinouchi, S. and B. Weisblum (1982). "Nucleotide sequence and functional map of pC194, a plasmid that specifies inducible chloramphenicol resistance." J Bacteriol 150(2): 815-825.

Horsburgh, M. J., J. L. Aish, I. J. White, L. Shaw, J. K. Lithgow and S. J. Foster (2002). "sigmaB modulates virulence determinant expression and stress resistance: characterization of a functional *rsbU* strain derived from *Staphylococcus aureus* 8325-4." J Bacteriol 184(19): 5457-5467.

Horsburgh, M. J., E. Ingham and S. J. Foster (2001). "In *Staphylococcus aureus*, fur is an interactive regulator with PerR, contributes to virulence, and Is necessary for oxidative stress resistance through positive regulation of catalase and iron homeostasis." J Bacteriol 183(2): 468-475.

Hu, L., A. Umeda, S. Kondo and K. Amako (1995). "Typing of *Staphylococcus aureus* colonising human nasal carriers by pulsed-field gel electrophoresis." J Med Microbiol 42(2): 127-132.

Huber, M., G. Siegenthaler, N. Mirancea, I. Marenholz, D. Nizetic, D. Breitkreutz, D. Mischke and D. Hohl (2005). "Isolation and characterization of human repetin, a member of the fused gene family of the epidermal differentiation complex." J Invest Dermatol 124(5): 998-1007.

Huesca, M., R. Peralta, D. N. Sauder, A. E. Simor and M. J. McGavin (2002). "Adhesion and virulence properties of epidemic Canadian methicillin-resistant *Staphylococcus aureus* strain 1: identification of novel adhesion functions associated with plasmin-sensitive surface protein." J Infect Dis 185(9): 1285-1296.

Hughes, J. and G. Mellows (1980). "Interaction of pseudomonic acid A with *Escherichia coli* B isoleucyl-tRNA synthetase." Biochem J 191(1): 209-219.

Ishida-Yamamoto, A., J. A. McGrath, H. Lam, H. Iizuka, R. A. Friedman and A. M. Christiano (1997). "The molecular pathology of progressive symmetric erythrokeratoderma: a frameshift mutation in the loricrin gene and perturbations in the cornified cell envelope." Am J Hum Genet 61(3): 581-589.

Iwase, T., Y. Uehara, H. Shinji, A. Tajima, H. Seo, K. Takada, T. Agata and Y. Mizunoe (2010). "*Staphylococcus epidermidis* Esp inhibits *Staphylococcus aureus* biofilm formation and nasal colonization." Nature 465(7296): 346-349.

Jarnik, M., P. A. de Viragh, E. Scharer, D. Bundman, M. N. Simon, D. R. Roop and A. C. Steven (2002). "Quasi-normal cornified cell envelopes in loricrin knockout mice imply the existence of a loricrin backup system." J Invest Dermatol 118(1): 102-109.

Jarnik, M., M. N. Simon and A. C. Steven (1998). "Cornified cell envelope assembly: a model based on electron microscopic determinations of thickness and projected density." J Cell Sci 111 (Pt 8): 1051-1060.

Jensen, P. R. and K. Hammer (1993). "Minimal Requirements for Exponential Growth of *Lactococcus lactis*." Appl Environ Microbiol 59(12): 4363-4366.

Ji, Y., B. Zhang, S. F. Van, Horn, P. Warren, G. Woodnutt, M. K. Burnham and M. Rosenberg (2001). "Identification of critical staphylococcal genes using conditional phenotypes generated by antisense RNA." Science 293(5538): 2266-2269.

Jonsson, I. M., S. K. Mazmanian, O. Schneewind, M. Verdrengh, T. Bremell and A. Tarkowski. (2002). "On the role of *Staphylococcus aureus* sortase and sortase-catalyzed surface protein anchoring in murine septic arthritis." J Infect Dis 185(10): 1417-1424.

Josefsson, E., O. Hartford, L. O'Brien, J. M. Patti and T. Foster. (2001). "Protection against experimental *Staphylococcus aureus* arthritis by vaccination with clumping factor A, a novel virulence determinant." J Infect Dis 184(12): 1572-1580.

Josefsson, E., K. W. McCrea, D. Ni Eidhin, D. O'Connell, J. Cox, M. Hook and T. J. Foster (1998). "Three new members of the serine-aspartate repeat protein multigene family of *Staphylococcus aureus*." Microbiology 144 (Pt 12): 3387-3395.

Juuti, K. M., B. Sinha, C. Werbick, G. Peters and P. I. Kuusela (2004). "Reduced adherence and host cell invasion by methicillin-resistant *Staphylococcus aureus* expressing the surface protein Pls." J Infect Dis 189(9): 1574-1584.

Karlsson, R., P. S. Katsamba, H. Nordin, E. Pol and D. G. Myszka (2006). "Analyzing a kinetic titration series using affinity biosensors." Anal Biochem 349(1): 136-147.

Kaufman, D. (2006). "Veronate (Inhibitex)." Curr Opin Investig Drugs 7(2): 172-179.

Kemp, E. H., R. L. Sammons, A. Moir, D. Sun and P. Setlow (1991). "Analysis of transcriptional control of the *gerD* spore germination gene of *Bacillus subtilis* 168." J Bacteriol 173(15): 4646-4652.

Kezic, S., P. M. Kemperman, E. S. Koster, C. M. de Jongh, H. B. Thio, L. E. Campbell, A. D. Irvine, W. H. McLean, G. J. Puppels and P. J. Caspers (2008). "Loss-of-function mutations in the filaggrin gene lead to reduced level of natural moisturizing factor in the stratum corneum." J Invest Dermatol 128(8): 2117-2119.

Khan, S. A. and R. P. Novick (1983). "Complete nucleotide sequence of pT181, a tetracycline-resistance plasmid from *Staphylococcus aureus*." Plasmid 10(3): 251-259.

Kim, H. K., A. G. Cheng, H. Y. Kim, D. M. Missiakas and O. Schneewind (2010). "Nontoxigenic protein A vaccine for methicillin-resistant *Staphylococcus aureus* infections in mice." J Exp Med 207(9): 1863-1870.

Kiser, K. B., J. M. Cantey-Kiser and J. C. Lee (1999). "Development and characterization of a *Staphylococcus aureus* nasal colonization model in mice." Infect Immun 67(10): 5001-5006.

Kluytmans, J. A., J. W. Mouton, M. F. VandenBergh, M. J. Manders, A. P. Maat, J. H. Wagenvoort, M. F. Michel and H. A. Verbrugh (1996). "Reduction of surgical-site infections in cardiothoracic surgery by elimination of nasal

carriage of *Staphylococcus aureus*." Infect Control Hosp Epidemiol 17(12): 780-785.

Koch, P. J., P. A. de Viragh, E. Scharer, D. Bundman, M. A. Longley, J. Bickenbach, Y. Kawachi, Y. Suga, Z. Zhou, M. Huber, D. Hohl, T. Kartasova, M. Jarnik, A. C. Steven and D. R. Roop (2000). "Lessons from loricrin-deficient mice: compensatory mechanisms maintaining skin barrier function in the absence of a major cornified envelope protein." J Cell Biol 151(2): 389-400.

Kohler, T., C. Weidenmaier and A. Peschel (2009). "Wall teichoic acid protects *Staphylococcus aureus* against antimicrobial fatty acids from human skin." J Bacteriol 191(13): 4482-4484.

Kokai-Kun, J. F., S. M. Walsh, T. Chanturiya and J. J. Mond (2003). "Lysostaphin cream eradicates *Staphylococcus aureus* nasal colonization in a cotton rat model." Antimicrob Agents Chemother 47(5): 1589-1597.

Korge, B. P., J. G. Compton, P. M. Steinert and D. Mischke (1992). "The two size alleles of human keratin 1 are due to a deletion in the glycine-rich carboxyl-terminal V2 subdomain." J Invest Dermatol 99(6): 697-702.

Korge, B. P., S. Q. Gan, O. W. McBride, D. Mischke and P. M. Steinert. (1992). "Extensive size polymorphism of the human keratin 10 chain resides in the C-terminal V2 subdomain due to variable numbers and sizes of glycine loops." Proc Natl Acad Sci U S A 89(3): 910-914.

Kreiswirth, B. N., S. Lofdahl, M. J. Betley, M. O'Reilly, P. M. Schlievert, M. S. Bergdoll and R. P. Novick (1983). "The toxic shock syndrome exotoxin structural gene is not detectably transmitted by a prophage." Nature 305(5936): 709-712.

Krishna Kumar, K., D. A. Jacques, G. Pishchany, T. Caradoc-Davies, T. Spirig, G. R. Malmirchegini, D. B. Langley, C. F. Dickson, J. P. Mackay, R. T. Clubb, E. P. Skaar, J. M. Guss and D. A. Gell (2011). "Structural basis for hemoglobin capture by *Staphylococcus aureus* cell-surface protein, IsdH." J Biol Chem 286(44): 38439-38447.

Kruger, R. G., B. Otvos, B. A. Frankel, M. Bentley, P. Dostal and D. G. McCafferty (2004). "Analysis of the substrate specificity of the *Staphylococcus aureus* sortase transpeptidase SrtA." Biochemistry 43(6): 1541-1551.

Kuipers, O. P., M. M. Beerthuyzen, P. G. de Ruyter, E. J. Luesink and W. M. de Vos (1995). "Autoregulation of nisin biosynthesis in *Lactococcus lactis* by signal transduction." J Biol Chem 270(45): 27299-27304.

Kuklin, N. A., D. J. Clark, S. Secore, J. Cook, L. D. Cope, T. McNeely, L. Noble, M. J. Brown, J. K. Zorman, X. M. Wang, G. Pancari, H. Fan, K. Isett, B. Burgess, J. Bryan, M. Brownlow, H. George, M. Meinz, M. E. Liddell, R. Kelly, L. Schultz, D. Montgomery, J. Onishi, M. Losada, M. Martin, T. Ebert, C. Y. Tan, T. L. Schofield, E. Nagy, A. Meineke, J. G. Joyce, M. B. Kurtz, M. J. Caulfield, K. U. Jansen, W. McClements and A. S. Anderson (2006). "A novel *Staphylococcus aureus* vaccine: iron surface determinant B induces rapid antibody responses in rhesus macaques and specific increased survival in a murine *S. aureus* sepsis model." Infect Immun 74(4): 2215-2223.

LaMarre, J. M., B. P. Howden and A. S. Mankin (2011). "Inactivation of the indigenous methyltransferase RlmN in *Staphylococcus aureus* increases linezolid resistance." Antimicrob Agents Chemother 55(6): 2989-2991.

Le Gouill, C. and C. V. Dery (1991). "A rapid procedure for the screening of recombinant plasmids." Nucleic Acids Res 19(23): 6655.

Lebon, A., J. A. Labout, H. A. Verbrugh, V. W. Jaddoe, A. Hofman, W. J. van Wamel, A. van Belkum and H. A. Moll (2009). "Role of *Staphylococcus aureus* nasal colonization in atopic dermatitis in infants: the Generation R Study." Arch Pediatr Adolesc Med 163(8): 745-749.

Lee, Y. L., T. Cesario, A. Pax, C. Tran, A. Ghouri and L. D. Thrupp (1999). "Nasal colonization by *Staphylococcus aureus* in active, independent, community seniors." Age Ageing 28(2): 229-232.

Lehrer, R. I. and T. Ganz (1999). "Antimicrobial peptides in mammalian and insect host defence." Curr Opin Immunol 11(1): 23-27.

Leszczynski, J. F. and G. D. Rose (1986). "Loops in globular proteins: a novel category of secondary structure." Science 234(4778): 849-855.

Leung, D. Y., R. Harbeck, P. Bina, R. F. Reiser, E. Yang, D. A. Norris, J. M. Hanifin and H. A. Sampson (1993). "Presence of IgE antibodies to staphylococcal exotoxins on the skin of patients with atopic dermatitis. Evidence for a new group of allergens." J Clin Invest 92(3): 1374-1380.

Leyden, J. J., R. R. Marples and A. M. Kligman (1974). "*Staphylococcus aureus* in the lesions of atopic dermatitis." Br J Dermatol 90(5): 525-530.

Li, M., X. Du, A. E. Villaruz, B. A. Diep, D. Wang, Y. Song, Y. Tian, J. Hu, F. Yu, Y. Lu and M. Otto (2012). "MRSA epidemic linked to a quickly spreading colonization and virulence determinant." Nat Med 18(5): 816-819.

Liew, C. K., B. T. Smith, R. Pilpa, N. Suree, U. Ilangovan, K. M. Connolly, M. E. Jung and R. T. Clubb (2004). "Localization and mutagenesis of the sorting signal binding site on sortase A from *Staphylococcus aureus*." FEBS Lett 571(1-3): 221-226.

Lina, G., F. Boutite, A. Tristan, M. Bes, J. Etienne and F. Vandenesch (2003). "Bacterial competition for human nasal cavity colonization: role of Staphylococcal *agr* alleles." Appl Environ Microbiol 69(1): 18-23.

Litvinov, R. I., O. V. Gorkun, D. K. Galanakis, S. Yakovlev, L. Medved, H. Shuman and J. W. Weisel (2007). "Polymerization of fibrin: Direct observation and quantification of individual B:b knob-hole interactions." Blood 109(1): 130-138.

Liu, M., W. N. Tanaka, H. Zhu, G. Xie, D. M. Dooley and B. Lei (2008). "Direct hemin transfer from IsdA to IsdC in the iron-regulated surface determinant (Isd) heme acquisition system of *Staphylococcus aureus*." J Biol Chem 283(11): 6668-6676.

Locke, J. B., G. Morales, M. Hilgers, C. K. G, S. Rahawi, J. Jose Picazo, K. J. Shaw and J. L. Stein (2010). "Elevated linezolid resistance in clinical cfr-positive *Staphylococcus aureus* isolates is associated with co-occurring

mutations in ribosomal protein L3." Antimicrob Agents Chemother 54(12): 5352-5355.

Lofgren, J. A., G. Morales, M. Hilgers, C. K. G, S. Rahawi, J. Jose Picazo, K. J. Shaw and J. L. Stein. (2007). "Comparing ELISA and surface plasmon resonance for assessing clinical immunogenicity of panitumumab." J Immunol 178(11): 7467-7472.

Lopez, O., M. Cocera, P. W. Wertz, C. Lopez-Iglesias and A. de la Maza (2007). "New arrangement of proteins and lipids in the stratum corneum cornified envelope." Biochim Biophys Acta 1768(3): 521-529.

Lorand, L., R. B. Credo and T. J. Janus (1981). "Factor XIII (fibrin-stabilizing factor)." Methods Enzymol 80 Pt C: 333-341.

Loughman, A., J. R. Fitzgerald, M. P. Brennan, J. Higgins, R. Downer, D. Cox and T. J. Foster. (2005). "Roles for fibrinogen, immunoglobulin and complement in platelet activation promoted by *Staphylococcus aureus* clumping factor A." Mol Microbiol 57(3): 804-818.

Loughman, A., T. Sweeney, F. M. Keane, G. Pietrocola, P. Speziale and T. J. Foster (2008). "Sequence diversity in the A domain of *Staphylococcus aureus* fibronectin-binding protein A." BMC Microbiol 8: 74.

Lowy, F. D. (1998). "*Staphylococcus aureus* infections." N Engl J Med 339(8): 520-532.

Luong, T. T. and C. Y. Lee (2002). "Overproduction of type 8 capsular polysaccharide augments *Staphylococcus aureus* virulence." Infect Immun 70(7): 3389-3395.

Machura, E., B. Mazur, E. Golemiec, M. Pindel and F. Halkiewicz (2008). "*Staphylococcus aureus* skin colonization in atopic dermatitis children is associated with decreased IFN-gamma production by peripheral blood CD4+ and CD8+ T cells." Pediatr Allergy Immunol 19(1): 37-45.

Maestrini, E., A. P. Monaco, J. A. McGrath, A. Ishida-Yamamoto, C. Camisa, A. Hovnanian, D. E. Weeks, M. Lathrop, J. Uitto and A. M. Christiano. (1996). "A molecular defect in loricrin, the major component of the cornified cell envelope, underlies Vohwinkel's syndrome." Nat Genet 13(1): 70-77.

Maguin, E., P. Duwat, T. Hege, D. Ehrlich and A. Gruss (1992). "New thermosensitive plasmid for gram-positive bacteria." J Bacteriol 174(17): 5633-5638.

Maira-Litran, T., L. V. Bentancor, C. Bozkurt-Guzel, J. M. O'Malley, C. Cywes-Bentley and G. B. Pier (2012). "Synthesis and evaluation of a conjugate vaccine composed of *Staphylococcus aureus* poly-N-acetyl-glucosamine and clumping factor A." PLoS One 7(9): e43813.

Manting, E. H. and A. J. Driessen (2000). "*Escherichia coli* translocase: the unravelling of a molecular machine." Mol Microbiol 37(2): 226-238.

Marshall, D., M. J. Hardman, K. M. Nield and C. Byrne (2001). "Differentially expressed late constituents of the epidermal cornified envelope." Proc Natl Acad Sci U S A 98(23): 13031-13036.

Marston, J. and W. J. Fahlberg (1960). "Coagulase production by *Staphylococcus aureus*. II. Growth and coagulase production in complex and chemically defined mediums--comparison of chemically defined mediums." J Infect Dis 106: 116-122.

Matsuka, Y. V., E. T. Anderson, T. Milner-Fish, P. Ooi and S. Baker (2003). "*Staphylococcus aureus* fibronectin-binding protein serves as a substrate for coagulation factor XIIIa: evidence for factor XIIIa-catalyzed covalent cross-linking to fibronectin and fibrin." Biochemistry 42(49): 14643-14652.

Mazmanian, S. K., E. P. Skaar, A. H. Gaspar, M. Humayun, P. Gornicki, J. Jelenska, A. Joachmiak, D. M. Missiakas and O. Schneewind (2003). "Passage of heme-iron across the envelope of *Staphylococcus aureus*." Science 299(5608): 906-909.

Mazmanian, S. K., H. Ton-That and O. Schneewind (2001). "Sortase-catalysed anchoring of surface proteins to the cell wall of *Staphylococcus aureus*." Mol Microbiol 40(5): 1049-1057.

Mazmanian, S. K., H. Ton-That, K. Su and O. Schneewind (2002). "An iron-regulated sortase anchors a class of surface protein during *Staphylococcus aureus* pathogenesis." Proc Natl Acad Sci U S A 99(4): 2293-2298.

McAdow, M., H. K. Kim, A. C. Dedent, A. P. Hendrickx, O. Schneewind and D. M. Missiakas (2011). "Preventing *Staphylococcus aureus* sepsis through the inhibition of its agglutination in blood." PLoS Pathog 7(10): e1002307.

McAleese, F. M. and T. J. Foster (2003). "Analysis of mutations in the *Staphylococcus aureus clfB* promoter leading to increased expression." Microbiology 149(Pt 1): 99-109.

McAleese, F. M., E. J. Walsh, M. Sieprawska, J. Potempa and T. J. Foster (2001). "Loss of clumping factor B fibrinogen binding activity by *Staphylococcus aureus* involves cessation of transcription, shedding and cleavage by metalloprotease." J Biol Chem 276(32): 29969-29978.

McDevitt, D., T. Nanavaty, K. House-Pompeo, E. Bell, N. Turner, L. McIntire, T. Foster and M. Hook (1997). "Characterization of the interaction between the *Staphylococcus aureus* clumping factor (ClfA) and fibrinogen." Eur J Biochem 247(1): 416-424.

McNamara, P. J., K. C. Milligan-Monroe, S. Khalili and R. A. Proctor. (2000). "Identification, cloning, and initial characterization of rot, a locus encoding a regulator of virulence factor expression in *Staphylococcus aureus*." J Bacteriol 182(11): 3197-3203.

Medina, M., E. Vintini, J. Villena, R. Raya and S. Alvarez. (2010). "*Lactococcus lactis* as an adjuvant and delivery vehicle of antigens against pneumococcal respiratory infections." Bioeng Bugs 1(5): 313-325.

Medved, L. V., O. V. Gorkun, V. F. Manyakov and V. A. Belitser (1985). "The role of fibrinogen alpha C-domains in the fibrin assembly process." FEBS Lett 181(1): 109-112.

Mehrel, T., D. Hohl, J. A. Rothnagel, M. A. Longley, D. Bundman, C. Cheng, U. Lichti, M. E. Bisher, A. C. Steven, P. M. Steinert (1990). "Identification of a major keratinocyte cell envelope protein, loricrin." Cell 61(6): 1103-1112.

Mendes, R. E., L. Deshpande, E. Rodriguez-Noriega, J. E. Ross, R. N. Jones and R. Morfin-Otero (2010). "First report of Staphylococcal clinical isolates in Mexico with linezolid resistance caused by cfr: evidence of *in vivo* cfr mobilization." J Clin Microbiol 48(8): 3041-3043.

Miajlovic, H., P. G. Fallon, A. D. Irvine and T. J. Foster (2010). "Effect of filaggrin breakdown products on growth of and protein expression by *Staphylococcus aureus*." J Allergy Clin Immunol 126(6): 1184-1190 e1183.

Miajlovic, H., A. Loughman, M. Brennan, D. Cox and T. J. Foster. (2007). "Both complement- and fibrinogen-dependent mechanisms contribute to platelet aggregation mediated by *Staphylococcus aureus* clumping factor B." Infect Immun 75(7): 3335-3343.

Miajlovic, H., M. Zapotoczna, J. A. Geoghegan, S. W. Kerrigan, P. Speziale and T. J. Foster (2010). "Direct interaction of iron-regulated surface determinant IsdB of *Staphylococcus aureus* with the GPIIb/IIIa receptor on platelets." Microbiology 156(Pt 3): 920-928.

Moks, T., et al. (1986). "Staphylococcal protein A consists of five IgG-binding domains." Eur J Biochem 156(3): 637-643.

Monk, I. R., P. G. Casey, M. Cronin, C. G. Gahan and C. Hill (2008). "Development of multiple strain competitive index assays for *Listeria monocytogenes* using pIMC; a new site-specific integrative vector." BMC Microbiol 8: 96.

Monk, I. R., Shah, I.M., Xu, M., Tan, M., Foster, T.J. (2012). "Transforming the Untransformable: Application of Direct Transformation To Manipulate

Genetically *Staphylococcus aureus* and *Staphylococcus epidermidis*." MBio 3 e00277-11(2).

Moore, G. E., R. E. Gerner and H. A. Franklin (1967). "Culture of normal human leukocytes." JAMA 199(8): 519-524.

Morales, G., J. J. Picazo, E. Baos, F. J. Candel, A. Arribi, B. Pelaez, R. Andrade, M. A. de la Torre, J. Fereres and M. Sanchez-Garcia (2010). "Resistance to linezolid is mediated by the cfr gene in the first report of an outbreak of linezolid-resistant *Staphylococcus aureus*." Clin Infect Dis 50(6): 821-825.

Moreillon, P., J. M. Entenza, P. Francioli, D. McDevitt, T. J. Foster, P. Francois and P. Vaudaux (1995). "Role of *Staphylococcus aureus* coagulase and clumping factor in pathogenesis of experimental endocarditis." Infect Immun 63(12): 4738-4743.

Munoz, P., J. Hortal, M. Giannella, J. M. Barrio, M. Rodriguez-Creixems, M. J. Perez, C. Rincon and E. Bouza (2008). "Nasal carriage of *S. aureus* increases the risk of surgical site infection after major heart surgery." J Hosp Infect 68(1): 25-31.

Muryoi, N., M. T. Tiedemann, M. Pluym, J. Cheung, D. E. Heinrichs and M. J. Stillman (2008). "Demonstration of the iron-regulated surface determinant (Isd) heme transfer pathway in *Staphylococcus aureus*." J Biol Chem 283(42): 28125-28136.

Navarre, W. W. and O. Schneewind (1999). "Surface proteins of gram-positive bacteria and mechanisms of their targeting to the cell wall envelope." Microbiol Mol Biol Rev 63(1): 174-229.

Nemes Z, S. P. (1999). "Bricks and Mortar of the Epidermal Barrier." Exp Mol Med 31(1): 5-19.

Ni Eidhin, D., Perkins, S., Francois, P., Vaudaux, P., Hook, M. & and T. J. Foster (1998). "Clumping factor B (ClfB), a new surface-located fibrinogen-binding adhesin of *Staphylococcus aureus*." Mol Microbiol(30): 245-257.

Nilsson, I. M., J. C. Lee, T. Bremell, C. Ryden and A. Tarkowski (1997). "The role of staphylococcal polysaccharide microcapsule expression in septicemia and septic arthritis." Infect Immun 65(10): 4216-4221.

Nouwen, J. L., M. W. Fieren, S. Snijders, H. A. Verbrugh and A. van Belkum (2005). "Persistent (not intermittent) nasal carriage of *Staphylococcus aureus* is the determinant of CPD-related infections." Kidney Int 67(3): 1084-1092.

Novakova, D., R. Pantucek, Z. Hubalek, E. Falsen, H. J. Busse, P. Schumann and I. Sedlacek (2010). "*Staphylococcus microti* sp. nov., isolated from the common vole (*Microtus arvalis*)." Int J Syst Evol Microbiol 60(Pt 3): 566-573.

Novick, R. P., S. J. Projan, J. Kornblum, H. F. Ross, G. Ji, B. Kreiswirth, F. Vandenesch and S. Moghazeh (1995). "The agr P2 operon: an autocatalytic sensory transduction system in *Staphylococcus aureus*." Mol Gen Genet 248(4): 446-458.

Novick, R. P., H. F. Ross, S. J. Projan, J. Kornblum, B. Kreiswirth and S. Moghazeh (1993). "Synthesis of staphylococcal virulence factors is controlled by a regulatory RNA molecule." EMBO J 12(10): 3967-3975.

O'Brien, L. M., E. J. Walsh, R. C. Massey, S. J. Peacock and T. J. Foster (2002). "*Staphylococcus aureus* clumping factor B (ClfB) promotes adherence to human type I cytokeratin 10: implications for nasal colonization." Cell Microbiol 4(11): 759-770.

O'Connell, D. P., T. Nanavaty, D. McDevitt, S. Gurusiddappa, M. Hook and T. J. Foster (1998). "The fibrinogen-binding MSCRAMM (clumping factor) of *Staphylococcus aureus* has a Ca2+-dependent inhibitory site." J Biol Chem 273(12): 6821-6829.

O'Neill, E., C. Pozzi, P. Houston, H. Humphreys, D. A. Robinson, A. Loughman, T. J. Foster and J. P. O'Gara (2008). "A novel *Staphylococcus aureus* biofilm phenotype mediated by the fibronectin-binding proteins, FnBPA and FnBPB." J Bacteriol 190(11): 3835-3850.

O'Regan, G. M. and A. D. Irvine (2008). "The role of filaggrin loss-of-function mutations in atopic dermatitis." Curr Opin Allergy Clin Immunol 8(5): 406-410.

O'Regan, G. M., A. Sandilands, W. H. McLean and A. D. Irvine (2008). "Filaggrin in atopic dermatitis." J Allergy Clin Immunol 122(4): 689-693.

O'Riordan, K. and J. C. Lee (2004). "*Staphylococcus aureus* capsular polysaccharides." Clin Microbiol Rev 17(1): 218-234.

O'Seaghdha, M., C. J. van Schooten, S. W. Kerrigan, J. Emsley, G. J. Silverman, D. Cox, P. J. Lenting and T. J. Foster (2006). "*Staphylococcus aureus* protein A binding to von Willebrand factor A1 domain is mediated by conserved IgG binding regions." FEBS J 273(21): 4831-4841.

Oeding, P., A. Grov and B. Myklestad. (1964). "Immunochemical Studies on Antigen Preparations from *Staphylococcus Aureus*. 2. Precipitating and Erythrocyte-Sensitizing Properties of Protein a (Antigen a) and Related Substances." Acta Pathol Microbiol Scand 62: 117-127.

Oku, Y., K. Kurokawa, M. Matsuo, S. Yamada, B. L. Lee and K. Sekimizu (2009). "Pleiotropic roles of polyglycerolphosphate synthase of lipoteichoic acid in growth of *Staphylococcus aureus* cells." J Bacteriol 191(1): 141-151.

Onell, A. and K. Andersson (2005). "Kinetic determinations of molecular interactions using Biacore--minimum data requirements for efficient experimental design." J Mol Recognit 18(4): 307-317.

Pal, M. and S. Dasgupta (2003). "The nature of the turn in omega loops of proteins." Proteins 51(4): 591-606.

Pallen, M. J., A. C. Lam, M. Antonio and K. Dunbar (2001). "An embarrassment of sortases - a richness of substrates?" Trends Microbiol 9(3): 97-102.

Palmer, C. N., A. D. Irvine, A. Terron-Kwiatkowski, Y. Zhao, H. Liao, S. P. Lee, D. R. Goudie, A. Sandilands, L. E. Campbell, F. J. Smith, G. M. O'Regan, R. M. Watson, J. E. Cecil, S. J. Bale, J. G. Compton, J. J. DiGiovanna, P. Fleckman, S. Lewis-Jones, G. Arseculeratne, A. Sergeant, C. S. Munro, B. El

Houate, K. McElreavey, L. B. Halkjaer, H. Bisgaard, S. Mukhopadhyay and W. H. McLean (2006). "Common loss-of-function variants of the epidermal barrier protein filaggrin are a major predisposing factor for atopic dermatitis." Nat Genet 38(4): 441-446.

Palmqvist, N., T. Foster, J. R. Fitzgerald, E. Josefsson and A. Tarkowski (2005). "Fibronectin-binding proteins and fibrinogen-binding clumping factors play distinct roles in staphylococcal arthritis and systemic inflammation." J Infect Dis 191(5): 791-798.

Panierakis, C., G. Goulielmos, D. Mamoulakis, S. Maraki, E. Papavasiliou and E. Galanakis (2009). "*Staphylococcus aureus* nasal carriage might be associated with vitamin D receptor polymorphisms in type 1 diabetes." Int J Infect Dis 13(6): e437-443.

Pankov, R. and K. M. Yamada (2002). "Fibronectin at a glance." J Cell Sci 115(Pt 20): 3861-3863.

Park, B., T. Iwase and G. Y. Liu (2011). "Intranasal application of *S. epidermidis* prevents colonization by methicillin-resistant *Staphylococcus aureus* in mice." PLoS One 6(10): e25880.

Patel, J. B., R. J. Gorwitz and J. A. Jernigan (2009). "Mupirocin resistance." Clin Infect Dis 49(6): 935-941.

Peacock, S. J., I. de Silva and F. D. Lowy (2001). "What determines nasal carriage of *Staphylococcus aureus*?" Trends Microbiol 9(12): 605-610.

Perkins, S., E. J. Walsh, C. C. Deivanayagam, S. V. Narayana, T. J. Foster and M. Hook. (2001). "Structural organization of the fibrinogen-binding region of the clumping factor B MSCRAMM of *Staphylococcus aureus*." J Biol Chem 276(48): 44721-44728.

Peschel, A., R. W. Jack, M. Otto, L. V. Collins, P. Staubitz, G. Nicholson, H. Kalbacher, W. F. Nieuwenhuizen, G. Jung, A. Tarkowski, K. P. van Kessel and J. A. van Strijp (2001). "*Staphylococcus aureus* resistance to human defensins

and evasion of neutrophil killing via the novel virulence factor MprF is based on modification of membrane lipids with l-lysine." J Exp Med 193(9): 1067-1076.

Peschel, A., M. Otto, R. W. Jack, H. Kalbacher, G. Jung and F. Gotz (1999). "Inactivation of the *dlt* operon in *Staphylococcus aureus* confers sensitivity to defensins, protegrins, and other antimicrobial peptides." J Biol Chem 274(13): 8405-8410.

Pilpa, R. M., E. A. Fadeev, V. A. Villareal, M. L. Wong, M. Phillips and R. T. Clubb (2006). "Solution structure of the NEAT (NEAr Transporter) domain from IsdH/HarA: the human hemoglobin receptor in *Staphylococcus aureus*." J Mol Biol 360(2): 435-447.

Ponnuraj, K., M. G. Bowden, S. Davis, S. Gurusiddappa, D. Moore, D. Choe, Y. Xu, M. Hook and S. V. Narayana (2003). "A "dock, lock, and latch" structural model for a staphylococcal adhesin binding to fibrinogen." Cell 115(2): 217-228.

Poole, L. B., D. A. Loveys, S. P. Hale, J. A. Gerlt, S. M. Stanczyk and P. H. Bolton (1991). "Deletion of the omega-loop in the active site of staphylococcal nuclease. 1. Effect on catalysis and stability." Biochemistry 30(15): 3621-3627.

Poutrel, B., F. B. Gilbert and M. Lebrun (1995). "Effects of culture conditions on production of type 5 capsular polysaccharide by human and bovine *Staphylococcus aureus* strains." Clin Diagn Lab Immunol 2(2): 166-171.

Prevaes, S. M., W. J. van Wamel, C. P. de Vogel, R. H. Veenhoven, E. J. van Gils, A. van Belkum, E. A. Sanders and D. Bogaert (2012). "Nasopharyngeal colonization elicits antibody responses to staphylococcal and pneumococcal proteins that are not associated with a reduced risk of subsequent carriage." Infect Immun 80(6): 2186-2193.

Prince, G. A. (1994). "The cotton rat in Biomedical Research." Anim. Welf. Inf. Cent. Newsl 5.

Prince, G. A., Jenson, A.B., Horswood, R.L., Camargo, E. & Chanock, R.M. (1978). "The pathogenesis of respiratory syncytial virus infection in cotton rats." Am. J. Pathol 93(3): 771–791.

Pynnonen, M., R. E. Stephenson, K. Schwartz, M. Hernandez and B. R. Boles (2011). "Hemoglobin promotes *Staphylococcus aureus* nasal colonization." PLoS Pathog 7(7): e1002104.

Que, Y. A., J. A. Haefliger, L. Piroth, P. Francois, E. Widmer, J. M. Entenza, B. Sinha, M. Herrmann, P. Francioli, P. Vaudaux and P. Moreillon (2005). "Fibrinogen and fibronectin binding cooperate for valve infection and invasion in *Staphylococcus aureus* experimental endocarditis." J Exp Med 201(10): 1627-1635.

Regev-Yochay, G., R. Dagan, M. Raz, Y. Carmeli, B. Shainberg, E. Derazne, G. Rahav and E. Rubinstein (2004). "Association between carriage of *Streptococcus pneumoniae* and *Staphylococcus aureus* in Children." JAMA 292(6): 716-720.

Reginald, K., K. Westritschnig, B. Linhart, M. Focke-Tejkl, B. Jahn-Schmid, J. Eckl-Dorna, A. Heratizadeh, A. Stocklinger, N. Balic, S. Spitzauer, V. Niederberger, T. Werfel, J. Thalhamer, S. Weidinger, N. Novak, M. Ollert, A. M. Hirschl and R. Valenta (2011). "*Staphylococcus aureus* fibronectin-binding protein specifically binds IgE from patients with atopic dermatitis and requires antigen presentation for cellular immune responses." J Allergy Clin Immunol 128(1): 82-91 e88.

Reichelt, J., H. Bussow, C. Grund and T. M. Magin (2001). "Formation of a normal epidermis supported by increased stability of keratins 5 and 14 in keratin 10 null mice." Mol Biol Cell 12(6): 1557-1568.

Rindi, S., S. Cicalini, G. Pietrocola, M. Venditti, A. Festa, T. J. Foster, N. Petrosillo and P. Speziale (2006). "Antibody response in patients with endocarditis caused by *Staphylococcus aureus*." Eur J Clin Invest 36(8): 536-543.

Risley, A. L., A. Loughman, C. Cywes-Bentley, T. J. Foster and J. C. Lee (2007). "Capsular polysaccharide masks clumping factor A-mediated adherence of *Staphylococcus aureus* to fibrinogen and platelets." J Infect Dis 196(6): 919-927.

Robinson, N. A., S. Lapic, J. F. Welter and R. L. Eckert. (1997). "S100A11, S100A10, annexin I, desmosomal proteins, small proline-rich proteins, plasminogen activator inhibitor-2, and involucrin are components of the cornified envelope of cultured human epidermal keratinocytes." J Biol Chem 272(18): 12035-12046.

Roche, F. M., R. Massey, S. J. Peacock, N. P. Day, L. Visai, P. Speziale, A. Lam, M. Pallen and T. J. Foster (2003). "Characterization of novel LPXTG-containing proteins of *Staphylococcus aureus* identified from genome sequences." Microbiology 149(Pt 3): 643-654.

Roche, F. M., M. Meehan and T. J. Foster (2003). "The *Staphylococcus aureus* surface protein SasG and its homologues promote bacterial adherence to human desquamated nasal epithelial cells." Microbiology 149(Pt 10): 2759-2767.

Roghmann, M., K. L. Taylor, A. Gupte, M. Zhan, J. A. Johnson, A. Cross, R. Edelman and A. I. Fattom (2005). "Epidemiology of capsular and surface polysaccharide in *Staphylococcus aureus* infections complicated by bacteraemia." J Hosp Infect 59(1): 27-32.

Rudchenko, S., I. Trakht and J. H. Sobel. (1996). "Comparative structural and functional features of the human fibrinogen alpha C domain and the isolated alpha C fragment. Characterization using monoclonal antibodies to defined COOH-terminal A alpha chain regions." J Biol Chem 271(5): 2523-2530.

Ruimy, R., C. Angebault, F. Djossou, C. Dupont, L. Epelboin, S. Jarraud, L. A. Lefevre, M. Bes, B. E. Lixandru, M. Bertine, A. El Miniai, M. Renard, R. M. Bettinger, M. Lescat, O. Clermont, G. Peroz, G. Lina, M. Tavakol, F. Vandenesch, A. van Belkum, F. Rousset and A. Andremont (2010). "Are host genetics the predominant determinant of persistent nasal *Staphylococcus aureus* carriage in humans?" J Infect Dis 202(6): 924-934.

Said-Salim, B., P. M. Dunman, F. M. McAleese, D. Macapagal, E. Murphy, P. J. McNamara, S. Arvidson, T. J. Foster, S. J. Projan and B. N. Kreiswirth. (2003). "Global regulation of *Staphylococcus aureus* genes by Rot." J Bacteriol 185(2): 610-619.

Sambrook, J., Fritsch, E. F. & Maniatis, T. (1989). Molecular cloning: a laboratory manual. Cold Spring Harbor, NY: Cold Spring Harbor Laboratory.

Savolainen, K., L. Paulin, B. Westerlund-Wikstrom, T. J. Foster, T. K. Korhonen and P. Kuusela (2001). "Expression of pls, a gene closely associated with the mecA gene of methicillin-resistant *Staphylococcus aureus*, prevents bacterial adhesion in vitro." Infect Immun 69(5): 3013-3020.

Schaffer, A. C., R. M. Solinga, J. Cocchiaro, M. Portoles, K. B. Kiser, A. Risley, S. M. Randall, V. Valtulina, P. Speziale, E. Walsh, T. Foster and J. C. Lee (2006). "Immunization with *Staphylococcus aureus* clumping factor B, a major determinant in nasal carriage, reduces nasal colonization in a murine model." Infect Immun 74(4): 2145-2153.

Schleifer, K. H. and O. Kandler (1972). "Peptidoglycan types of bacterial cell walls and their taxonomic implications." Bacteriol Rev 36(4): 407-477.

Schutte, B. C. and P. B. McCray, Jr. (2002). "[beta]-defensins in lung host defense." Annu Rev Physiol 64: 709-748.

Selva, L., D. Viana, G. Regev-Yochay, K. Trzcinski, J. M. Corpa, I. Lasa, R. P. Novick and J. R. Penades (2009). "Killing niche competitors by remote-control bacteriophage induction." Proc Natl Acad Sci U S A 106(4): 1234-1238.

Shinefield, H., S. Black, A. Fattom, G. Horwith, S. Rasgon, J. Ordonez, H. Yeoh, D. Law, J. B. Robbins, R. Schneerson, L. Muenz, S. Fuller, J. Johnson, B. Fireman, H. Alcorn and R. Naso (2002). "Use of a *Staphylococcus aureus* conjugate vaccine in patients receiving hemodialysis." N Engl J Med 346(7): 491-496.

Shuter, J., V. B. Hatcher and F. D. Lowy (1996). "*Staphylococcus aureus* binding to human nasal mucin." Infect Immun 64(1): 310-318.

Silverman, G. J. (1992). "Human antibody responses to bacterial antigens: studies of a model conventional antigen and a proposed model B cell superantigen." Int Rev Immunol 9(1): 57-78.

Sinha, B., P. P. Francois, O. Nusse, M. Foti, O. M. Hartford, P. Vaudaux, T. J. Foster, D. P. Lew, M. Herrmann and K. H. Krause (1999). "Fibronectin-binding protein acts as *Staphylococcus aureus* invasin via fibronectin bridging to integrin alpha5beta1." Cell Microbiol 1(2): 101-117.

Sitkiewicz, I., I. Babiak and W. Hryniewicz (2011). "Characterization of transcription within *sdr* region of *Staphylococcus aureus*." Antonie Van Leeuwenhoek 99(2): 409-416.

Skaar, E. P. and O. Schneewind (2004). "Iron-regulated surface determinants (Isd) of *Staphylococcus aureus*: stealing iron from heme." Microbes Infect 6(4): 390-397.

Smith, E. J., L. Visai, S. W. Kerrigan, P. Speziale and T. J. Foster (2011). "The Sbi protein is a multifunctional immune evasion factor of *Staphylococcus aureus*." Infect Immun 79(9): 3801-3809.

Sprecher, E., A. Ishida-Yamamoto, O. M. Becker, L. Marekov, C. J. Miller, P. M. Steinert, K. Neldner and G. Richard (2001). "Evidence for novel functions of the keratin tail emerging from a mutation causing ichthyosis hystrix." J Invest Dermatol 116(4): 511-519.

Stackebrandt, E. and M. Teuber (1988). "Molecular taxonomy and phylogenetic position of lactic acid bacteria." Biochimie 70(3): 317-324.

Stapleton, M. R., M. J. Horsburgh, E. J. Hayhurst, L. Wright, I. M. Jonsson, A. Tarkowski, J. F. Kokai-Kun, J. J. Mond and S. J. Foster (2007). "Characterization of IsaA and SceD, two putative lytic transglycosylases of *Staphylococcus aureus*." J Bacteriol 189(20): 7316-7325.

Steinert, P. M. (1993). "Structure, function, and dynamics of keratin intermediate filaments." J Invest Dermatol 100(6): 729-734.

Steinert, P. M. and R. K. Liem (1990). "Intermediate filament dynamics." Cell 60(4): 521-523.

Steinert, P. M., J. W. Mack, B. P. Korge, S. Q. Gan, S. R. Haynes and A. C. Steven (1991). "Glycine loops in proteins: their occurrence in certain intermediate filament chains, loricrins and single-stranded RNA binding proteins." Int J Biol Macromol 13(3): 130-139.

Steinert, P. M. and D. R. Roop (1988). "Molecular and cellular biology of intermediate filaments." Annu Rev Biochem 57: 593-625.

Steven, A. C. and P. M. Steinert (1994). "Protein composition of cornified cell envelopes of epidermal keratinocytes." J Cell Sci 107 (Pt 2): 693-700.

Stranden, A. M., K. Ehlert, H. Labischinski and B. Berger-Bachi (1997). "Cell wall monoglycine cross-bridges and methicillin hypersusceptibility in a *femAB* null mutant of methicillin-resistant *Staphylococcus aureus*." J Bacteriol 179(1): 9-16.

Stranger-Jones, Y. K., T. Bae and O. Schneewind (2006). "Vaccine assembly from surface proteins of *Staphylococcus aureus*." Proc Natl Acad Sci U S A 103(45): 16942-16947.

Stringfellow, W. T., B. Dassy, M. Lieb and J. M. Fournier (1991). "*Staphylococcus aureus* growth and type 5 capsular polysaccharide production in synthetic media." Appl Environ Microbiol 57(2): 618-621.

Studier, F. W. and B. A. Moffatt (1986). "Use of bacteriophage T7 RNA polymerase to direct selective high-level expression of cloned genes." J Mol Biol 189(1): 113-130.

Supre, K., S. De Vliegher, I. Cleenwerck, K. Engelbeen, S. Van Trappen, S. Piepers, O. C. Sampimon, R. N. Zadoks, P. De Vos and F. Haesebrouck (2010). "*Staphylococcus devriesei* sp. nov., isolated from teat apices and milk of dairy cows." Int J Syst Evol Microbiol 60(Pt 12): 2739-2744.

Sutra, L., P. Rainard and B. Poutrel (1990). "Phagocytosis of mastitis isolates of *Staphylococcus aureus* and expression of type 5 capsular polysaccharide are influenced by growth in the presence of milk." J Clin Microbiol 28(10): 2253-2258.

Tegmark, K., A. Karlsson and S. Arvidson (2000). "Identification and characterization of SarH1, a new global regulator of virulence gene expression in *Staphylococcus aureus*." Mol Microbiol 37(2): 398-409.

Ten Broeke-Smits, N. J., J. A. Kummer, R. L. Bleys, A. C. Fluit and C. H. Boel (2010). "Hair follicles as a niche of *Staphylococcus aureus* in the nose; is a more effective decolonisation strategy needed?" J Hosp Infect 76(3): 211-214.

Terada, M., H. Tsutsui, Y. Imai, K. Yasuda, H. Mizutani, K. Yamanishi, M. Kubo, K. Matsui, H. Sano and K. Nakanishi (2006). "Contribution of IL-18 to atopic-dermatitis-like skin inflammation induced by *Staphylococcus aureus* product in mice." Proc Natl Acad Sci U S A 103(23): 8816-8821.

Thakker, M., J. S. Park, V. Carey and J. C. Lee (1998). "*Staphylococcus aureus* serotype 5 capsular polysaccharide is antiphagocytic and enhances bacterial virulence in a murine bacteremia model." Infect Immun 66(11): 5183-5189.

Thumm, G. and F. Gotz (1997). "Studies on prolysostaphin processing and characterization of the lysostaphin immunity factor (Lif) of *Staphylococcus simulans biovar staphylolyticus*." Mol Microbiol 23(6): 1251-1265.

Tomi, N. S., B. Kranke and E. Aberer (2005). "Staphylococcal toxins in patients with psoriasis, atopic dermatitis, and erythroderma, and in healthy control subjects." J Am Acad Dermatol 53(1): 67-72.

Torii, N., T. Nozaki, M. Masutani, H. Nakagama, T. Sugiyama, D. Saito, M. Asaka, T. Sugimura and K. Miki (2003). "Spontaneous mutations in the *Helicobacter pylori rpsL* gene." Mutat Res 535(2): 141-145.

Traber, K. and R. Novick (2006). "A slipped-mispairing mutation in AgrA of laboratory strains and clinical isolates results in delayed activation of *agr* and

failure to translate delta- and alpha-haemolysins." Mol Microbiol 59(5): 1519-1530.

Traber, K. E., E. Lee, S. Benson, R. Corrigan, M. Cantera, B. Shopsin and R. P. Novick (2008). "*agr* function in clinical *Staphylococcus aureus* isolates." Microbiology 154(Pt 8): 2265-2274.

Travis, S. M., P. K. Singh and M. J. Welsh (2001). "Antimicrobial peptides and proteins in the innate defense of the airway surface." Curr Opin Immunol 13(1): 89-95.

Tsurupa, G., L. Tsonev and L. Medved (2002). "Structural organization of the fibrin(ogen) alpha C-domain." Biochemistry 41(20): 6449-6459.

Tung, H., B. Guss, U. Hellman, L. Persson, K. Rubin and C. Ryden (2000). "A bone sialoprotein-binding protein from *Staphylococcus aureus*: a member of the staphylococcal Sdr family." Biochem J 345 Pt 3: 611-619.

Uehara, Y., H. Nakama, K. Agematsu, M. Uchida, Y. Kawakami, A. S. Abdul Fattah and N. Maruchi (2000). "Bacterial interference among nasal inhabitants: eradication of *Staphylococcus aureus* from nasal cavities by artificial implantation of *Corynebacterium* sp." J Hosp Infect 44(2): 127-133.

van Belkum, A., N. J. Verkaik, C. P. de Vogel, H. A. Boelens, J. Verveer, J. L. Nouwen, H. A. Verbrugh and H. F. Wertheim (2009). "Reclassification of *Staphylococcus aureus* nasal carriage types." J Infect Dis 199(12): 1820-1826.

van den Akker, E. L., J. L. Nouwen, D. C. Melles, E. F. van Rossum, J. W. Koper, A. G. Uitterlinden, A. Hofman, H. A. Verbrugh, H. A. Pols, S. W. Lamberts and A. van Belkum (2006). "*Staphylococcus aureus* nasal carriage is associated with glucocorticoid receptor gene polymorphisms." J Infect Dis 194(6): 814-818.

van Gils, E. J., E. Hak, R. H. Veenhoven, G. D. Rodenburg, D. Bogaert, J. P. Bruin, L. van Alphen and E. A. Sanders (2011). "Effect of seven-valent pneumococcal conjugate vaccine on *Staphylococcus aureus* colonisation in a randomised controlled trial." PLoS One 6(6): e20229.

van Rijen, M. M., M. Bonten, R. P. Wenzel and J. A. Kluytmans (2008). "Intranasal mupirocin for reduction of *Staphylococcus aureus* infections in surgical patients with nasal carriage: a systematic review." J Antimicrob Chemother 61(2): 254-261.

Vaudaux, P., D. Pittet, A. Haeberli, P. G. Lerch, J. J. Morgenthaler, R. A. Proctor, F. A. Waldvogel and D. P. Lew (1993). "Fibronectin is more active than fibrin or fibrinogen in promoting *Staphylococcus aureus* adherence to inserted intravascular catheters." J Infect Dis 167(3): 633-641.

Veiga, H. and M. G. Pinho (2009). "Inactivation of the SauI type I restriction-modification system is not sufficient to generate *Staphylococcus aureus* strains capable of efficiently accepting foreign DNA." Appl Environ Microbiol 75(10): 3034-3038.

Vergara-Irigaray, M., T. Maira-Litran, N. Merino, G. B. Pier, J. R. Penades and I. Lasa (2008). "Wall teichoic acids are dispensable for anchoring the PNAG exopolysaccharide to the *Staphylococcus aureus* cell surface." Microbiology 154(Pt 3): 865-877.

Vernachio, J., A. S. Bayer, T. Le, Y. L. Chai, B. Prater, A. Schneider, B. Ames, P. Syribeys, J. Robbins and J. M. Patti (2003). "Anti-clumping factor A immunoglobulin reduces the duration of methicillin-resistant *Staphylococcus aureus* bacteremia in an experimental model of infective endocarditis." Antimicrob Agents Chemother 47(11): 3400-3406.

Visai, L., N. Yanagisawa, E. Josefsson, A. Tarkowski, I. Pezzali, S. H. Rooijakkers, T. J. Foster and P. Speziale (2009). "Immune evasion by *Staphylococcus aureus* conferred by iron-regulated surface determinant protein IsdH." Microbiology 155(Pt 3): 667-679.

von Eiff C, B. K., Machka K, Stammer H, Peters G. (2001). "Nasal carriage as a Source of *Staphylococcus aureus* Bactemia, Study Group." N Engl J Med 344(1): 11-16.

von Eiff, C., J. F. Kokai-Kun, K. Becker and G. Peters (2003). "*In vitro* activity of recombinant lysostaphin against *Staphylococcus aureus* isolates from anterior nares and blood." Antimicrob Agents Chemother 47(11): 3613-3615.

Waldron, D. E. and J. A. Lindsay (2006). "Sau1: a novel lineage-specific type I restriction-modification system that blocks horizontal gene transfer into *Staphylococcus aureus* and between *S. aureus* isolates of different lineages." J Bacteriol 188(15): 5578-5585.

Walsh, E. J., H. Miajlovic, O. V. Gorkun and T. J. Foster (2008). "Identification of the *Staphylococcus aureus* MSCRAMM clumping factor B (ClfB) binding site in the alphaC-domain of human fibrinogen." Microbiology 154(Pt 2): 550-558.

Walsh, E. J., L. M. O'Brien, X. Liang, M. Hook and T. J. Foster (2004). "Clumping factor B, a fibrinogen-binding MSCRAMM (microbial surface components recognizing adhesive matrix molecules) adhesin of *Staphylococcus aureus*, also binds to the tail region of type I cytokeratin 10." J Biol Chem 279(49): 50691-50699.

Ward, J. B. (1981). "Teichoic and teichuronic acids: biosynthesis, assembly, and location." Microbiol Rev 45(2): 211-243.

Weidenmaier, C., J. F. Kokai-Kun, S. A. Kristian, T. Chanturiya, H. Kalbacher, M. Gross, G. Nicholson, B. Neumeister, J. J. Mond and A. Peschel (2004). "Role of teichoic acids in *Staphylococcus aureus* nasal colonization, a major risk factor in nosocomial infections." Nat Med 10(3): 243-245.

Weidenmaier, C., J. F. Kokai-Kun, E. Kulauzovic, T. Kohler, G. Thumm, H. Stoll, F. Gotz and A. Peschel (2008). "Differential roles of sortase-anchored surface proteins and wall teichoic acid in *Staphylococcus aureus* nasal colonization." Int J Med Microbiol 298(5-6): 505-513.

Weidenmaier, C. and A. Peschel (2008). "Teichoic acids and related cell-wall glycopolymers in Gram-positive physiology and host interactions." Nat Rev Microbiol 6(4): 276-287.

Weidenmaier, C., A. Peschel, V. A. Kempf, N. Lucindo, M. R. Yeaman and A. S. Bayer (2005). "DltABCD- and MprF-mediated cell envelope modifications of *Staphylococcus aureus* confer resistance to platelet microbicidal proteins and contribute to virulence in a rabbit endocarditis model." Infect Immun 73(12): 8033-8038.

Weidenmaier, C., A. Peschel, Y. Q. Xiong, S. A. Kristian, K. Dietz, M. R. Yeaman and A. S. Bayer (2005). "Lack of wall teichoic acids in *Staphylococcus aureus* leads to reduced interactions with endothelial cells and to attenuated virulence in a rabbit model of endocarditis." J Infect Dis 191(10): 1771-1777.

Weigel, L. M., D. B. Clewell, S. R. Gill, N. C. Clark, L. K. McDougal, S. E. Flannagan, J. F. Kolonay, J. Shetty, G. E. Killgore and F. C. Tenover (2003). "Genetic analysis of a high-level vancomycin-resistant isolate of *Staphylococcus aureus*." Science 302(5650): 1569-1571.

Weiss, W. J., E. Lenoy, T. Murphy, L. Tardio, P. Burgio, S. J. Projan, O. Schneewind and L. Alksne (2004). "Effect of *srtA* and *srtB* gene expression on the virulence of *Staphylococcus aureus* in animal models of infection." J Antimicrob Chemother 53(3): 480-486.

Wertheim, H. F., D. C. Melles, M. C. Vos, W. van Leeuwen, A. van Belkum, H. A. Verbrugh and J. L. Nouwen (2005). "The role of nasal carriage in *Staphylococcus aureus* infections." Lancet Infect Dis 5(12): 751-762.

Wertheim, H. F., M. C. Vos, A. Ott, A. van Belkum, A. Voss, J. A. Kluytmans, P. H. van Keulen, C. M. Vandenbroucke-Grauls, M. H. Meester and H. A. Verbrugh (2004). "Risk and outcome of nosocomial *Staphylococcus aureus* bacteraemia in nasal carriers versus non-carriers." Lancet 364(9435): 703-705.

Wertheim, H. F., M. C. Vos, A. Ott, A. Voss, J. A. Kluytmans, C. M. Vandenbroucke-Grauls, M. H. Meester, P. H. van Keulen and H. A. Verbrugh (2004). "Mupirocin prophylaxis against nosocomial *Staphylococcus aureus* infections in nonsurgical patients: a randomized study." Ann Intern Med 140(6): 419-425.

Wertheim, H. F., E. Walsh, R. Choudhurry, D. C. Melles, H. A. Boelens, H. Miajlovic, H. A. Verbrugh, T. Foster and A. van Belkum (2008). "Key role for clumping factor B in *Staphylococcus aureus* nasal colonization of humans." PLoS Med 5(1): e17.

Whittock, N. V., F. J. Smith, H. Wan, R. Mallipeddi, W. A. Griffiths, P. Dopping-Hepenstal, G. H. Ashton, R. A. Eady, W. H. McLean and J. A. McGrath (2002). "Frameshift mutation in the V2 domain of human keratin 1 results in striate palmoplantar keratoderma." J Invest Dermatol 118(5): 838-844.

Wu, J. A., C. Kusuma, J. J. Mond and J. F. Kokai-Kun (2003). "Lysostaphin disrupts *Staphylococcus aureus* and *Staphylococcus epidermidis* biofilms on artificial surfaces." Antimicrob Agents Chemother 47(11): 3407-3414.

Wuite, J., B. I. Davies, M. J. Go, J. C. Lambers, D. Jackson, G. Mellows and T. C. Tasker (1985). "Pseudomonic acid, a new antibiotic for topical therapy." J Am Acad Dermatol 12(6): 1026-1031.

Xia, G., T. Kohler and A. Peschel (2010). "The wall teichoic acid and lipoteichoic acid polymers of *Staphylococcus aureus*." Int J Med Microbiol 300(2-3): 148-154.

Xiang, H., Y. Feng, J. Wang, B. Liu, Y. Chen, L. Liu, X. Deng and M. Yang (2012). "Crystal Structures Reveal the Multi-Ligand Binding Mechanism of *Staphylococcus aureus* ClfB." PLoS Pathog 8(6): e1002751.

Xu, S. Y., A. R. Corvaglia, S. H. Chan, Y. Zheng and P. Linder (2011). "A type IV modification-dependent restriction enzyme SauUSI from *Staphylococcus aureus* subsp. aureus USA300." Nucleic Acids Res 39(13): 5597-5610.

Yokoyama, K., H. Mizuguchi, Y. Araki, S. Kaya and E. Ito (1989). "Biosynthesis of linkage units for teichoic acids in gram-positive bacteria: distribution of related enzymes and their specificities for UDP-sugars and lipid-linked intermediates." J Bacteriol 171(2): 940-946.

Yoneda, K., D. Hohl, O. W. McBride, M. Wang, K. U. Cehrs, W. W. Idler and P. M. Steinert (1992). "The human loricrin gene." J Biol Chem 267(25): 18060-18066.

Yoneda, K., O. W. McBride, B. P. Korge, I. G. Kim and P. M. Steinert (1992). "The cornified cell envelope: loricrin and transglutaminases." J Dermatol 19(11): 761-764.

Yu, V. L., A. Goetz, M. Wagener, P. B. Smith, J. D. Rihs, J. Hanchett and J. J. Zuravleff. (1986). "*Staphylococcus aureus* nasal carriage and infection in patients on hemodialysis. Efficacy of antibiotic prophylaxis." N Engl J Med 315(2): 91-96.

Zanger, P., D. Nurjadi, B. Vath and P. G. Kremsner (2011). "Persistent nasal carriage of *Staphylococcus aureus* is associated with deficient induction of human beta-defensin 3 after sterile wounding of healthy skin in vivo." Infect Immun 79(7): 2658-2662.

Zapotoczna, M., Z. Jevnikar-Rojnik, H. Miajlovic, J. Kos and T. J. Foster (2012). "Iron regulated surface determinant B (IsdB) promotes *Staphylococcus aureus* adherence to and internalization by non-phagocytic human cells." Cell Microbiol.

Zhou, X. M., W. W. Idler, A. C. Steven, D. R. Roop and P. M. Steinert (1988). "The complete sequence of the human intermediate filament chain keratin 10. Subdomainal divisions and model for folding of end domain sequences." J Biol Chem 263(30): 15584-15589.

Zhu, H., G. Xie, M. Liu, J. S. Olson, M. Fabian, D. M. Dooley and B. Lei (2008). "Pathway for heme uptake from human methemoglobin by the iron-regulated surface determinants system of *Staphylococcus aureus*." J Biol Chem 283(26): 18450-18460.

Zong, Y., T. W. Bice, H. Ton-That, O. Schneewind and S. V. Narayana (2004). "Crystal structures of *Staphylococcus aureus* sortase A and its substrate complex." J Biol Chem 279(30): 31383-31389.